Quantitative Genetic Analysis of *C. elegans* Vulval Development

---

Dissertation

zur Erlangung der naturwissenschaftlichen Doktorwürde

(Dr. sc. nat.)

vorgelegt der

Mathematisch-naturwissenschaftlichen Fakultät

der

Universität Zürich

von

Tobias Jan Schmid

aus Schübelbach SZ

Promotionskomitee

Prof. Dr. Alex Hajnal (Vorsitz)

Prof. Dr. Ueli Grossniklaus

Prof. Dr. Homayoun Bagheri

Prof. Dr. Ralf Sommer

Zürich, 2014

Zusammenfassung:

Natürlich vorkommende Variationen im Erbgut stellen den Ursprung individueller Veranlagungen für bestimmte Krankheiten und deren Ausgang dar. Komplexe Krankheiten wie Krebs beruhen insbesondere auf dem Zusammenspiel zwischen genetischen Veranlagungen und der Umwelt. Um solche komplexen Sachverhalte besser zu verstehen und Strategien zur Krebsbekämpfung zu entwickeln, ist die Identifizierung solcher Risiko Faktoren essentiell.

In dieser Studie verwendeten wir die Entwicklung der *C. elegans* Vulva als Modell der Krebsentstehung, da wichtige, krebsrelevante Signalwege wie EGFR/RAS/MAPK, Notch und Wnt involviert sind. Dafür haben wir das Erbgut zweier Wildtyp Stämme, N2 Bristol und CB4856 Hawaii kombiniert. Zusätzlich fügten wir noch Mutationen in Onkogenen wie Ras(gf) oder β-catenin(lf) ein. Mit den so entstandenen, mutationsinkludierten rekombinanten Inzucht Linien (miRILs) waren wir in der Lage, Regionen quantitativer Merkmale (QTLs) zu identifizieren, welche Signale von Ras und Wnt beeinflussen. Eine nähere Untersuchung der QTLs für Ras(gf) Prozesse führte zur Entdeckung mehrerer Kandidatengenen. Das vielversprechendste Gen ist *amx-2*. Der Vergleich mit der homologen humanen Sequenz deutet auf eine Ähnlichkeit zu Monoamine Oxidase A (MAOA) hin, welche eine wichtige Rolle in der Erforschung von psychischen Erkrankungen spielte. Erst kürzlich wurde die Herunterregulation von MAOA als Indikator für aggressives Krebswachstum in mehreren Spezies beschrieben ((Rybaczyk, Bashaw, Pathak, & Huang, 2008)). In gleicher Weise zeigen wir hier, dass der Verlust von *amx-2* eine Erhöhung der RAS/MAPK Aktivität während der Vulvaentwicklung zur Folge hat, was darauf hindeutet, dass *amx-2* ein negativer Regulator der Signalübertragung ist. Zudem zeigen wir, dass nur N2 Bristol ein funktionelles *amx-2* Gen besitzt. Des Weiteren genügt die Expression von *amx-2* in Darmzellen, um die Funktion von *amx-2* wieder herzustellen. Im Anschluss konnten wir zeigen, das AMX-2 Substrat Serotonin (5-HT), aber nicht Dopamin, in der Lage ist, eine Überaktivität von RAS/MAPK in einer Ras(gf) Mutante zu supprimieren. Interessant ist dabei, dass die Suppression durch den 5-HT Metaboliten 5-Hydroxyindolessigsäure (5-HIAA) und teils auch Melatonin (MT) bewirkt wird.

Wir haben zudem die Funktion von 5-HIAA in humanen Krebszellen untersucht und festgestellt, dass 5-HIAA die RAS/MAPK Signaleübertragung inhibiert durch eine Hemmung der MAP Kinase ERK2. 5-HIAA war auch in der Lage, das Wachstum von Krebszellen zu.

Zusammengefasst lässt sich sagen, dass wir in *C. elegans amx-2* über einen quantitativen genetischen Ansatz als negativen Regulator des RAS/MAPK Signalwegs gefunden haben und dass der 5-HAT Metabolit 5-HIAA, welcher durch *amx-2* produziert wird ebenfalls die MAP Kinase hemmt. Wir schlagen deshalb vor, dass die Menge des durch *amx-2*/MAOA produzierten

5-HIAA massgeblichen Einfluss hat, RAS/MAPK Signale zu modulieren und dass dieser Mechanismus in auch in Vertebraten existiert.

Summary:

Natural genetic variation constitutes the source of an individual's predisposition to develop certain diseases more frequently and with poorer outcome. Complex diseases such as cancer in particular rely on the interplay between the genetic background and the environment. The identification of genetic risk factors is necessary to understand the entire complexity of such diseases and might uncover novel drug targets for treatment.

In this study, we used *C. elegans* vulval development as a model for complex cancer signalling, since vulval fate specification relies on the interplay between the EGFR/RAS/MAPK, Notch and Wnt pathway, that are all misregulated in human cancer. We mixed the genomes of two well established wild-type strains, N2 Bristol and CB4856 Hawaii, and introduced mutations in oncogenes such as ras(gf) or β-catenin(gf). We established mutation included recombinant inbred lines (miRILs) and mapped quantitative trait loci (QTLs) affecting Ras and Wnt signalling. Further studes of the QTLs in the Ras(gf) containing miRILs revealed several candidate genes, the most promising called *amx-2*. Sequence homology comparison between the human and the *C. elegans* genomes indicated that *amx-2* is most similar to Monoamine Oxidase A (MAOA), a gene well known for its pivotal role in the study of mental disorders. Recently, the down-regulation of MAOA mRNA has been reported as an indicator of more aggressive cancer in various species ((Rybaczyk et al., 2008)). Similarly, we show that loss of *amx-2* function increases RAS/MAPK signalling during *C. elegans* vulval development. Therefore, *amx-2* represents a negative regulator of the pathway. In addition, we demonstrate that only the N2 Bristol allele exerts this inhibitory function and that CB4856 Hawaii has a non-functional allele. We further identified the gut lineage as the tissue necessary for the suppressive role of *amx-2* on RAS/MAPK signalling. We next analysed the role of the substrates of *amx-2*, Serotonin (5-HT) and Dopamine (L-DOPA) on RAS/MAPK signalling. Surprisingly, only Serotonin inhibited over activation of the RAS/MAPK pathway in a Ras(gf) background. Interestingly, this was due to the Serotonin metabolite 5-Hydroxyindoleacedic acid (5-HIAA) and in part also to Melatonin (MT).

We further tested the effect of 5-HIAA to inhibit RAS/MAPK signalling in different human cancer cell lines and show that the 5-HT metabolite suppresses RAS/MAPK signalling by a reduction of phosphorylated ERK2. In addition, 5-HIAA slows down cell proliferation.

In summary, we found in *C. elegans amx-2* as a novel negative regulator of RAS/MAPK signalling using a quantitative genetics approach. In addition, we identified 5-HIAA, whose production relies on the enzymatic activity of *amx-2,* as a substance able to inhibit RAS/MAPK signalling. We

therefore propose that the levels of 5-HIAA produced by *amx-2*/MAOA are crucial to modulate RAS/MAPK signalling in *C. elegans* and that this mechanism also exists in vertebrates.

Table of Contents

Introduction

1.1 *Caenorhabditis Elegans*

C. elegans is a free-living organism that belongs to the Nematodes. The adult worm is less than 1mm in length and 0.2 mm in diameter, unsegmented and bilaterally symmetrical. In nature it inhabits temperate soil environment. *C. elegans* feeds on bacteria and fungi that arise on decaying organic material. *C. elegans* exists in two sexes, hermaphrodites and males (Figure 1, Figure 2), the latter of which comprising only comprise 0.5% of the total population. Hermaphrodites produce both sperm and eggs and are able to self-fertilize. One hermaphrodite normally gives rise to 300 offspring (Brenner, 1974). Sex in *C. elegans* is determined by the X0-system, by which the hermaphrodite has two X-chromosomes (XX) in contrast to the male, with only one (X0).

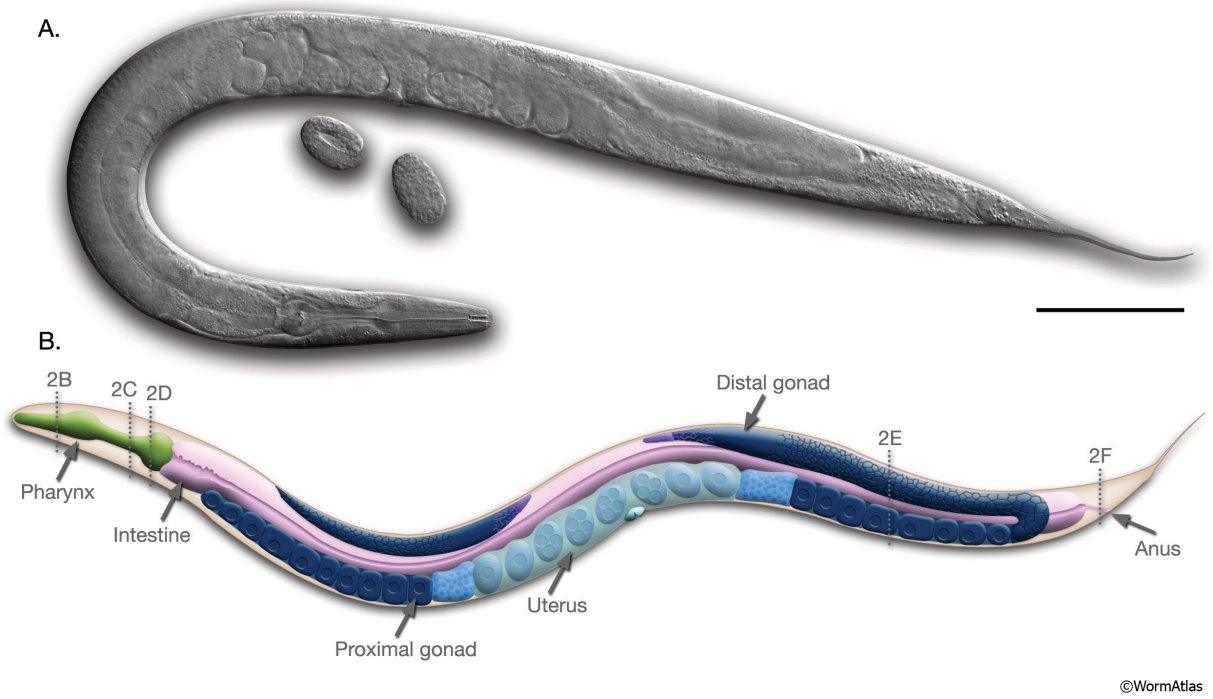

Figure 1: Hermaphrodite anatomy: *C. elegans* is simple, it consists of mainly the pharynx (green) a feeding gut (purple) and two gonad arms (dark blue), where oocyte maturation takes place from distal to proximal. Sperm is produced early during postembryonic development and stored in the two spermathecae (blue). Eggs are pushed through one of the spermathecae to get fertilized and to start developing in the uterus (light blue) until they get laid through the vulval opening.

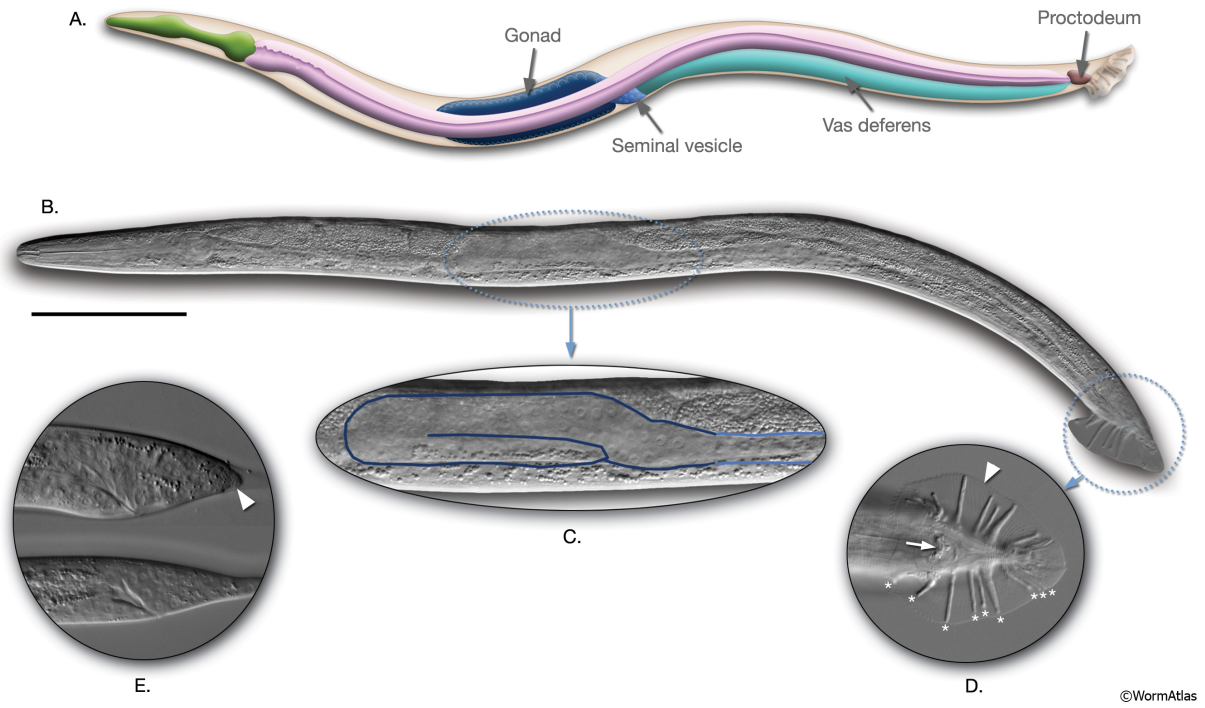

Figure 2: Male anatomy: *C. elegans* males occur infrequently in wild population (0.5%). Males have a pharynx (green) and a feeding gut (purple). They only have one gonad arm (blue), where they produce sperm. The male tale resembles a fan and consists of sensory rays and spicules. The rays help to find the vulval opening of the hermaphrodite, into which the spicules are inserted to release sperm. Figure adapted from WormAtlas

The *C. elegans* genome is approximately 100'000'000 base pairs long and harbours roughly 20'000 genes. These genes are distributed over five pairs of autosomes and one pair of sex chromosomes.

C. elegans development follows an invariant cell lineage; therefore, the developmental fate of each cell can therefore be determined. Wild type adult hermaphrodites always comprise of 959 cells, since 131 out of 1090 cells are eliminated by programmed cell death. Additionally, *C. elegans* presents one of the simplest model organisms with a nervous system. The connectivity pattern of the 302 neurons has been mapped completely, which makes it easy to study fundamental processes in an otherwise very complex organ.

In the mid sixties, Sidney Brenner chose *C. elegans* as a model organism because of its cheap and easy handling. *C. elegans* can be held on agar plates or in liquid medium. Since the animal is transparent, each developmental stage is accessible to study using conventional light microscopy. *C. elegans* tolerates freezing in liquid nitrogen and storage at -80°C for many years. Despite its simple body plan, *C. elegans* harbour, all characteristics of a real animal, e.g. a nervous system for complex behaviours, tissue development, a feeding gut and musculature (Rankin, 2002; de Bono *et al.*, 2002) and can therefore serve as a model for several human disease mechanisms.

1.2 Anatomy of *C. elegans*

The anatomy of *C. elegans* is simple (Brenner, 1974). The animal consists of the head containing the nerve ring and the pharynx, the main body that is filled with intestine and the gonad that contains the vulva, the uterus and the spermatheca in the case of the hermaphrodite (Figure 1). Gonad and intestine are surrounded by the pseudocoelomic space. A layer of epidermal sheath cells, called the hypodermis and protected by a secreted cuticle, surrounds the cylindrical body. *C. elegans* has no circulatory system and is able to extract oxygen from the environments by free diffusion due to its small size. Nutrients are released directly into the pseudocoelomic space to be taken up by various cells. The main body muscles of *C. elegans* are arranged in four rows, two on the dorsal and two on the ventral side. The major nerve cords are localized along the whole body on the dorsal and ventral midline. Locomotion occurs by coordinated contraction of the body muscle cells on one side that leads to a bending of the animal and in alternating sequence to a sinusoidal movement.

1.3 Life Cycle of *C. elegans*

A *C. elegans* embryo hatches after 14 hours of embryogenesis. During postembryonic development at 20°C, the animal develops through four larval stages to reach adulthood after 3.5 days. The larval stages of *C. elegans* are intermitted by moults, during which the animal sheds its cuticle followed by secretion of a new stage-specific cuticular layer. *C. elegans* L1 larva have the ability to enter into the dauer stage under conditions of crowding or food limitation ((Riddle, 1982)). The robust dauer larva is then able to survive unfavourable environmental conditions and to re-enter the normal life cycle if the situtation improves (Figure 3) (Cassada & Russell, 1975; Wormatlas).

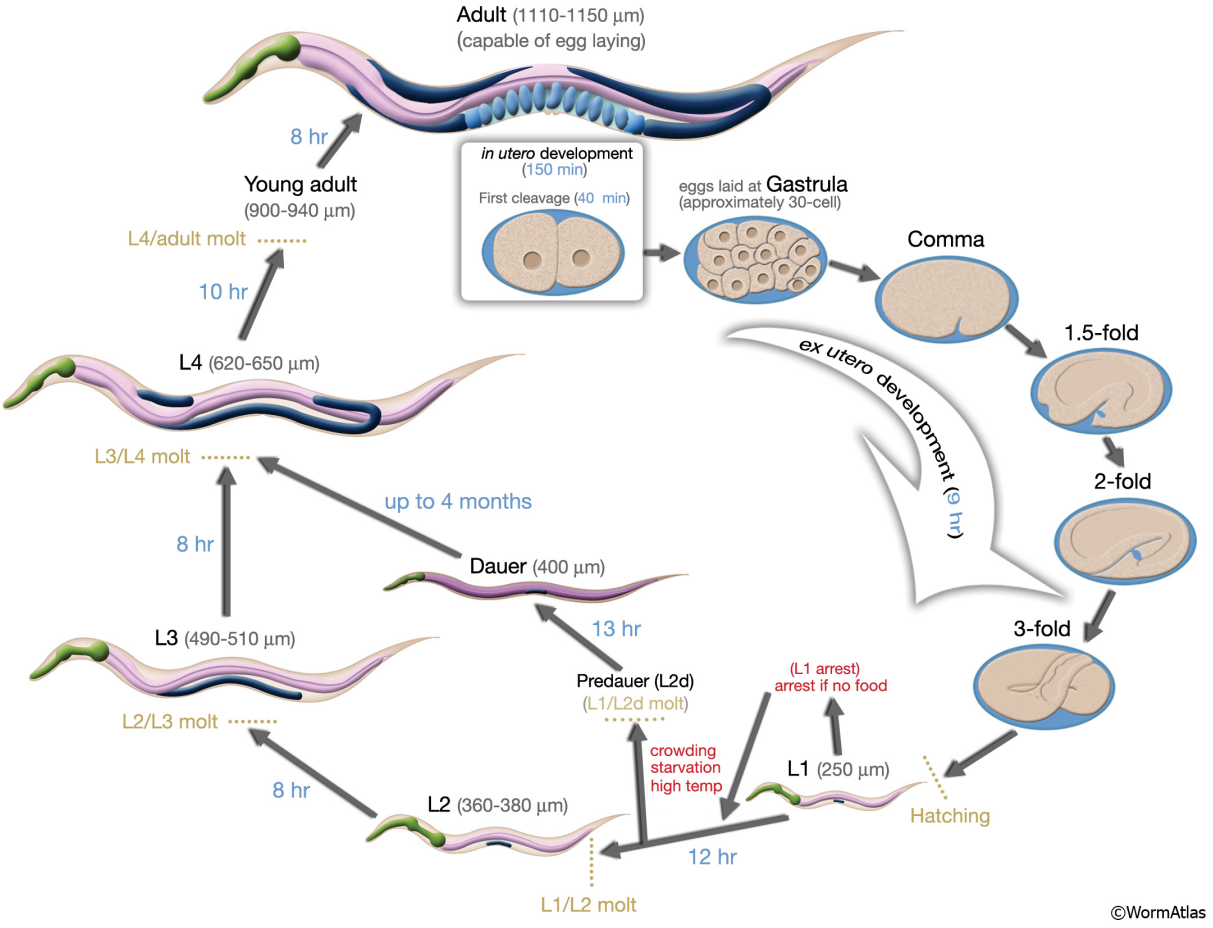

Figure 3: Life cycle of *C. elegans* at 22°C. Life starts with the fertilization of the oocyte inside the hermaphrodite. The developing embryo will be laid through the vulva at gastrulation stage. After 9 more hours it hatches and starts its postembryonic development as an L1 larva. It grows and moults after 12 hours into an L2 larva and moults again after 8 more hours to start L3 stage. L4 stage begins at 8 hours post L3 and eventually, the larva develops into a young adult and starts producing its own eggs after 10 hours post L4. Adapted from WormAtlas.

1.4 *C. elegans* Vulval Development

The vulva of *C. elegans* is the egg-laying organ of the hermaphrodite and is dispensable for life. Since the key signalling pathways RTK/RAS, WNT and NOTCH are involved during vulval development (Sternberg, 2005), the vulva can serve as a model system for complex disease signalling, such as cancer (Chang et al., 1999). Additionally, alterations in these signalling pathways are often associated with cancer in humans.

Vulval development starts during the third larval stage.12 Pn.p cells, P1.p – P12.p are located on the ventral side of the developing larva. Six of those termed P3.p – P8.p compose the equivalence group of the vulva and are called vulval precursor cells (VPCs). Each of those six VPCs has the potential to adopt a vulval cell fate. During the L3 larval state the anchor cell (AC), a specialized polarized cell in the somatic gonad, secretes the EGF-like ligand LIN-3 to activate the EGF receptor LET-23 in the receiving cells, P3.p – P8.p. Since LIN-3 is secreted in a graded manner,

the cell in closest proximity to the AC, P6.p receives the strongest signal, activates downstream components of the RAS/ MAPK pathway and thereby adopts the 1° cell fate. The activation of the RAS/ MAPK pathway in P6.p leads to the expression of Notch ligands eventually preventing the neighbouring cells P5.p and P7.p via lateral inhibition from adopting a 1° cell fate. Upregulation of Notch signalling in P5.p and P7.p induces the 2° cell fate in those cells. The induced cells, P5.p – P7.p undergo three further rounds of cell divisions to generate 22 cells, whereas the uninduced cells, P3.p, P4.p and P8.p divide once and then fuse to the hypodermal syncytium hyp7. During L4, vulval development is completed by Morphogenesis (Figure 4).

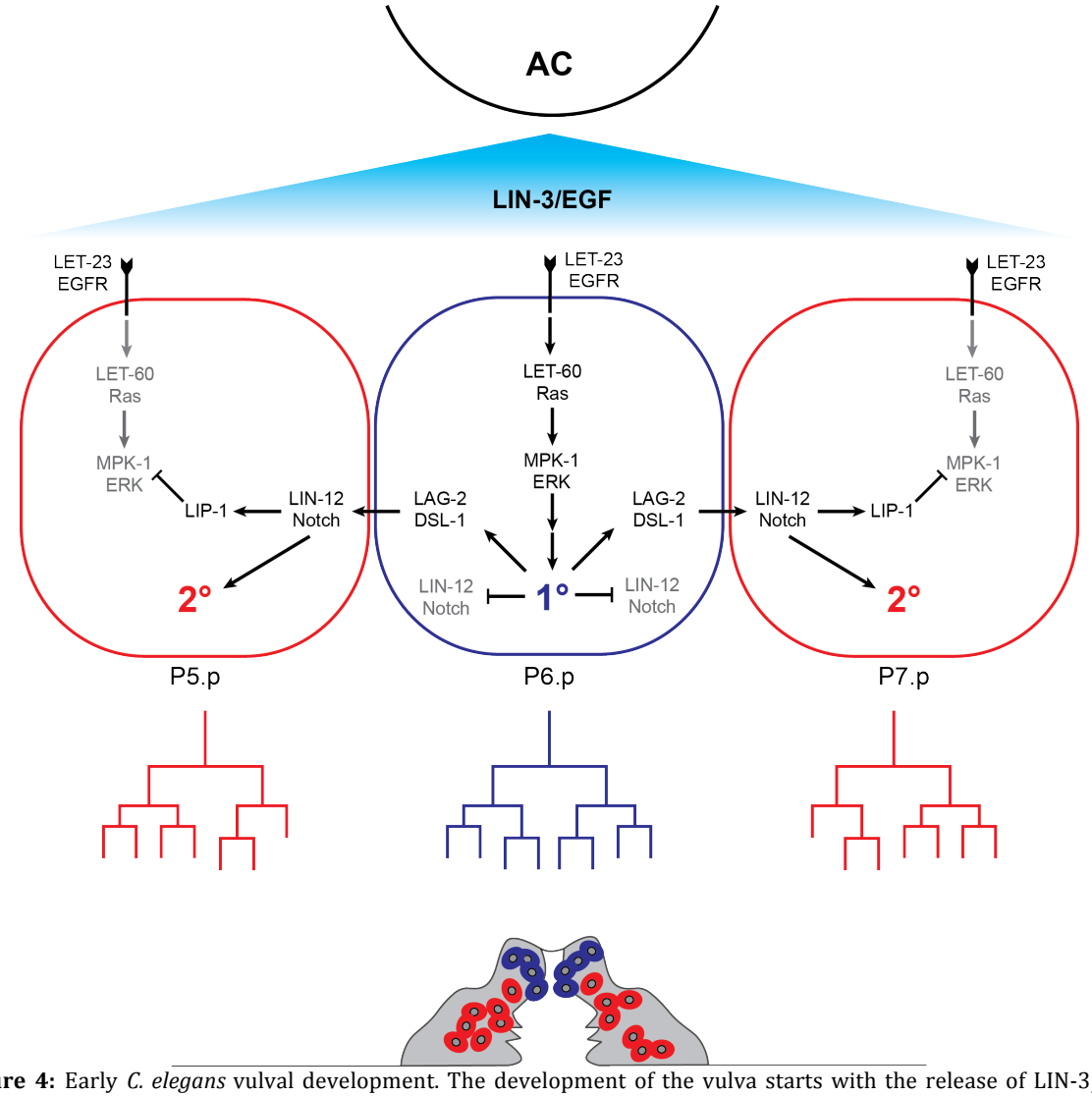

Figure 4: Early *C. elegans* vulval development. The development of the vulva starts with the release of LIN-3/EGF from the anchor cell. Highest activation of the EGFR/RAS/MAPK pathway is observed in P6.p due to its proximity to the anchor cell inducing the 1° cell fate. Subsequent lateral inhibition via the Delta/Notch pathway suppresses adoption of the 1° cell fate and leads to the induction of the 2° cell fate in P5.p and P6.p. P5.p – P7.p will divide three more times to produce 22 daughter cells that through further events of morphogenesis form the adult vulva

1.4.1 1° Cell Fate Specification via the EGF/RAS/MAPK Pathway

The anchor cell secretes LIN-3/EGF (Hill & Sternberg, 1992) in a graded manner to activate LET-23/EGFR molecules at the baso-lateral site of the underlying vulval precursor cells (VPCs). LIN-3/EGF binding leads to receptor dimerization and auto phosphorylation of its C-terminal domain (Sternberg & Horvitz, 1986). A ternary complex consisting of LIN-2/CASK, LIN-7/VELIS and LIN-10/MINT is necessary correct localisation of LET-23/EGFR to ensure sufficient receptor activation by LIN-3/EGF (Charles W Whitfield, 1999). The phosphorylated residues of LET-23/EGFR serve as docking sites for SEM-5/Grb2 and recruit SOS-1/GEF to activate LET-60/RAS (Aroian, Koga, Mendel, Ohshima, & Sternberg, 1990), (C. Chang, 2000). Active LET-60/RAS binds and stabilises LIN-45/Raf at the plasma- or other endomembrane, where it is activated. LIN-45 phosphorylates MEK-2 thereby triggering the MAPK cascade. MEK-2, further phosphorylates MPK-1 leading to its translocation into the nucleus, to either activate or inactivate various target proteins. LIN-1/ETS and LIN-31/WH are targets of activated nuclear MPK-1 and form a complex to inhibit vulval induction (Beitel, Tuck, Greenwald, & Horvitz, 1995), (L. M. Miller, Gallegos, Morisseau, & Kim, 1993). Upon nuclear translocation of activated MPK-1 followed by phosphorylation of LIN-31, this inhibitory complex is disrupted and phosphorylated LIN-31 may act as positive regulator of vulval development by increasing the transcription of LIN-39/HOX tha eventually induces the 1° cell fate (Clark, Chisholm, & Horvitz, 1993), (Salser, Loer, & Kenyon, 1993). During vulval development LIN-3 is secreted gradually such that P6.p receives the highest dose and subsequently adopts the 1° cell fate. P6.p divides three times, leading to eight daughter cells that will later on form the vulE and vulF toroid.

1.4.2 2° Cell Fate Specification via the Delta/Notch Pathway

The adoption of the 1° cell fate in P6.p leads to the upregulation and higher expression of the redundant Notch ligands *lag-2*, *dsl*-1 and *apx-1.* These secreted Notch ligands activate Notch receptors in the neighbouring P5.p and P7.p cells to induce 2° cell fate and to prevent them from adopting the 1° cell fate via activation of negative EGFR/RAS/MAPK regulators such as *gap-1*, *lip-1*, *dpy-23* and the *lst* genes (Alex Hajnal, 1997), (Berset, 2001), (Yoo, Bais, & Greenwald, 2004). 2° cells divide three times leading to seven daughter cells each. These 14 cells form cells required for the establishment of the vulA vulB1 vulB2 vulC and vulD toroid. Together with the vulE and vulF toroid from the 1° cell lineage a stack of seven rings is formed. Subsequent morphogenesis initiates eversion of this stack to complete the adult egg-laying organ (R. K. Herman & Hedgecock, 1990), (Antoshechkin & Han, 2002), (Sharma-Kishore, White, Southgate, & Podbilewicz, 1999), (Kishore & Sundaram, 2002), (Dalpé, Brown, & Culotti, 2005).

1.5 RAS and its Signalling

In 1981, the rat genes homologous to the viral Harvey and Kirsten transforming sequences were identified and named ras (rat sarcoma virus) (DeFeo et al., 1981). Subsequently, the genes were found in mice and humans (E. H. Chang, Gonda, Ellis, Scolnick, & Lowy, 1982). Interestingly, many of the different human cancer cell lines revealed mutations in RAS. Frequently, point mutations affecting the amino acid residues 12 and less often 13 and 61 were found (Tabin et al., 1982), (Reddy, Reynolds, Santos, & Barbacid, 1982), (Taparowsky et al., 1982), (Capon, Chen, Levinson, Seeburg, & Goeddel, 1983). Mutations in K-Ras are the predominantly found in human cancer (20%), whereas H-Ras is found mutated less frequently (2-3%). In 1983 N-ras was identified in neuroblastoma and leukaemia cell lines discovered to share the same characteristics as H- and K-ras (Shimizu et al., 1983), (Hall, Marshall, Spurr, & Weiss, 1983), (Taparowsky, Shimizu, Goldfarb, & Wigler, 1983). RAS are small G-proteins with an intrinsic GTPase activity, they shuttle between an active GTP and an inactive GDP bound form (Gilman, 1987). Mutations in the GTPase domain rendering it constitutively active are characteristic for cancer patients (Santos et al., 1984), (Nakano et al., 1984), (R H Hruban, 1993), (Hand et al., 1984).

1.5.1 Subcellular Localisation of RAS

RAS is post-translationally modified with lipids to achieve full function. All three Isoforms of RAS share a CAAX motif at the very C-terminal end. In a first step, the cysteine is isporenylated by a farnesyl protein transferase (Casey, Solski, Der, & Buss, 1989), (Sefton, Trowbridge, Cooper, & Scolnick, 1982), enabling RAS to associate with the ER, where the residual AAX motif is cleaved off. In a second step, the farnesylated cysteine is carboxymethylated by isoprenyl cysteine transferase (Omerovic, Laude, & Prior, 2007). This initially weak membrane binding is supported by additional palmitoyl groups or by other C-terminal motifs such as stretches of positively charged lysine that can interact with the negatively charged phospholipid head groups of membranes (Hancock, Paterson, & Marshall, 1990). The latter two modifications are reversible and thereby enable RAS to interact with various subcellular compartments. Depending on the presence of palmitoyl groups, RAS shuttles between the Golgi apparatus (depalmitoylated) and the plasmamembrane (palmitoylated), while the number of palmitoyl groups determines the half-life of RAS at the membrane. Although RAS is located predominantly at the plasma membrane, it is also observed in endosomes that affect its recycling dynamics (Ghai et al., 2011) and on mitochondria, where it induces apoptosis (Bivona et al., 2006) through

a still unknown mechanism. Constitutively active RAS has been found to prevent mitochondria induced apoptosis through the activation of ERK that reduces the sensitivity of the mitochondrial permeability transition pore (Rasola et al., 2010).

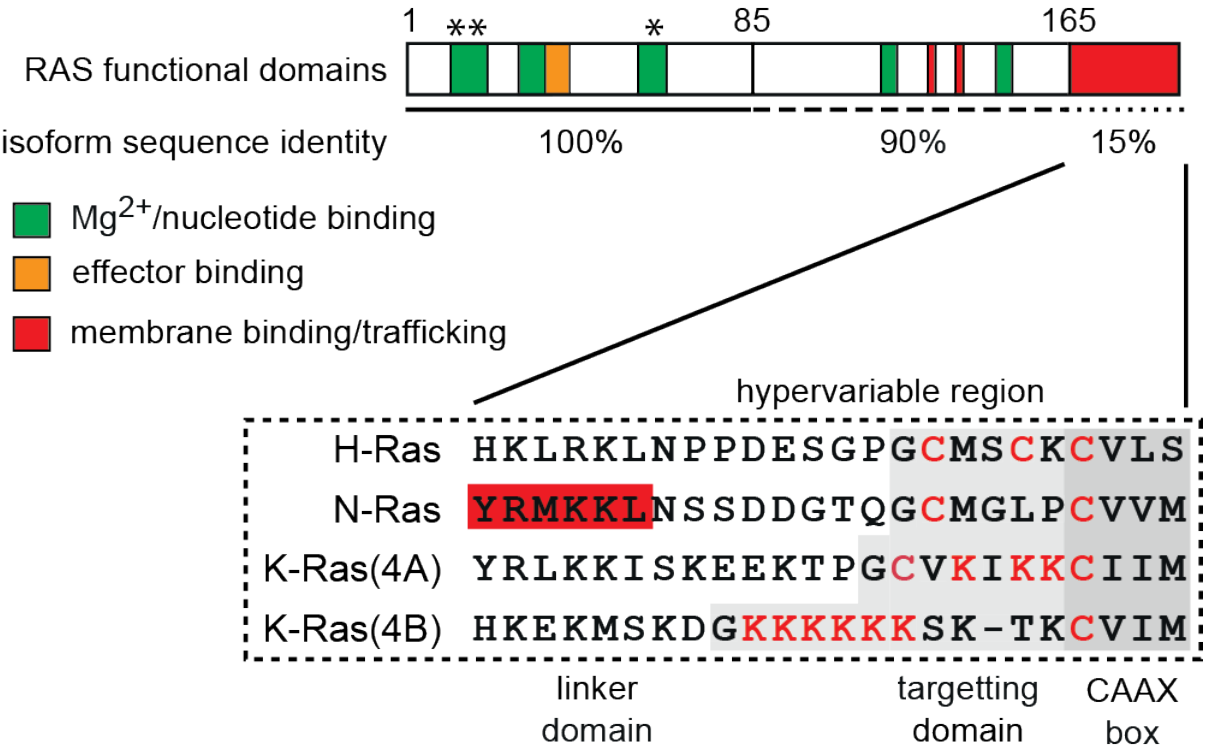

Figure 5: RAS domains. Depicted are the 3 different human RAS isoforms and their conservation. The only striking difference between the isoforms is in the hypervariable region (HVR), whose difference (red) is important for the differening subcellular localisation of the three isoforms. Asterisks mark the site of the oncogenic mutations. Adapted from (Prior & Hancock, 2012).

RAS is thought to either freely diffuse or localise into signalling modules, which are nanoclusters of 12-24 nm containing 6-7 proteins with a half life of 0.1-1s. (Plowman, Muncke, Parton, & Hancock, 2005). Each type of RAS isoform is assembled into a specific nanocluster, depending on the HVR, C-terminal anchor and G domain. These nanoclusters possess unique structural properties, regarding the dependency or dispensability of cholesterol and the employment of scaffold proteins such as galectin-1 and galectin-3 (Roy et al., 2005), (Niv, 2002). RAS nanoclusters serve as a scaffold for downstream signalling.

1.5.2 Regulation and interacting signalling partners of RAS

RAS is negatively regulated through the action of GTPase activating proteins (GAPs) that will enhance RAS the intrinsic GTPase activity over 1000 fold. Active RAS requires guanine nucleotide-exchange factors (GEFs) such as son of sevenless (SOS) (Boguski & McCormick, 1993). SOS preferentially interacts with the GDP bound form of RAS to activate it. Recently, a

positive feedback loop was discovered implicating SOS to also interact with the GTP bound form of RAS to further stimulate RAS activation (Mor et al., 2007). SOS was shown to interact with the growth factor receptor-bound protein-2 (GRB2) that in turn interacts with the EGF receptor and thereby connects mitogenic signalling to RAS. The RAF1 Ser/Thr kinase was the first downstream effector protein found to be activated by RAS (P. Li, Wood, Mamon, Haser, & Roberts, 1991). RAF1 signals downstream to MEK which signals to ERK1,2 ((Kyriakis et al., 1992)) eventually activating E26 transcription factors (ETS) to facilitate the entry into S-phase by an upregulation of the G1 cyclin D1 (Figure 6). There are many more effector molecules such as FOS, serum response factor (SRF), leucine zipper protein JUN, activating transcription factor 2 (ATF2) and the nuclear factor-κB (NF-κB) (Pylayeva-Gupta, Grabocka, & Bar-Sagi, 2011).

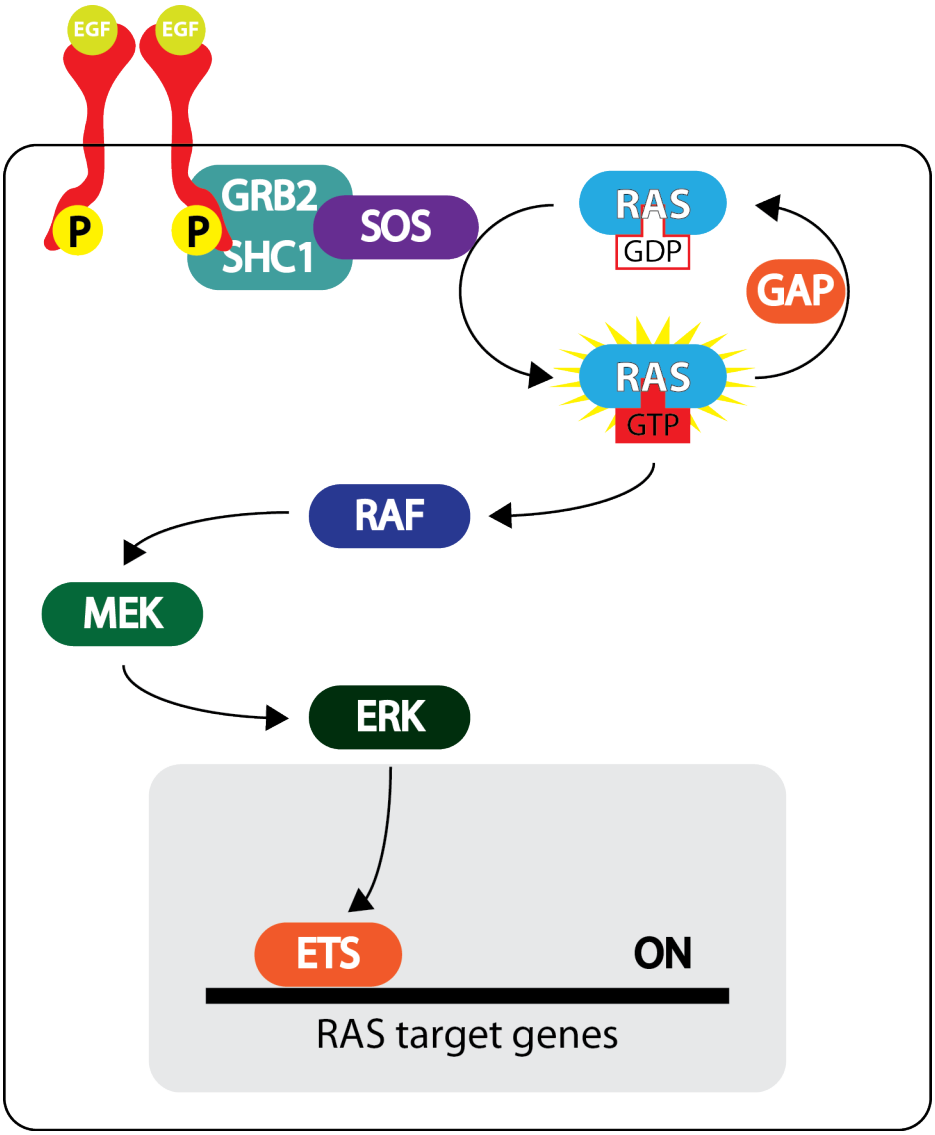

Figure 6: Schematic representation of classical EGFR/RAS/MAPK signalling. EGF molecules activate the EGF receptor (red) by receptor dimerization and subsequent auto-phosphorylation of its C-terminal kinase domains. The adaptor proteins SHC1 and GRB2 act as a docking site for the nucleotide exchange factor SOS-1 that in turn activates the small

G protein RAS via exchange of its GDP with GTP to render RAS active. The downstream target of RAS, the Ser/Thr kinase RAF further transduces the signalling to MEK and MEK signals to ERK as terminal member of the pathway. ERK translocates into the nucleus and activates RAS target gene expression that is necessary for the numerous functions of RAS like cell proliferation and survival, invasion and metastasis as well as angiogenesis.

1.5.3 RAS in Vulval Development

One of the *C. elegans* genes necessary during the development of the vulva is *let-60* with highest similarity to the human KRAS2B. A number of further ras like genes have been identified in *C. elegans*, most of them are still uncharacterized. The human and *C. elegans* RAS homologues exhibit remarkably strong sequence similarity, within which even the mutation sites are conserved. The *let-60(n1046)* gain-of-function allele replaces a G for an E at position 13 rendering it constitutively active and so does the mutated allele of human RAS. As expected from elevated RAS signalling, the vulval tissue of *let-60(n1046)* mutants display a hyperinduction phenotype.

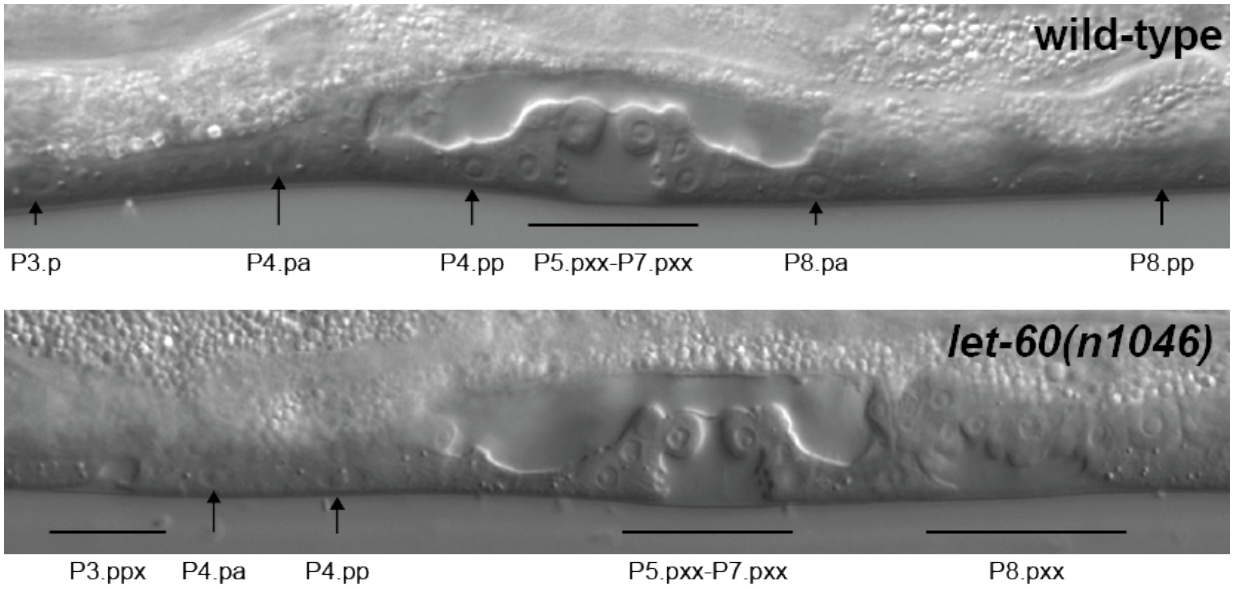

Figure 7: L4 vulva in the wild-type (top) and in *let-60(n1046)* gain-of-function mutant (bottom). In the wild-type, only P5.p-P7.p receive enough inductive signal and divide three times (black line). The *let-60(n1046)* mutant has additional cells induced, such as P8.p and part of P3.p. (black lines).

1.6 WNT Signalling

Wnt signalling is highly conserved throughout the animal kingdom. It regulates many developmental processes ranging from cell polarity over cell migration, cell proliferation and cell differentiation. Wnt ligands encode secreted glycoproteins that either function as short

range signalling molecules or as morphogens providing positional information to cells in a complex organ. Wnt signalling can be divided into canonical and non-canonical processes (Rao & Kühl, 2010).

Mutations in ß-catenin can prevent its degradation by the APC/Axin/CK1/GSK-3 ß complex. Stabilised ß-catenin constitutively activates Wnt target genes, a number of which were identified in various cancerous cell types, such as melanoma, colorectal cancer and prostate cancer (Morin, 1997), (Korinek, 1997), (Rubinfeld et al., 1997), (Chesire, Ewing, Sauvageot, Bova, & Isaacs, 2000). Masckauchán, Shawber, Funahashi, Li, & Kitajewski, 2005 further demonstrated that Wnt/beta-catenin signalling promotes cell proliferation and survival via angiogenic regulators.

Canonical Wnt signalling is best studied and relies on the action of ß-catenin. In the off state, the destruction complex consisting of the scaffold protein Axin, the tumour suppressor gene product APC and the two kinases CK1 and GSK3ß captures ß-catenin, to promote phosphorylation within its N-terminal domain and induce ubiquitination followed by proteasomal degradation of ß-catenin (Maniatis, 1999). In the on state, binding of Wnt ligands to the Wnt receptors Frizzled and LRP6 lead to the inactivation of the destruction complex via recruitment of Axin to LRP6 at the plasma membrane and through the action of Dishevelled. Stabilised ß-catenin is able to enter into the nucleus where it interacts with transcription factors of TCF/Lef1 HMG-box containing proteins to co-activate target genes (Eastman & Grosschedl, 1999).

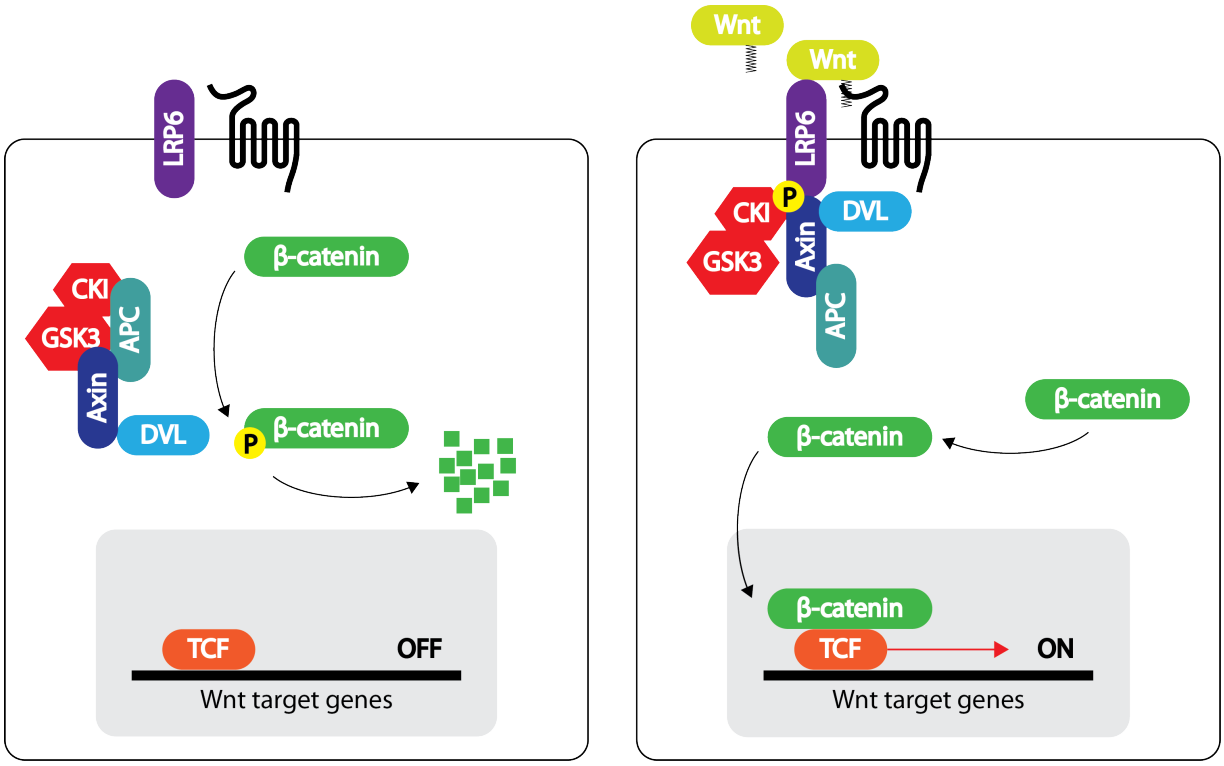

Figure 8: Canonical Wnt signalling. In the absence of a Wnt ligands ß-catenin is targeted for degradation via the destruction complex consisting of CK1, GSK3ß, APC and Axin. In the presence of a Wnt ligands, Axin is recruited to the plasma membrane and the destruction complex cannot be formed. ß-catenin is stabilised and able to transfer into the nucleus to interact with TCF/Lef transcription factors to co-activate target genes.

Non-canonical Wnt signalling regulates all ß-catenin independent processes such as planar cell polarity and Ror and Ryk dependent pathways.

1.6.1 ß-catenin as Key Mediator in Canonical Wnt Signalling Processes

C. elegans possesses four ß-catenin orthologues. These are ß-catenin-armadillo-related (BAR-1), worm-armadillo (WRM-1), humpback (HMP-2) (Eisenmann, Maloof, Simske, Kenyon, & Kim, 1998), (Korswagen, Herman, & Clevers, 2000), (Natarajan, Witwer, & Eisenmann, 2001) and symmetrical-sister-cell-hermaphrodite-gonad-defect (SYS-1) (Liu, Phillips, Amaya, Kimble, & Xu, 2008). In contrast, *Drosophila melanogaster* and vertebrates only possess one ß-catenin with dual function in cell adhesion and signalling. ß-catenin is not only able to anchor adherens junctions with the cytoskeleton by binding to tail regions of both α-catenin and cadherins but also to bind transcription factors of the TCF/Lef family to activate Wnt target gene expression (J. R. Miller & Moon, 1996), (Willert & Nusse, 1998). However, in *C. elegans* this dual function is split onto the four different ß-catenin orthologoues. BAR-1 is mainly the signalling molecule in canonical Wnt signalling, WRM-1 is involved in non-canonical Wnt signalling, HMP-2 exerts the

function as the bridge molecule in adherens junction (Costa, 1998) and SYS-1 regulates asymmetric cell division (Miskowski, Li, & Kimble, 2001).

BAR-1 is the main signalling ß-catenin involved in canonical Wnt signalling. It harbours a phosphodegron sequence that is phosphorylated in the presence of the destruction complex. It has further been found to interact with the Axin orthologues PRY-1 and AXL-1, with APR-1/APC and GSK-3/GSK3ß. Therefore, BAR-1 seems to be regulated by a similar destruction complex as seen in *Drosophila melanogaster* and vertebrates. At last, BAR-1 is able to bind the transcription factor POP-1/TCF to co-activate genes (Korswagen et al., 2000). Canonical Wnt signalling in *C. elegans* is observed during the migration of Q neuroblast progeny, during VPC fate specification, the specification of the P12 fate and the contact mediated inhibition of gene expression in posterior seam cells.

SYS-1 and WRM-1 are more divergent ß-Catenin orthologoues and control asymmetric cell division along the anteroposterior axis. During the establishment of somatic gonad asymmetry, SYS-1 is not regulated by the destruction complex, although the process seems to depend on APR-1. In addition, SYS-1 co-activates Wnt target genes together with POP-1, similar to BAR-1. WRM-1 functions as an activator of LIT-1 that eventually exports POP-1 from the nucleus and by that downregulates Wnt signalling.

HMP-2 colocalises to adherens junctions where it links α-catenin, HMP-1 and the classical cadherin HMR-1. HMP-2 neither interacts with POP-1 nor with PRY-1 highlighting its specific role in adhesion, while both BAR-1 and WRM-1 do not interact with HMR-1 and thus seem to be signalling molecules without any adhesive properties (Hardin & King, 2008).

1.6.2 Canonical Wnt Signalling During *C. elegans* Vulval Development

The competence of vulval precursor cells (VPCs) is conferred/ensured by the inhibition of early VPC fusion to the hypodermal syncytium hyp7 and is crucial for the inductive signalling from the anchor cell. The Hox gene LIN-39 maintains the competence by repressing the fusogen EFF-1 in the VPCs, whereas P1.p, P2.p, P9.p to P12.p lack lin-39 function and fuse to hyp7 during the L1 stage ({Clark:1993wm}, {Shemer:2002vq}). During the L2 stage, intercellular Wnt signalling maintains the VPC competence, possibly via BAR-1, to ensure LIN-39 expression. This finding is based on studies employing/using *bar-1* null mutants, in which the increase of fused fates could be rescued by the overexpression of *lin-39* fused to the *bar-1* promoter. However in these mutants (?), P5.p to P7.p often fail to fuse, indicating that other components might regulate *lin-39* and VPC competence (Eisenmann et al., 1998). Recent evidence suggests that LIN-3 plays a role in maintaining VPC competence by direct expression of *lin-39* in addition to its well-known

function in vulval induction (Myers & Greenwald, 2007). Still, LIN-3 mainly functions during vulval induction since loss of *lin-3* does not lead to excessive cell fusion events. Only when Wnt signalling is reduced does absence of *lin-3* lead to VPC fusion. During the L3 stage, EGFR/RAS/MAPK and Wnt signalling coordinately regulate *lin-39* expression in order to specify the vulval cell fates (Clandinin, Katz, & Sternberg, 1997), (Maloof & Kenyon, 1998), (Gleason, 2002) This might explain why P5.p to P7.p are more resistant than P3.p and P4.p to adopting a fused fate in a *bar-1* null mutant (Eisenmann & Kim, 2000).

Since the function of LIN-39 is required multiple times during vulval development, it is challenging to elucidate components affecting vulval competence or induction singularly. One might speculate that the level of LIN-39 will be key to separate those two processes and that LIN-39 maintains competence at low levels and a certain threshold is required for successful induction. However, LIN-39 is not able to promote vulval induction in the absence of inductive signalling, which implies the involvement of additional factors (Maloof & Kenyon, 1998). The role of Wnt signalling during vulval development is primarily to maintain competence of the VPCs, since its role in vulval induction is hardly understood.

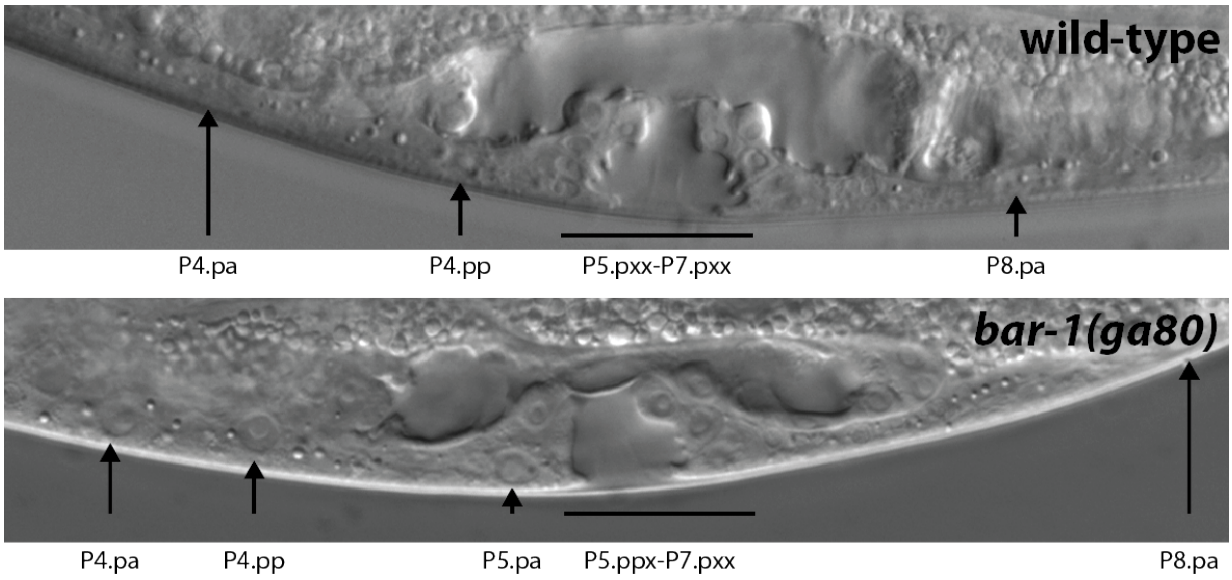

Figure 9: L4 vulva in the wild-type (top) and in *bar-1(ga80)* loss-of-function mutant (bottom). In the wild-type, P5.p-P7.p receive enough inductive signal and divide three times (black line). The *bar-1(ga80))* mutant has fewer cells induced, such as P5.pa which remains undivided.

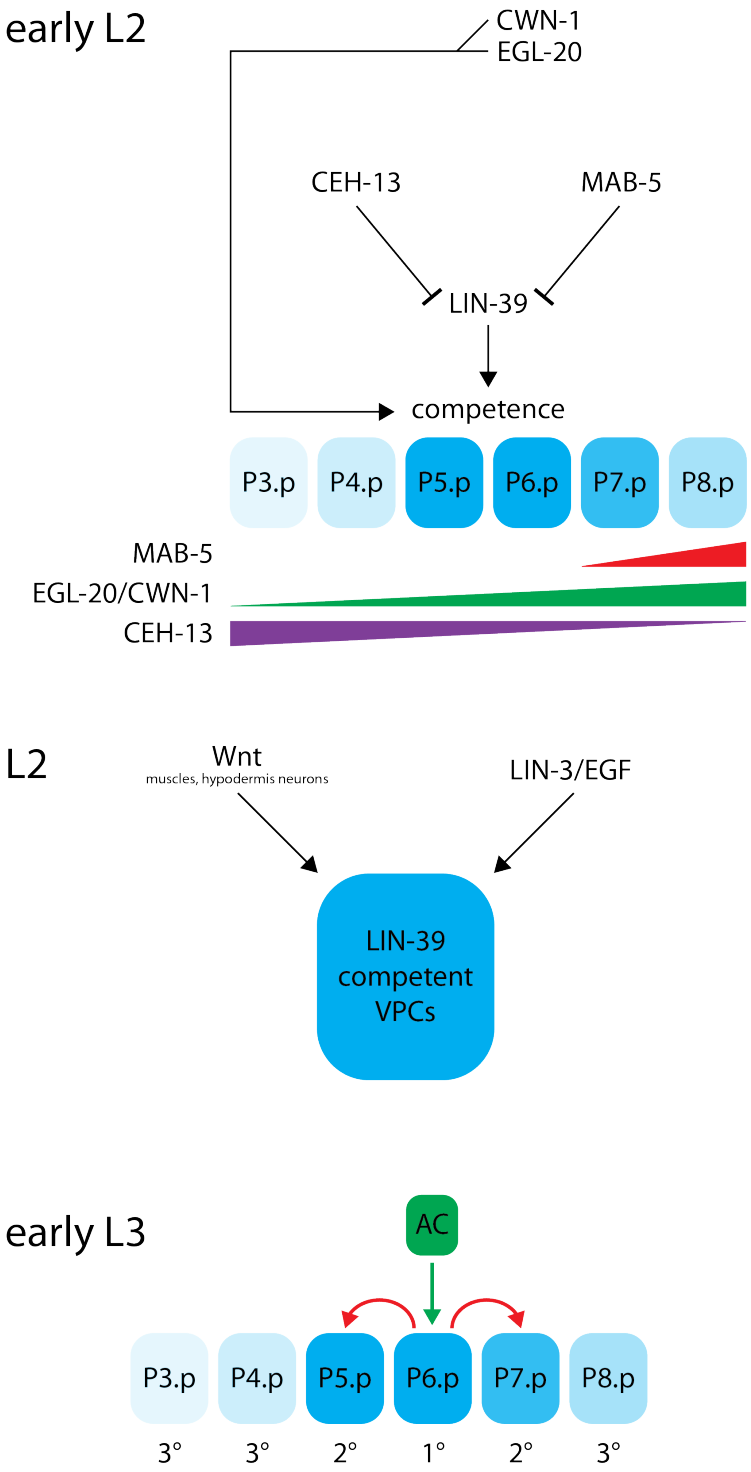

Figure 10: Wnt signalling during vulval development. During early L2 stage, the hox gene CEH-13 inhibits the competence of anterior VPCs P3.p, P4.p and P5.p via the reduction of LIN-39 levels. CWN-1 and EGL-20 triggered Wnt signalling activates the competence in anterior VPCs independent of LIN-39. In addition, EGL-20 decreases competence in posterior VPCs through the hox gene MAB-5, leaving the highest LIN-39 levels to P5.p to P7.p. There is evidence that LIN-3 together with Wnt signalling from multiple tissues maintains competence of the VPCs. In the L3 stage coordinated action of EGFR/RAS/MAPK and Wnt signalling will regulate *lin-39*. The inductive signal from the AC induces 1° cell fate in P6.p and via lateral inhibition 2° cell fate in P5.p and P7.p, the remaining cells receive too little inductive signal and eventually adopt the 3° cell fate.

Aim

In the past, extensive research focused on rare monogenetic diseases and their pathophysiology in humans. The discovery of new monogenetic diseases has reached saturation. Today, the more common complex diseases, such as cancer are the major cause of death in modern society, with almost 60% of the adult population dying. They arise from interactions between various signalling networks and the environment. It is known that the genetic background has a considerable effect on the pathogenesis of many complex diseases, but further investigation is needed to decipher the underlying genetic risk factors. Complex diseases and their multigenic characteristics have long been neglected due to their high complexity and the combination of low impact alleles with no obvious effect on the phenotype. In recent years, with the discovery of novel techniques in the field of genomics, it has become feasible to study the underlying complexity of such signalling networks. Abundant evidence suggests a tight link between the genetic background and disease susceptibility. Freemann and colleagues 2006 showed that the genotype has a profound influence on both the onset and the spectrum of tumour formation. Seitz et. al. 2006 demonstrated that tumour formation strongly depends on the genetic background found in various cancer cell lines. This is not only true for cancer signalling, it also applies to other complex diseases, where the genetic background acts as a modifier of disease signalling. The genetic factors underlying these modifiers remain to be identified.

Numerous human genome wide association studies (GWAS) have helped in predicting many new susceptibility loci associated with certain diseases. However, these GWAS are limited by the investigation of the genotype underlying a specific phenotype and therefore, the potential for personalized medicine and therapy is restricted.

The model organism *C. elegans* can help to circumvent those limitations by providing excellent tools to study natural variation in complex disease signalling. Introduced in 1974 by Sidney Brenner, *C. elegans* proved to be an excellent model to study human biology in a simple way. For many years, *C. elegans* biology has exclusively focused on one genetic background, N2 isolated from Bristol. Using N2 with induced mutations, *C. elegans* researchers were able to discover many aspects in the field of developmental biology with respect to conservation in humans. Several key signalling networks are conserved, some of which were shown misregulated during cancer formation and progression. The EGFR/RAS/MAPK, WNT and Notch pathways are prime examples and were extensively reported being involved in cancer signalling in humans. The most common mutation found in cancer genomes affects the RAS proto-oncogene and renders it constantly active; ß-catenin, the master regulator during WNT signalling is mutated in approximately 10% of all cancer types. In addition, Notch deregulation plays a role in many cancer types. Since *C. elegans* vulval development relies on the interplay of those three key

signalling pathways, the use of vulval development to model complex cancer signalling in humans is obvious. Recently, *C. elegans* research has evolved into a platform for quantitative systems genetics (Gaertner & Phillips, 2010) to allow for the identification of novel modifiers of well-established signalling network, which would be missed using classical forward or reverse genetic approaches such as mutagenesis or RNAi. The aim is to study natural genetic variation, which is essential to understand gene function in a continuously changing living system. Allelic interactions between different backgrounds often influence complex traits and are therefore crucial for investigation. To decipher the effects of naturally occurring alleles on the phenotype in a segregating wild population, it is therefore necessary to extend the genetic background in which they are studied and to not only rely on one single wild type strain. By now, there are approximately 27 different *C. elegans* wild isolates available and still more are being sequenced. However, the most divergent strain from N2 found so far is CB4856, which contains approximately one single nucleotide polymorphism per 800 bps (Vergara et al., 2014). This amount of variability is small compared to *Drosophila* or higher model organisms and stems from the hermaphroditic mode of reproduction; therefore not much change is to be expected.

Natural, quantitative genetic variation in complex cancer signalling can be studied during *C. elegans* vulval development. Therefore an adapted set of recombinant inbred lines (RILs) was established to uncover such variation in EGFR/RAS/MAPK signalling during vulval development.

Natural Variation in Signalling Networks

To investigate natural genetic variation during vulval development, we crossed different mutants, available in the N2 Bristol reference background with CB4856 Hawaii (and others); eventually establishing mutation included recombinant inbred lines (miRILs). In a first pre-screen we focused on mutants affecting genes in the RTK/RAS/MAPK (light blue), the Notch (not shown) and the Wnt (light green) pathway, the three key signalling networks involved during the development of the hermaphrodite vulva. All the candidates screened are summarized in Table 1. To detect most phenotypic variation we selected the miRILs from F2 generation on for strong phenotypic deviations from the mutant in the N2 background. With this approach we were able to preselect possible sensitized backgrounds where we would expect most of the variation in regard to the phenotype vulva malformations. The major disadvantage of this method is the low mapping resolution, since we select for specific genotype combinations and are therefore limited for further quantitative trait identification. We screened for cryptic variation in *CB4856* (Hawaii), *CB4858* (Pasadena) and *AB1* (Adelaide) wild isolates.

Natural variation was observed for the RTK/RAS/MAPK and the Wnt pathway (Table 1); no change could be detected for mutants affecting Notch signalling (not shown). Therefore we further concentrated our attention on those two pathways, taking the most promising candidate miRILs, the *let-60(n1046)* and the *bar-1(ga80)* sets. For better mapping resolution of quantitative traits we enlarged the two miRIL sets by establishing additional lines. Eventually we established 228 miRILs for the *let-60(n1046)* and 79 miRILs for the *bar-1(ga80)* sensitized background. In order to map quantitative traits in those two MIRIL sets, we assessed both genotype and phenotype of each individual line. As for phenotypic analysis, we chose vulval induction counting as readout for pathway activity (*let-60(n1046)* and *bar-1(ga80)*) and gonad migration for quantitative changes in gradient and guidance cues (*bar-1(ga80)* only). In general, the number of induced vulval precursor is positively correlated to the activity of either RTK/RAS/MAPK or Wnt signaling, meaning the more cells that were induced, the higher the pathway activity (Sternberg & Horvitz, 1986). Since the *bar-1(ga80)* MIRILs also showed variation in gonad migration, we were also assessing this as additional phenotype. For genotypic analysis we used 72 fragment length polymorphisms (FLPs) equally spanning all the six chromosomes to asses either N2 or CB4856 genotype (Zipperlen et al., 2005).

Allele	Wild isolate			Phenotype	
	CB4856	CB4858	AB1	vulva	other
let-23(sy1)	6	7	5	weak suppression	
let-60(n1046)	43	0	0	strong enhancement	swollen, lethals
gap-1(ga133)	2	6	6	unchanged	muscle degradation
mpk-1(ga111)	lost	lost	lost	unchanged	sterility suppressed
hs::mpk-1	3	4	3	weak enhancement	tail defect enhanced
lin-2(n397)	4	4	4	weak suppression	
bar-1(ga80)	38	0	30	strong enhancement	lethality increased

Table 1: Initial pre-screen in *CB4856*, *CB4858* and *AB1* revealed putative modifier backgrounds used for further analysis. Light blue boxes indicate signalling components of EGR/RAS/MAPK pathway, light green boxes components of WNT signalling.

1.7 Natural Variation in Signalling Networks: EGFR/RAS/MAPK Signalling

The 228 *let-60(n1046)* miRILs displayed small linkage disequilibria. As expected, there is a low recombination frequency at the position of the included mutation (Figure 11, Chromosome IV). In addition there is hardly any recombination observed on the left side of Chromosome I (Figure 11, Chromosome I). In agreement with (Hannah S Seidel, 2008) there is a naturally occurring genome incompatibility between N2 and CB4856. Otherwise recombination frequencies spanning the chromosomes seem equal with expected lower recombination towards the telomere regions.

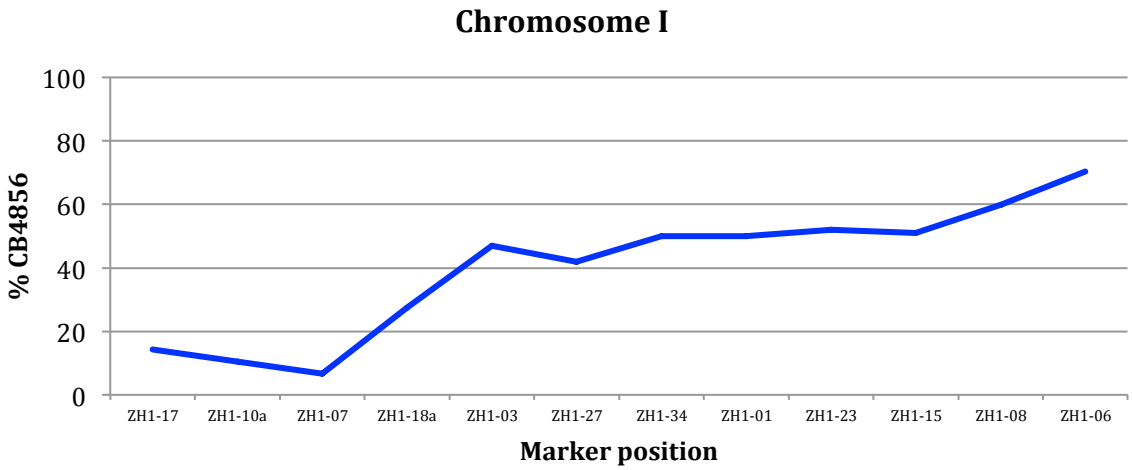
Chromosome I
100
80
60
40
20
0
% CB4856
ZH1-17
ZH1-10a
ZH1-07
ZH1-18a
ZH1-03
ZH1-27
ZH1-34
ZH1-01
ZH1-23
ZH1-15
ZH1-08
ZH1-06
Marker position

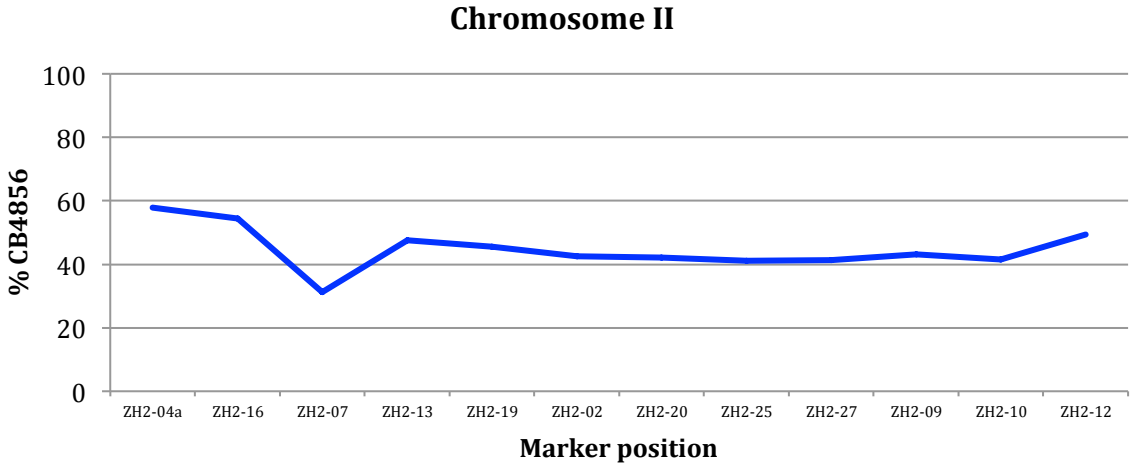
Chromosome II
100
80
60
40
20
0
% CB4856
ZH2-04a
ZH2-16
ZH2-07
ZH2-13
ZH2-19
ZH2-02
ZH2-20
ZH2-25
ZH2-27
ZH2-09
ZH2-10
ZH2-12
Marker position

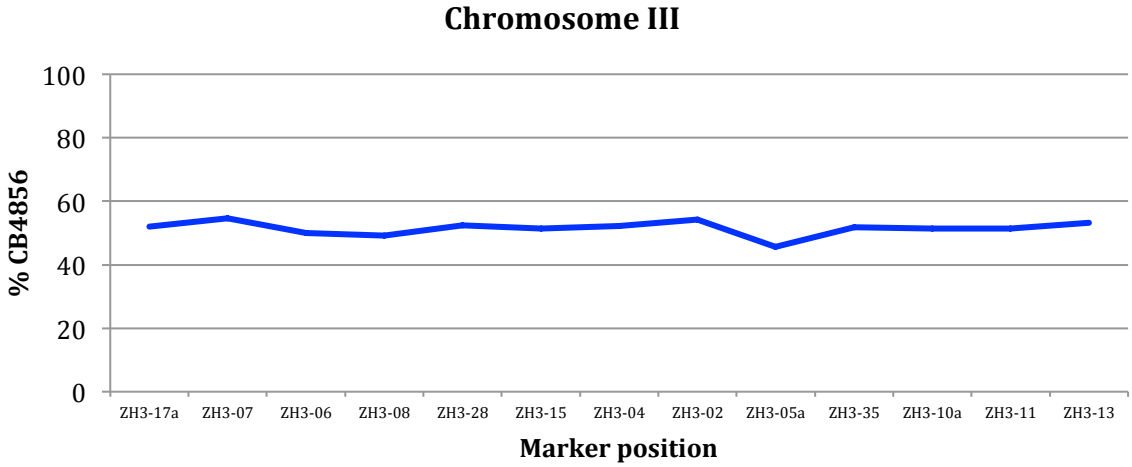
Chromosome III
100
80
60
40
20
0
% CB4856
ZH3-17a
ZH3-07
ZH3-06
ZH3-08
ZH3-28
ZH3-15
ZH3-04
ZH3-02
ZH3-05a
ZH3-35
ZH3-10a
ZH3-11
ZH3-13
Marker position

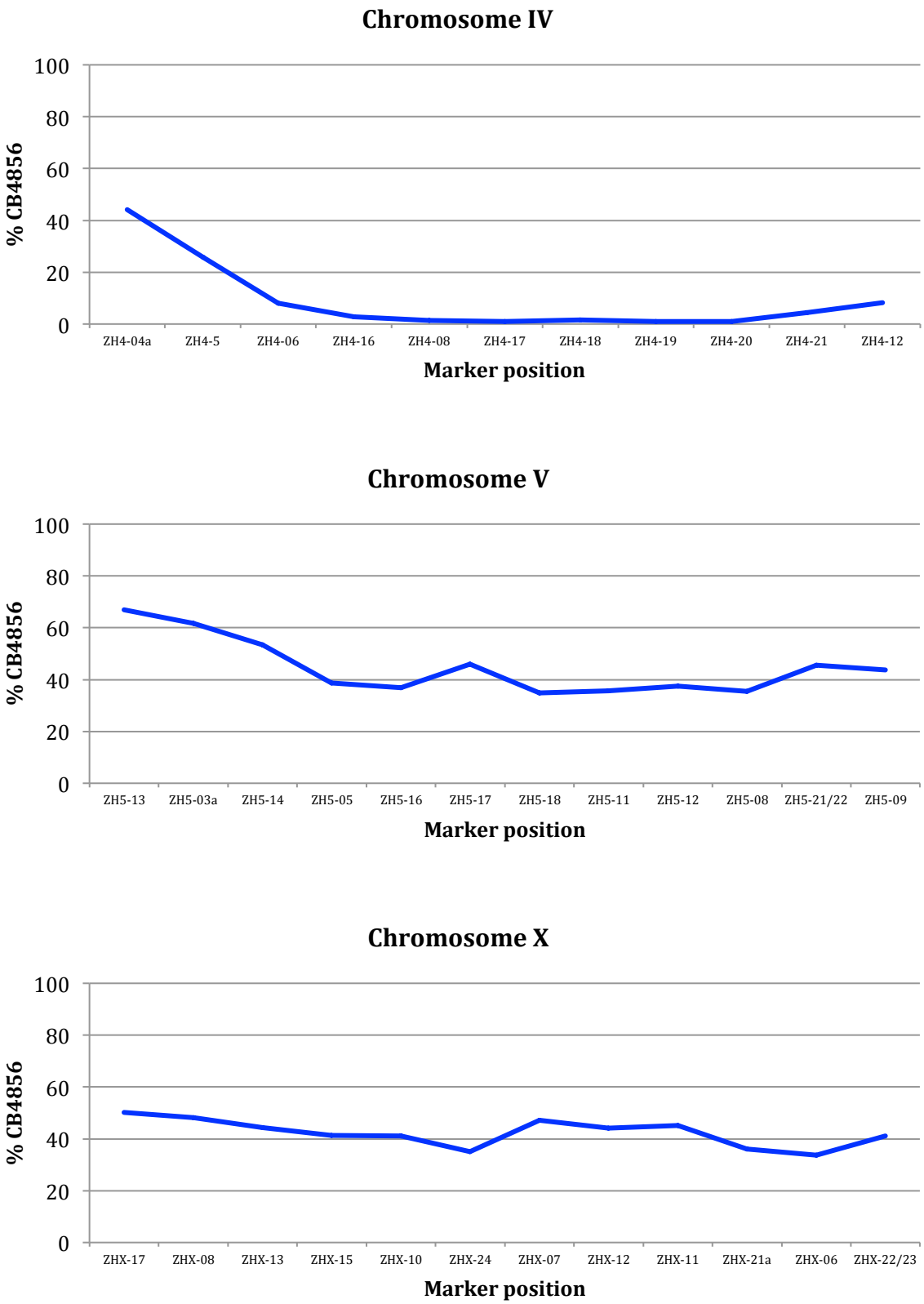

Figure 11: Genotype summary of the *let-60(n1046)* miRILs. Plotted as blue line is marker positions vs. % of CB4856 genome at that position.

1.7.1 Natural Variation in *let-60(n1046)* MIRILs: Vulval Induction Index

Vulval induction counting was used as the method to determine EGFR/RAS/MAPK pathway activity during *C. elegans* vulval development ((Sternberg & Horvitz, 1986)). In Table 2, increasing vulval induction index is shown for every miRIL; its broad phenotypic range from 3.0 – 5.7 indicates the presence of several genomic loci involved in the modification of the phenotype. There is no vulval induction recorded smaller than 3, possibly due to buffering and robustness of vulval development in this sensitized background. Therefore further QTL mapping can help to localise and identify those modifier regions.

MIRIL	#	VI	STDEV	s.e.m.
97	20	3.00	0.00	0.00
101	21	3.00	0.00	0.00
167	20	3.00	0.00	0.00
183	20	3.00	0.00	0.00
196	20	3.00	0.00	0.00
208	20	3.00	0.00	0.00
176	20	3.03	0.11	0.03
149	25	3.04	0.20	0.04
141	23	3.07	0.23	0.05
84	20	3.08	0.18	0.04
140	20	3.08	0.24	0.05
205	20	3.10	0.26	0.06
171	21	3.12	0.22	0.05
124	20	3.13	0.32	0.07
146	20	3.13	0.22	0.05
105	22	3.14	0.32	0.07
202	22	3.14	0.35	0.07
194	20	3.15	0.49	0.11
225	22	3.16	0.36	0.08
224	23	3.20	0.36	0.08
69	20	3.20	0.50	0.11
92	22	3.23	0.59	0.13
88	21	3.31	0.37	0.08
61	20	3.33	0.63	0.14
94	20	3.33	0.54	0.12
187	20	3.33	0.54	0.12
43	26	3.35	0.56	0.11
115	20	3.35	0.49	0.11
134	20	3.35	0.40	0.09
198	20	3.35	0.59	0.13
216	20	3.35	0.61	0.14
219	20	3.38	0.48	0.11
109	21	3.38	0.38	0.08

MIRIL	#	VI	STDEV	s.e.m.
51	22	3.39	0.51	0.11
67	20	3.40	0.62	0.14
90	20	3.40	0.60	0.13
209	21	3.40	0.52	0.11
31	50	3.41	0.64	0.09
79	21	3.43	0.64	0.14
182	21	3.43	0.64	0.14
104	42	3.44	0.58	0.09
91	22	3.45	0.63	0.14
186	21	3.48	0.62	0.14
111	22	3.48	0.59	0.13
174	24	3.50	0.53	0.11
207	21	3.50	0.69	0.15
132	25	3.52	0.55	0.11
204	21	3.52	0.70	0.15
150	20	3.53	0.68	0.15
218	20	3.53	0.70	0.16
188	23	3.54	0.64	0.13
157	20	3.55	0.74	0.17
118	24	3.56	0.60	0.12
114	21	3.57	0.62	0.13
96	26	3.58	0.87	0.17
108	20	3.60	0.68	0.15
139	20	3.60	0.62	0.14
N2	100	3.60	0.59	0.06
210	21	3.62	0.65	0.14
131	20	3.63	0.70	0.16
161	21	3.64	0.65	0.14
192	21	3.64	0.59	0.13
200	22	3.68	0.59	0.13
197	21	3.69	0.60	0.13
21	24	3.71	0.91	0.19
166	21	3.71	0.68	0.15
15	43	3.72	0.80	0.12
37	52	3.75	0.92	0.13
107	20	3.75	0.66	0.15
221	23	3.76	0.69	0.14
53	21	3.76	0.85	0.18
199	20	3.78	0.68	0.15
35	21	3.79	0.87	0.19
70	21	3.79	0.90	0.20
10	43	3.79	0.85	0.13
2	44	3.81	0.91	0.14
163	22	3.82	0.66	0.14
129	20	3.83	0.71	0.16
11	34	3.84	0.84	0.14
55	22	3.84	0.66	0.14

MIRIL	#	VI	STDEV	s.e.m.
130	22	3.84	0.70	0.15
162	22	3.86	0.74	0.16
160	20	3.88	0.76	0.17
190	27	3.94	0.64	0.12
68	20	3.98	0.77	0.17
116	20	3.98	0.77	0.17
137	20	3.98	0.75	0.17
211	20	3.98	0.62	0.14
168	24	3.98	0.74	0.15
106	21	4.00	0.71	0.15
112	21	4.00	0.69	0.15
144	22	4.02	0.72	0.15
87	20	4.05	0.69	0.15
164	21	4.07	1.04	0.23
122	22	4.09	0.67	0.14
7	53	4.12	0.90	0.12
6	48	4.13	0.81	0.12
222	22	4.14	0.71	0.15
14	42	4.15	0.89	0.14
26	20	4.18	0.67	0.15
80	20	4.18	1.00	0.22
102	21	4.19	0.87	0.19
195	20	4.23	0.97	0.22
128	22	4.23	0.88	0.19
8	39	4.23	0.85	0.14
3	58	4.23	0.86	0.11
65	21	4.24	0.80	0.17
136	23	4.24	0.85	0.18
62	22	4.25	0.92	0.20
180	22	4.27	0.80	0.17
39	20	4.28	0.66	0.15
191	21	4.29	0.89	0.19
20	45	4.29	1.01	0.15
142	20	4.30	1.01	0.22
152	20	4.30	0.82	0.18
185	20	4.30	0.88	0.20
4	48	4.32	0.93	0.13
19	54	4.32	0.85	0.12
148	20	4.35	0.89	0.20
89	21	4.36	0.92	0.20
5	44	4.36	0.90	0.14
34	49	4.37	0.80	0.11
213	30	4.40	0.72	0.13
220	20	4.43	0.80	0.18
27	21	4.43	0.99	0.22
66	21	4.43	0.93	0.20
113	21	4.43	1.03	0.22

MIRIL	#	VI	STDEV	s.e.m.
9	53	4.45	0.83	0.11
119	23	4.46	0.96	0.20
78	20	4.48	1.12	0.25
123	20	4.48	0.66	0.15
81	22	4.50	0.95	0.20
175	20	4.50	1.00	0.22
12	49	4.51	0.90	0.13
155	23	4.52	0.80	0.17
93	20	4.53	0.85	0.19
59	21	4.55	0.86	0.19
1	43	4.56	0.93	0.14
41	25	4.56	0.88	0.18
151	21	4.57	0.60	0.13
127	20	4.58	0.80	0.18
32	22	4.59	0.87	0.19
47	22	4.59	0.83	0.18
49	20	4.60	0.85	0.19
103	20	4.60	0.93	0.21
156	23	4.61	0.77	0.16
203	22	4.61	0.75	0.16
147	21	4.62	0.74	0.16
36	20	4.63	0.63	0.14
121	20	4.63	0.84	0.19
46	23	4.63	1.08	0.22
126	26	4.63	0.76	0.15
228	21	4.64	0.84	0.18
135	21	4.67	0.75	0.16
227	25	4.68	0.93	0.19
120	20	4.70	0.83	0.19
143	20	4.70	0.97	0.22
33	62	4.71	0.86	0.11
73	21	4.71	0.89	0.19
75	21	4.71	0.82	0.18
100	22	4.75	0.74	0.16
85	22	4.77	0.75	0.16
98	22	4.77	0.81	0.17
13	51	4.77	0.92	0.13
74	20	4.78	0.68	0.15
184	20	4.78	0.72	0.16
56	23	4.78	0.86	0.18
57	23	4.78	0.69	0.14
214	20	4.80	0.66	0.15
217	23	4.83	0.83	0.17
52	22	4.84	0.85	0.18
189	22	4.84	0.86	0.18
193	22	4.84	0.70	0.15
170	20	4.85	0.78	0.17

MIRIL	#	VI	STDEV	s.e.m.
173	20	4.85	0.61	0.14
99	21	4.86	0.59	0.13
48	24	4.88	0.82	0.17
83	21	4.88	0.85	0.19
42	27	4.91	0.83	0.16
28	65	4.91	0.86	0.11
18	66	4.95	0.83	0.10
82	23	4.96	0.93	0.19
133	21	4.98	0.78	0.17
169	21	4.98	0.54	0.12
181	21	4.98	0.66	0.14
226	24	4.98	0.88	0.18
16	38	4.99	0.78	0.13
76	21	5.00	0.42	0.09
125	20	5.00	0.92	0.21
158	22	5.00	0.76	0.16
23	57	5.01	0.76	0.10
77	22	5.05	0.92	0.20
24	51	5.07	0.86	0.12
17	76	5.08	0.82	0.09
64	23	5.09	0.67	0.14
63	20	5.10	0.68	0.15
54	24	5.10	0.74	0.15
29	58	5.16	0.87	0.11
30	37	5.16	0.59	0.10
215	24	5.19	0.64	0.13
86	30	5.20	0.76	0.14
206	21	5.24	0.68	0.15
44	16	5.25	0.68	0.17
22	71	5.26	0.68	0.08
223	21	5.26	0.75	0.16
178	23	5.28	0.67	0.14
117	23	5.30	0.47	0.10
71	44	5.33	0.75	0.11
154	22	5.34	0.54	0.12
153	23	5.35	0.46	0.10
177	24	5.35	0.48	0.10
58	21	5.36	0.62	0.13
38	41	5.41	0.58	0.09
72	24	5.42	0.55	0.11
165	25	5.42	0.55	0.11
212	25	5.42	0.55	0.11
145	29	5.43	0.65	0.12
179	22	5.43	0.62	0.13
138	21	5.45	0.71	0.15
110	20	5.48	0.60	0.13
40	43	5.48	0.60	0.09

MIRIL	#	VI	STDEV	s.e.m.
25	55	5.56	0.53	0.07
201	30	5.62	0.45	0.08
172	24	5.63	0.68	0.14
95	45	5.63	0.49	0.07
45	22	5.64	0.52	0.11
60	23	5.70	0.39	0.08
50	20	5.70	0.34	0.08
159	27	5.70	0.37	0.07

Table 2: *let-60(n1046)* miRIL phenotype. Lines are sorted with increasing vulval induction index.

1.7.2 QTL Mapping to Determine Modifier Regions

(This section is based and adapted from the report of L. Basten Snoek from 2011)

Some prior adjustments to the miRIL set are needed before QTL mapping can deliver reliable results. This set was scanned for certain abnormalities listed below.

1. miRILs that are completely N2; no recombination
2. Identical miRILs; leads to unequal distribution of alleles and genotypes
3. Some lines are less well genotyped or markers are switched
4. miRILs without the *n1046* allele

The following table depicts MIRILs falling in one of those four classes.

Class	miRILs	Remarks
1	79, 88, 116, 125, 152, 204	almost completely N2
2	2, 3, 4, 5, 25, 26, 27 6, 7, 41, 42 8, 9, 36, 37 11, 31, 12, 32, 13, 33 14, 19, 34, 15, 21, 35 16, 17, 18, 22, 23, 24, 28, 29, 30, 38, 39, 40 53, 69, 56, 57, 58, 59, 62, 65, 75, 76, 81, 83 161, 162, 175, 181 176, 182, 189, 177, 183 178, 184, 179, 185, 180, 186	almost identical
3	195	genotype error
4	97, 196	no *n1046* allele

Table 3: Excluded miRILs from QTL analysis.

In all those cases, miRILs were excluded in the QTL mapping

QTL mapping identified four loci that affect vulval induction in the miRILs. One QTL was identified at the far end of Chromosome I, two linked QTLs with opposing effects were mapped to the middle of Chromosome II and a fourth QTL was identified in the middle of Chromosome V (Figure 12). In addition, the effect size for each QTL on the VI was determined. QTL 1 and 2 rely on the CB4856 allele, with an effect size of 0.52 and 0.55 respectively. The effects of QTL 3 and 4 are influenced through the N2 allele with strength of 1.1 and 0.42 (Table 4). In total, this leads to an increase in vulval induction of 2.58 above a wild type value of 3, therefore to a highest VI of 5.58. This QTL model explains 40% of the variation in VI between the miRILs

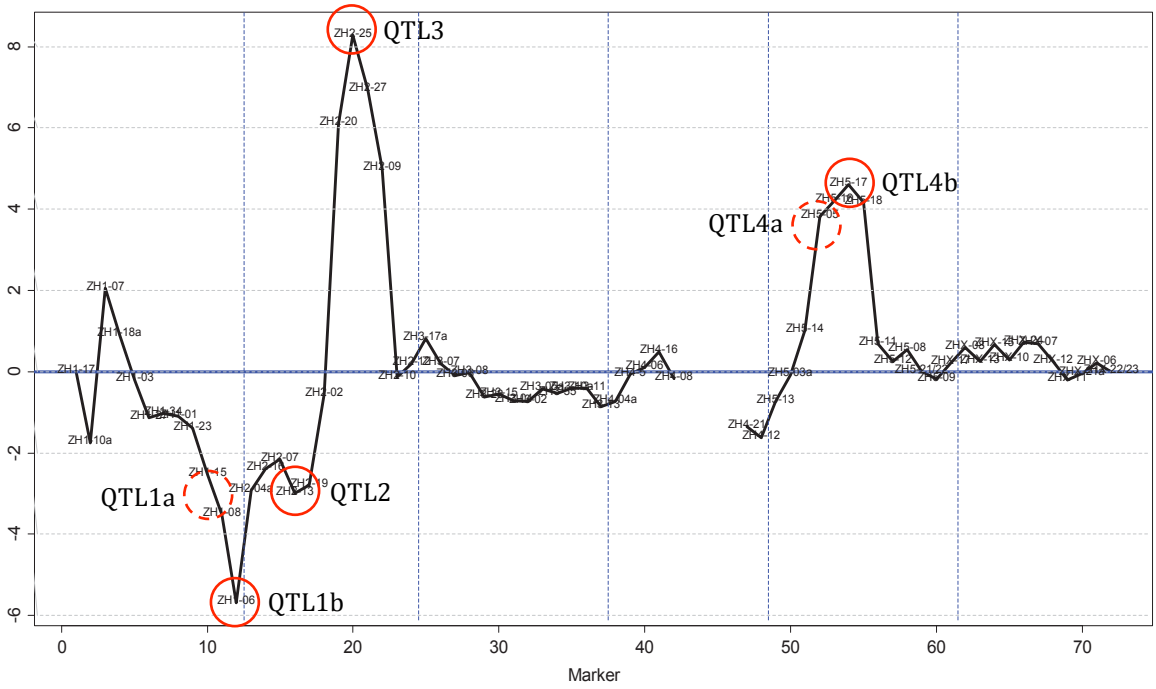

Figure 12: QTL mapping predicted 4 genomic regions affecting vulval induction in the miRILs. QTL peaks are indicated with red circles. In addition, two more unpredicted QTLs were experimentally identified (dashes red circles). Fragment length polymorphism markers are indicated on the x-axis and LOD*significance effect on the y-axis.

QTL 1	CB4856 allele increases VI by 0.52
QTL 2	CB4856 allele increases VI by 0.55
QTL 3	CB4856 allele decreases VI by 1.1
QTL 4	CB4856 allele decreases VI by0.42

Table 4: Quantitative trait effect size prediction. Depicted are the effect sizes for the Hawaiian alleles; the opposite would be true for the Bristol alleles.

1.7.2.1 Verification of QTL Regions: Introgression Lines

We evaluated the existence of each QTL region using corresponding introgression lines from (Doroszuk, Snoek, Fradin, Riksen, & Kammenga, 2009) (Figure 14). We crossed the *let-60(n1046)* Bristol mutant with introgression lines ewIR2, 5, 7, 9, 10, 11, 17 for Chromosome 1 (Figure 15), ewIR21, 23, 26 for Chromosome II (Figure 16) and ewIR66, 67, 68 for Chromosome V (Figure 19).

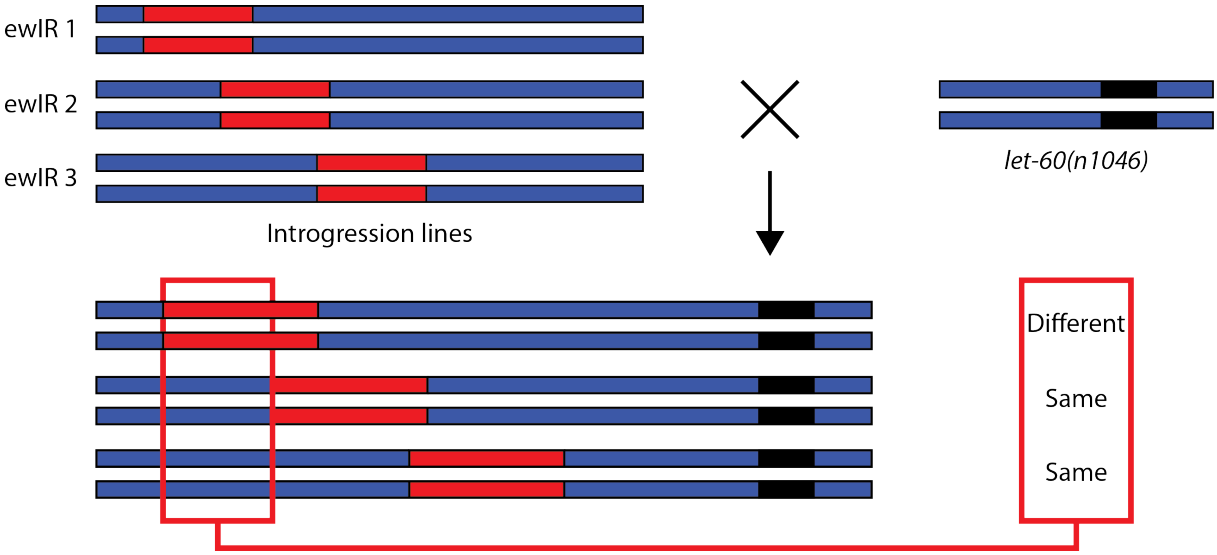

Figure 13: Introgression lines principle. Depicted is the situation for any chromosome. Different corresponding and preferentially overlapping introgression lines are crossed with the *let-60(n1046)* Bristol mutant.

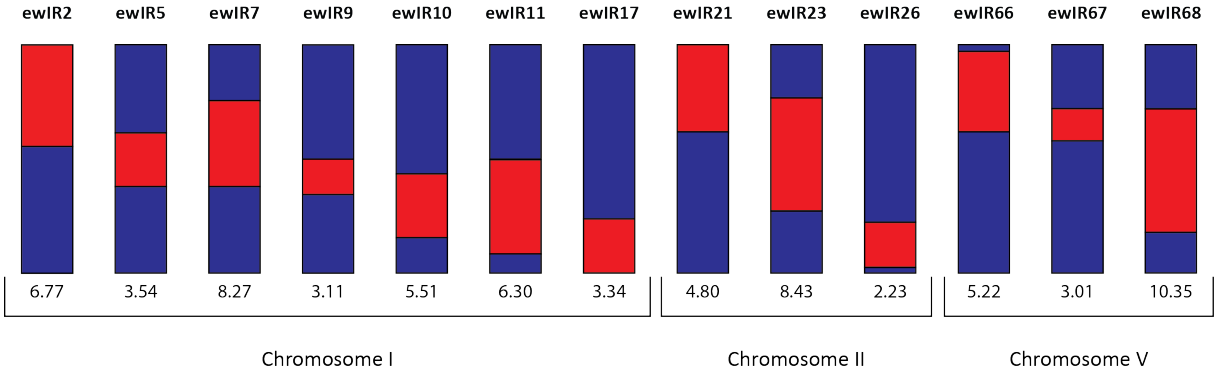

Figure 14: Introgression lines used in this study. Depicted is the location of the CB4856 introgression (red) surrounded by the N2 background (blue) for each ewIR.. line. Corresponding introgression sizes are indicated below.

We analysed lines homozygous for the introgression and the *let-60(n1046)* allele vs. lines that contain the mutation only. Introgression line crosses for chromosome I verified the previously identified QTL1b region to be between ewIR10 and ewIR17, a genomic interval of approximately 0.6 Mb. The QTL model predicts the CB4856 allele to increase the VI by 0.52 (see Report *let-60* from L. Basten Snoek), which is in good agreement with the experimentally verified data of approximately 0.55 in VI. In addition the region between ewIR5 and ewIR7 harbours another QTL named QTL1a with the size of approximately 1.2 Mb and a CB4856 allele QTL effect of approximately +0.61 in VI (Figure 15).

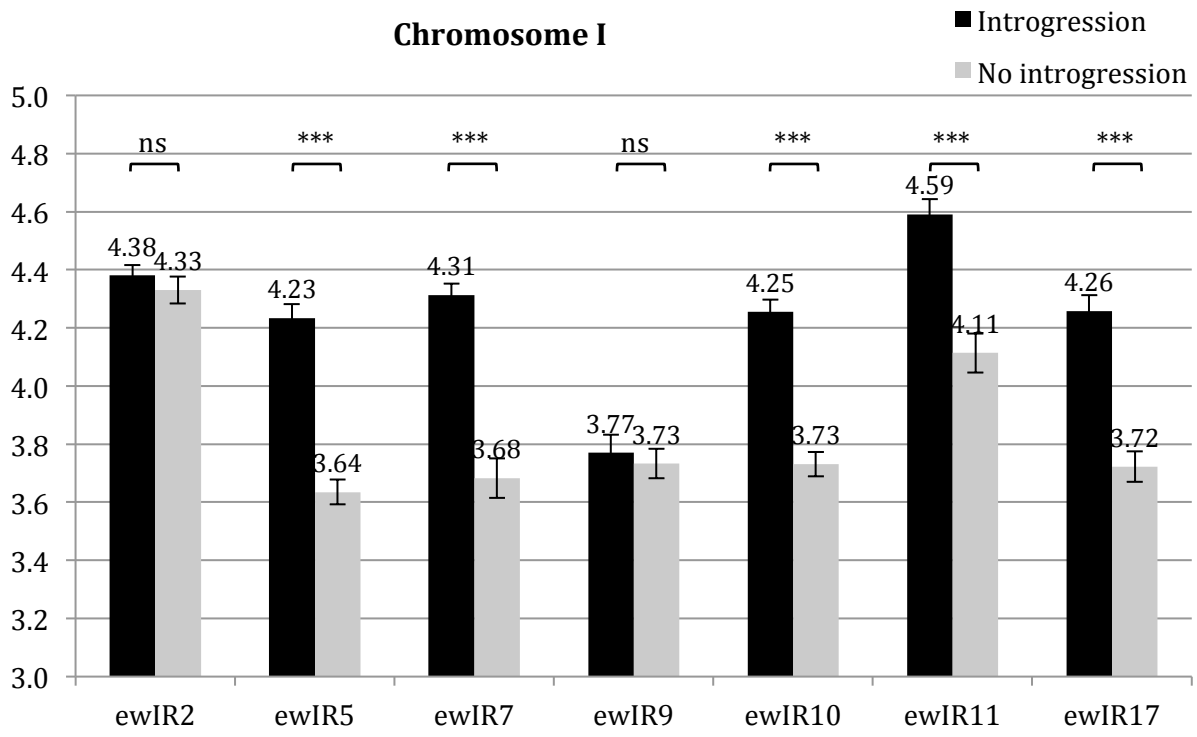

Figure 15: Introgression line crosses for chromosome I. All depicted lines carry the *n1046* allele and either the introgression (black bars) or no introgression (grey bars). Differences within an introgression line indicate the QTL region to be located there. Error bars = SE, Mann-Whitney-U test, * p<0.05, ** p<0.01, *** p<0.001

The QTLs two and three are located on chromosome II and are tightly linked. There are no introgression lines available to separate these two regions. It is therefore only possible to test them as one large QTL. As seen in Table 4, the predicted theoretical effect of this combined QTL on VI is -0.55 for the Hawaiian allele. Experimentally we could estimate a change in induction of -0.33, which is slightly higher than what was expected. Nevertheless, we could demonstrate that ewIR23 genomic region harbours the modifiers, since neither ewIR21 nor ewIR26 genomic region had any effect on vulval induction (Figure 16).

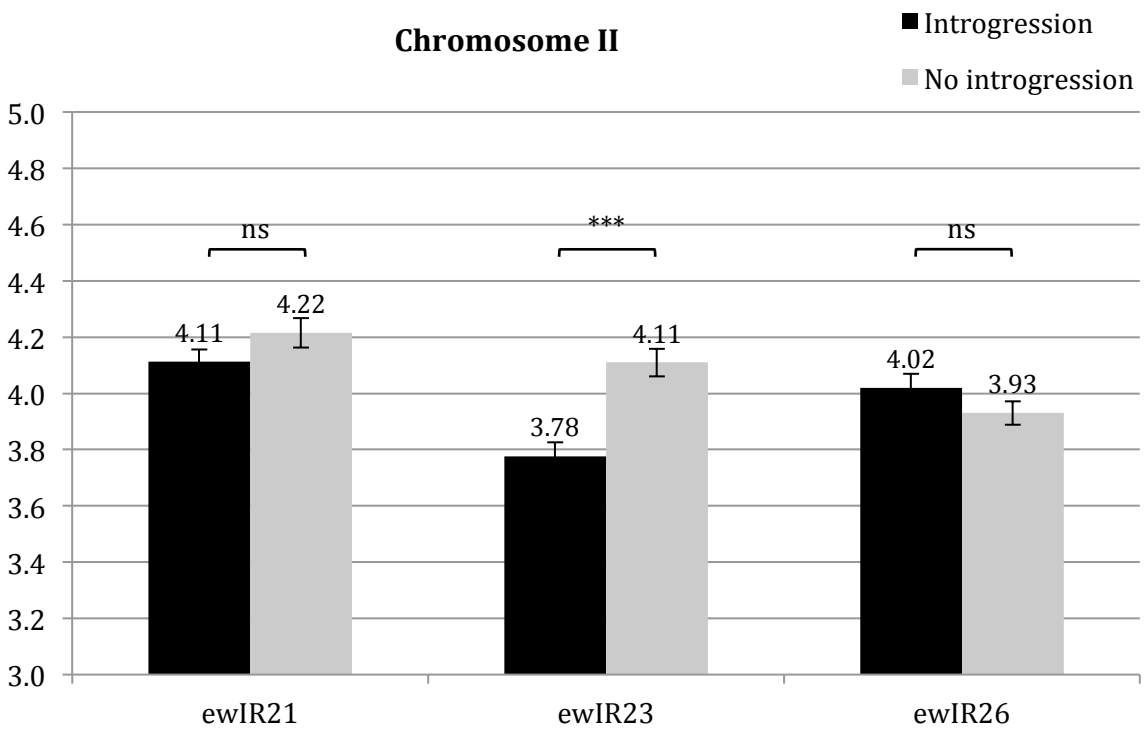

Figure 16: Introgression line crosses for chromosome II. All depicted lines carry the *n1046* allele and either the introgression (black bars) or no introgression (grey bars). Differences within an introgression line indicate the QTL region to be located there. Error bars = SE, Mann-Whitney-U test, * p<0.05, ** p<0.01, *** p<0.001

QTL 4 lies on chromosome V and the CB4856 allele is predicted to lower the VI by 0.42. We used ewIR66, 67 and 68 to verify and narrow the region. This approach was unsuccessful (Figure 18). We speculated that vulval induction in the *let-60(n1046)* mutant is robust against lows and highs, therefore one can never achieve a VI of 6 nor of 3. In addition the effect of QTL4 is predicted to depend on the presence of CB4856 at QTL1b position. The presence of CB4856 on chromosome 5 only slightly decreases VI (Figure 17, green vs. yellow). The additional presence of CB4856 on chromosome 1, together with CB4856 on chromosome 5 more strongly inhibits VI (Figure 17, purple vs red). Therefore, in a second attempt we sensitized the *let-60(n1046)* using ewIR17 to artificially raise VI to 4.26. This should allow for more variability in phenotype and indeed using this approach we were able to detect QTL4. To our surprise, QTL 4 was further divided into two sub-QTL (QTL4a and b) separated by the ewIR67 introgression (Figure 19). Additionally, we noted that QTL 4 indeed synthetically interacts with QTL 1b, since the presence of either ewI67 or 68 alone does not affect vulval induction in the *let-60(n1046)* mutant (Figure 19, red vs. blue bars). For unknown reason, there is some discrepancy in the ewIR17;66 no introgression lines (Figure 19, first column blue bar). Theoretically those lines should be similar to *the let-60(n1046)* single mutant or to ewIR17;67 and -;68 no introgression lines (residual blue bars). Nevertheless, we could identify the QTL4a and b effects to be -0.68 and -0.41 respectively.

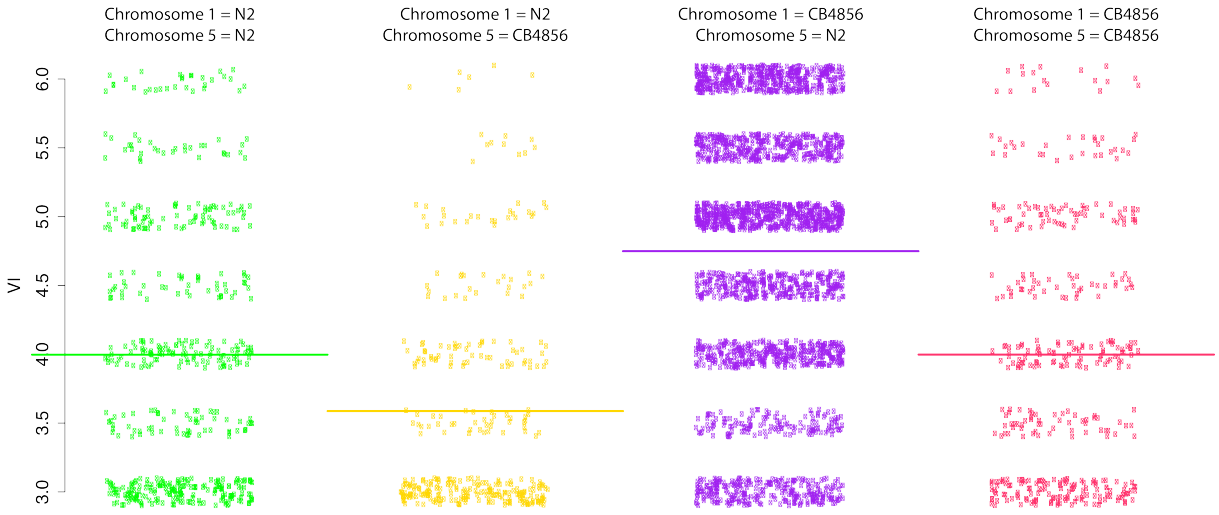

Figure 17: Synergistic effect of QTLs 1 and 5. All data is plotted and average vulval induction is shown as coloured line. Indicated on top are the different combinatorial cases.

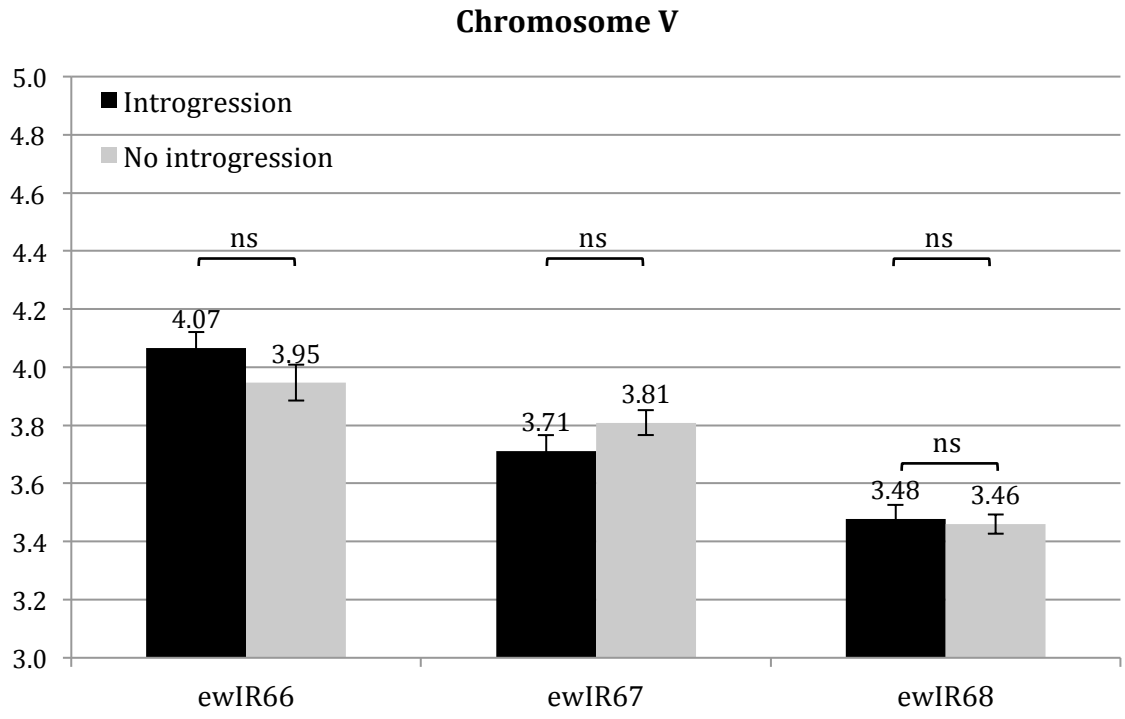

Figure 18: Introgression line crosses for chromosome V. All depicted lines carry the *n1046* allele and either the introgression (black bars) or no introgression (grey bars). No QTL could be detected. Error bars = SE, Mann-Whitney-U test

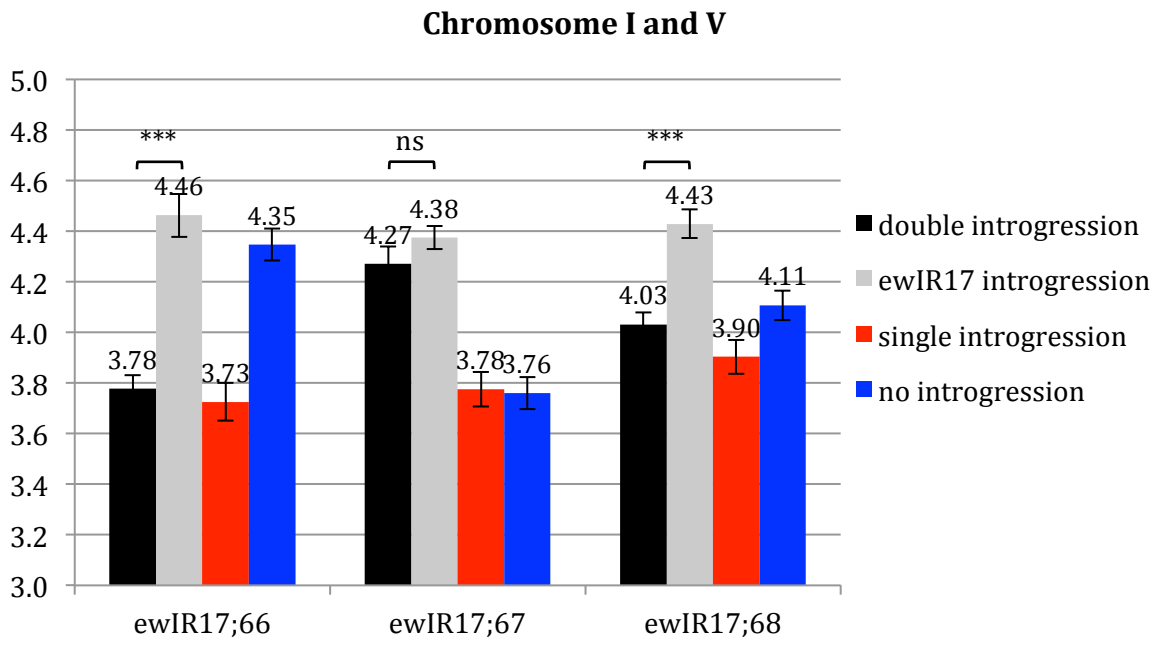

Figure 19: Introgression line crosses for chromosomes I and V. All depicted lines carry the *n1046* allele and either both introgressions (black bars), only one introgression (grey bar for ewIR17 and red bar for either ewIR66, 67 or 68) or no introgression (blue bar). Two sub-QTLs could be detected on ewIR66 and ewIR68 region, only separated by ewIR67 introgression. Error bars =SE, Mann-Whitney-U test, * p<0.05, ** p<0.01, *** p<0.001

In summary, we could demonstrate the reliability of the QTL mapping algorithm by verification of all the four genomic regions. In addition we fine mapped QTL regions to smaller genomic intervals, to facilitate follow up analysis. Surprisingly we identified two more QTLs (QTL1a and QTL5a), which were not detected by the mapping algorithm. We chose QTL 1b for further investigation due to the fact of a perfect overlap with QTL1 in the *bar-1(ga80)* MIRIL set (Figure 44).

1.7.3 expression QTLs (eQTLs) Overlap with QTLs for Vulval Induction

(The results from this section were carried out in collaboration with the group of Jan Kammenga, Wageningen University, The Netherlands)

We investigated a subset of 36 MIRILs for eQTL analysis, in which the transcript of every single gene is taken as phenotypic measurement and compared with the genotype (Figure 20). Whole worm RNA was extracted and analysed on microarrays. We can expect two possible eQTL cases: cis eQTLs are regions on the genome that affect the transcription of their own mRNA, e.g. regulatory sequences such as variations in promoter or 3'UTR regions. In addition, there are trans eQTL in which a specific region affects many targets, e.g. variation in transcription factors that will eventually lead to a change in expression for many genes. If we plot marker position on

the y-axis and eQTL position on the x-axis, then cis eQTL are visible in the diagonal and trans eQTL manifest as vertical trans bands.

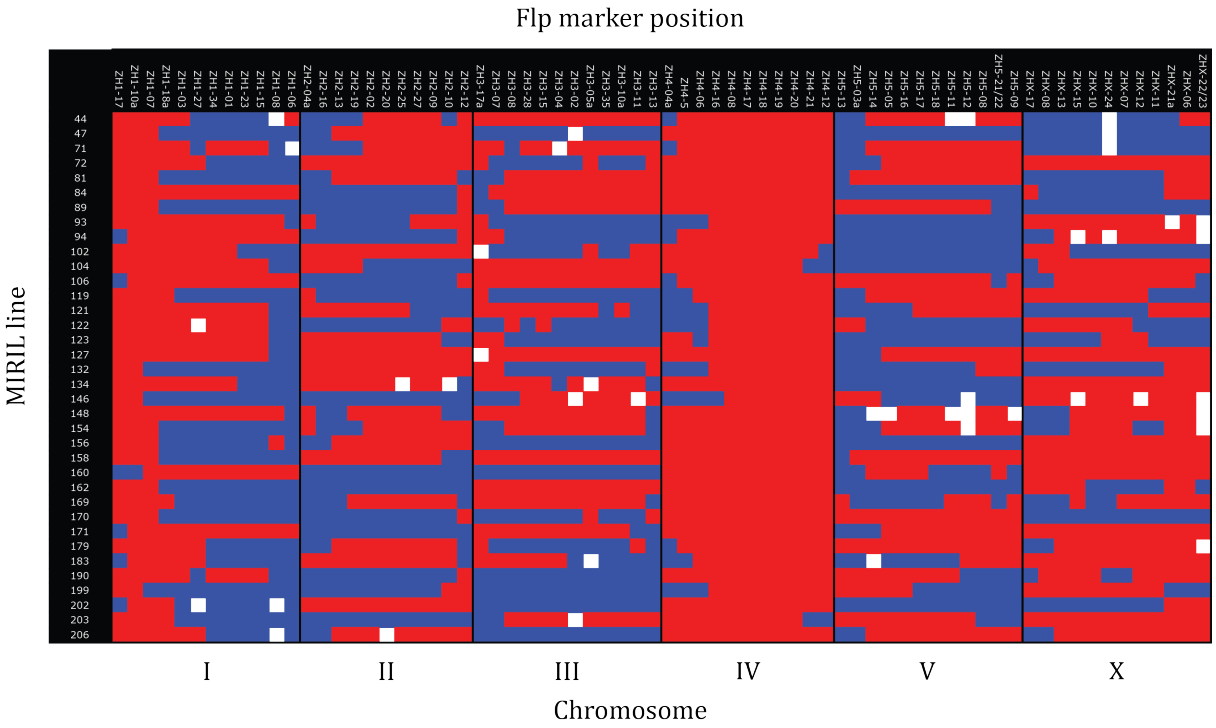

Figure 20: MIRILs used for genetical genomics analysis to identify eQTLs. Blue indicates N2 and red CB4856 genomic loci.

After analysis of the data by the group of Jan Kammenga, eQTLs were visualised and found to overlap with the previously found QTLs for vulval induction (Figure 21, red boxes). As expected, we identified eQTL regions not known for vulval induction (e.g. on chromosome X). The strong eQTL peak at the left side of chromosome I might be an artefact. The fact that QTLs and eQTLs overlap indicates that the observed effects in the vulva might be as well true for the entire animal and therefore reflect a more global function.

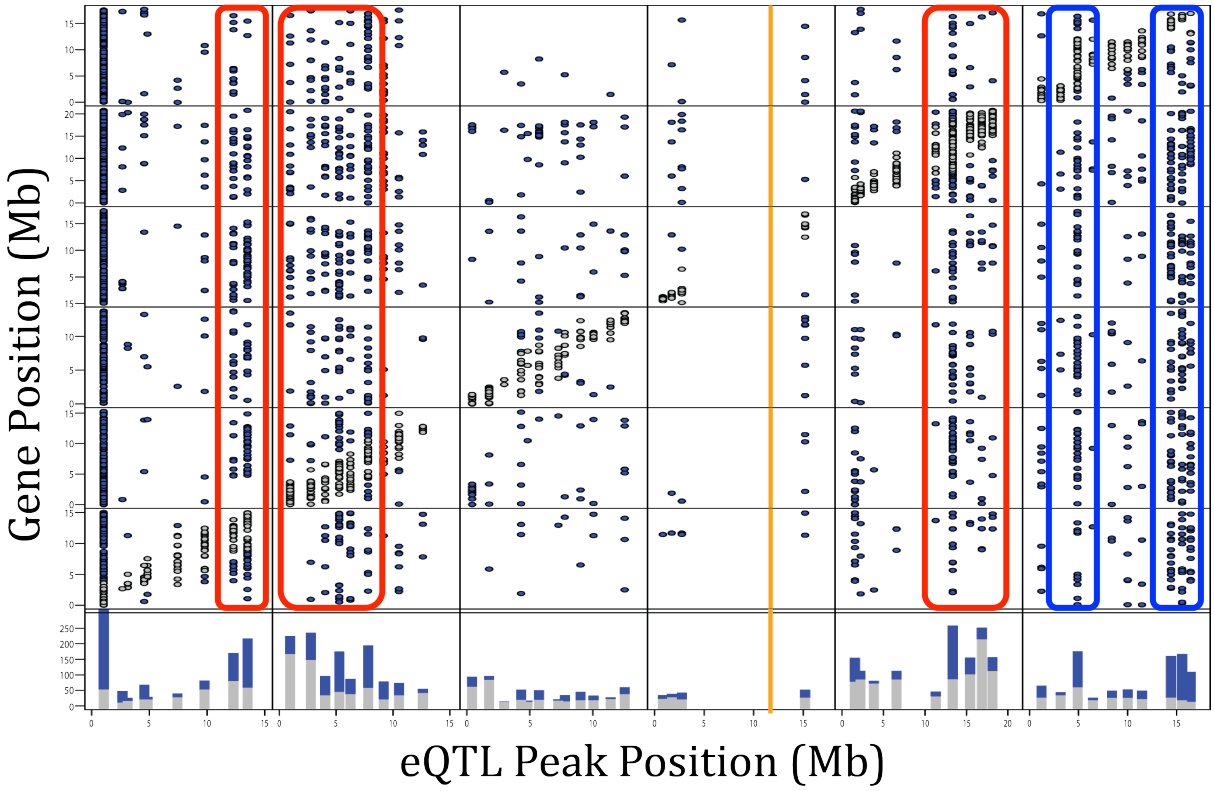

Figure 21: eQTL analysis: cis eQTLs are visualised as white dots, whereas trans eQTLs are marked in blue. The orange line marks the site of the *n1046* allele, where there is hardly any recombination allowed. At the bottom a sum up of the changed transcript per location is shown. The genomic regions for the QTLs in vulval induction are encircled in red and additional eQTL are indicated in blue. There is a high correlation between the eQTLs for whole worm transcriptome and for vulval induction as red boxes nicely overlap with the eQTLs.

1.7.4 Identification of Candidate Genes for *let-60(n1046)* miRILs:

Whole genome sequencing was used to have the most accurate identification of polymorphic genes between the two parental genetic backgrounds *let-60(n1046)* and CB4856. For this purpose we extracted total genomic DNA for both the parental strains and used the service of the Functional Genomics Center Zürich to sequence. The strains were paired end sequenced with mean coverage of approximately 17x. Alignments with the reference genome WS220 and further SNP calling were accomplished using CLC genomics workbench (see electronic supplementary information for more details).

1.7.4.1 Candidate Genes in QTL1b Region

With the help of the introgression line crosses, we were able to narrow down QTL1b to a region of approximately 0.6 Mb. We further sequenced the whole genome of the parentals *let-60(n1046)* and CB4856. We aligned both sequences to the reference N2 genome and focused on non synonymous single nucleotide polymorphisms (SNPs) and included genes missing in the Hawaiian genome ((Maydan, Lorch, Edgley, Flibotte, & Moerman, 2010)) to filter for most likely candidates. In total this list eventually contained 143 putative candidate genes (Table 5).

Gene Name	non synonymous SNPs
E03H4.11	Asn369His
C54C8.2	Gly245Glu
C54C8.4	Met141Ile
glct-5	Lys264Glu
T27F6.1	Arg3Gly
pars-2	Ala13Va Ser411Pro, Ser123Pro, Ser71Pro Gln412His, Gln124His, Gln72His
K11D2.4	Thr158Pro, Thr146Pro, Thr84Pro, Thr18Pro Tyr368Asn, Tyr356Asn, Tyr294Asn, Tyr228Asn, Tyr150Asn
W02D9.4	Ser76Pro
W02D9.9	Leu58Ile
dlk-1	Thr43Pro, Thr116Pro
F33E2.4	
F33E2.6	Glu259Val Asp824Glu
T07D10.1	Val8Ile
ntr-1	Thr373Ile
T07D10.3	Gln273Pro

Gene Name	non synonymous SNPs
H16D19.4	Ser153Ile Gly189Arg Leu295Pro Asn307His
H28O16.2	Ala2Ser
clec-103	Ser22Ile
ndx-1	Val197Ile
T26E3.5	Lys59Thr Glu70Lys
T26E3.6	Glu66Stp Asp53Glu
T26E3.8	CB4856 deletion
sra-25	Arg307Gln
sra-17	Glu277Asp Leu298Phe
sra-20	Ile66Thr
sra-23	Gly18Val
T06G6.5*	Ser120Stp
T06G6.6	Val46Met; Val73Met
srw-88	Gly175Glu
pfd-3	Ala5Val
W02A11.1	Ile287Thr Phe200Ser
vps-25	Leu132Pro
toe-4	Leu132Pro
uba-2	Thr166Ala
bath-34*	CB4856 deletion
W02A11.6	CB4856 deletion
bath-35	Tyr16Thr Gly18Glu Ala97Gly Asn120Lys Lys142Glu Leu216Met
amx-2	Asn535Ser Arg521Gly Thr532Ser
B0019.2	Ala30Val
Y18D10A.1	Ile169Met Ser557Leu Glu700Gly Thr871Pro Gln1046Pro

Gene Name	non synonymous SNPs
Y18D10A.2	Glu144Gly
ptr-17	Val560Phe; Val576Phe Arg782Cys
Y18D10A.8	Ser283Ala
Y18D10A.9	Ala324Ser
clec-104	Cys74Stp Ala102Thr Val189Phe
clec-106	Ser51Pro Ser80Trp Asp209His Gly210Asp
pad-1	Gly1667Asn
F08A8.1	Ile26Thr; Ile109Thr; Ile138Thr
F08A8.4	Val10Gly
F08A8.5	Leu15Ser,Ser
fbxa-140	Gln311Stp
C47B2.2	Phe92Leu
gale-1	Thr327Asn
selb-1	Met98Ile,Ile Leu139Ile; Leu180Ile Asn268Lys; Asn309Lys Lys292Thr; Lys333Thr
prx-11	Glu142Ala
smu-1	Ile270Met Thr6Ala,Ala; Thr83Ala
clec-108	Val135Gly
Y26D4A.8	Thr319Ile
Y26D4A.9	Ile869Phe
C17H1.4	Asp319Gly
C17H1.7	Asp343Tyr
F22G12.5	His697Asp
F17B5.1	Asp158Asn Ser463Phe Lys524Glu
oac-17	Met452Val
clec-109	Ser46Phe
F17B5.4	Gln100Lys
clec-110	Ala104Val
ZK1225.1	Thr213Asn

Gene Name	non synonymous SNPs
ZK1225.2	Lys123Glu Lys179Stp Gly184Cys Lys258Glu Lys280Glu Leu393Met Met429Ile
ZK1225.4	Lys154Gln Val188Ile Lys231Glu Cys278Tyr Ile389Leu Thr447Ile
ZK1225.5	Thr19Ala Phe27Leu Asp54Glu Thr392Ala Ile401Val Tyr457His Ile468Thr Ile494Leu
ssp-31	Ser18Leu Gly94Ser
ZK1053.3	Glu32Lys Asn56Ser Arg365Ile Cys429Tyr
F44F1.1	CB4856 deletion
F44F1.3	Gly131Ser His217Leu Asn257Lys Pro408Gln Ala418Thr Asp468Gly
F44F1.4	Ser348Ile
F44F1.6	Val3Ile,Ile
vet-6	Thr157Ala Ile336Thr
sepa-1	Arg179Gly Arg383Gln Ala680Ser
T04D3.1	Ala121Pro

Gene Name	non synonymous SNPs
gcy-35	Ile163Thr Arg484His Gly566Ala
T04D3.5	in gcy-35 CDS
W08E3.4	Lys65Gln Lys175Thr
Y40B1A.1	Met22Val
C01A2.3	Ala119Val
C01A2.6	Ala21Pro Asp28Glu His39Asn Ala43Val Pro60Ser Val110Ile
W05H12.2	Ser285Thr
fbxb-66	Val88Met
eif-3.J	Glu164Gly
agef-1	Gln1136Pro; Gln1170Pro
W09C5.7	Lys394Arg
W04A4.3	Gly85Ser
W04A4.5	Ser241Thr Ser34Arg
Y6B3B.1	Asp143Gly Phe201Ser Gln794Arg Ile914Arg Glu1058Val Leu1192Pro Pro1496Gln Ile1577Thr
Y6B3B.3	Lys229Thr Asp396Gly Arg946Cys Thr1085Lys
Y6B3B.4	Ser617Asn
Y6B3B.5	Leu126Ser; Leu135Ser
Y6B3B.9	Asn170Ser
Y37H9A.2	in Y37H9A.3
Y37H9A.3	Phe126Ser
W04A8.1	Trp501Ser; Trp630Ser
W04A8.2	Cys218Ser
W04A8.3	Val187Ile

Gene Name	non synonymous SNPs
W04A8.5	Ser178Cys Phe217Ile
W04A8.6	Phe521Leu
ins-30	Lys37Glu
fbxb-101	Asn27Asp Leu305Phe
tfg-1	Lys142Gln Phe151Leu
kal-1	Val277Met
fipr-24	Ser45Thr
ZK849.1	Cys313Arg
ZK849.5	Ser58Arg
K05C4.9	CB4856 deletion
C01A2.9	Cys108Phe
C37A5.11	Thr15Ala
fbxa-101	Leu256Val
F17B5.6	Phe4Ile Ser254Asn
F17B5.9	His4Arg
T26E3.10	Ile49Val
nhr-85	Lys96Thr
W09G3.6	Lys470Thr Met412Thr Met187Thr
W09G3.7	Pro332Leu
fkb-8	Ile226Thr
Y26D4A.10	Pro103Gln Asn256Ser
Y26D4A.14	Asn496Ser
dnj-29	Tyr429His,His
Y71A12B.10	Ala390Val
Y71A12B.15	Arg7Cys
Y71A12B.17	Lys176Glu Ser553Arg
trp-4	Met36Ile Gly41Ser
clec-111	Ser133Pro Thr141Ala Leu145Ile
clec-112	Asp83Asn Gly195Ser Val233Leu Val263Ala

Gene Name	non synonymous SNPs
Y71A12B.8	Asn119Gly Thr359Ile
Y71A12B.9	Gln215His
Y87G2A.11	Met513Val
Y87G2A.12	Ala50Val
cyn-15	Ile183Val
Y87G2A.7	Gly369Glu Gly38Arg
ZK1053.1	Glu135Gly
ZK1053.4	Thr201Ser Phe251Ile
ZK1053.7	Glu12Asp
pmr-1	Gln700His
ZK849.6	Ser28Tyr

Table 5: Chosen candidate genes for RNAi knockdown in overlap of ewIR10 and ewIR17 region. Gene names and respective polymorphisms are indicated.

1.7.4.2 RNAi to Identify Modifier Genes that Alter RAS Signalling

In a next step we applied RNAi gene knockdown to further screen the list of candidates for modifiers of the EGFR/RAS/MAPK signalling pathway during vulval development. We chose to screen the candidates in two different genetic backgrounds for changes in vulval induction. As first strain, we chose *let-60(n1046*) in a complete N2 background and as the second strain, we took *ewIR17;let-60(n1046).* With this approach we are able to investigate the function of both, the Bristol (*let-60(n1046)*) and the Hawaiian alleles (*ewIR17;let-60(n1046)*). From the original 143 candidates genes, only 113 were available in the Ahringer RNAi library and eventually 107 candidates were screened. The results from the RNAi are summarized in Table 6.

Gene Name	RNAi					
	Bristol allele	s.e.m.	p	Hawaii allele	s.e.m.	p
E03H4.11	4.50	0.20		5.10	0.14	
C54C8.2	4.25	0.22		4.55	0.24	3.2E-03
C54C8.4	4.55	0.16		5.38	0.11	
glct-5	4.30	0.22		5.15	0.18	
T27F6.1	4.48	0.19		5.35	0.17	
pars-2	4.40	0.22		5.03	0.14	
K11D2.4	4.55	0.19		5.48	0.12	
W02D9.4	5.23	0.17	1.2E-03	5.08	0.20	
W02D9.9	4.53	0.19		4.75	0.19	

Gene Name	RNAi					
	Bristol allele	s.e.m.	p	Hawaii allele	s.e.m.	p
dlk-1	4.58	0.19		5.20	0.15	
F33E2.4	4.15	0.25		4.78	0.19	
F33E2.6	4.55	0.21		5.10	0.19	
T07D10.1	4.20	0.18		4.88	0.18	2.3E-02
ntr-1	4.90	0.21		5.20	0.15	
T07D10.3	4.03	0.23		5.00	0.11	2.6E-02
H16D19.4	na	na		na	na	
H28O16.2	na	na		na	na	
clec-103	4.68	0.13		5.35	0.16	
ndx-1	4.08	0.22		4.98	0.18	
T26E3.5	4.25	0.16		5.38	0.14	
T26E3.6	3.95	0.16	3.6E-02	4.73	0.19	6.1E-03
T26E3.8	na	na		na	na	
sra-25	4.55	0.21		5.08	0.15	
sra-17	4.98	0.17		5.65	0.16	
sra-20	3.58	0.12	9.0E-04	3.95	0.13	4.2E-03
sra-23	4.23	0.17		4.98	0.19	
*T06G6.5**	4.15	0.16		5.40	0.12	
T06G6.6	3.90	0.20	4.3E-02	5.23	0.18	
srw-88	3.38	0.10	1.2E-06	4.70	0.16	1.5E-03
pfd-3	3.98	0.19		4.60	0.18	7.5E-04
W02A11.1	3.83	0.15	7.7E-03	5.05	0.14	
vps-25	4.65	0.20		5.58	0.10	
toe-4	3.65	0.17	1.4E-03	4.38	0.20	1.4E-04
uba-2	4.70	0.17		5.38	0.18	
*bath-34**	4.10	0.16		4.85	0.21	2.9E-02
W02A11.6	na	na		na	na	
bath-35	4.18	0.22		5.05	0.14	
amx-2	5.05	0.18	1.2E-02	5.38	0.21	
B0019.2	3.95	0.21		5.30	0.16	
Y18D10A.1	4.28	0.20		5.08	0.14	
Y18D10A.2	3.68	0.16	1.5E-03	4.48	0.19	3.0E-04
ptr-17	4.65	0.22		5.13	0.14	
Y18D10A.8	4.45	0.17		4.48	0.19	
Y18D10A.9	3.58	0.16	8.9E-05	4.38	0.19	
clec-104	4.70	0.23		5.15	0.17	
clec-106	4.10	0.17		5.10	0.13	
pad-1	3.90	0.24		4.73	0.16	2.5E-03
F08A8.1	4.35	0.16		5.08	0.16	
F08A8.4	4.25	0.20		5.50	0.14	

Gene Name	RNAi					
	Bristol allele	s.e.m.	p	Hawaii allele	s.e.m.	p
F08A8.5	3.93	0.18	3.9E-02	4.48	0.16	5.0E-05
fbxa-140	4.43	0.18		4.73	0.19	
C47B2.2	4.05	0.14		5.45	0.12	
gale-1	4.48	0.19		4.05	0.21	3.8E-02
selb-1	4.23	0.16		5.15	0.21	
prx-11	4.23	0.13		4.98	0.21	
smu-1	3.83	0.15	6.9E-03	4.75	0.24	2.2E-02
clec-108	4.65	0.17		5.28	0.19	
Y26D4A.8	3.93	0.20		5.68	0.13	
Y26D4A.9	4.38	0.18		5.48	0.11	
C17H1.4	4.75	0.21		5.68	0.09	
C17H1.7	4.90	0.17		5.23	0.14	
F22G12.5	4.85	0.17		5.30	0.14	
F17B5.1	4.80	0.21		4.85	0.16	
oac-17	4.48	0.23		5.13	0.18	
clec-109	4.58	0.18		5.05	0.18	
F17B5.4	5.00	0.14	8.2E-03	5.40	0.15	
clec-110	4.33	0.25		5.40	0.14	
ZK1225.1	4.58	0.20		5.18	0.17	
ZK1225.2	4.68	0.24		5.40	0.12	
ZK1225.4	3.55	0.16	2.7E-04	5.05	0.21	
ZK1225.5	4.00	0.17		4.93	0.18	3.5E-02
ssp-31	4.48	0.16		5.25	0.12	
ZK1053.3	4.05	0.17		5.03	0.20	
F44F1.1	5.33	0.11	1.8E-03	5.18	0.18	
F44F1.3	4.80	0.17		na	na	
F44F1.4	5.20	0.14	6.1E-04	5.63	0.12	
F44F1.6	3.65	0.15	9.3E-04	4.55	0.18	5.4E-04
vet-6	4.28	0.18		5.33	0.12	
sepa-1	4.95	0.18		5.48	0.08	5.0E-02
T04D3.1	4.63	0.18		4.80	0.16	
gcy-35	4.38	0.17		5.15	0.19	
T04D3.5	3.95	0.20		5.00	0.20	
W08E3.4	4.63	0.18		5.28	0.18	
Y40B1A.1	3.98	0.20	2.2E-02	4.58	0.16	1.6E-02
C01A2.3	4.43	0.20		na	na	
C01A2.6	4.63	0.14		na	na	
W05H12.2	4.43	0.21		4.75	0.15	
fbxb-66	4.33	0.24		4.68	0.20	
eif-3.J	4.13	0.21		4.28	0.14	1.3E-04

Gene Name	RNAi					
	Bristol allele	s.e.m.	p	Hawaii allele	s.e.m.	p
agef-1	3.98	0.22	2.8E-02	na	na	
W09C5.7	4.63	0.18		5.25	0.17	
W04A4.3	4.33	0.19		5.43	0.16	
W04A4.5	4.30	0.18		4.78	0.18	
Y6B3B.1	4.40	0.23		5.30	0.16	
Y6B3B.3	4.48	0.16	2.6E-02	4.83	0.21	
Y6B3B.4	3.53	0.14	8.4E-05	4.78	0.20	1.2E-02
Y6B3B.5	4.25	0.18		4.45	0.18	
Y6B3B.9	na	na		3.73	0.17	1.5E-09
Y37H9A.2	3.88	0.16	1.7E-02	5.05	0.17	
Y37H9A.3	4.08	0.20		5.13	0.16	
W04A8.1	4.13	0.17		5.38	0.12	
W04A8.2	4.35	0.24		4.95	0.19	
W04A8.3	4.43	0.18		5.63	0.11	
W04A8.5	4.53	0.14		5.13	0.13	
W04A8.6	3.93	0.15	2.4E-02	4.95	0.18	4.7E-02
ins-30	4.43	0.20		5.33	0.18	
fbxb-101	4.53	0.21		5.50	0.15	
tfg-1	3.83	0.17	1.2E-02	4.08	0.22	9.1E-06
kal-1	4.35	0.20		4.90	0.21	4.7E-02
fipr-24	na	na		na	na	
ZK849.1	4.53	0.20		5.23	0.19	
ZK849.5	4.93	0.16		5.40	0.12	
K05C4.9	na	na		na	na	
empty vector	4.55	0.07		5.16	0.06	

Table 6: RNAi gene knockdown of putative modifier genes. All candidates were screened for changes in vulval induction in either a *let-60(n1046)* single (Bristol allele) or an ewIR17 introgression *let-60(n1046)* mutant (Hawaii allele). Student's t-test indicates the level of significance for each of the candidates. Beige rows indicate allele unspecific and grey rows allele specific effects of the RNAi. na: no data available

Natural variation describes a situation in which there is a difference between the behaviour of at least two alleles in a population. In the RNAi candidate screen we tested for two possible outcomes. We are now able to distinguish between candidate genes that alter RAS pathway activity allele-independently (Table 6, beige rows) and candidate genes that react in an allele-specific manner (Table 6, grey rows). Allele-independent effects represent novel candidate genes that play a role in RAS signalling independent of their genetic background. Nevertheless those would be good candidates for further investigation. Since the interest of this project lies in the discovery of novel natural variations, we further focused on genes that significantly altered

RAS pathway activity in an allele-specific manner, thereby supporting their role as natural modifier genes. We extracted these candidates from Table 6 for more detailed analysis (Table 7).

1.7.4.3 Transgenesis Experiments as Supportive Evidence for Natural Modifier Genes.

Next, we evaluated the candidates for their allele-specificity in overexpression studies. In contrast to gene knockdown via RNAi (see section 1.7.4.2), we injected PCR fragments of either the Bristol or Hawaii genomic locus in the *let-60(n1046)* mutant and assessed vulval induction. We further used *sur-5::gfp* as co-injection marker to distinguish between overexpressing and control animals. We were able to test the following genes: *amx-2, F44F1.3, F44F1.1, tfg-1, toe-4, F17B5.4, Y18D10A.2, F08A8.5, W02D9.4, srw-88* and *C54C8.2*, which are summarized below in Table 7.

Gene	Allele	Line	Extrachromosomal array				p
			+	s.e.m.	-	s.e.m.	
amx-2	N2	7	3.88	0.16	3.93	0.20	0.8467
		8	4.13	0.13	3.95	0.17	0.3858
		9	4.08	0.22	4.18	0.22	0.7463
	CB4856	1	3.49	0.14	4.15	0.19	0.0013
		2	3.75	0.16	4.28	0.18	0.0353
		3	3.63	0.20	4.48	0.17	0.0025
		4	3.58	0.15	4.03	0.21	0.0897
		5	3.43	0.16	4.23	0.13	0.0004
F44F1.3	N2	1	3.65	0.14	4.00	0.18	0.3700
		3	3.00	0.00	3.58	0.13	0.0002
		4	3.28	0.10	3.98	0.14	0.0001
	CB4856	1	3.38	0.10	4.08	0.22	0.0061
		2	4.08	0.20	4.65	0.21	0.0537
		3	3.98	0.18	4.68	0.18	0.0088
		4	3.70	0.13	4.40	0.25	0.0172
F44F1.1	N2	1	3.90	0.15	4.05	0.14	0.4658
		2	3.62	0.16	3.68	0.16	0.8043
		5	3.80	0.19	4.05	0.18	0.3511
		6	4.33	0.20	4.40	0.22	0.8032
	CB4856	1	3.26	0.13	3.76	0.15	0.0151
		2	3.45	0.15	4.03	0.18	0.0184
		3	3.18	0.08	3.78	0.13	0.0001
		4	3.45	0.17	4.18	0.16	0.0035
		5	3.20	0.10	3.70	0.17	0.0106
tfg-1	N2	1	4.50	0.44	4.34	0.19	0.6993
	CB4856	1	3.42	0.08	3.65	0.10	0.0592
toe-4	N2	2	3.56	0.08	3.45	0.08	0.9013

Gene	Allele	Line	Extrachromosomal array				p
			+	s.e.m.	-	s.e.m.	
		3	3.57	0.13	3.61	0.13	0.8571
		4	3.25	0.09	3.65	0.21	0.0839
		5	3.65	0.16	4.03	0.17	0.1214
	CB4856	1	3.21	0.05	3.76	0.10	0.0001
		2	3.29	0.06	3.97	0.09	0.0000
		3	3.53	0.12	4.18	0.18	0.0053
F17B5.4	CB4856	1	3.78	0.17	4.13	0.15	0.1297
		2	3.52	0.10	3.76	0.13	0.8082
		3	3.35	0.12	4.15	0.18	0.0006
Y18D10A.2	CB4856	1	3.55	0.17	3.46	0.10	0.6397
		2	3.80	0.18	3.45	0.14	0.1368
		6	3.30	0.14	3.73	0.19	0.0815
F08A8.5	CB4856	1	4.06	0.15	4.34	0.17	0.2278
		2	3.23	0.09	3.54	0.12	0.0415
		4	3.54	0.14	4.00	0.22	0.0731
W02D9.4	CB4856	1	4.75	0.25	4.10	0.18	0.2698
		2	3.85	0.16	3.80	0.17	0.8065
srw-88	CB4856	1	3.68	0.15	3.58	0.15	0.6368
		2	3.68	0.21	4.23	0.18	0.0513
		3	3.88	0.20	4.23	0.18	0.2027
C54C8.2	CB4856	3	3.62	0.19	3.34	0.12	0.8693
		5	3.46	0.11	3.50	0.26	0.2116
sur-5::gfp	control	na	3.80	0.19	3.75	0.15	0.8399

Table 7: Transgenic lines generated via micro-injection of PCR fragments spanning the corresponding genomic region from either the N2 or the CB4856 genetic background. Vulval induction was compared between intraline animals carrying the extrachromosomal array vs. animals without the array. Student's t-test was used to calculate the level of significance (light grey: $p < 0.05$, dark grey: $p < 0.01$, black: $p < 0.001$). s.e.m.: standard error of mean

The presented data is to handle with care, since microinjection generates large multicopy extrachromosomal arrays with non-mendelian segregation that does not represent wildtype conditions. There might be still biological artifacts due to the massive overexpression of all genetic information in the extrachromosomal array. Nevertheless we could verify several of the candidate genes to be putative RAS modifiers with allele-specific effects. *amx-2* and *F44F1.1* seemed to be the best candidates to follow up also due to their high sequence divergence between N2 and CB4856.

1.7.5 *amx-2* is as Modifier of RAS/MAPK Signalling

amx-2 is by sequence homology similar to human monoamine oxidases A and B (MAO) (Figure 22). In humans, monoamine oxidases are located in the outer mitochondrial membrane and are

responsible for the deamination of a wide variety of monoamines such as serotonin (5-HT), dopamine (DA), norephinephrine, , tyramine and 2-phenylethylamine (PEA). MAOA and MAOB differ in their substrate specificity, where MAOA prefers serotonin and norephinephrine as substrates in contrast to MAOB that oxidises 2-phenylethylamine and benzylamine. Dopamine

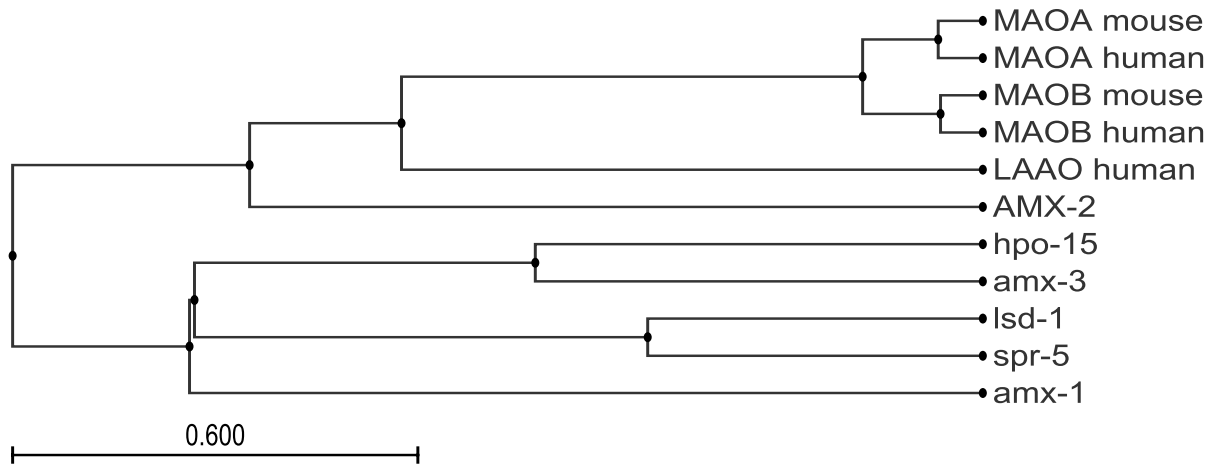

Figure 22: Amino-acid sequence homology of *C. elegans* AMX-2 compared to *C. elegans*, human and mouse homologues. *amx-2* is most similar to MAOA and MAOB or to LAAO.

and tyramine seem to be substrates for both isozymes ((Kalgutkar, Dalvie, & Castagnoli, 2001)).

An *amx-2* knockout mutant *ok1235* is available from the *C. elegans* gene knockout consortium. *ok1235* is a deletion/insertion allele deleting 1735 bp in exons 7, 8, 9 and part of 10 and inserting 126bp. We suppose *ok1235* to be a putative null allele (Figure 23).

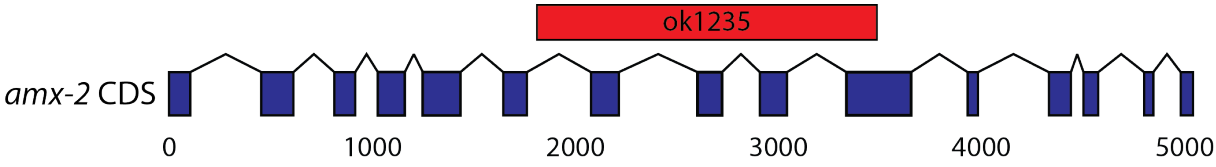

Figure 23: Intron exon structure of *amx-2*. *amx-2* possesses 15 exons and codes for a protein of 724 amino acids. The ok1235 allele removes exons 7, 8, 9 and part of 10 leading to a splice site mutation that presumably activates nonsense-mediated decay

We crossed the *amx-2(ok1235)* putative null mutant with the *let-60(n1046)* strain to verify the results from the RNAi knockdown. We compared vulval induction of single *let-60(n1046)* vs. *amx-2(ok1235);let-60(n1046)* double mutant lines from the same cross. The presence of the *amx-2(ok1235)* allele is able to further enhance the *let-60(n1046)* mutation (Figure 24). We included three more mutants in the EGFR/RAS/MAPK pathway to exclude that our observation

is *let-60(n1046)* specific. We used a gain-of-function and a reduction-of-function allele in let-23/EGFR (*sa62* and *sy1* respectively) and a reduction-of-function allele in let-60/RAS (*n2021*) to study. In all three cases, the absence of *amx-2* leads to an enhancement of signalling and to more vulval induction (Figure 24). We conclude that *amx-2* negatively regulates EGFR/RAS/MAPK signalling, possibly downstream of *let-60* or in a parallel pathway.

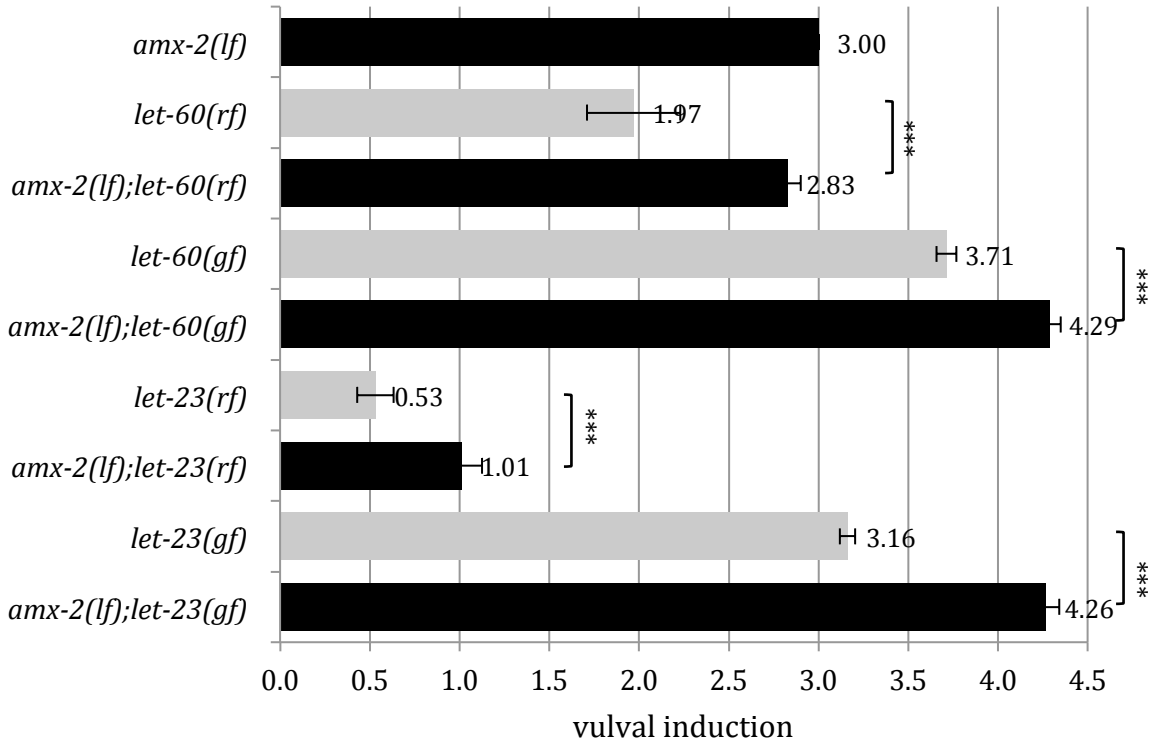

Figure 24: Epistastis analysis of *amx-2* in the EGFR/RAS/MAPK pathway. Enhancement of signalling as seen by increased vulval induction is notable as soon as *amx-2* is missing (black vs. grey bars). Error bars =SE, Mann-Whitney-U test, ** p<0.01, *** p<0.001

1.7.5.1 Single Copy Insertion of *amx-2* Uncovers Cryptic Natural Variation

We continued our study by integrating two copies of the *amx-2* locus into the genome. We chose the recently established MosSCI technique for this purpose ((Frøkjær-Jensen et al., 2008)), which should circumvent the problem of overexpression, which is often seen via more conventional methods (gene bombardment or gamma ray integration). We introduced two copies of either the N2 or the CB4856 *amx-2* locus into the genome. We further assessed the functionality of the N2 and the CB4856 allele by rescue experiments with the *amx-2(ok1235)* mutant. Therefore we crossed the N2 or CB4856 insertion lines with *amx-2(ok1235);let-60(n1046)* double mutants. As seen below, two copies of either N2 or CB4856 in the *let-60(n1046)* mutant do not affect signalling, assuming that the endogenous N2 *amx-2* allele is

dominant (Figure 25, first three bars). After removal of the endogenous N2 *amx-2*, using *amx-2(ok1235)* we could demonstrate the functionality of the N2 allele to rescue for the loss of the endogenous *amx-2* gene and to restore vulval induction similar to the *let-60(n1046)* mutant (Figure 25, fourth row). The CB4856 allele instead failed to rescue and could only slightly reduce vulval induction as compared to the double mutant *amx-2(ok1235);let-60(n1046)* (Figure 25, fifth row). We conclude that we could uncover cryptic natural variation in the *amx-2* locus between the two genetic backgrounds N2 and CB4856.

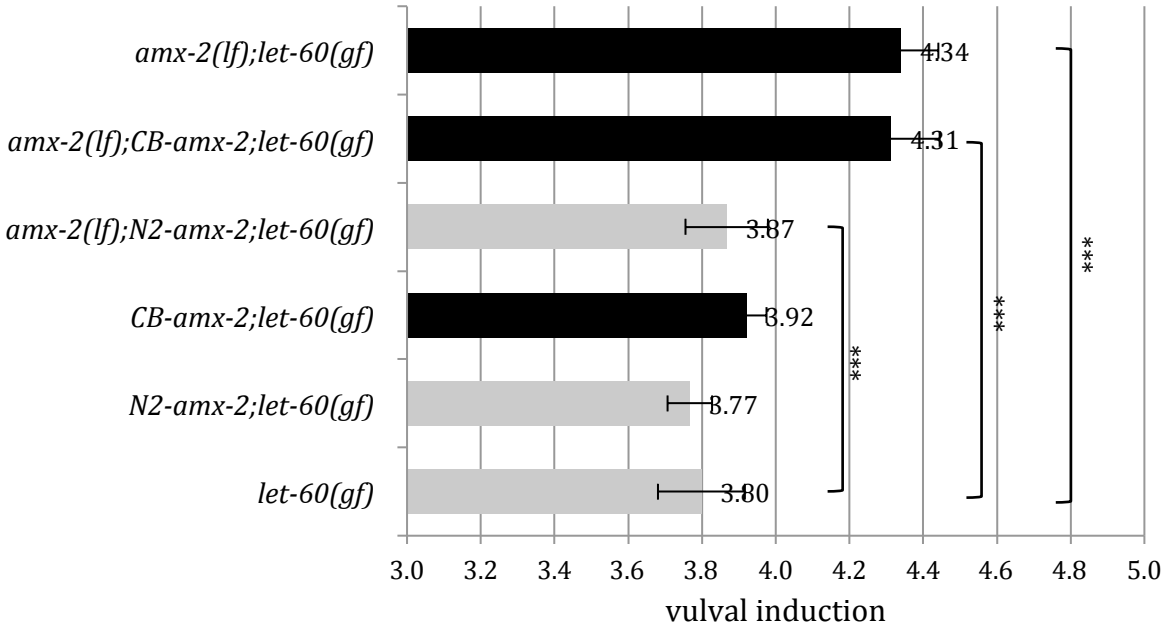

Figure 25: MoSCI line crosses. Insertion lines were generated and crossed with the *let-60(n1046)* and *amx-2(ok1235);let-60(n1046)* mutant. Vulval induction was compared between the lines. N2-amx-2 as well as CB-amx-2 indicates the presence of two copies of the artificially introduced Mos insertions. Error bars =SE, Mann-Whitney-U test, *** p<0.001

1.7.5.2 Expression of *amx-2* in the Gut is Necessary and Sufficient to Exert its Function

Since *amx-2* might be responsible for the deamination of the worms' neurotransmitter, we expected it to be strongly expressed in the nervous system (Figure 26A), but we also suspected it to be expressed in other tissues as well. Therefore, we generated a transcriptional reporter. Surprisingly, *amx-2* is not expressed in the developing vulva; but *amx*-2::gfp expression becomes visible much later in the adult structure (Figure 26B). In addition, *amx-2* is strongly expressed in the gut lineage (Figure 26C) and in some unidentified cells in the tail (Figure 26D).

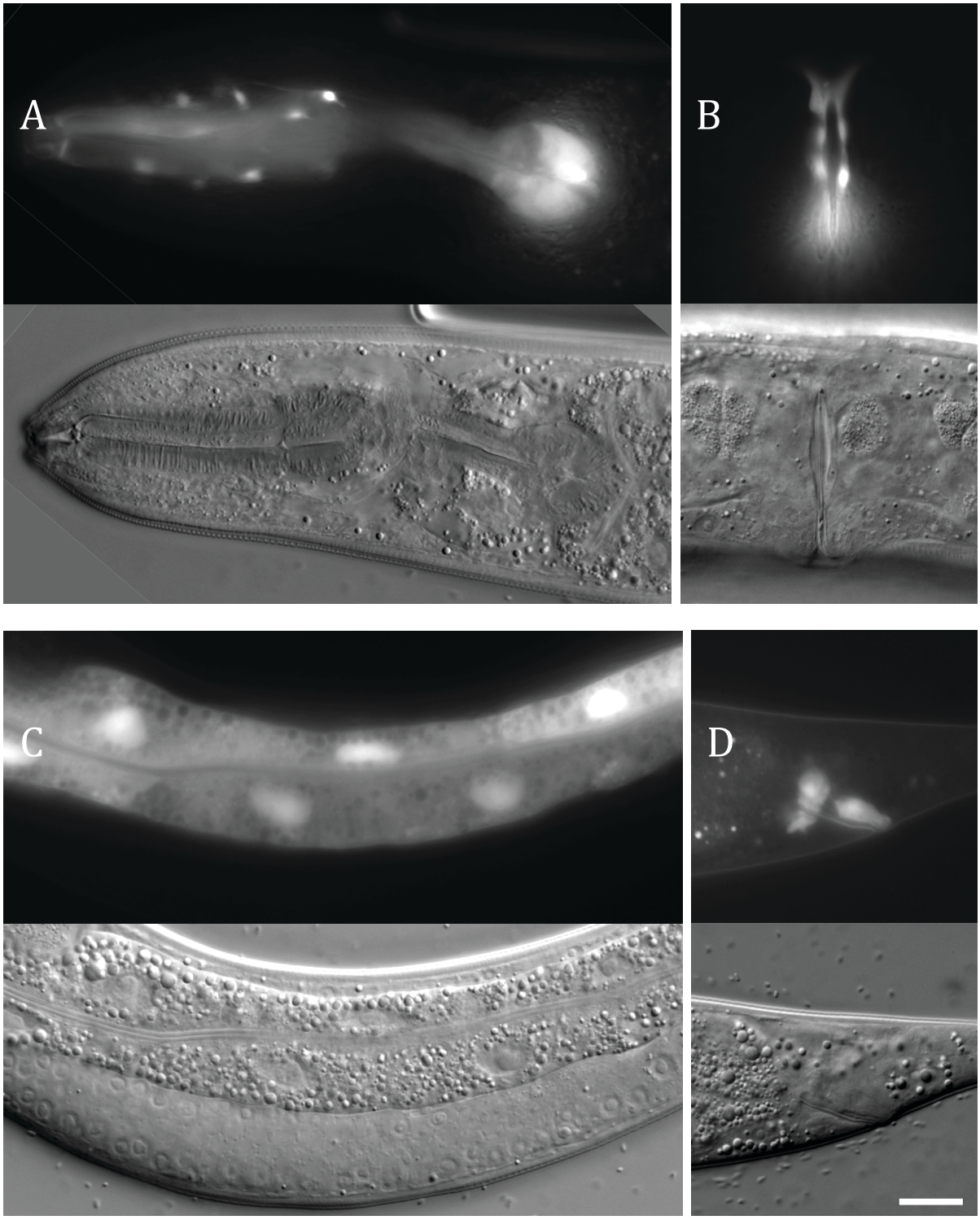

Figure 26: Expression of *amx-2*. The *amx-2* promoter was used to drive gfp expression. A: head neurons, B: adult vulva structure, C: entire gut cells, D: unidentified cells in the tail.

In a next step, we wanted to identify the tissue necessary for *amx-2* to function. Since the nervous system is widely refractory to RNAi ((Barstead, 2001)) and *amx-2* RNAi phenocopied the mutant, we excluded it to be the tissue necessary for *amx-2* to function. We made use of tissue-specific RNAi to test *amx-2* in the vulva and the gut. We used *rde-1(ne219)* to make *C.*

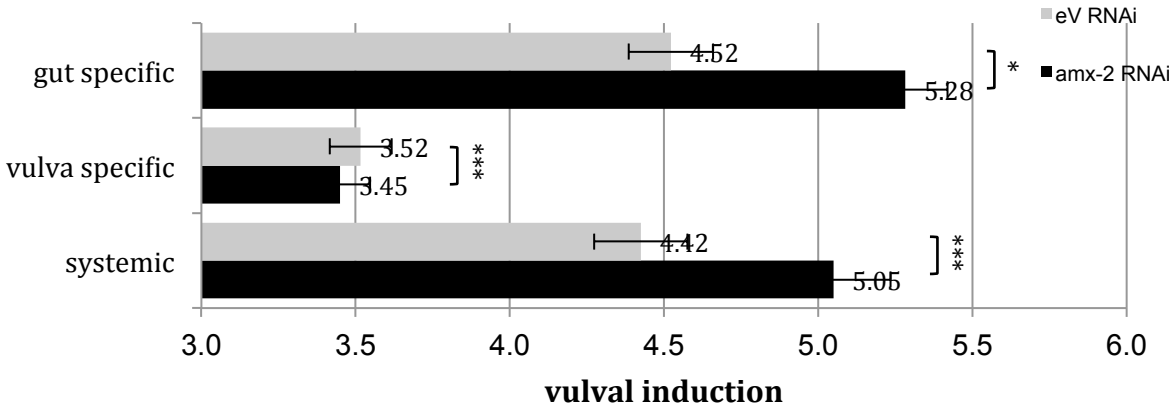

Figure 27: Tissue specific RNAi in the gut and the vulva compared to systemic. Expression of the dsRNA in the gut is able to fully phenocopy the systemic effects, indicating that RNAi in the gut is necessary and sufficient for *amx-2* to exert its function. Error bars =SE, Mann-Whitney-U test, *p<0.05, *** p<0.001

elegans resistant to RNAi. We further expressed the *rde-1(+)* rescue construct under a tissue-specific promoter to make the tissue of interest RNAi sensitive again. Eventually, we reduced *amx-2* via RNAi in the vulva or in the gut and checked for changes in vulval induction . *amx-2* knock-down in the gut lead to the same decrease in vulval induction as systemic RNAi (Figure 27, first and third row). *amx-2* knockdown only in the vulva did not alter vulval induction (Figure 27, seond row).

In conclusion, we could show that *amx-2* is widely expressed in the entire animal and that absence of *amx-2* in the gut fully phenocopies the systemic RNAi effect as negative regulator of RAS signalling.

1.7.5.3 Expression Levels of *amx-2* Measured by quantitative PCR are not Different Between N2 and CB4856

The expression level of *amx-2* was measured using quantitative PCR. We designed primer pairs specific for the mRNA of *amx-2* and as control for *amx-1*. Three primer pairs were used to detect the *amx-2* (OTS 234/235, 236/237, 238/239) and two primer pairs for the *amx-1* mRNA (OTS 242/243, 244/245). We carried out experiments in biological triplicates for the N2, CB4856 and *amx-2(ok1235)* strains (Figure 28). As expected, the putative loss-of-function mutant *amx-2(ok1235)* has significantly lower expression of *amx-2* as compared to N2 and CB4856, possibly

due to nonsense-mediated decay (NMD). There is a slight, but non-significant reduction in CB4856 *amx-2* expression as compared to N2. Levels of *amx-1* seem equal with the exception of higher *amx-1* expression in the *amx-2(ok12235)* strain, which might reflect a mechanism to compensate for the loss of *amx-2*.

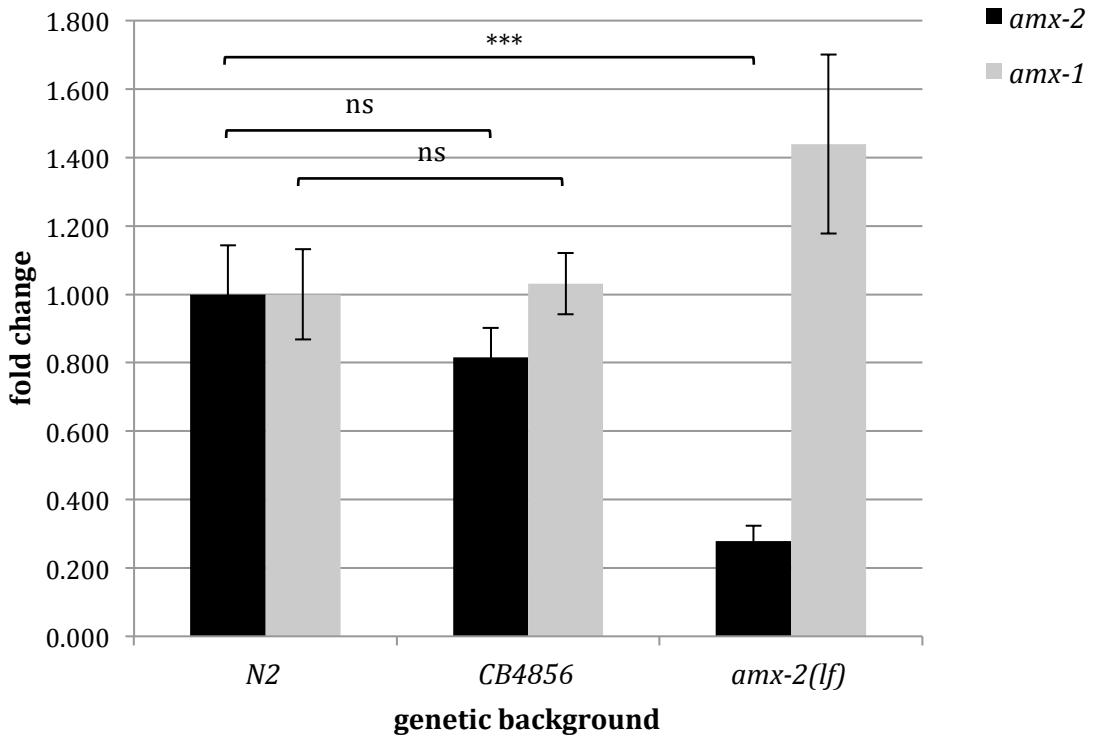

Figure 28: Quantitative PCR of *amx-2* and *amx-1*. The expression level of *amx-2* (black) and *amx-1* (grey) for the three background N2, CB4856 and *amx-2(lf)* are indicated. Fold change is normalised to N2, three biological replicates, error bars = SD. Students t-test ***p<0.001

1.7.5.4 Measuring Enzymatic Activity of *amx-2* in Whole Worm Protein Extracts

Since there was no difference between the expression of *amx-2* in N2 and CB4856 we measured *amx-2* enzymatic activity, relying on the homology of *amx-2* being a monoamine oxidase. We used the Amplex Red Monoamine Oxidase kit (lifetechnologies, cat # A12214) to measure enzyme activity. Upon substrate addition, monoamine oxidases will metabolise substrates producing metabolites and H_2O_2 as by-product. The amount of H_2O_2, therefore, indirectly reflects the activity of monoamine oxidase and in this case *amx-2*. H_2O_2 can be measured in a horseradish peroxidase dependent reaction of 1:1 H_2O_2:Amplex Red, producing resorufin. The concentration of resorufin can be measured with an excitation at 530-560 nm and emission detection at 590 nm. Preliminary promising data suggested, that the protein activity differ between N2, CB4856 and *amx-2(ok1235)* (Figure 29). Surprisingly the *let-60(n1046)* mutation

decreased amount of *amx-2* activity. After many more biological replicates, we were not able to reproduce the data obtained before and averaging all biological removed differences in activity due to very high experimental variability (data not shown). Next, to reduce variability we decided to centrifuge the crude worm protein samples to purify the mitochondrial fraction, which should be the organelle where *amx-2* is located. Unfortunately we were not able to reduce the variability and therefore results still remain inconclusive (Figure 30) and conclusions should not be drawn.

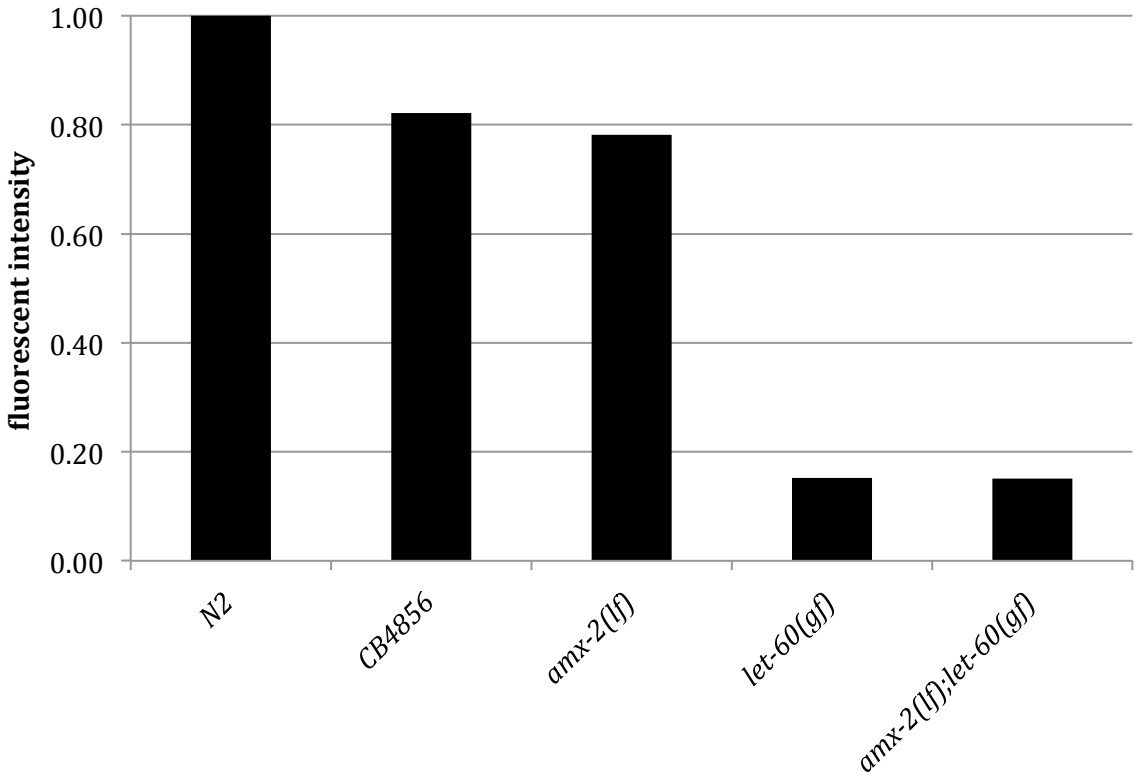

Figure 29: Enzymatic activity of *amx-2*. The enzymatic activity was measured and indicated as fluorescent intensity for the corresponding genetic backgrounds. Fluorescent intensity is normalized to N2.

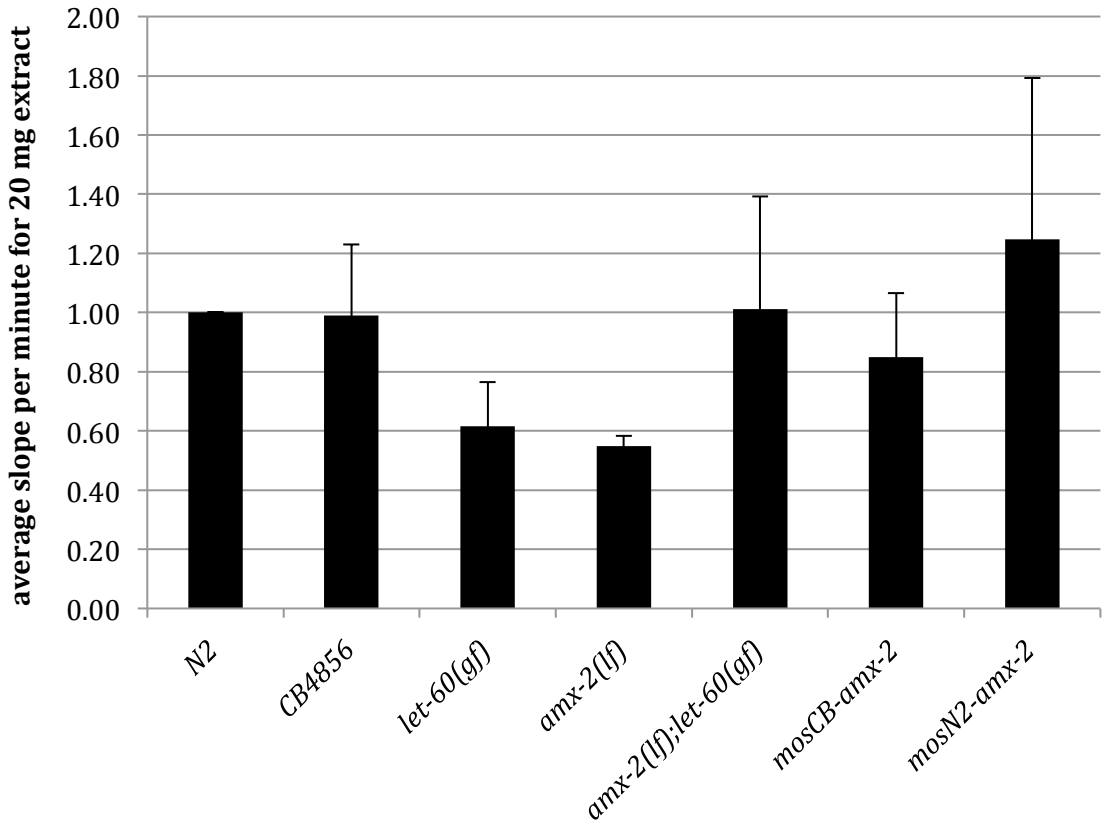

Figure 30: Enzymatic activity of *amx-2*. Mitochondrial fractions of the corresponding genetic backgrounds were measured. Average slope is normalized to N2. Three biological replicates, error bars = SE.

1.7.5.5 *amx-2* Acts on MAPK Signalling

To test if the effect of *amx-2* does involve terminal members of the pathway such as the mpk-1/MAPK and its phosphorylation, we probed western blots of *let-60(n1046)* and *amx-2(ok1235);let-60(n1046)* with antibodies against phosphorylated and total ERK. The double mutant displays a slightly higher but non-significant phospho/total ERK ratio as compared to the single mutant (Figure 31).

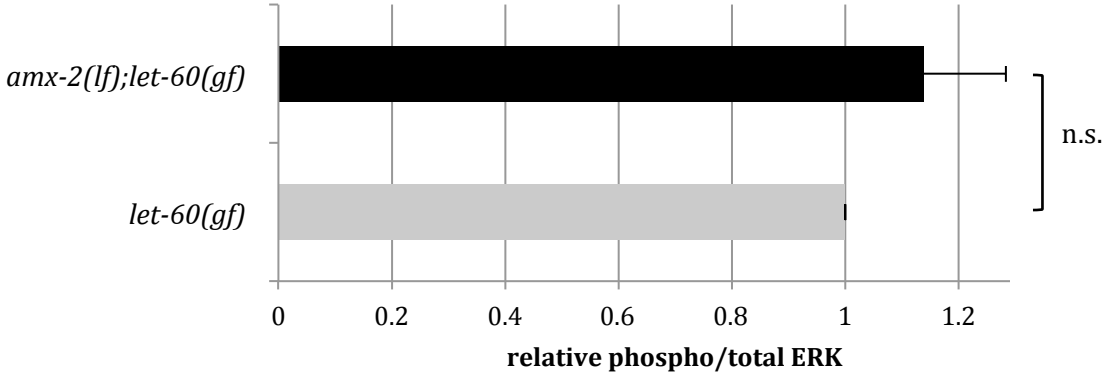

Figure 31: Western blot semi-quantitative analysis: *amx-2(lf);let-60(gf)* mutants have a slightly higher ratio of phosphorylated/total ERK indicating higher signalling strength.

1.7.6 Putative Substrates of AMX-2: Serotonin and Dopamine.

The human homologues of AMX-2, MAOA and MAOB are able to metabolize and deaminate monoamines such as Serotonin and Dopamine, which are built up from the precursors Tryptophan and Tyrosine, respectively (Figure 32). The action of MAO is necessary to oxidize those compounds, ultimately leading to the metabolites 5-hydroxyindolacetic acid and dihydroxyphenylacetic acid (Figure 33).

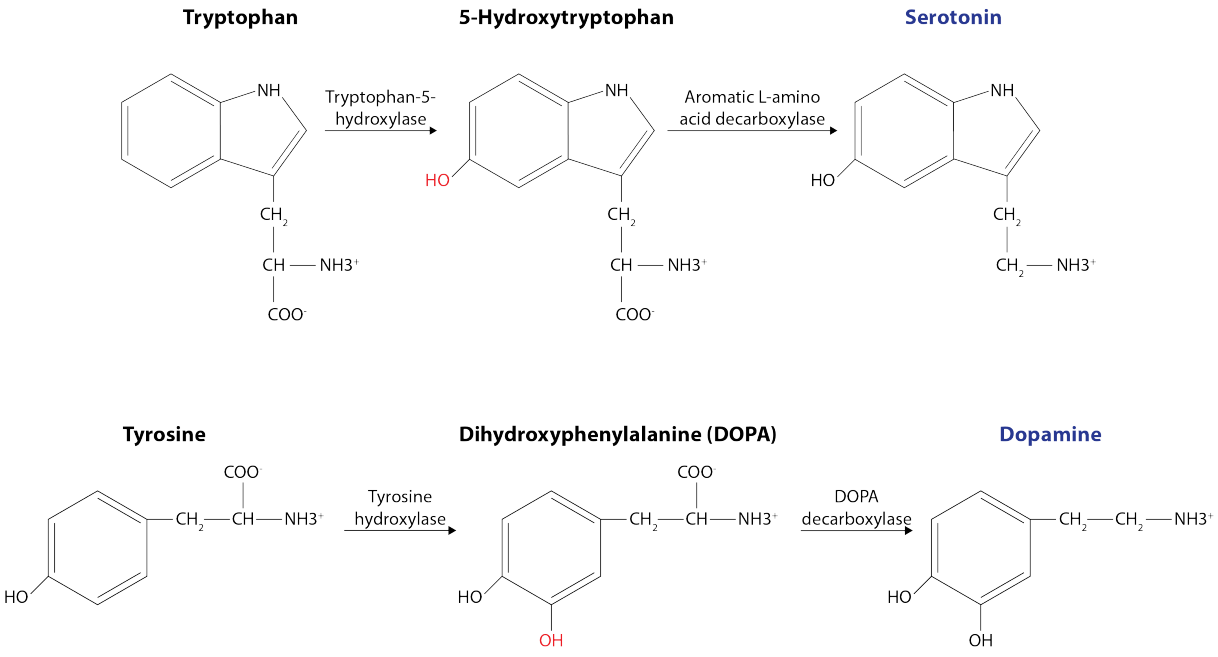

Figure 32: Synthesis of Serotonin and Dopamine. During the Synthesis of Serotonin, the amino acid Tryptophan is converted into 5-Hydroxytryptophan and further decarboxylated to Serotonin (5-hydroxytryptamine, 5-HT). The synthesis of Dopamine uses Tyrosine as precursor amino acid, which is converted in a similar manner as Sertotonin to

Dihydroyphenylalanine and further to Dopamine (DP). In both processes the first hydroxylations are the limiting steps.

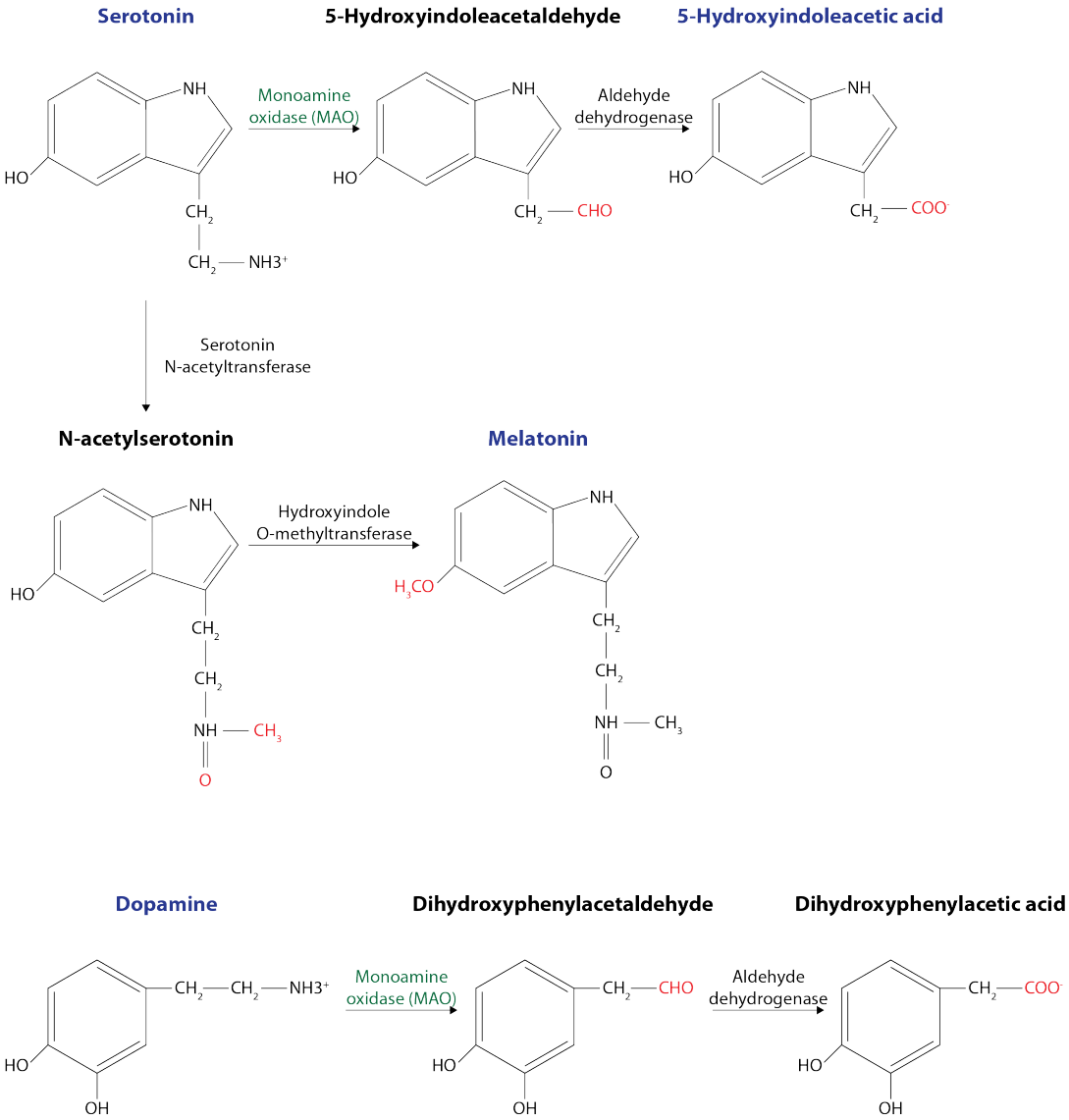

Figure 33: Metabolism of Serotonin and Dopamine. Serotonin is metabolized via the action of MAOA to 5-hydroxyindolacetaldehyde and subsequently into 5-hydroxyindolacetic acid (5-HIAA). Serotonin can further serve as precursor for the synthesis of Melatonin through the action of Serotonin N-acetyltransferase and hydroxyindole O-methyltransferase. Dopamine is further oxidised into dyhydroxyphenylacetaldehyde and subsequently converted to Dihydroxyphenylacetic acid (DOPAC)

Therefore, we hypothesised that *amx-2* may use those substrates and tested those putative upstream *amx-2* substrates and products to further their role in RAS signalling. We included Serotonin and Dopamine in the agar of conventional NGM plates at different concentrations and analysed vulval induction of either *let-60(n1046)* single and *amx-2(ok1235);let-60(n1046)* double mutants. Surprisingly, Serotonin was able to completely suppress vulval hyperinduction

in both backgrounds (Figure 34), whereas Dopamine was not able to significantly affect vulval induction (Figure 35, black bars). Depending on the concentration of 5-HT, we were able to identify a critical concentration in which the difference between the presence or absence of *amx-2* became apparent (Figure 34, red arrows).

In addition, we tested Melatonin as an *amx-2* independent substance, but built up from Serotonin (Figure 33). Indeed Melatonin affects vulval induction as well and independently of *amx-2* (Figure 35, lime green bars).

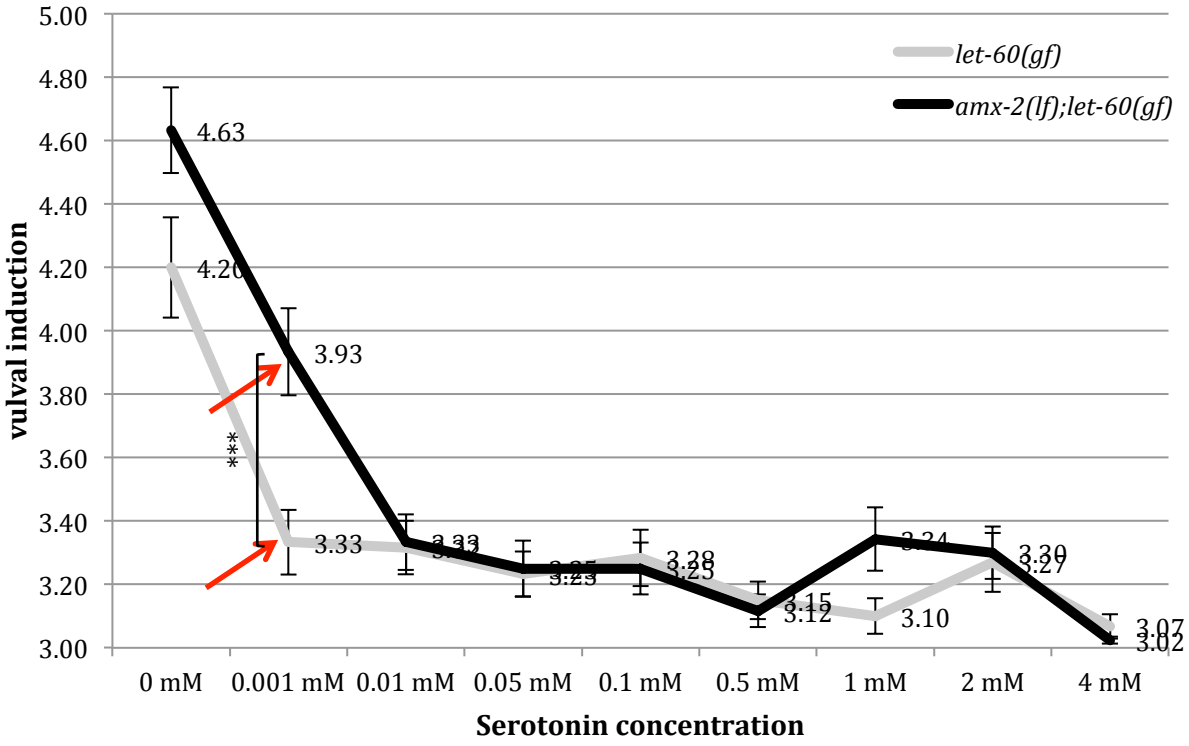

Figure 34: Effect of Serotonin on vulval induction in *let-60(gf)* and *amx-2(lf);let-60(gf) animals.* Serotonin at high concentration is able to almost completely suppress vulval induction in both the mutants. At a critical concentration of 0.001 mM the difference between the mutants become apparent. Error bars =SE, Mann-Whitney-U test, *** p<0.001

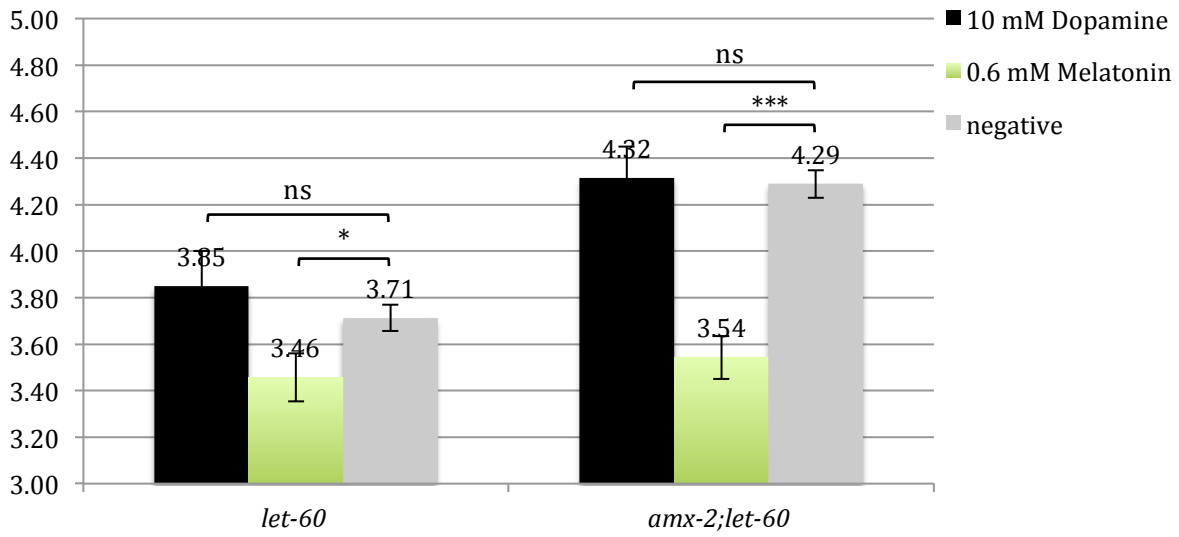

Figure 35: Effect of Dopamine and Melatonin on vulval induction in *let-60(gf)* and *amx-2(lf);let-60(gf) animals.* Dopamine (black) does not affect either mutant vulval induction. Melatonin instead inhibits vulval induction in both the lines, independent of *amx-2* (lime green). Error bars =SE, Mann-Whitney-U test, *p<0.05, *** p<0.001

In conclusion it seems that *amx-2* primarily uses Serotonin but not Dopamine as substrate to suppress EGFR/RAS/MAPK signalling during vulval development. In addition, Melatonin, which uses Serotonin as precursor molecule, showed similar suppressive effects.

1.7.6.1 5-HIAA Affects EGFR/RAS/MAPK Signalling

Since Melatonin had an effect on RAS signalling, we tested the main Serotonin metabolite 5-HIAA for an effect on signalling. Indeed, 5-HIAA was able to suppress vulval hyperinduction in both genetic backgrounds *let-60(n1046)* and *amx-2(ok1235);let-60(n1046)* (Figure 36). In contrast to the effects observed with Serotonin, there is no critical concentration identified, suggesting that the effect of 5-HIAA is independent of *amx-2*. This is to be expected, since 5-HIAA is metabolically downstream of *amx-2* function.

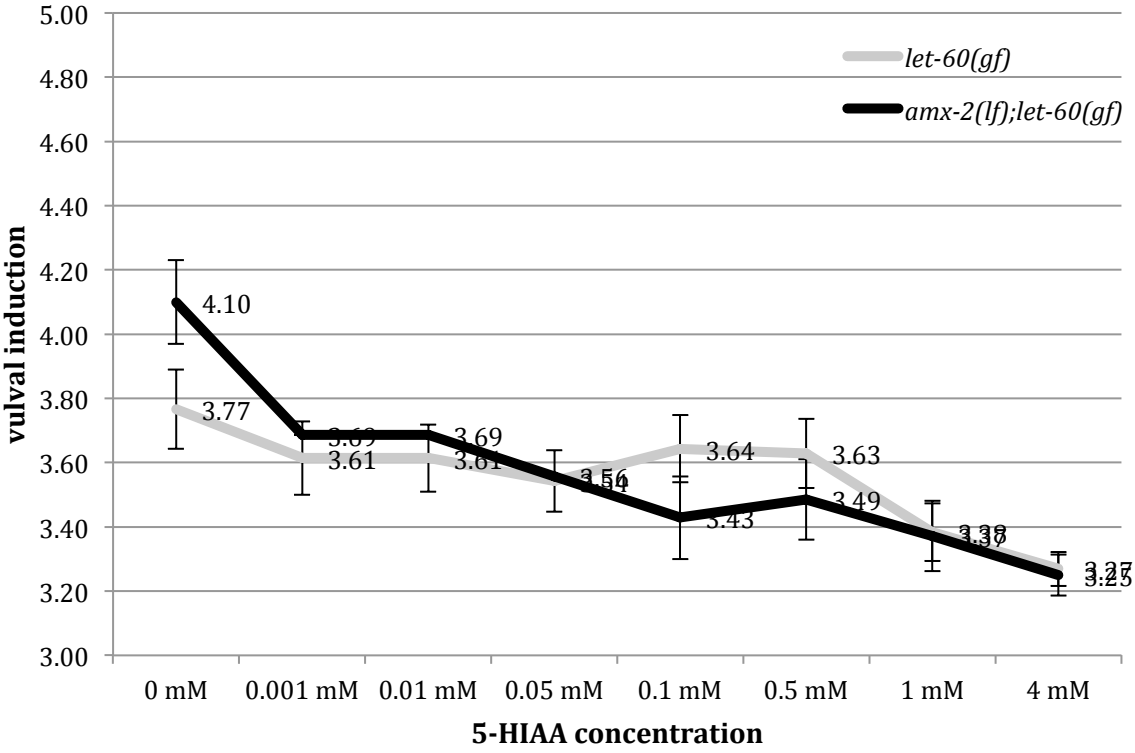

Figure 36 Effect of 5-HIAA on vulval induction in *let-60(gf)* and *amx-2(lf);let-60(gf) animals.* 5-HIAA at high concentration is able to strongly suppress vulval induction in both the mutants. No critical concentration between the genetic backgrounds can be identified. Error bars =SE

In summary, 5-HIAA, maybe in combination with Melatonin, is able to strongly inhibit EGFR/RAS/MAPK signalling during vulval development. The fact that 5-HIAA has a weaker effect than Serotonin might arise from the possibility of Serotonin still being able to be converted into both Melatonin and 5-HIAA that together more strongly repress. If only 5-HIAA is applied, this additional inhibitory branch is not present.

1.7.6.2 5-HIAA Acts Downstream of RAS or in a Parallel Pathway

We further wanted to know at what position 5-HIAA exerts its function in the pathway. We investigated the suppressive action of 5-HIAA in two more mutants of the EGFR/RAS/MAPK pathway. In *mpk-1(gf)* and *lin-1(lf)* mutants we could demonstrate that 5-HIAA does not have an effect anymore, suggesting its role upstream of *mpk-1* (Figure 37). We cannot exclude 5-HIAA to act in a yet unknown parallel pathway.

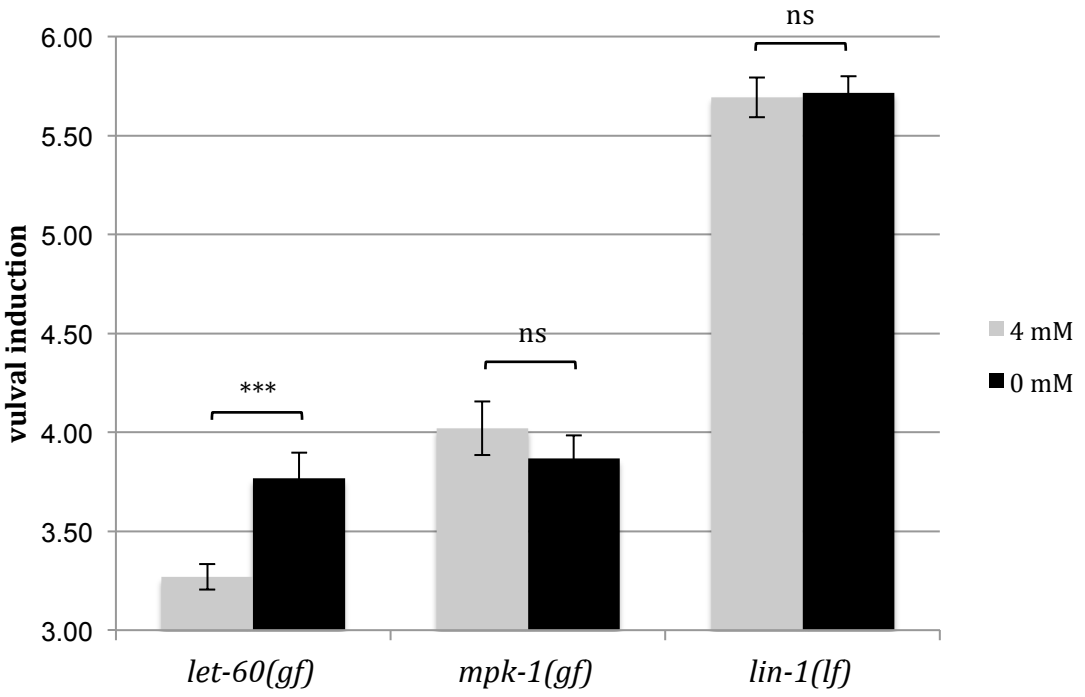

Figure 37: Epistatic analysis of 5-HIAA action on EGFR/RAS/MAPK signalling. In contrast to *let-60(gf)*, 5-HIAA is not able to suppress vulval induction in *mpk-1(gf)* and *lin-1(lf)* mutants and therefore has to act upstream of *mpk-1* and downstream of *let-60* or in a parallel pathway. Error bars =SE, Mann-Whitney-U test, *** p<0.001

1.7.6.3 Global, Systemic Role of 5-HIAA

5-HIAA might besides its role to repress RAS signalling in the developing vulva have a more global role and will act in other tissues likewise. To test this hypothesis we analysed the development of two more RAS dependent tissues, the development of the excretory system and oocyte maturation in the adult germ line. Under hyperactivated RAS conditions, the development of the excretory system will produce 2 duct cells instead of only one (Berset, 2005), and improper maturation of oocytes will lead to accumulation of oocytes at the proximal end of the germ line (Stetak, Gutierrez, & Hajnal, 2008). Duct cell duplications were scored in a *let-60(n1046)* with the help of *lin-48::gfp* reporter that marks the duct cells. Oocyte maturation was scored in a *let-60(ga89ts)* mutant at 25°C Application of 5-HIAA was able to supress both phenotypes, similar to the vulva (Figure 38, Figure 39). In conclusion, 5-HIAA seems to affect RAS signalling tissue-independent.

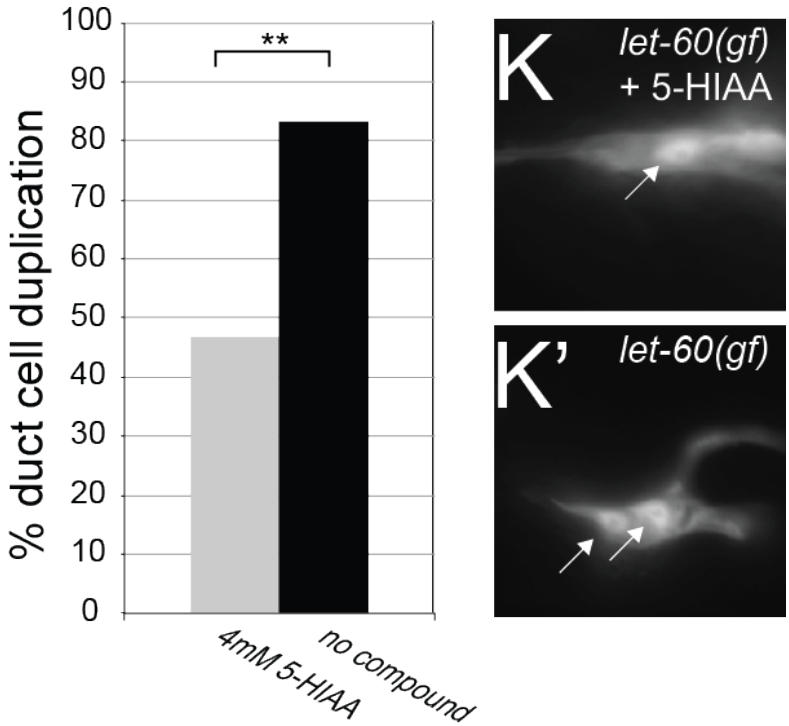

Figure 38: Global effect of 5-HIAA. Overacting RAS during the development of the excretory system. Application of 4 mM 5-HIAA reduced the number of duplicated ducts significantly. Fisher's exact test, ** p<0.01

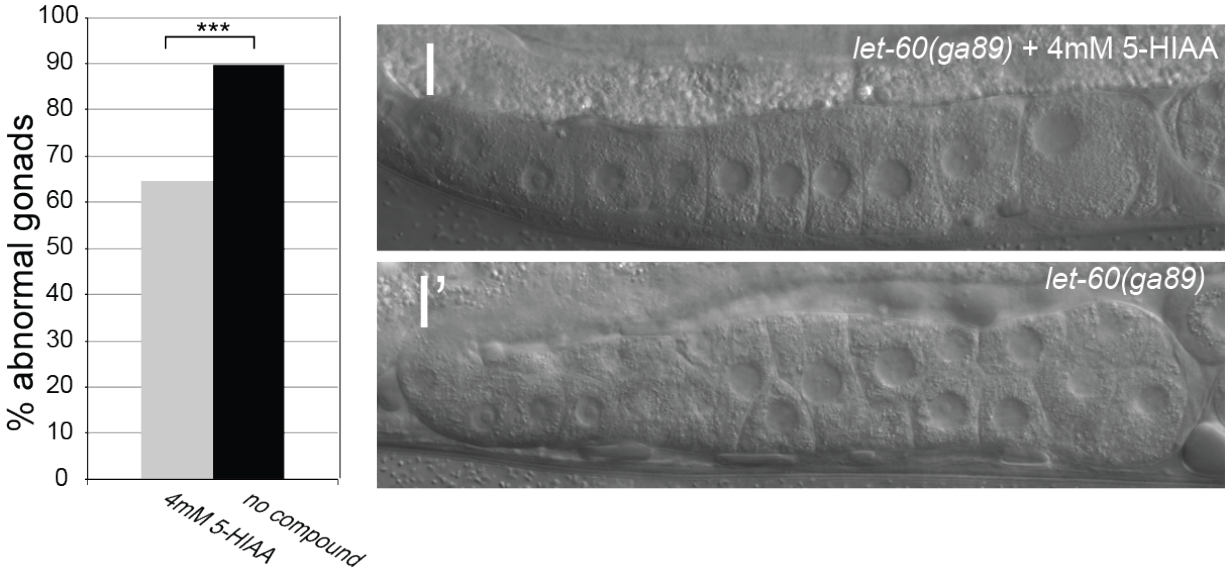

Figure 39: Global effect of 5-HIAA. Overacting RAS during oocyte maturation. Application of 4 mM 5-HIAA reduced the development of abnormal oocytes, stacking up in the proximal region of the adult germline. Fisher's exact test, ** p<0.01, *** p< 0.001

1.7.6.4 5-HIAA Decreases the Ratio of Phosphorylated vs Total Forms of ERK1,2

The ratio of phosphorylated vs. total ERK usually serves as a downstream readout for RAS signalling activity. One of the possibilities could be that 5-HIAA affects this ratio and therefore

decreases signalling strength. We analysed western blots probed with antibodies recognising phosphorylated and total form of ERK and were able to demonstrate that 5-HIAA significantly decreases the ratio of phospho/total ERK (Figure 40).

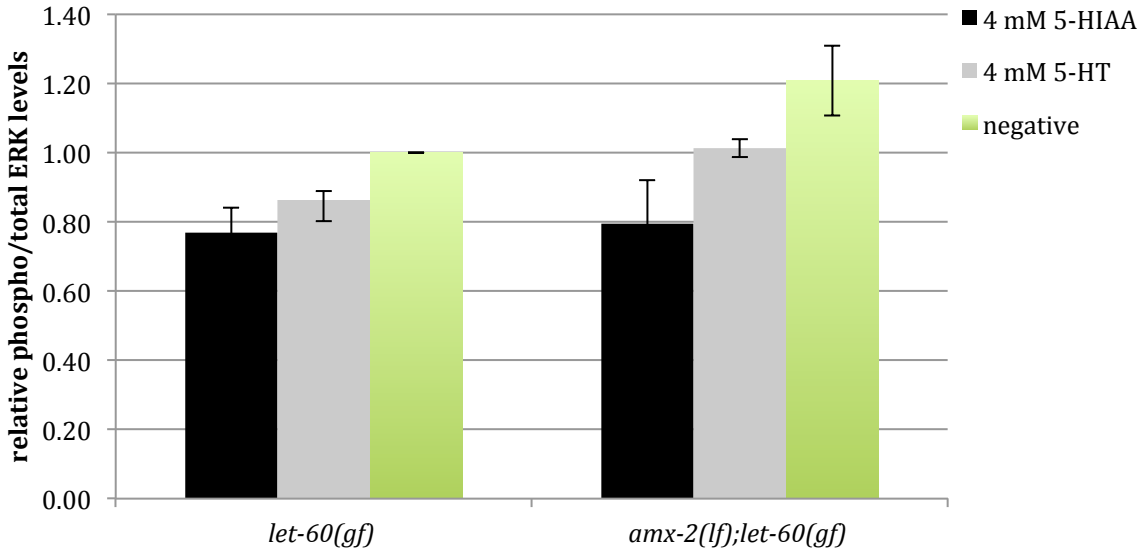

Figure 40: Ratio of phospho/total ERK. Treatment with high dose of 5-HIAA leads to strong reduction in the phospho/total ERK ratio. Serotonin has the same effect, although weaker.

1.7.7 Functional Conservation of 5-HIAA in Higher Organisms

Since 5-HIAA exerts such a consistent, tissue-independent effect, we tested if this mechanism is alsoconserved in vertebrates. We therefore chose different human cell lines to study and included the M010817 melanoma, HCT116 colon carcinoma and MB-MDA223 breast adenocarcinoma cells, that all contain K-Ras mutations.

1.7.7.1 5-HIAA Decreases the Ratio of Phosphorylated ERK/total ERK

We first investigated phosphorylation of ERK in M010817 cells and could show that the ratio of phospho/total ERK decreases with increasing 5-HIAA concentration (Figure 41).

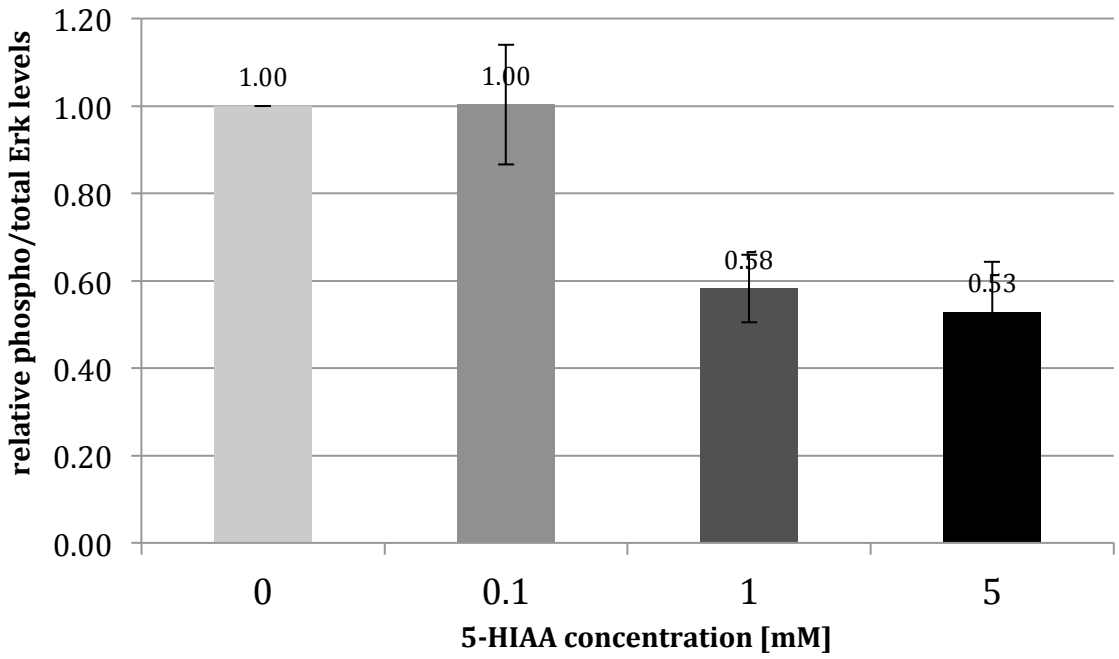

Figure 41: Effect of increasing 5-HIAA concentration on phospho/total ERK ratio in M010817 melanoma cells. With increasing concentration, the ratio of phospho/total ERK decreases.

Results from the HCT116 and MB-MDA223 cell lines were inconclusive due to high variability between biological samples (data not shown).

1.7.7.2 5-HIAA Affects Growth and/or Survival of Cells

Since semi-quantitative analysis of western blots only captures a still image and suffers from limitations, we examined the role of 5-HIAA more deeply in MTT (3-(4, 5-dimethylthiazolyl-2)-2,

5-diphenyltetrazolium bromide) growth assays. MTT is a substance that is converted to insoluble purple formazan in the presence of NAD(P)H-dependent cellular oxidoreductase enzymes, indirectly reflecting the viability of the cell. Therefore, the more formazan built, the more cells are alive and growing. We tested growth and/or survival of the three different cell lines M010817, HCT116 and MB-MDA223 under increasing concentrations of 5-HIAA and could show that different concentrations of 5-HIAA suppressed the growth and/or survival of the cells (Figure 42).

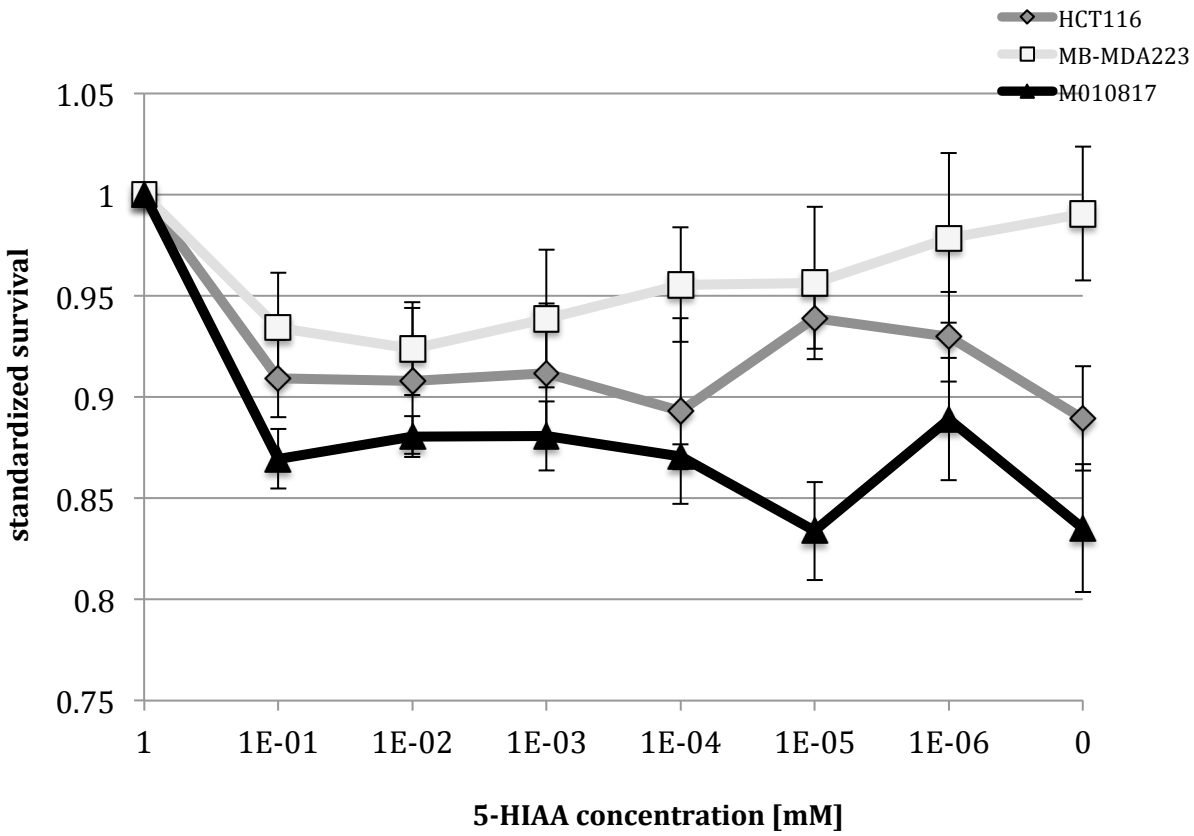

Figure 42: MTT assay with cell lines M010817, HCT116 and MB-MDA223 and increasing concentration of 5-HIAA. Strongest effect is visible in M010817 cells, as those are probably the least cancerous like cell lines.

We will further evaluate the role of 5-HIAA on phosphorylated/total ERK level using a more precise FRET based system In addition we will assess the function of 5-HIAA on the growth of cancer cells using the more precise soft agar method (Sato & Kan, 2001). In addition, we will include the analysis of HEK cells as less cancerous and still growth factor stimulus dependent.

1.8 AMX-2 publication manuscript draft:

Systemic regulation of RAS/MAPK signaling by the Serotonin metabolite 5-HIAA

T. Schmid[1,2], B. Snoek[3], M. Rordiguez[3], E. Fröhli[1], L. van der Bent[3], J. Kamenga[3], A. Hajnal[1,*]

[1]University of Zurich, Institute of Molecular Life Sciences, Winterthurerstrasse 190 CH-8057 Zurich, Switzerland.

[2]PhD Program in Molecular Life Sciences

[3]Laboratory of Nematology, Wageningen University, Droevendaalsesteeg 1, 6708PB, Wageningen, The Netherlands

[*]Correspondence to: alex.hajnal@imls.uzh.ch

Keywords: signal transduction, MAP kinase, serotonin, *Caenorhabditis elegans*.

Running Title: Systemic regulation of RAS/MAPK signaling

18. Juli 2014 16:15

Abstract

The genetic background profoundly affects the outcome of oncogenic mutations in signal transduction pathways. Here, we have used a quantitative genetics approach in *C. elegans* to identify modifiers of the conserved RAS/MAPK signaling cascade. A RIL set containing a mutation in the RAS homologue *let-60(gf)* in a mixed Hawaii/Bristol background shows strong variation in the penetrance and expressivity of the phenotype when compared to the mutant *let-60(gf)* in the "pure" Bristol background. We further mapped QTL regions and identified AMX-2, homologous to human MAOA as a negative regulator of RAS signaling. We further demonstrate that the metabolite produced by MAOA, 5-HIAA is responsible for the down-regulation of RAS signaling both in *C. elegans* and in human cancer cell lines. This finding indicates a similar mechanism for 5-HIAA to suppress RAS signaling in vertebrates and may serve as novel adjuvant in the treatment of cancer.

One Sentence Summary:

Monoamine oxidase-A globally regulates RAS/MAPK signaling through production of the serotonin metabolite 5-HIAA.

Human cancer is a complex multigenic disease caused by the combination of somatic mutations in oncogenes and tumor suppressor genes together with background mutations in cancer susceptibility genes. While many of the oncogenes and tumor suppressor genes that acquire mutations in different types of cancer are well characterized, relatively little is known about the effect of the genetic background, in which these oncogenic mutations occur, on the progression and outcome of the disease.

Individual components of the EGFR/RAS/MAPK signaling pathway are mutated in the majority of all human carcinoma. In particular, activating ("gain-of-function") mutations in HRAS and KRAS are among the most prevalent mutations found in tumor cells {Prior:2012dr}. Thanks to the strong conservation of the EGFR/RAS/MAPK pathway in metazoans, genetic studies in model organisms have provided new insights into various factors regulating EGFR/RAS/MAPK signaling. The Nematode *C. elegans* is an excellent model to study how the genetic background modifies the effects of EGFR/RAS/MAPK pathway mutations. Here, we have used quantitative genetics (Gaertner & Phillips, 2010) to explore how the genetic background affects the phenotypes caused by the activating G13E mutation *n1046* in the *ras* gene *let-60,* which is similar to the HRAS and KRAS mutations found in many cancers {Prior:2012dr}.

We compared RAS/MAPK signaling in the two most diverse genetic backgrounds available, *C. elegans* varieties Bristol (N2) and Hawaii (CB4856) (Koch, van Luenen, van der Horst, Thijssen, & Plasterk, 2000), (Andersen et al., 2012). To measure the activity of the RAS/MAPK pathway, we initially used vulval induction as a reliable and quantifiable readout. During larval development, the anchor cell (AC) in the somatic gonad secretes the EGF-like ligand LIN-3 to activate the EGF receptor LET-23 in the vulval precursor cells (VPCs) P3.p through P8.p (Sternberg, 2005). The VPC closest to the AC (P6.p), which receives most of the EGF signal, exhibits highest MAPK activation and adopts the 1° cell fate (**Fig. 1A**). P6.p then expresses DSL family ligands that activate the NOTCH pathway in the neighboring VPCs to induce the 2° vulval cell fate in P5.p and P7.p. The remaining VPCs, P3.p, P4.p and P8.p, that receive low levels of EGF and DSL signals adopt the 3° uninduced cell fate. In the wild-type, three of the six VPCs adopt a vulval cell fate. Mutations that hyperactivate EGFR/RAS/MAPK signaling, such as the *n1046* allele, cause the differentiation of more than three and up to six VPCs and a Multivulva phenotype, while mutations that reduce EGFR/RAS/MAPK signaling result in the induction of fewer than three VPCs and a Vulvaless phenotype. Hence, the average number of induced VPCs per animal (VI index) is a quantitative measure of EGFR/RAS/MAPK activity in the VPCs (Sternberg & Horvitz, 1986) (Sternberg, 2005).

We generated a set of 228 recombinant inbred lines (RILs) between the Bristol strain MT2125 that carries the activating *ras* mutation *let-60(n1046gf)* and a wild isolate from Hawaii (CB4856) (**Fig. 1B**). Since small genetic variations are efficiently buffered in a wild-type genome (Milloz, Duveau, Nuez, & Félix, 2008), the inclusion of the *let-60(gf)* allele created a sensitized genetic background, allowing us to identify genetic modifiers that increase or decrease RAS/MAPK signaling. After 10 generations of inbreeding, 162 of the RILs were genotyped using 72 fragment length polymorphisms (FLPs) as described in (Zipperlen et al., 2005) (**Fig. 1C**, top). In addition, we quantified EGFR/RAS/MAPK activity in each RIL by measuring the VI index (Sternberg & Horvitz, 1986). While the *let-60(gf)* allele in the Bristol background exhibits a VI of 3.7±0.06, the VIs of the RILs varied between 3.0 and 5.6 (**Fig. 1C**, bottom). Quantitative trait loci (QTL) mapping identified at least four loci on chromosomes I (QTL1), II (QTL 2 and 3) and V (QTL 4) above the threshold LOD of ±3. (**Fig. 1D**, see Methods). Since the *let-60(gf)* mutation maps to chromosome IV, our approach did not permit us to identify QTLs on this chromosome. To confirm and refine the mapping of the QTLs, introgression lines (ILs) carrying portions of the Hawaii genome in regions of interest (Doroszuk, Snoek, Fradin, Riksen, & Kammenga, 2009) were crossed to the *let-60(gf)* Bristol strain. Lines homozygous for the introgressions and the *let-60(gf)* mutation were compared to siblings obtained from the same crosses that did not carry the introgressions to identify those introgressions that cause differences in the VI. The results for the fine mapping of QTL1 are shown in **Fig. 2A** and for all QTLs in **suppl Fig S1**. IL mapping

revealed that QTL1 is composed of two adjacent QTLs 1a and 1b and that QTL1b maps to an interval of 1.43 Mbp containing 142 polymorphic genes (**Fig. 2A**). We next performed RNAi knockdown of 110 of the 142 candidates in *let-60(gf)* single mutants and *let-60(gf)* mutants carrying the *ewIR17* introgression (**suppl Tab. S1**). Of particular interest were candidates exhibiting alleles specific RNAi effects, i.e.knockdowns changing VI in the *ewIR17; let-60(gf)* but not the *let-60(gf)* background or vice versa, as they likely define polymorphic modifiers of RAS signaling. Among the 36 RNAi clones altering the VI, *amx-2* was chosen for further analysis because it fulfilled all the criteria as polymorphic modifier. *amx-2i* had no significant effect on the *ewIR17; let-60(gf)* background, but increased the VI of *let-60(gf)* mutants (**Fig. 2B**). Furthermore, the *amx-2(ok1235)* deletion allele, which probably represents a null allele (Wormbase, pers. communication), increased the VI of *let-60(gf)* mutants in the Bristol background (**Fig. 2C**). To individually asses the activities of the Bristol and Hawaii *amx-2* variants, we generated single copy insertions (Frøkjær-Jensen et al., 2008) of an 7.8 kb genomic fragment spanning the *amx-2* locus isolated from the Bristol or Hawaiian genomes and introduced them into *amx-2(lf); let-60(gf)* double mutants. Insertion of the Bristol but not the Hawaii *amx-2* variant reduced the VI of *amx-2(lf); let-60(gf)* double mutants to the value observed in *let-60(gf)* single mutants (**Fig. 2C**). These results confirm the different physiological activities of the two *amx-2* variants. In addition, *amx-2(lf)* partially suppressed reduction-of-function mutations in *let-60 ras* and the EGFR homolog *let-23*, in which the VI is decreased below wild-type levels, and the *let-23* gain-of-function mutation *sa62* was further enhanced by *amx-2(lf)* (**Fig. 2D**). Thus, *amx-2* negatively regulates EGFR/RAS/MAPK signaling in the VPCs. To determine the site of *amx-2* action, we generated transcriptional $P_{amx\text{-}2}$*>gfp* reporters. *amx-2* is expressed in head neurons, the intestine and, a subset of cells of the rectum and in the adult vulva (**Fig. 2E-H**). We did not detect any *amx-2* expression in the vulval cells during induction. Moreover, neurons generally have a low sensitivity to RNAi (Timmons, Court, & Fire, 2001), yet *amx-2i* efficiently phenocopied the *amx-2(lf)* phenotype. We thus suspected that *amx-2* might act in the intestinal cells where we detected prominent expression. Intestine-specific *amx-2i* using an *rde-1(lf); let-60(gf);* $P_{elt\text{-}2}$*>rde-1(+)* strain (Pilipiuk, Lefebvre, Wiesenfahrt, Legouis, & Bossinger, 2009) increased the VI to a similar degree as systemic RNAi, while vulva-specific RNAi using $P_{lin\text{-}31}$*>rde-1(+)*(Haag et al., 2014) had no detectable effect (**Fig. 2I**, note that the overall lower VI in the vulva-specific RNAi strain is due to the genetic background). Finally, we measured the transcript levels of *amx-2* and its paralog *amx-1* by quantitative real-time PCR. The abundance of *amx-2* and *amx-1* transcripts was not significantly different between the Bristol and Hawaii backgrounds (**Fig. 2J**). However, *amx-2* levels were around 60% decreased and *amx-1* levels were 40% increased in *amx-2(lf)* mutants.

amx-2 encodes a member of the mitochondrial monoamine oxidase (MAO) family (**suppl.**

Fig. S2) (Tipton, Boyce, O'Sullivan, Davey, & Healy, 2004). AMX-2 is most similar to human MAO-A with 20% sequence identity between the catalytic domains followed by MAO B (19% identity) and L-amino oxidase (15% identity). The Hawaii AMX-2 possesses two coding polymorphisms in its catalytic domain (V410I and N416S) and 4 are located in the C-terminal region (R521G, T532S, N535S and L617P) (**suppl. Fig. S3**). MAOs are key enzymes in the degradation of the neurotransmitters serotonin (5-HT) and Dopamine (L-DOPA) (**Fig. 3A**) (Kalgutkar, Dalvie, & Castagnoli, 2001). The products of the L-DOPA and 5-HT deamination reactions, 3,4-Dihydroxyphenylacetaldehyde and 5-Hydroxyindole-acetaldehyde respectively, are further oxidised by aldehyde dehydrogenases into 3,4-Dihydroxyphenylacetic acid and 5-Hydroxyindole-acetic acid (5-HIAA), which in humans is secreted through the kidneys (**Fig. 3A**).

We thus investigated if the MAO AMX-2 inhibits RAS/MAPK signaling by controlling the levels of L-DOPA, 5-HT or one of its metabolites. The addition of 10mM L-DOPA into the growth medium had no significant effect on the VI of *let-60(gf)* single or *amx-2(lf); let-60(gf)* double mutants (**Fig. 3B**). However, addition of 1mM 5-HT as well as 1mM of the 5-HT metabolite 5-HIAA caused a strong reduction of the VI in both backgrounds (**Fig. 3B,C,C'**). Also, 0.6mM melatonin (MT) had a slightly weaker yet significant effect on the VI. We therefore conclude that the 5-HT metabolites, in particular 5-HIAA, inhibit RAS/MAPK signaling. To test the sensitivity of the RAS/MAPK pathway to 5-HT and 5-HIAA, we performed dose-response experiments in the presence and absence of *amx-2*. For both compounds, the maximum reduction of the VI was observed at concentrations above 1mM (**Fig. 3D,E**). However, *let-60(gf)* single mutants displayed a higher sensitivity to low concentrations (1µM) of 5-HT than *amx-2(lf); let-60(gf)* double mutants, while the effects of 5-HIAA were independent of the *amx-2* genotype. Overall, 5-HT exerted a slightly stronger effect than 5-HIAA, suggesting that additional 5-HT metabolites besides 5-HIAA may inhibit RAS/MAPK signaling. To determine at which step 5-HIAA regulates the RAS/MAPK pathway, we examined a strain expressing an activated form of the MAPK MPK-1 along with the MAPKK MEK-2 (*mpk-1(gf)*) (Lackner & Kim, 1998). Application of 4mM 5-HIAA did not alter the VI of *mpk-1(gf)* mutants, indicating that 5-HIAA inhibits signaling upstream of MPK-1 (**suppl. Figure S4**). Furthermore, 5-HIAA did not affect a *lf* mutation in *lin-1*, which encodes and ETS family transcription factor that represses vulval induction downstream of MPK-1 and is inactivated through MPK-1 phosphorylation (**suppl. Figure S4**) (Jacobs, Beitel, Clark, Horvitz, & Kornfeld, 1998) (Sternberg, 2005). We further quantified total phospho-MPK-1 levels in extracts of L4 larvae as described (Lackner & Kim, 1998). 5-HT and 5-HIAA caused a similar reduction in phospho-MPK-1 levels in *let-60(gf)* mutants, yet in the *amx-2(lf); let-60(gf)* background 5-HIAA exerted a stronger effect than 5-HT (**Fig. 4A**). Since the RAS/MAPK signaling is required in multiple tissues of *C. elegans* (Lackner & Kim, 1998), we tested if 5-HIAA acts as a global inhibitor of the RAS/MAPK pathway. For example, the temperature-sensitive *let-*

60(ga89gf) allele causes accelerated exit of meiotic germ cells from the pachytene stage, resulting in the accumulation of many immature oocytes in the proximal gonad arm at the restrictive temperature (**Fig. 3F,G'**) (Stetak, Gutierrez, & Hajnal, 2008). In addition, *let-60(n1046gf)* mutants frequently contain two duct cells (**Fig. 3H,I'**). Application of 4mM 5-HIAA partially suppressed the *let-60(gf)* phenotypes in the germ line and the duct cell (**Fig. 3F,G,H,I**). Thus, 5-HIAA exerts a systemic effect to globally inhibit RAS/MAPK signaling in different organs of *C. elegans*.

Finally, we tested if 5-HIAA exerts similar effects on the RAS/MAPK pathway in mammalian cells. We first measured the growth rates of 3 human cell lines derived from melanoma (M010817), colon (HCT116) and breast (MDA-MB231) cancers that all contain activating G13D mutations in KRAS (**Fig. 4C**) (Civenni et al., 2011), (Scholl et al., 2009). Direct addition of 5-HIAA into the culture medium exerted a growth inhibiting effect at concentrations as low as 1nM. Interestingly, in some cell lines, most pronounced in MDA-MB231, the growth inhibiting effect was diminished at concentrations above 1µM, suggesting a hormetic dose response (Calabrese, 2013). Consistent with the results obtained in *C. elegans*, phospho-ERK2 levels in serum-stimulated HEK293 cells were reduced after pretreatment with 5-HIAA (**Fig. 4B**). We conclude that 5-HIAA reduces ERK2 activation in human cells.

Increasing evidence indicates that the genetic background profoundly influences the onset and progression of human cancer, yet the molecular identities of these genetic risk factors are largely unknown (Freeman et al., 2006). By using quantitative genetics to compare the genetic background of two *C. elegans* isolates, we have identified genetic modifiers of the oncogenic RAS/MAPK signaling pathway. These modifiers could not have been found in conventional forward genetic screens, as each locus alone only exerts a minor effect. In particular, our approach has led to the identification of the MAO AMX-2 as a global negative regulator of RAS/MAPK signaling in multiple organs of *C. elegans*. AMX-2 functions in intestinal cells by catalyzing the production of 5-HT metabolites such as 5-HIAA. The fact that 5-HT exerts some inhibitory effects even in *amx-2* mutants may be explained by the presence of additional redundant MAOs, especially AMX-1. Epistasis analysis indicates that the systemic application of 5-HIAA inhibits MAPK activation at a step downstream of RAS and upstream of MAPK. Thus, AMX-2 in the intestine may globally tune the activity of the RAS/MAPK pathway in response to changes in environmental conditions or food intake by releasing 5-HIAA and other 5-HT metabolites.

The role of 5-HT as a neurotransmitter in the nervous system is well studied. However, over 90% of the 5-HT in the human body is found outside of the nervous system, especially in enterochromaffin cells of the intestine (Tipton et al., 2004). Remarkably, (Rybaczyk, Bashaw,

Pathak, & Huang, 2008) reported that the expression of the 5-HT degrading enzyme MAO-A, the closest AMX-2 homolog, is consistently down-regulated across many human tumor types and model organisms. The functional implications and mechanism of reduced MAO-A expression in tumors has been unclear. Our findings that systemic application of the 5-HT metabolite 5-HIAA inhibits RAS/MAPK signaling and proliferation in *C. elegans* and human cells may explain the physiological consequences of reduced MAO-A expression. Tumors expressing low levels of MAO-A generate less oncostatic 5-HIAA and at the same time contain higher levels of 5-HT. Moreover, 5-HT can promote tumour growth and survival via cross-talk to the RAS/MAPK pathway (Soll et al., 2009), (Pai, Marshall, Hernandez, Buckley, & Horseman, 2009) (Alpini et al., 2008). Thus, MAO-A levels may set a global threshold for the activation of the RAS/MAPK cascade by various extracellular signals. To our knowledge, the 5-HT metabolite 5-HIAA is the first endogenous small molecule that acts as a systemic inhibitor of the RAS/MAPK pathway.

Figures

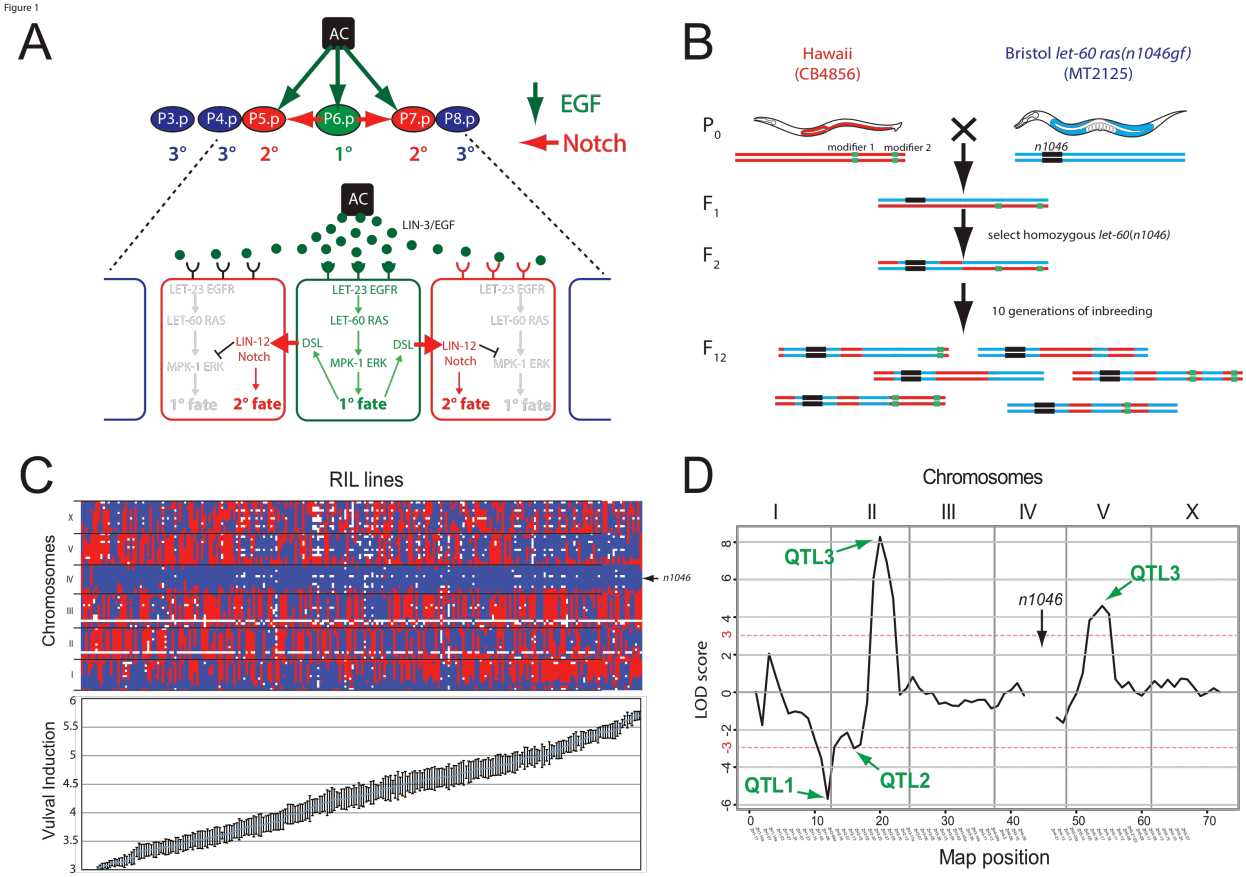

Figure 1. QTL mapping of *let-60 ras* modifiers

(A) Vulval development of *C. elegans*. P6.p receives the highest dose of the inductive EGF-like signal released by the Anchor cell (AC) thereby activating EGFR/RAS/MAPK signalling and adopting the 1° cell fate (green arrows). Lateral inhibition via components of the Delta-Notch pathway induces the 2° cell fate in the neighbouring cells P5.p and P7.p (red arrows). The remaining cells (blue) that neither receive the inductive nor the inhibitory signal will adopt the uninduced 3° cell fate. **(B)** Crossing scheme of the *let-60(gf)* mutation included recombinant inbred lines (miRILs). Hawaii males (red) were crossed with Bristol ras(gf) mutants (blue). Random segregation of the two parental genomes was allowed with the exception of the ras mutation, that was recovered homozygous from F2 generation onwards. Ten more rounds of self-reproduction was carried out to drive all regions to homozygosity and eventually generating the miRIL population. **(C)** Genotype and phenotype of the *let-60(gf)* miRIL population sorted by increasing vulval induction, error bars = SE. Depicted for the genotype are fragment length polymporphisms (FLPs) for the entire genome (y-axis) and miRIL number (x-axis); Hawaii genomic regions are indicated in red and Bristol genomic regions in blue. The phenotype of the corresponding genotype is shown below on the y-axis. **(D)** QTL mapping of the miRILs. Displayed are the four genomic regions above a threshold of LOD > 3. The effect on the phenotype for the *let-60(gf)* mutant is shown, where regions with negative LOD will decrease and regions with positive LOD will increase vulval induction; the opposite situation would be true for the CB4856 strain.

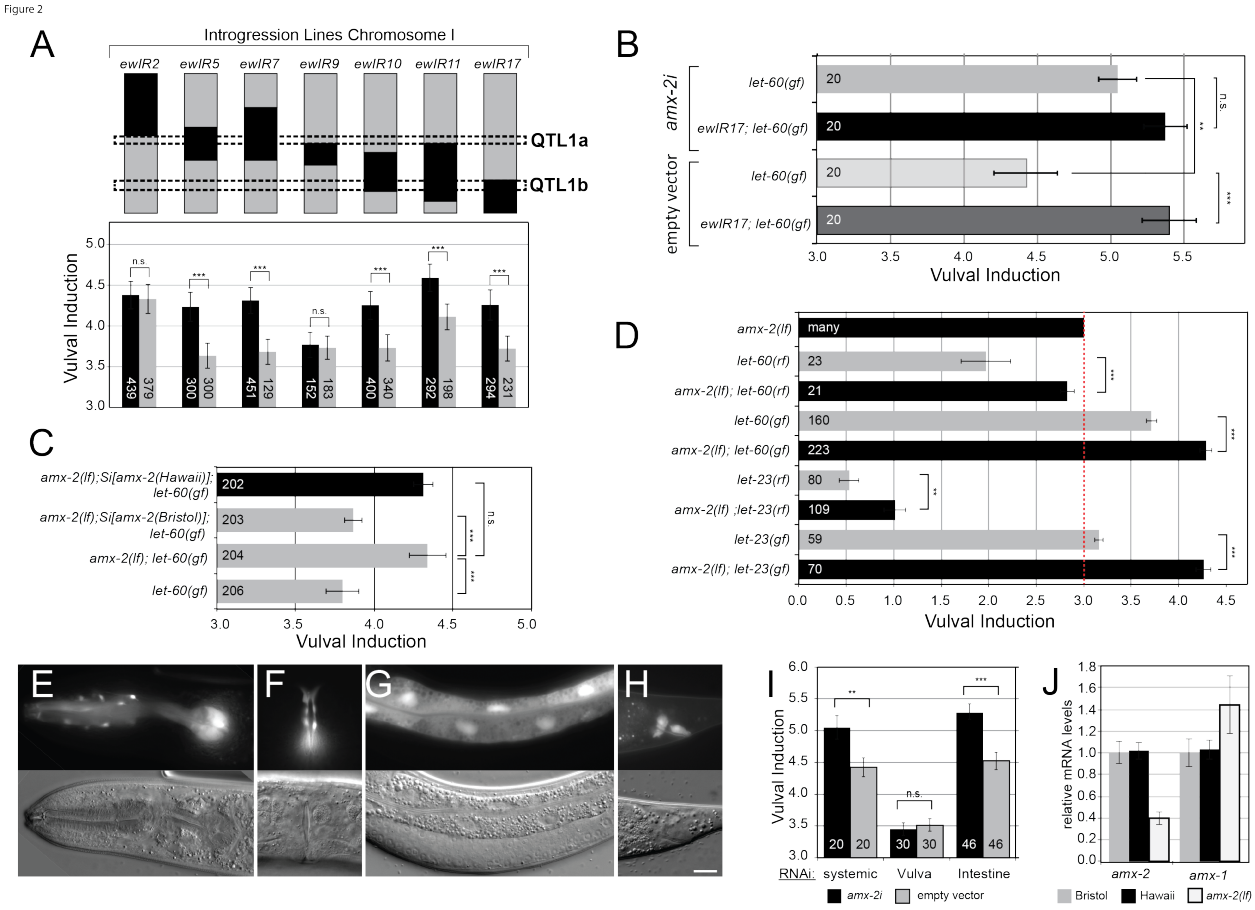

Figure 2. AMX-2 negatively regulates RAS/MAPK signaling

(A) Introgression line verification. The genomic regions for Bristol (blue) and Hawaii (red) are indicated on the corresponding lines. Vulval induction of siblings from the same cross was recorded for lines carrying the CB4856 introgression (red bars) vs. lines that are N2 (blue bars). Error bars = SE. **(B)** *amx-2* allele specific effects on ras signalling. Knockdown of *amx-2* via RNAi was carried out for the N2 (blue bar) and the CB4856 allele(red bar) and compared to empty vector control (light blue and red). Error bars = SE. **(C)** Differential activity of *amx-2* in N2 vs. CB4856. *amx-2(ok1235);let-60(n1046)* double mutants were rescued with two copies of the N2 (blue) or the CB4856 allele (red). Error bars = SE. **(D)** Epistasis analysis of *amx-2*. The loss of *amx-2* in mutants carrying the *let-23(rf)*, *let-23(gf)* and *let-60(rf)* alleles is indicated. Error bars = SE. **(E-H)** *amx-2* expression. The transcript of amx-2 is seen in head and pharyngeal neurons **(E)**, in the adult vulva **(F)**, in the complete gut lineage **(G)** and in a subset of cell of the rectum **(H)**. **(I)** Tissue specific RNAi of *amx-2*. In addition to systemic RNAi, knockdown of *amx-2* in the intestine and the vulva was carried out. **(J)** Quantitative PCR of *amx-2* and *amx-1*. Expression levels of *amx-2* and *amx-1* for N2, CB4856 and *amx-2(lf)* are indicated as fold change normalized to N2. Error bars = SD. Student's t-test * p<0.05, ** p<0.01, *** p<0.001

Figure 3

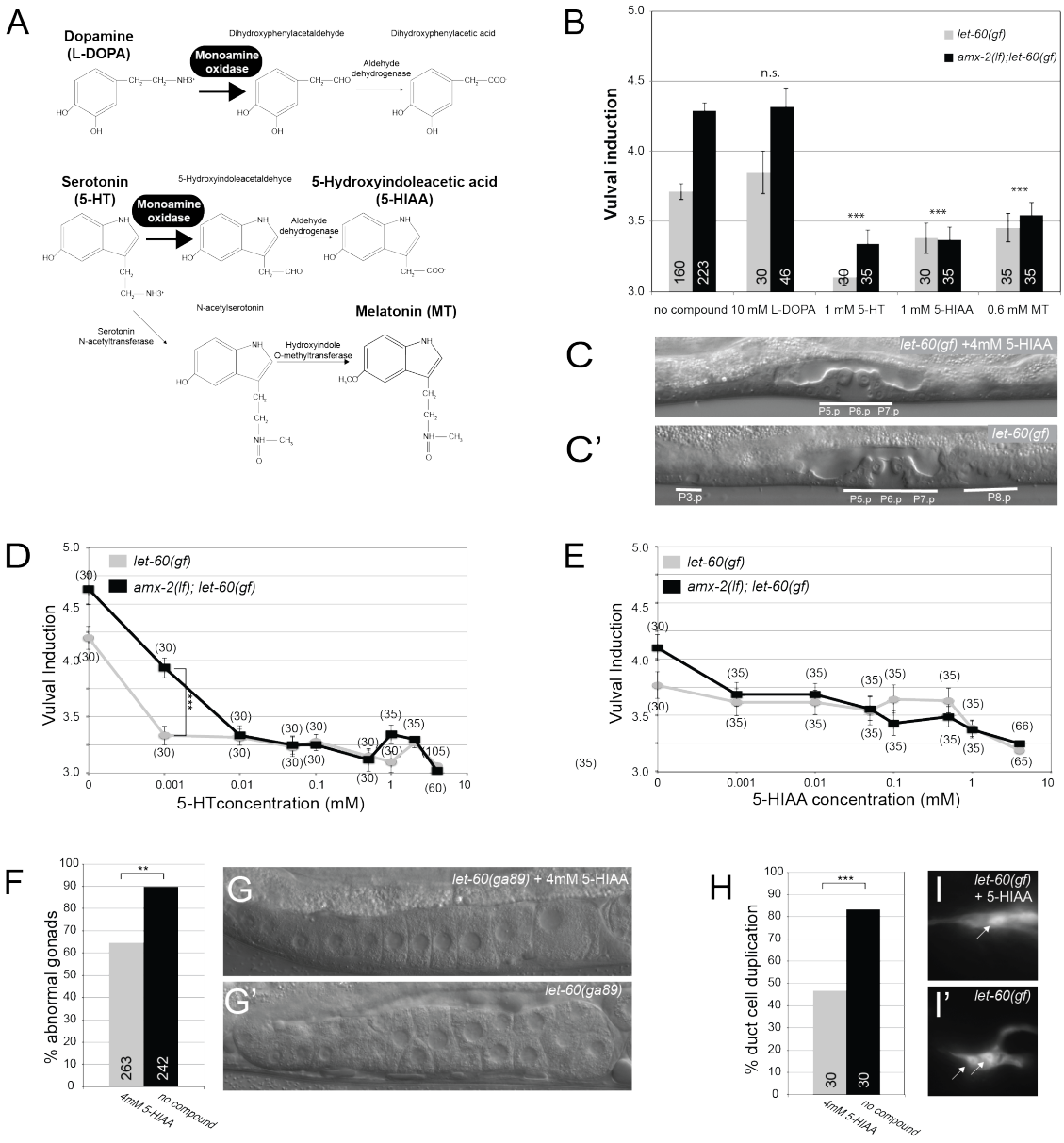

Figure 3. Systemic inhibition of RAS/MAPK signaling by serotonin and its metabolites

(A) Action of monoamine oxidase A on the metabolism of Dopamine (L-DOPA) Serotonin (5-HT) and Melatonin (MT). **(B)** Effect of L-DOPA, 5-HT and MT on vulval induction. *let-60(gf)* single and *amx-2(lf);let-60(gf)* genotypes are indicated in grey and black, respectively. Error bars = SE. Significance values as compared to the no compound treatment are indicated. **(C-C')** Effect of 5-HIAA on *let-60(gf)* mutants under Nomarski optics. **(D-E)** Dose dependence of 5-HT **(D)** and 5-HIAA **(E)** to reduce vulval induction in the *let-60(gf)* and *amx-2(lf);let-60(gf)* strains. Error bars = SE. **(F)** Effect of 5-HIAA on EGFR/RAS/MAPK signalling. Different mutant and their response to a high dose (grey) and no dose (black) of 5-HIAA is indicated. Error bars = SE. **(G)** Semi-quantitative analysis of MPK-1/ERK phosphorylation. The situation of *let-60(gf)* (grey bars) and *amx-2(lf);let-60(gf)* (black bars) for high doses of 5-HT and 5-HIAA are shown. Error bars = SE. **(H-J)** Global effects of 5-HIAA on different EGFR/RAS/MAPK dependent developmental processes; germline development **(H)** and development of the excretory system **(J)** is depicted. Student's

t-test: ** $p<0.01$, *** $p<0.001$.

Figure 4

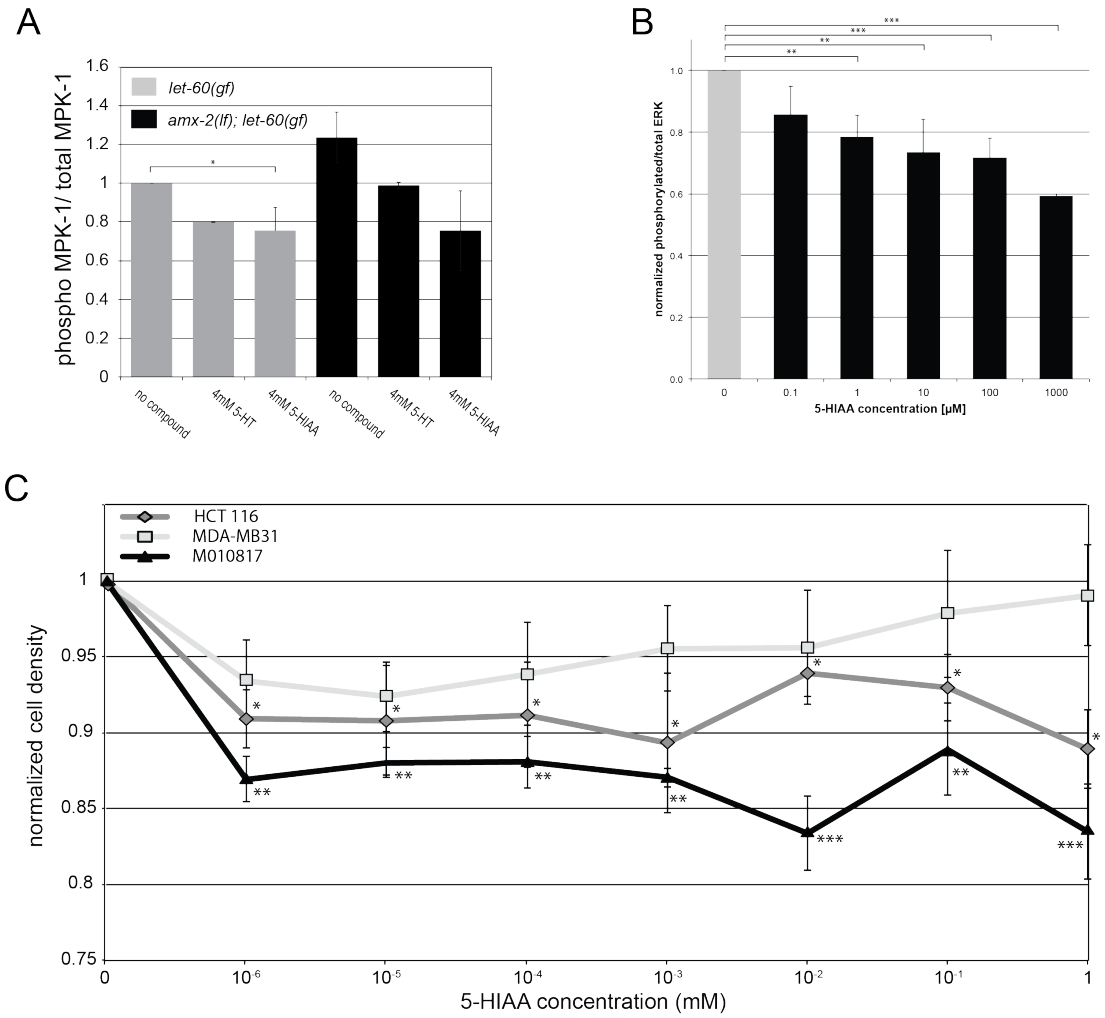

Figure 4. 5-HIAA inhibits ERK2 activation and proliferation in *C. elegans* and human cells

(A) Effect of 5-HT and 5-HIAA on the activation of ERK1,2. Whole worm protein extracts were probed with antibodies recognizing the phosphorylated and total form of ERK1,2 in the genetic backgrounds *let-60(n1046)* and *amx-2(ok1235);let-60(n1046)*. Error bars = SE. **(B)** Effect of different concentrations of 5-HIAA on the activation of ERK1,2 was tested in HEK 293 cells. Error bars = SE.**(C)** Different concentrations of 5-HIAA were applied to HCT116, MDA-MB231 and M010817 cell and cell proliferation was measured as normalized cell density in MTT assays. Error bars = SE from 4 replicates.

Supplementary Materials

Materials and Methods:

General methods and strains used:

Strains were maintained on NGM agar and on OP50 bacteria at 20°C, otherwise stated (Brenner, 1974).

Genetics strains: LGI: RB1190: *amx-2(ok1235)*; **LGII:** PS1839: *let-23(sa62)*, AH13: *let-23(sy1)*; **LGIV:** SD551: *let-60(ga89)*, MT2124: *let-60(n1046)*, MT4866: *let-60(n2021)*, MT822: *lin-1(n304)*

Transgenic strains: OLB11: r*de-1(ne219)*;Ex[elt-2p::rde-1(+);pRF4], AH2927: *let-60(n1046);rde-1(ne209);zh*Ex418[l*in-31p::rde-1;myo-2::mCherry*], SD1059: gaIS37[HS-*mpk-1*, HS-dmek], AH552: *let-60(n1046)*;saIS14[*lin-48p::gfp*]

Generation of miRILs: miRILs were generated by crossing CB4856 males with MT2124 hermaphrodites. In the F2 generation, lines homozygous for the *n1046* allele were singled out and selfed for 10 more generations of inbreeding. At generation F12, lines were regarded as isogenic and frozen for long-term storage.

Introgression lines for QTL confirmation: The mentioned ewIR from (Doroszuk et al., 2009) were crossed with the MT2124 mutant. FLP mapping as described in (Zipperlen et al., 2005) was further used to detect lines containing the introgression and the multivulva phenotype for the presence of the homozygous *n1046* allele. For analysis, Introgression lines harbouring the n1046 allele were compared to sibling lines containing the *n1046* allele only.

Double mutants and MosSCI integration lines: Transgenic line generation was carried out as described in (Frøkjær-Jensen et al., 2008). AH3007, AH3008, AH3013, AH3014, AH3024, AH3041, AH3042, AH3043: *amx-2(ok1235);zhIS73[N2-amx-2(+)];let-60(n1046),* AH3011, AH3012, AH3036, AH3040, AH3046, AH3047, AH3048, AH3049: *amx-2(ok1235);zhIS74[CB4856-amx-2(+)];let-60(n1046)* strains were compared to sibling lines containing l*et-60(n1046)* or *amx-2(ok1235);let-60(n1046)* only.

Transcriptional reporter of *amx-2*: Primers OTS219 (AAAAGGATCCTTAGGTTTATTGCTGGAAAAAT) and OTS220 (AAAAGGATCCCCTTAACCAAATTTCATACCC) were used to amplify 4kb of upstream promoter region. The PCR fragment was further cloned into BamHI restriction site of pPD95.67 to generate an N-terminal GPF fusion. Animals were co-injected with the pharyngeal marker p*myo-2*::mcherry.

Phenotyping: Vulval induction counting was used as the method to determine

EGFR/RAS/MAPK pathway activity during *C. elegans* vulval development as described in (Sternberg & Horvitz, 1986). The duct cell duplication phenotype was scored using AH552 (Berset, 2005), the presence of either one or two duct cells was scored using fluorescence microscopy. The oocyte maturation phenotype was scored using conventional light microscopy with nomarski optics (Stetak et al., 2008).

QTL mapping:

RNAi: Gene knockdown in *C. elegans* was carried out using RNAi feeding according to (Kamath, Martinez-Campos, Zipperlen, Fraser, & Ahringer, 2000). For intestine specific RNAi, OLB11 was crossed with the MT2124 mutant, for vulval specific RNAi, AH2927 was crossed with the MT2124 mutant.

Compound treatments: Standard NGM plates were supplemented with varying concentrations of Serotonin (5-HT) (H9523, Sigma**)**, 5-Hydroxyindoleacetic acid (5-HIAA) (H8876, Sigma), Dopamine (DOPA) (H8502, Sigma) or Melatonin (MT) (M5250 Sigma) and kept in dark at 4°C prior to use.

Western blot: The following Antibodies were used:

Anti-MAP Kinase (ERK-1, ERK-2): Sigma-Aldrich, M5670

Anti-MAP Kinase, Activated (Diphosphorylated ERK-1&2): Sigma-Aldrich, M8159

Anti-α-Tubulin: Sigma-Aldrich, T6074

I. elegans:

20 L4 hermaphrodites were placed in 20µl of 1x Laemmli sample buffer. Samples were boiled for 10 minutes at 95°C, then briefly centrifuged for 10-30 seconds at fullspeed and loaded on a 8% SDS gel. The gel was subsequently blotted on a PVDF (Milipore) membrane. The membrane was probed with the 1° antibody in 4% fat free milk/TBST (1:5000 for Anti-MAP Kinase and 1:1000 for Anti-MAP Kinase, Activated) overnight at 4°C. After washing the membrane, the membrane was probed with the 2° host specific antibody conjugated with HRP, 1:1000 in 4% fat free milk/TBST for 2 hours at room temperature. The Amersham ECL Prime Western Blotting Detection Reagent (RPN2332) was used and blots were imaged on an gel imager. Western blots were analysed using ImageJ with the integrated density function.

Cell culturing:

Human cancer cell lines were kept in culture flasks or on coated plates in an incubator at 37°C with 5% CO_2.

M010817

Cells were kept in RPMI medium (Dulbecco) supplemented with 10% FCS.

HCT116, MB-MDA223, HEK

Cells were kept in DMEM medium (Dulbecco) supplemented with 10% FCS.

Western blots:

HEK 293 cell were grown in media containing different concentrations of 5-HIAA. Prior to harvesting, cells were stimulated with EGF and subsequently harvested after 5 min of exposure to the growth factor.

Passaging and Trypsination: Cells were conventionally passaged/ harvested using trypsination.

MTT assay:

The method was adapted from (Mosmann, 1983).

Reagents:

PBS

MTT solution: 5mg/ml in PBS, freshly prepared and kept in dark at 4°C

Lysis solution: 0.1 N HCl in isopropanol

Procedure:

Cells were collected from a culture bottle and counted using a haemocytometer. Next, 4000 cells per well were seeded into 96 well culture plates and kept in 200 µl of either RPMI supplemented with 10% FCS (M010817) or in 200 µl of DMEM supplemented with 10% FCS (HCT116, MB-MDA231) for 24 h at 37°C 5% CO_2. The next day, almost all growth medium was aspired and 200 µl of fresh medium supplemented with different concentrations of 5-HIAA was added. Cells were incubated at 37°C 5% CO_2 for 48 h. Next, 40 µl of MTT solution was added per well and cells were left for 3-4 hours at 37°C 5% CO_2. Medium was aspired completely and 200 µl of Lysis solution was added. Pipetting up and down thereby helped to dissolve any formazan clumps. 94 well plates were covered with aluminium foil and absorption at 600 nm was read on a plate reader.

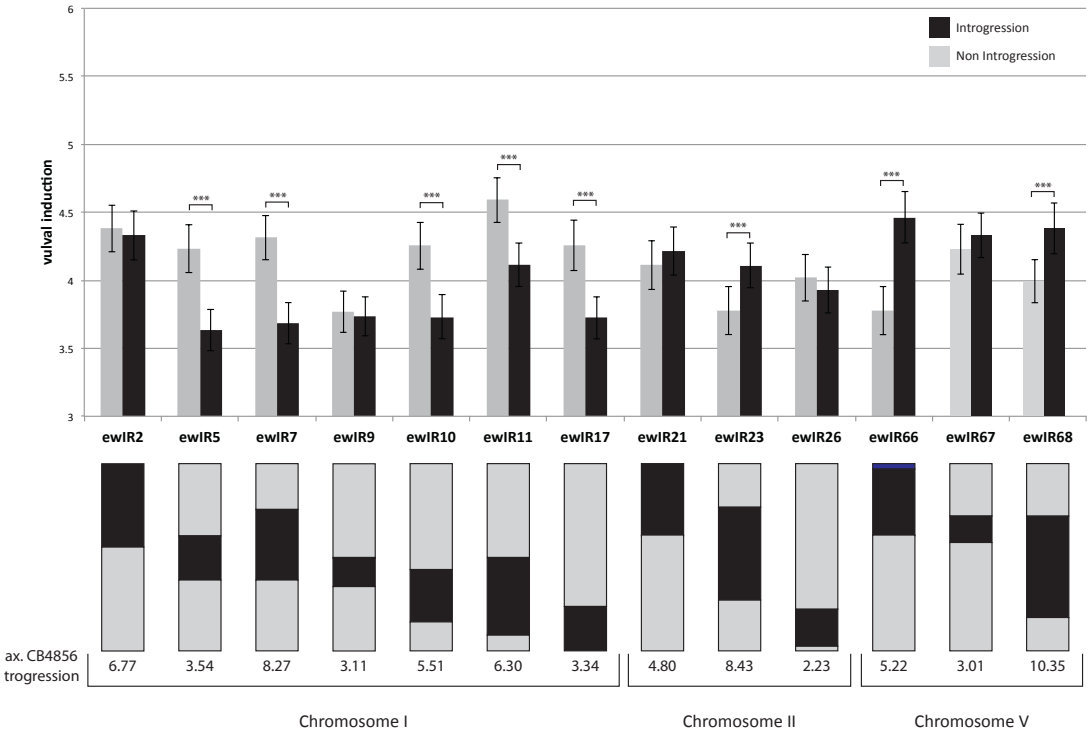

Figure S1. Fine-mapping of the QTLs shown in Figure 1D using ILs

Lines matching the corresponding putative QTL regions were chosen from (Doroszuk et al., 2009) and crossed with the *let-60(n1046)* mutant. Differences in vulval induction between the sibling lines with or without introgression verified the predicted QTL region. The use of several overlapping introgression lines was used to further narrow the genomic interval to smaller regions for follow up studies. The sizes and positions of the ewIR introgressions are depicted below. Error bars: SE, Student's t-test *** p<0.001.

suppl. Figure S2

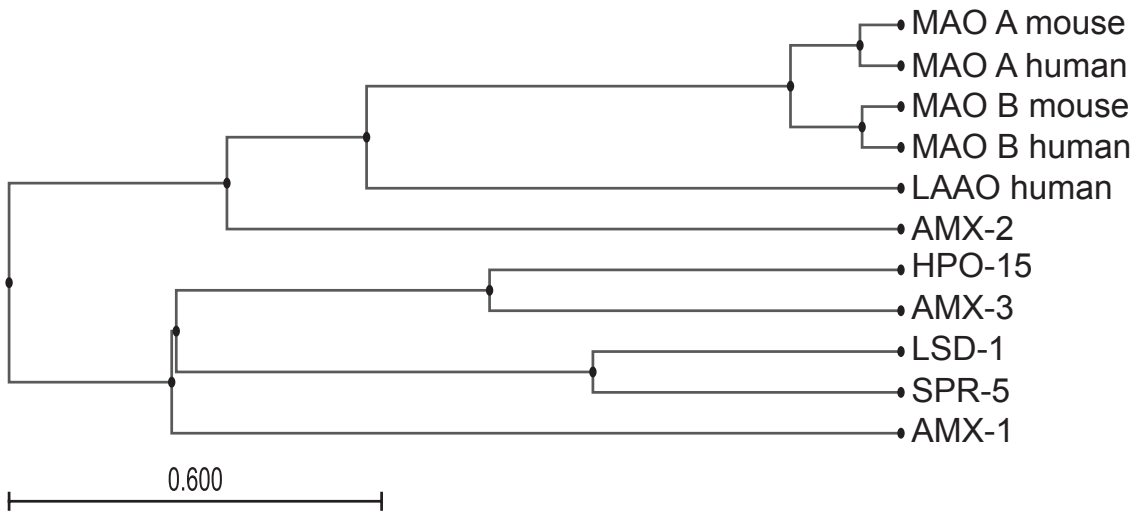

Figure S2. Sequence similarity between AMX-2 and monoamine oxidases.

AMX-2 is most similar to human MAOA or MAOB, less conserved to LAAO.The *C. elegans* genome harbours five more paralogues as indicated.

suppl. Figure S3

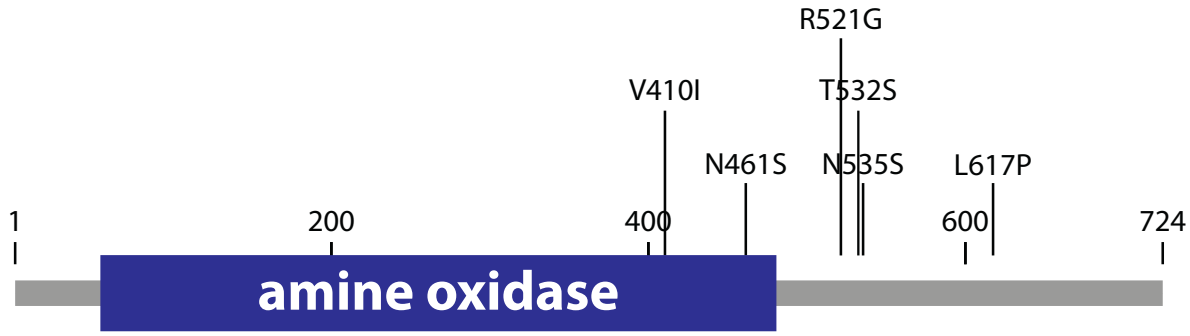

Figure S3. Coding polymorphisms between *C.elegans* Bristol and Hawaii AMX-2.

Indicated is the AMX-2 protein structure and its conserved amine oxidase domain. Coding SNPs are prevalently found in the C-terminal region of the protein (R521G, T532S, N535S and L617P), only two non-synonymous SNPs are found to affect the catalytic amine oxidase domain (V410I and N461S)

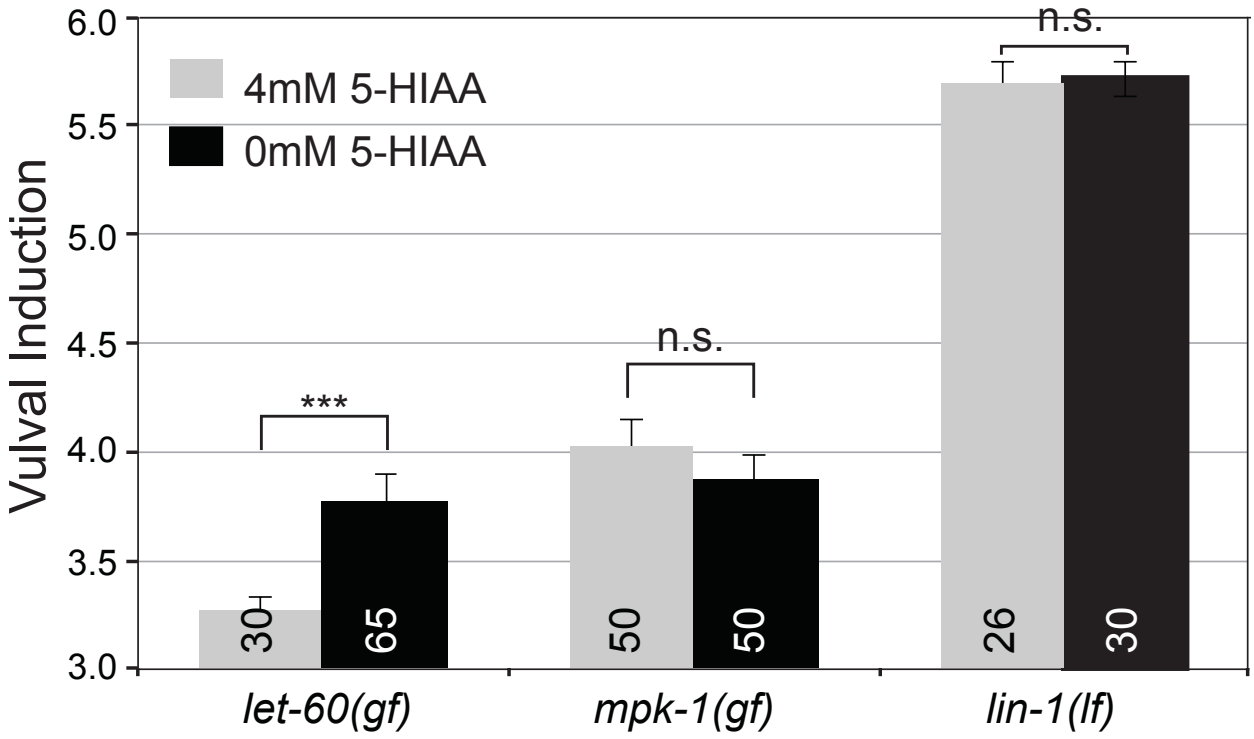

Figure S4. Epistatic analysis on the function of 5-HIAA.

The effect of 5-HIAA on EGFR/RAS/MAPK signalling pathway during vulval development was test in SD1059: gaIS37[HS-*mpk-1*, HS-dmek] *and* MT822: *lin-1(n304).* Error bars: SE, Student's t-test *** p<0.001.

Gene Name	RNAi					
	Bristol allele	SE	p	Hawaii allele	SE	p
E03H4.11	4.50	0.20		5.10	0.14	
C54C8.2	4.25	0.22		4.55	0.24	3.2E-03
C54C8.4	4.55	0.16		5.38	0.11	
glct-5	4.30	0.22		5.15	0.18	
T27F6.1	4.48	0.19		5.35	0.17	
pars-2	4.40	0.22		5.03	0.14	
K11D2.4	4.55	0.19		5.48	0.12	
W02D9.4	5.23	0.17	1.2E-03	5.08	0.20	
W02D9.9	4.53	0.19		4.75	0.19	
dlk-1	4.58	0.19		5.20	0.15	
F33E2.4	4.15	0.25		4.78	0.19	
F33E2.6	4.55	0.21		5.10	0.19	
T07D10.1	4.20	0.18		4.88	0.18	2.3E-02
ntr-1	4.90	0.21		5.20	0.15	
T07D10.3	4.03	0.23		5.00	0.11	2.6E-02
H16D19.4	na	na		na	na	
H28O16.2	na	na		na	na	
clec-103	4.68	0.13		5.35	0.16	
ndx-1	4.08	0.22		4.98	0.18	
T26E3.5	4.25	0.16		5.38	0.14	
T26E3.6	3.95	0.16	3.6E-02	4.73	0.19	6.1E-03
T26E3.8	na	na		na	na	
sra-25	4.55	0.21		5.08	0.15	
sra-17	4.98	0.17		5.65	0.16	
sra-20	3.58	0.12	9.0E-04	3.95	0.13	4.2E-03

Gene Name	RNAi					
	Bristol allele	SE	p	Hawaii allele	SE	p
sra-23	4.23	0.17		4.98	0.19	
*T06G6.5**	4.15	0.16		5.40	0.12	
T06G6.6	3.90	0.20	4.3E-02	5.23	0.18	
srw-88	3.38	0.10	1.2E-06	4.70	0.16	1.5E-03
pfd-3	3.98	0.19		4.60	0.18	7.5E-04
W02A11.1	3.83	0.15	7.7E-03	5.05	0.14	
vps-25	4.65	0.20		5.58	0.10	
toe-4	3.65	0.17	1.4E-03	4.38	0.20	1.4E-04
uba-2	4.70	0.17		5.38	0.18	
*bath-34**	4.10	0.16		4.85	0.21	2.9E-02
W02A11.6	na	na		na	na	
bath-35	4.18	0.22		5.05	0.14	
amx-2	5.05	0.18	1.2E-02	5.38	0.21	
B0019.2	3.95	0.21		5.30	0.16	
Y18D10A.1	4.28	0.20		5.08	0.14	
Y18D10A.2	3.68	0.16	1.5E-03	4.48	0.19	3.0E-04
ptr-17	4.65	0.22		5.13	0.14	
Y18D10A.8	4.45	0.17		4.48	0.19	
Y18D10A.9	3.58	0.16	8.9E-05	4.38	0.19	
clec-104	4.70	0.23		5.15	0.17	
clec-106	4.10	0.17		5.10	0.13	
pad-1	3.90	0.24		4.73	0.16	2.5E-03
F08A8.1	4.35	0.16		5.08	0.16	
F08A8.4	4.25	0.20		5.50	0.14	
F08A8.5	3.93	0.18	3.9E-02	4.48	0.16	5.0E-05

Gene Name	RNAi					
	Bristol allele	SE	p	Hawaii allele	SE	p
fbxa-140	4.43	0.18		4.73	0.19	
C47B2.2	4.05	0.14		5.45	0.12	
gale-1	4.48	0.19		4.05	0.21	3.8E-02
selb-1	4.23	0.16		5.15	0.21	
prx-11	4.23	0.13		4.98	0.21	
smu-1	3.83	0.15	6.9E-03	4.75	0.24	2.2E-02
clec-108	4.65	0.17		5.28	0.19	
Y26D4A.8	3.93	0.20		5.68	0.13	
Y26D4A.9	4.38	0.18		5.48	0.11	
C17H1.4	4.75	0.21		5.68	0.09	
C17H1.7	4.90	0.17		5.23	0.14	
F22G12.5	4.85	0.17		5.30	0.14	
F17B5.1	4.80	0.21		4.85	0.16	
oac-17	4.48	0.23		5.13	0.18	
clec-109	4.58	0.18		5.05	0.18	
F17B5.4	5.00	0.14	8.2E-03	5.40	0.15	
clec-110	4.33	0.25		5.40	0.14	
ZK1225.1	4.58	0.20		5.18	0.17	
ZK1225.2	4.68	0.24		5.40	0.12	
ZK1225.4	3.55	0.16	2.7E-04	5.05	0.21	
ZK1225.5	4.00	0.17		4.93	0.18	3.5E-02
ssp-31	4.48	0.16		5.25	0.12	
ZK1053.3	4.05	0.17		5.03	0.20	
F44F1.1	5.33	0.11	1.8E-03	5.18	0.18	
F44F1.3	4.80	0.17		na	na	

Gene Name	RNAi					
	Bristol allele	SE	p	Hawaii allele	SE	p
F44F1.4	5.20	0.14	6.1E-04	5.63	0.12	
F44F1.6	3.65	0.15	9.3E-04	4.55	0.18	5.4E-04
vet-6	4.28	0.18		5.33	0.12	
sepa-1	4.95	0.18		5.48	0.08	5.0E-02
T04D3.1	4.63	0.18		4.80	0.16	
gcy-35	4.38	0.17		5.15	0.19	
T04D3.5	3.95	0.20		5.00	0.20	
W08E3.4	4.63	0.18		5.28	0.18	
Y40B1A.1	3.98	0.20	2.2E-02	4.58	0.16	1.6E-02
C01A2.3	4.43	0.20		na	na	
C01A2.6	4.63	0.14		na	na	
W05H12.2	4.43	0.21		4.75	0.15	
fbxb-66	4.33	0.24		4.68	0.20	
eif-3.J	4.13	0.21		4.28	0.14	1.3E-04
agef-1	3.98	0.22	2.8E-02	na	na	
W09C5.7	4.63	0.18		5.25	0.17	
W04A4.3	4.33	0.19		5.43	0.16	
W04A4.5	4.30	0.18		4.78	0.18	
Y6B3B.1	4.40	0.23		5.30	0.16	
Y6B3B.3	4.48	0.16	2.6E-02	4.83	0.21	
Y6B3B.4	3.53	0.14	8.4E-05	4.78	0.20	1.2E-02
Y6B3B.5	4.25	0.18		4.45	0.18	
Y6B3B.9	na	na		3.73	0.17	1.5E-09
Y37H9A.2	3.88	0.16	1.7E-02	5.05	0.17	
Y37H9A.3	4.08	0.20		5.13	0.16	

Gene Name	RNAi					
	Bristol allele	SE	p	Hawaii allele	SE	p
W04A8.1	4.13	0.17		5.38	0.12	
W04A8.2	4.35	0.24		4.95	0.19	
W04A8.3	4.43	0.18		5.63	0.11	
W04A8.5	4.53	0.14		5.13	0.13	
W04A8.6	3.93	0.15	2.4E-02	4.95	0.18	4.7E-02
ins-30	4.43	0.20		5.33	0.18	
fbxb-101	4.53	0.21		5.50	0.15	
tfg-1	3.83	0.17	1.2E-02	4.08	0.22	9.1E-06
kal-1	4.35	0.20		4.90	0.21	4.7E-02
fipr-24	na	na		na	na	
ZK849.1	4.53	0.20		5.23	0.19	
ZK849.5	4.93	0.16		5.40	0.12	
K05C4.9	na	na		na	na	
empty vector	4.55	0.07		5.16	0.06	

Tables S1. Results of the RNAi screen in the QTL1b region.

Shown are the results for RNAi knockdown of either the N2 Bristol or the CB4856 Hawaii allele. Grey colored genes indicate allele specific, beige allele independent changes in vulval induction. p values according to Student's t-test. * indicates partly or completely missing genes in CB4856.

Alpini, G., Invernizzi, P., Gaudio, E., Venter, J., Kopriva, S., Bernuzzi, F., et al. (2008). Serotonin metabolism is dysregulated in cholangiocarcinoma, which has implications for tumor growth. *Cancer research*, *68*(22), 9184–9193. doi:10.1158/0008-5472.CAN-08-2133

Andersen, E. C., Gerke, J. P., Shapiro, J. A., Crissman, J. R., Ghosh, R., Bloom, J. S., et al. (2012). Chromosome-scale selective sweeps shape Caenorhabditis elegans genomic diversity. *Nature Genetics*, *44*(3), 285–290. doi:10.1038/ng.1050

Berset, T. A. (2005). The C. elegans homolog of the mammalian tumor suppressor Dep-1/Scc1 inhibits EGFR signaling to regulate binary cell fate decisions. *Genes & Development*, *19*(11), 1328–1340. doi:10.1101/gad.333505

Brenner, S. (1974). The genetics of Caenorhabditis elegans. *Genetics*, *77*(1), 71–94.

Calabrese, E. J. (2013). Hormetic mechanisms. *Critical reviews in toxicology*, *43*(7), 580–606. doi:10.3109/10408444.2013.808172

Civenni, G., Walter, A., Kobert, N., Mihic-Probst, D., Zipser, M., Belloni, B., et al. (2011). Human CD271-positive melanoma stem cells associated with metastasis establish tumor heterogeneity and long-term growth. *Cancer research*, *71*(8), 3098–3109. doi:10.1158/0008-5472.CAN-10-3997

Doroszuk, A., Snoek, L. B., Fradin, E., Riksen, J., & Kammenga, J. (2009). A genome-wide library of CB4856/N2 introgression lines of Caenorhabditis elegans. *Nucleic Acids Research*, *37*(16), e110–e110. doi:10.1093/nar/gkp528

Freeman, D., Lesche, R., Kertesz, N., Wang, S., Li, G., Gao, J., et al. (2006). Genetic background controls tumor development in PTEN-deficient mice. *Cancer research*, *66*(13), 6492–6496. doi:10.1158/0008-5472.CAN-05-4143

Frøkjær-Jensen, C., Wayne Davis, M., Hopkins, C. E., Newman, B. J., Thummel, J. M., Olesen, S.-P., et al. (2008). Single-copy insertion of transgenes in Caenorhabditis elegans. *Nature Genetics*, *40*(11), 1375–1383. doi:10.1038/ng.248

Gaertner, B. E., & Phillips, P. C. (2010). Caenorhabditis elegans as a platform for molecular quantitative genetics and the systems biology of natural variation. *Genetics research*, *92*(5-6), 331–348. doi:10.1017/S0016672310000601

Haag, A., Gutierrez, P., Bühler, A., Walser, M., Yang, Q., Langouët, M., et al. (2014). An in vivo EGF receptor localization screen in C. elegans Identifies the Ezrin homolog ERM-1 as a temporal regulator of signaling. *PLoS Genetics*, *10*(5), e1004341. doi:10.1371/journal.pgen.1004341

Jacobs, D., Beitel, G. J., Clark, S. G., Horvitz, H. R., & Kornfeld, K. (1998). Gain-of-function mutations in the Caenorhabditis elegans lin-1 ETS gene identify a C-terminal regulatory

domain phosphorylated by ERK MAP kinase. *genetics.org*, *149*(4), 1809.

Kalgutkar, A. S., Dalvie, D. K., & Castagnoli, N. (2001). Interactions of nitrogen-containing xenobiotics with monoamine oxidase (MAO) isozymes A and B: SAR studies on MAO substrates and inhibitors. *Chemical research in …*.

Kamath, R. S., Martinez-Campos, M., Zipperlen, P., Fraser, A. G., & Ahringer, J. (2000). Effectiveness of specific RNA-mediated interference through ingested double-stranded RNA in Caenorhabditis elegans. *Genome Biology*, *2*(1), research0002.1. doi:10.1186/gb-2000-2-1-research0002

Koch, R., van Luenen, H. G., van der Horst, M., Thijssen, K. L., & Plasterk, R. H. (2000). Single nucleotide polymorphisms in wild isolates of Caenorhabditis elegans. *Genome Research*, *10*(11), 1690–1696.

Lackner, M. R., & Kim, S. K. (1998). Genetic analysis of the Caenorhabditis elegans MAP kinase gene mpk-1. *Genetics*, *150*(1), 103–117.

Milloz, J., Duveau, F., Nuez, I., & Félix, M.-A. (2008). Intraspecific evolution of the intercellular signaling network underlying a robust developmental system. *Genes & Development*, *22*(21), 3064–3075. doi:10.1101/gad.495308

Mosmann, T. (1983). Rapid colorimetric assay for cellular growth and survival: Application to proliferation and cytotoxicity assays. *Journal of Immunological Methods*, *65*(1-2), 55–63. doi:10.1016/0022-1759(83)90303-4

Pai, V. P., Marshall, A. M., Hernandez, L. L., Buckley, A. R., & Horseman, N. D. (2009). Altered serotonin physiology in human breast cancers favors paradoxical growth and cell survival. *Breast Cancer Research*, *11*(6), R81. doi:10.1186/bcr2448

Pilipiuk, J., Lefebvre, C., Wiesenfahrt, T., Legouis, R., & Bossinger, O. (2009). Increased IP 3/Ca 2+ signaling compensates depletion of LET-413/DLG-1 in C. elegans epithelial junction assembly. *Developmental Biology*, *327*(1), 34–47.

Rybaczyk, L. A., Bashaw, M. J., Pathak, D. R., & Huang, K. (2008). An indicator of cancer: downregulation of Monoamine Oxidase-A in multiple organs and species. *BMC Genomics*, *9*(1), 134. doi:10.1186/1471-2164-9-134

Scholl, C., Fröhling, S., Dunn, I. F., Schinzel, A. C., Barbie, D. A., Kim, S. Y., et al. (2009). Synthetic lethal interaction between oncogenic KRAS dependency and STK33 suppression in human cancer cells. *Cell*, *137*(5), 821–834. doi:10.1016/j.cell.2009.03.017

Soll, C., Jang, J. H., Riener, M.-O., Moritz, W., Wild, P. J., Graf, R., & Clavien, P.-A. (2009). Serotonin promotes tumor growth in human hepatocellular cancer. *Hepatology*, *51*(4), 1244–1254.

doi:10.1002/hep.23441

Sternberg, P. W. (2005). Vulval development. *WormBook*. doi:10.1895/wormbook.1.6.1

Sternberg, P. W., & Horvitz, H. R. (1986). Pattern formation during vulval development in C. elegans. *Cell*, *44*(5), 761–772. doi:10.1016/0092-8674(86)90842-1

Stetak, A., Gutierrez, P., & Hajnal, A. (2008). Tissue-specific functions of the Caenorhabditis elegans p120 Ras GTPase activating protein GAP-3. *Developmental Biology*, *323*(2), 166–176. doi:10.1016/j.ydbio.2008.08.026

Timmons, L., Court, D. L., & Fire, A. (2001). Ingestion of bacterially expressed dsRNAs can produce specific and potent genetic interference in Caenorhabditis elegans. *Gene*, *263*(1-2), 103–112.

Tipton, K. F., Boyce, S., O'Sullivan, J., Davey, G. P., & Healy, J. (2004). Monoamine oxidases: certainties and uncertainties. *Current medicinal chemistry*, *11*(15), 1965–1982.

Zipperlen, P., Nairz, K., Rimann, I., Basler, K., Hafen, E., Hengartner, M., & Hajnal, A. (2005). A universal method for automated gene mapping. *Genome Biology*, *6*(2), R19. doi:10.1186/gb-2005-6-2-r19

1.9 Natural Variation in Signalling Networks: Wnt Signalling

(part of this section was carried out as Masterthesis of Fabienne Largey 2011-2012 and in collaboration with the group of Jan Kammenga)

1.9.1 Natural Variation in *bar-1(ga80)* miRILs: Genotype

The 79 *bar-1(ga80)* miRILs displayed small linkage disequilibria. As expected, there is a low recombination frequency at the position of the included mutation (Figure 43, Chromosome X). In addition, there is hardly any recombination observed on the left side of Chromosome I (Figure 43, Chromosome I). In agreement with (Hannah S Seidel, 2008) there is a naturally occurring genome incompatibility between N2 and CB4856. Chromosome III has an overall lower than expected ratio of CB4856/N2. Otherwise recombination frequencies spanning the chromosomes seem equal with expected lower recombination towards the telomere regions. Interestingly, Chromosome 5 is mostly CB4856. There is even a fixed region for CB4856 around ZH5-09, which we cannot explain.

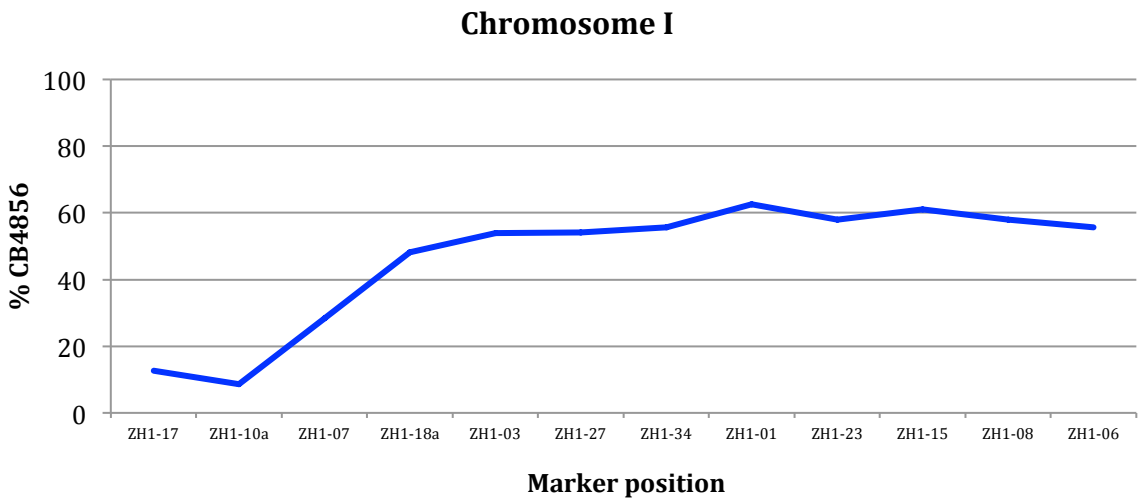

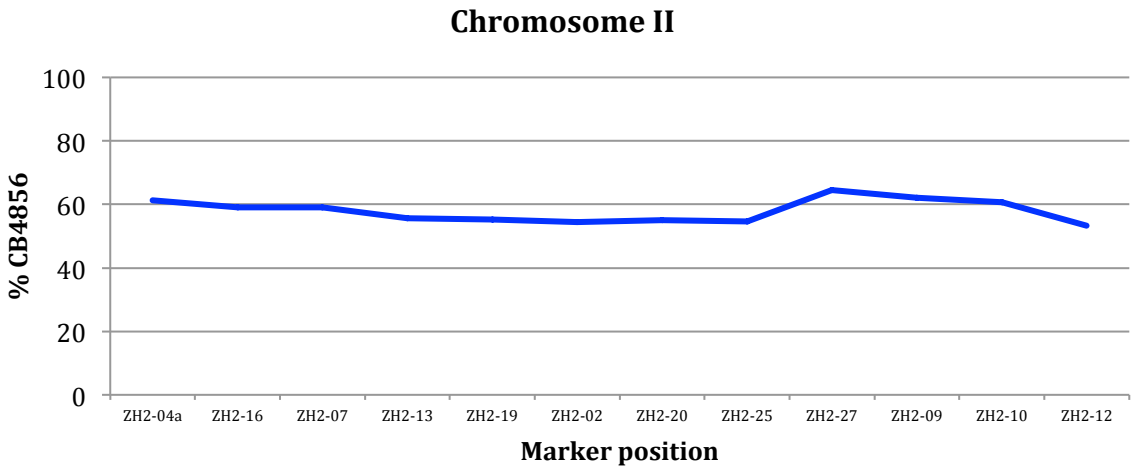
Chromosome II
100
80
60
40
20
0
% CB4856
ZH2-04a
ZH2-16
ZH2-07
ZH2-13
ZH2-19
ZH2-02
ZH2-20
ZH2-25
ZH2-27
ZH2-09
ZH2-10
ZH2-12
Marker position

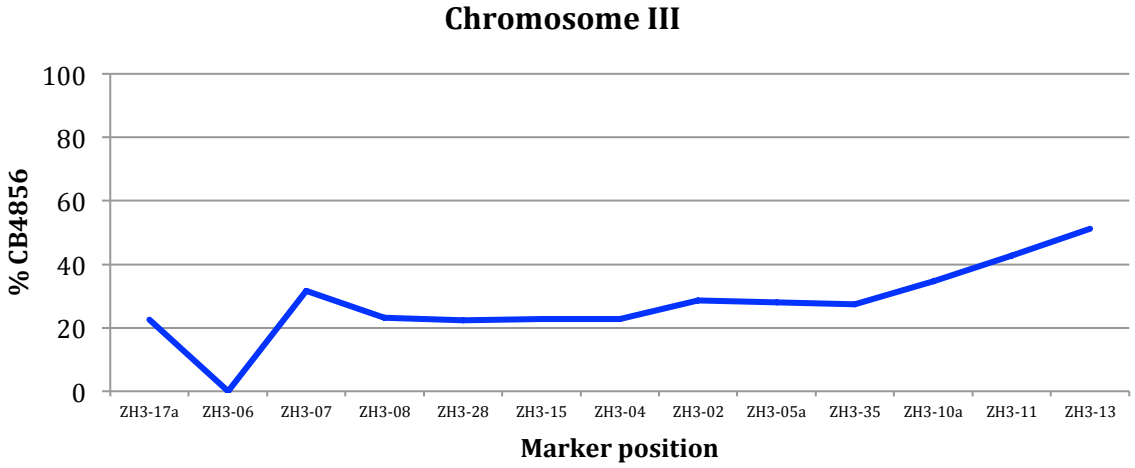
Chromosome III
100
80
60
40
20
0
% CB4856
ZH3-17a
ZH3-06
ZH3-07
ZH3-08
ZH3-28
ZH3-15
ZH3-04
ZH3-02
ZH3-05a
ZH3-35
ZH3-10a
ZH3-11
ZH3-13
Marker position

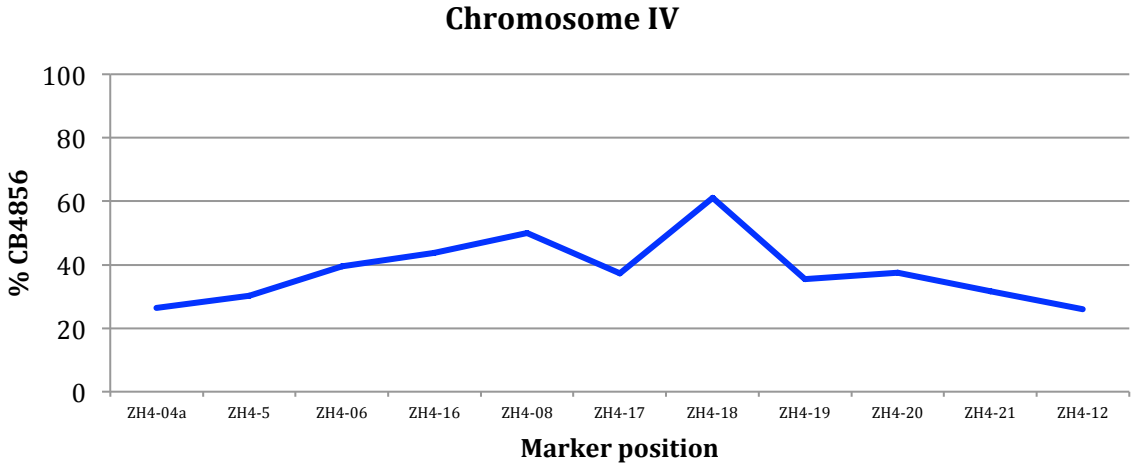
Chromosome IV
100
80
60
40
20
0
% CB4856
ZH4-04a
ZH4-5
ZH4-06
ZH4-16
ZH4-08
ZH4-17
ZH4-18
ZH4-19
ZH4-20
ZH4-21
ZH4-12
Marker position

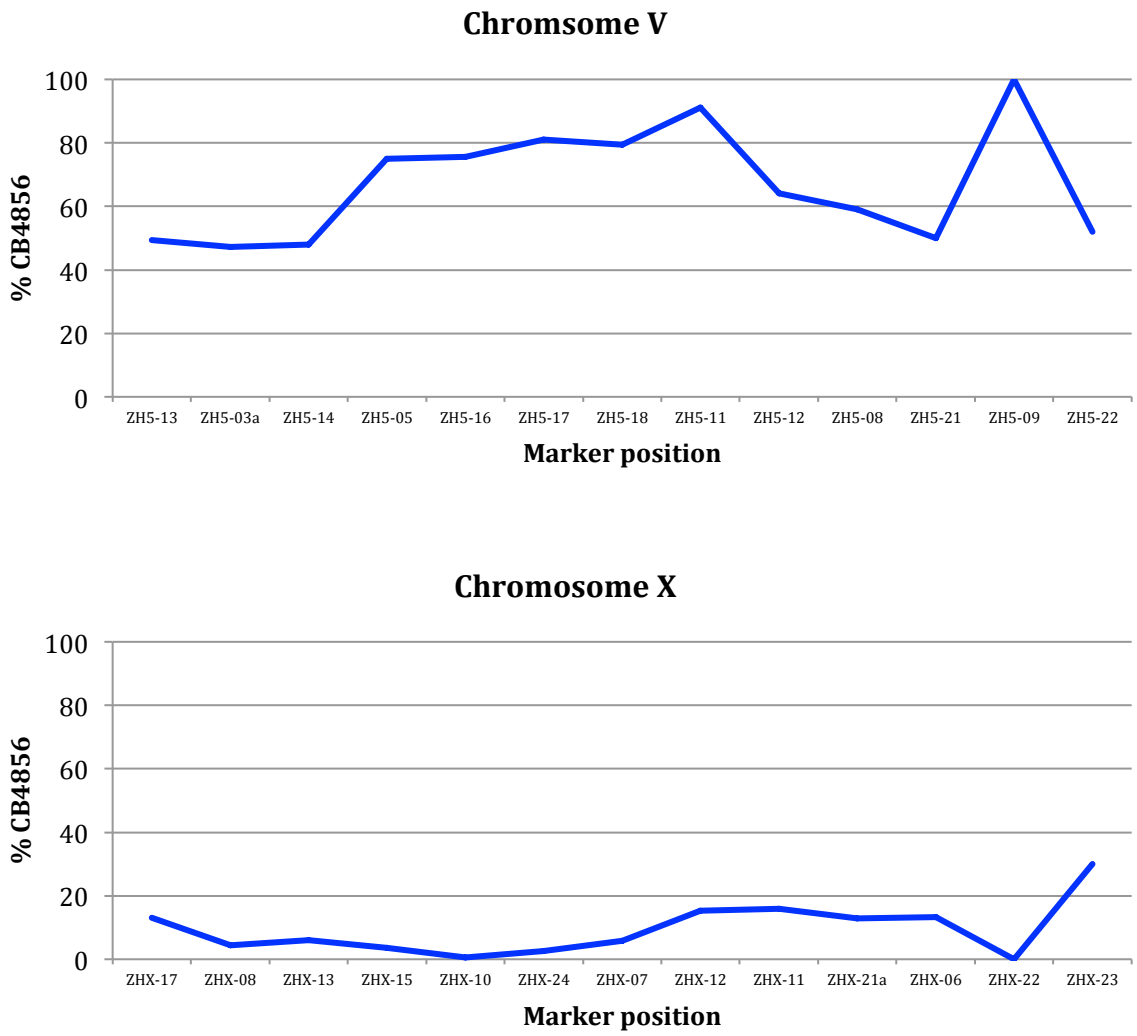

Figure 43: Genotype summary of the *bar-1(ga80)* miRILs. Plotted, as blue line is marker position vs. % of CB4856 genome at that position.

1.9.2 Natural Variation in *bar-1(ga80)* miRILs: Phenotype

Again, vulval induction (VI) counting was used as the method to determine Wnt pathway activity during *C. elegans* vulval development ((Sternberg & Horvitz, 1986)). In addition, we scored the mismigration of the gonad arms as gonadal index (GI), defined as the number of mismigrated gonad arms divided by two for total number of gonad arms and averaged for the total of animals scored. In Table 8, an increasing vulval induction index is shown for every miRIL. The broad phenotypic range from 0.14 – 2.94 indicates the presence of several genomic loci involved in the modification of the phenotype. There is no vulval induction recorded higher than the wild-type level of 3, possibly due to buffering and robustness of vulval development in this sensitized

background. Gonad mismigration defects range from 0 to a highest value of 88.2 (Table 9). Further QTL mapping will help to localise and identify those modifier regions.

MIRIL	#	VI	STDEV	s.e.m.
39	22	0.14	0.64	0.07
57	21	0.48	0.90	0.10
32	40	0.51	0.99	0.11
1	21	1.26	1.02	0.11
3	61	1.34	1.21	0.14
50	22	1.41	1.30	0.14
70	25	1.44	1.42	0.16
47	22	1.50	1.23	0.14
54	21	1.55	1.19	0.13
61	24	1.71	1.26	0.14
48	27	1.76	1.24	0.14
26	22	1.84	1.10	0.12
12	20	1.88	1.13	0.13
25	22	1.91	1.30	0.14
34	22	1.91	1.24	0.14
2	37	1.96	1.29	0.14
6	28	2.02	1.02	0.11
31	46	2.09	1.13	0.13
63	22	2.09	1.19	0.13
51	22	2.18	1.25	0.14
55	21	2.19	1.04	0.12
53	20	2.20	1.16	0.13
18	43	2.21	1.04	0.12
52	23	2.26	1.11	0.12
22	42	2.26	1.11	0.12
5	45	2.27	1.04	0.12
45	21	2.36	0.67	0.08
42	22	2.36	0.86	0.10
67	20	2.43	0.91	0.10
36	22	2.43	0.89	0.10
28	62	2.44	1.01	0.11
33	25	2.44	0.81	0.09
19	21	2.48	0.72	0.08
49	22	2.48	0.87	0.10
15	26	2.54	0.72	0.08
4	22	2.55	0.84	0.09
24	36	2.57	0.69	0.08
35	26	2.58	0.72	0.08
77	22	2.59	0.77	0.09
62	21	2.60	0.46	0.05
72	26	2.60	0.40	0.04
13	28	2.61	0.57	0.06
79	22	2.61	0.67	0.08

MIRIL	#	VI	STDEV	s.e.m.
59	21	2.62	0.69	0.08
21	31	2.65	0.57	0.06
78	20	2.65	0.37	0.04
73	20	2.68	0.37	0.04
64	22	2.68	0.72	0.08
43	22	2.70	0.37	0.04
68	26	2.71	0.38	0.04
16	21	2.71	0.68	0.08
23	23	2.72	0.65	0.07
29	41	2.72	0.61	0.07
20	73	2.76	0.55	0.06
60	22	2.77	0.37	0.04
74	20	2.80	0.68	0.08
41	23	2.80	0.36	0.04
56	23	2.80	0.33	0.04
30	39	2.81	0.53	0.06
11	47	2.81	0.40	0.04
9	22	2.82	0.50	0.06
75	22	2.82	0.29	0.03
14	21	2.83	0.33	0.04
38	21	2.83	0.29	0.03
58	23	2.85	0.32	0.04
69	20	2.85	0.37	0.04
44	27	2.85	0.33	0.04
17	25	2.86	0.37	0.04
37	22	2.86	0.23	0.03
8	20	2.88	0.36	0.04
71	21	2.88	0.31	0.03
46	22	2.89	0.21	0.02
76	22	2.89	0.21	0.02
7	23	2.89	0.26	0.03
66	21	2.90	0.20	0.02
65	20	2.93	0.18	0.02
40	21	2.93	0.18	0.02
10	27	2.94	0.16	0.02
27	dead	-	-	-

Table 8: *bar-1(ga80)* miRIL vulval induction phenotype. Lines are sorted with increasing vulval induction index.

RIL	#	GI
3	20	0
9	22	0
12	20	0
13	21	0
16	21	0
21	31	0
28	20	0
29	21	0

RIL	#	GI
30	20	0
36	22	0
37	22	0
38	21	0
41	23	0
61	24	0
64	22	0
69	20	0
76	22	0
11	26	3.8
31	24	4.2
23	23	4.3
18	22	4.5
25	22	4.5
6	28	4.6
10	21	4.8
14	21	4.8
45	21	4.8
5	20	5
22	20	5
1	21	5.8
20	35	8.6
56	23	8.6
7	23	8.7
58	23	8.7
63	22	9.1
32	20	10
26	22	13.6
46	22	13.6
24	21	14.3
66	21	14.3
35	26	14.5
44	27	14.8
8	20	15
4	22	16.6
75	22	16.6
19	21	17.3
65	20	18
79	22	18.1
57	21	19.1
68	26	19.2
33	25	20
67	20	22
60	22	22.2
43	22	22.7
55	21	23
70	25	24
17	25	25

RIL	#	GI
62	21	28.8
78	20	30
2	22	31.8
52	23	32.1
40	21	34.6
54	21	34.6
74	20	40
48	27	42.3
42	22	44.4
77	22	45.4
71	21	46.1
50	22	55.5
72	26	58.2
53	20	60
49	22	61
73	20	66
34	22	66.5
39	22	66.5
59	21	69.1
51	22	72.1
47	22	88.2

Table 9: Gonadal Index (GI), as Wnt polarity readout. miRILs are sorted with increasing GI. Since GI only gives yes or no values, there are no STDEV and s.e.m. to be calculated.

1.9.3 QTL Mapping of *bar-1(ga80)* miRILs Reveals Two QTLs for Vulval Induction and One QTL for Gonad Migration

(this section is based and adapted from the Report on *bar-1(ga80)* MIRILs from L.Basten Snoek)

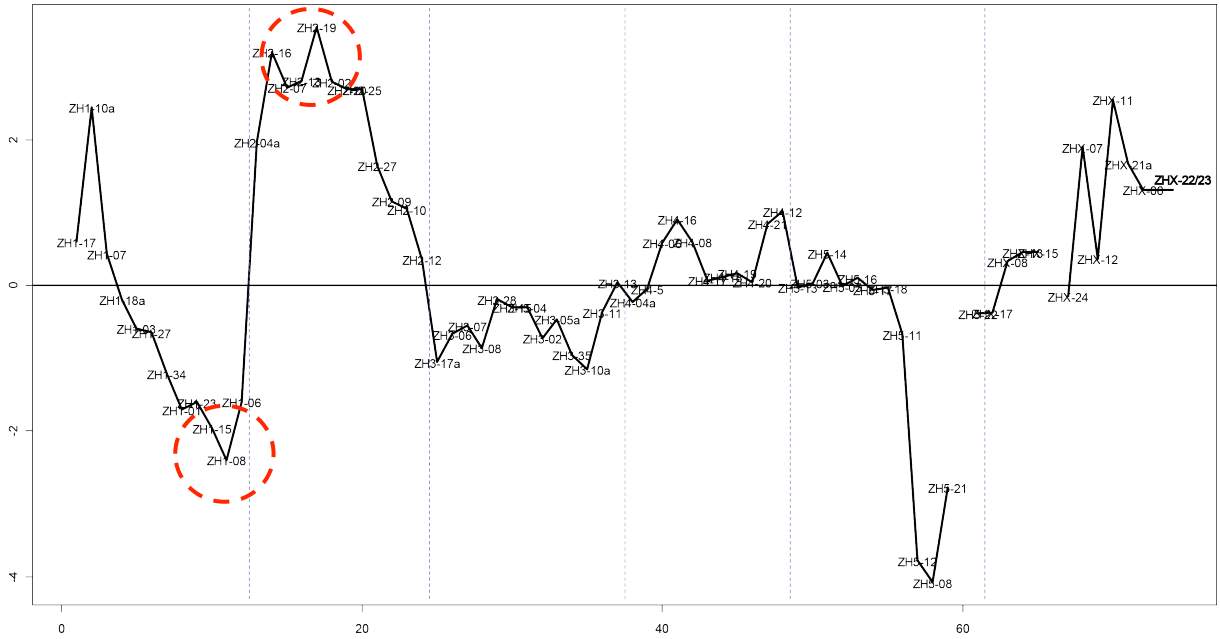

Figure 44: QTL mapping predicted two genomic regions affecting vulval induction in the miRILs. QTL peaks are encircled in red. Fragment length polymorphism markers are indicated on the x-axis and LOD*significance effect on the y-axis.

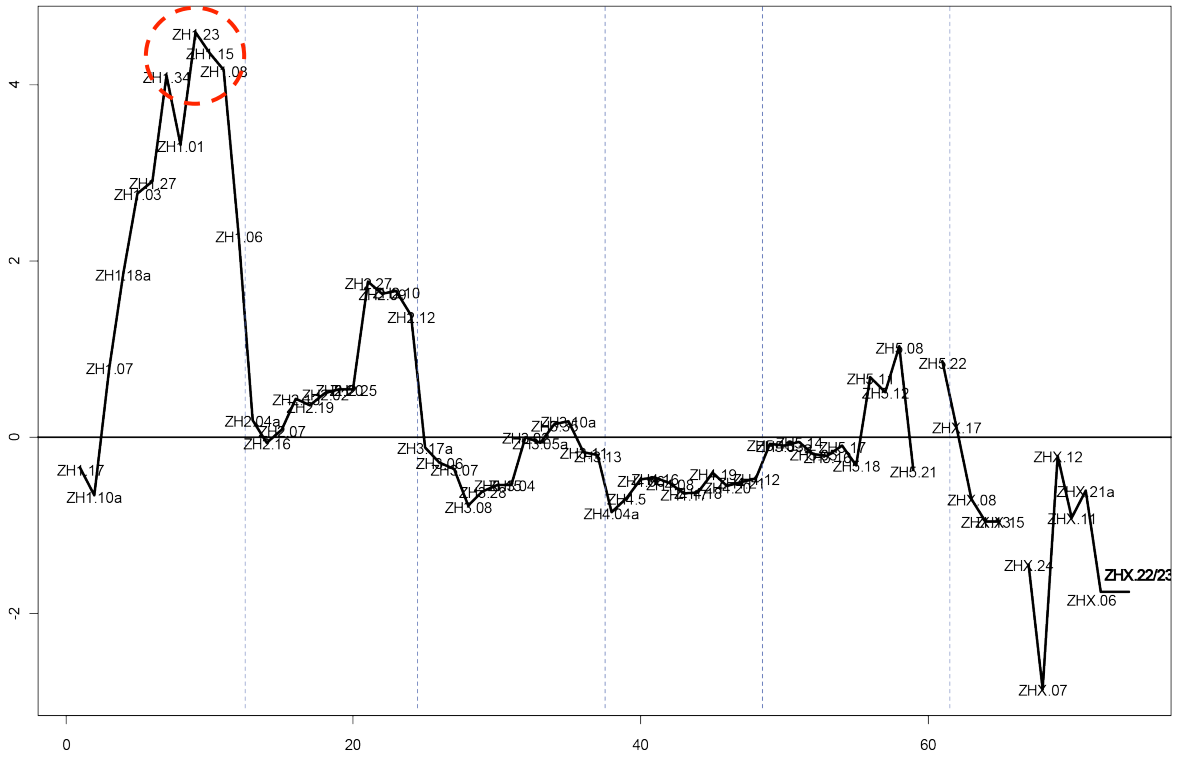

Figure 45: QTL mapping predicted only one genomic regions affecting gonad migration in the miRILs. The QTL peak is encircled in red. Fragment length polymorphism markers are indicated on the x-axis and LOD*significance effect on the y-axis.

1.9.3.1 Verification of QTL Regions: Introgression Lines

Introgression lines crosses were carried out only for chromosome I and did not reveal the exact position of the QTLs for vulval induction or gonad migration, but indicated the ewIR9 region to be involved. In the meantime, the group of Jan Kammenga performed additional crosses for chromosome I (ewIR13 and ewIR14) and II (ewIR21 and ewIR23) to verify QTL 1 and QTL 2 affecting vulval induction.

Together, we could verify the existence of QTL 1 for vulval induction using the introgression lines ewIR13 and ewIR14 (Figure 46).

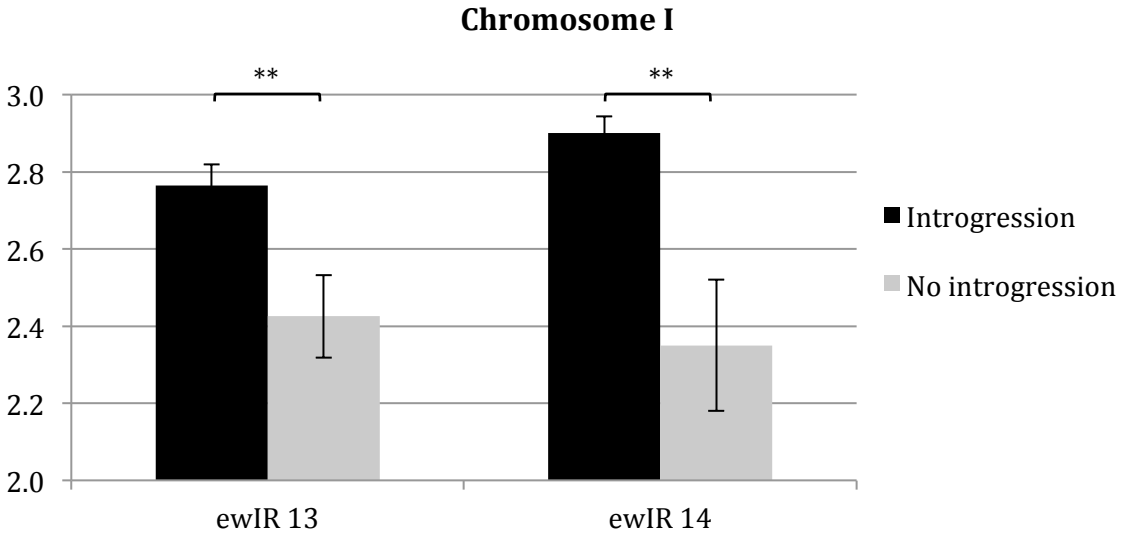

Figure 46: Introgression line crosses to verify QTL 1 for vulval induction in the bar-1 MIRILs. All depicted lines carry the *ga80* allele and either the introgression (black bars) or no introgression (grey bars). Differences within an introgression line indicate the QTL region to be located there. Since both ewIR13 and ewIR14 show an effect the QTL has to lie in the shared region. Error bars =SE, Mann-Whitney-U test, ** p<0.01

In addition, the QTL for vulval induction on chromosome two was checked with introgression lines ewIR21 and ewIR23. We could further demonstrate that as well as in Figure 46, both the regions have to harbour the modifier (Figure 47).

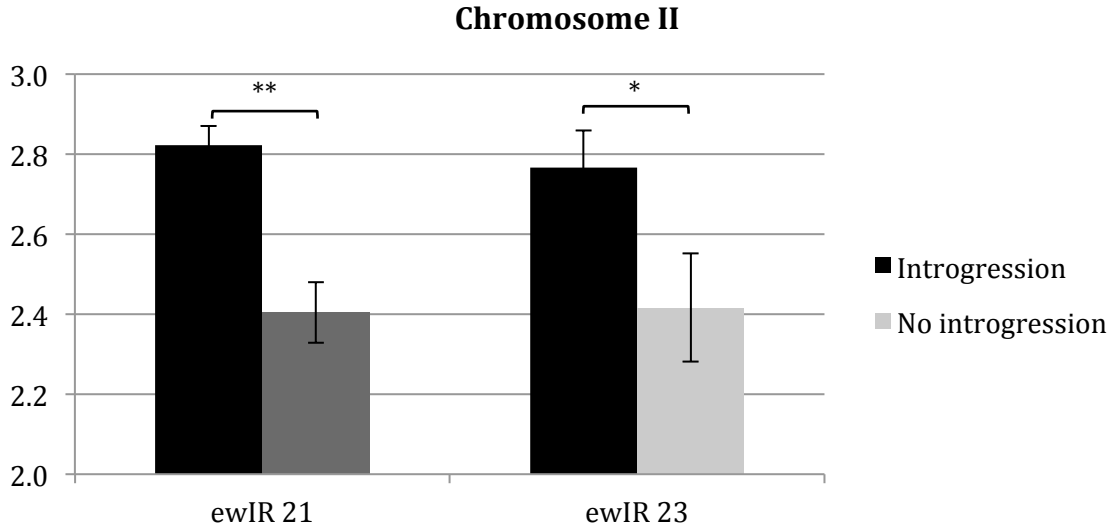

Figure 47: Introgression line crosses to verify QTL 2 for vulval induction in the bar-1 miRILs. All depicted lines carry the *ga80* allele and either the introgression (black bars) or no introgression (grey bars). Differences within an introgression line indicate the QTL region to be located there. Since both ewIR21 and ewIR23 show an effect the QTL has to lie in the shared region. Note: The data for no introgression in the ewIR21 is missing and was replaced with average VI of all previous no introgression lines. Error bars =SE, Mann-Whitney-U test, * p<0.05, ** p<0.01

1.9.4 expression QTLs (eQTLs) Overlap with QTLs for Vulval Induction

(The results from this section were carried out in collaboration with the group of Jan Kammenga, Wageningen University, The Netherlands)

We investigated a subset of 36 MIRILs for eQTL based on the seletion of Basten Snoek for analysis, as we did for the let-60(n1046) MIRILs. in section 1.7.3. The eQTLs overlap with the QTLs for gonad migration and vulval induction and therefore reflect a more globally acting modifier, affecting gonad migration and/or vulval induction (Figure 48).

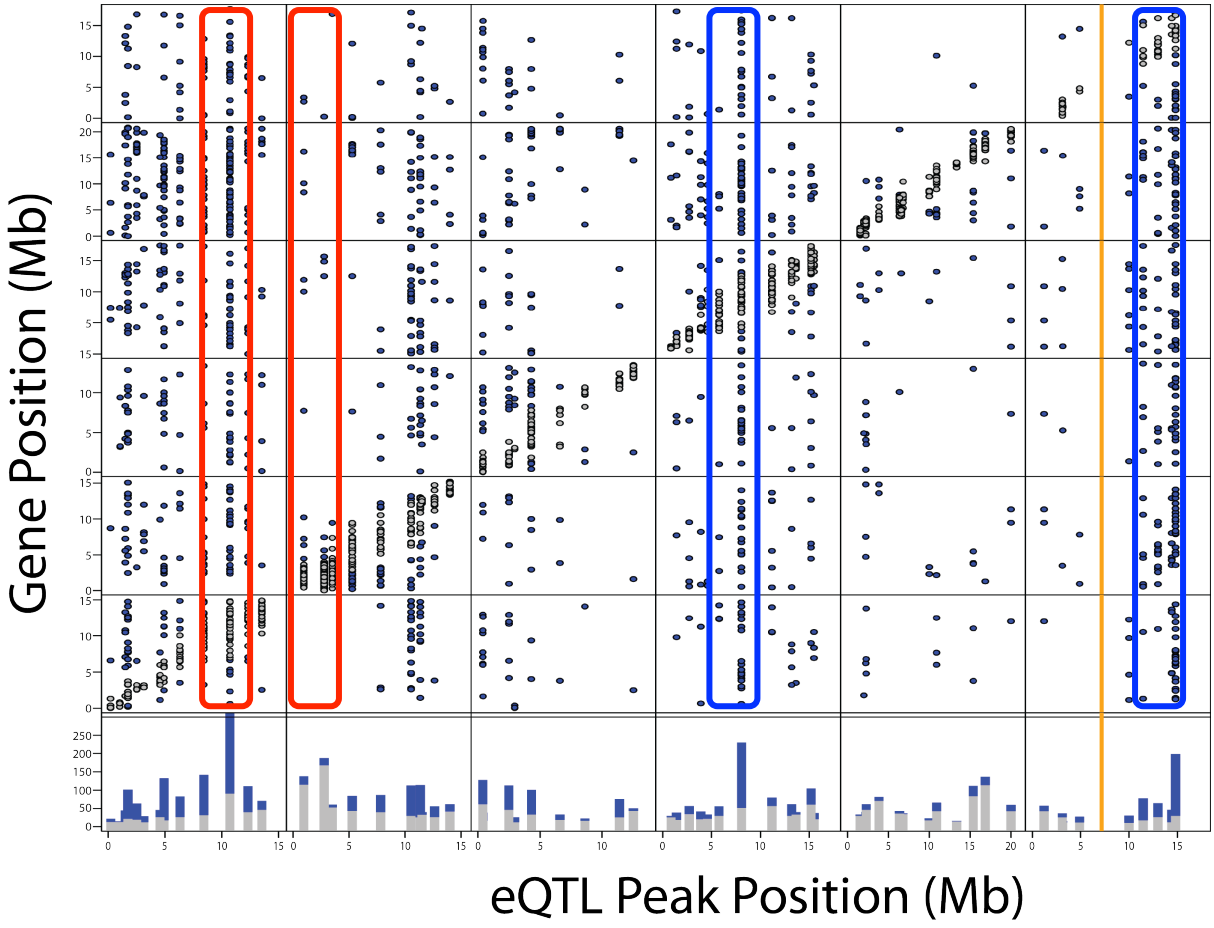

Figure 48: eQTL analysis: cis eQTLs are visualised as white dots, whereas trans eQTLs are marked in blue. The orange line marks the site of the *ga80* allele, where there is hardly any recombination allowed. At the bottom a sum up of the changed transcript per location is shown. The genomic regions for the QTLs in vulval induction/ gonad migration are encircled in red. There is a high correlation between the eQTLs for whole worm transcriptome and for vulval induction and gonad migration. In addition, there are strong trans eQTL peaks on chromosome 4 and X (blue), which are not seen as conventional QTL.

1.9.5 Identification of Candidate Genes:

1.9.5.1 Candidate Genes in QTL 1 Region Affecting Vulval Induction and Gonad Migration

We selected polymorphic genes in the ewIR9 and ewIR11 regions that are annotated to produce a protruding vulva phenotype when mutated or knocked down and tested for their ability to modify gonad migration and vulval induction (see Masterthesis Fabienne Largey).

1.9.5.2 RNAi to Identify Modifier Genes that Alter WNT Signalling

After re-screening some of the candidates (complete list, see Masterthesis Fabienne Largey) in a second RNAi experiment for differences in vulval induction, we ended up with the following significant candidate genes:

Gene	Vulval induction	% Vul	n	p-value	Homology
hsr-9	1.30	84.0	25	0.047	Dentin sialophosphoprotein
C15C6.3	1.15	82.7	24	0.015	Serine/arginine repetitive matrix protein 1
glct-2	1.10	86.4	52	0.002	Galactosylgalactosylxylosylprotein 3-beta-glucuronosyltransferase 1
eV	1.93	63.3	30		

Table 10: Significant candidate genes at QTL 1 position that alter Wnt signalling in the *bar-1(ga80)* mutant, readout by measuring vulval induction.

1.9.6 *sqv-2* is a Modifier of WNT Signalling

In addition, the group of Jan Kammega identified *sqv-2* as a possible modifier for vulval induction in the *bar-1(ga80)* MIRILs as part of QTL2 (pers. communication).

sqv-2 or squashed vulva 2 is a glycosaminoglycan galactosyltransferase II (Hwang, Olson, Brown, Esko, & Horvitz, 2003). Its function is needed for vulval morphogenesis. *sqv-2* is thought to secrete hydroscopic proteoglycans into the vulval lumen, which in turn attracts water molecules and therefore fills it up. Without *sqv-2*, there is a reduced lumen formed.

We crossed the *sqv-2(n2826)* allele with *bar-1(ga80)* and counted vulval induction. Surprisingly, the *sqv-2(n2826);bar-1(ga80)* double mutant show increased vulval induction compared to *bar-1(ga80)* alone (Figure 49).

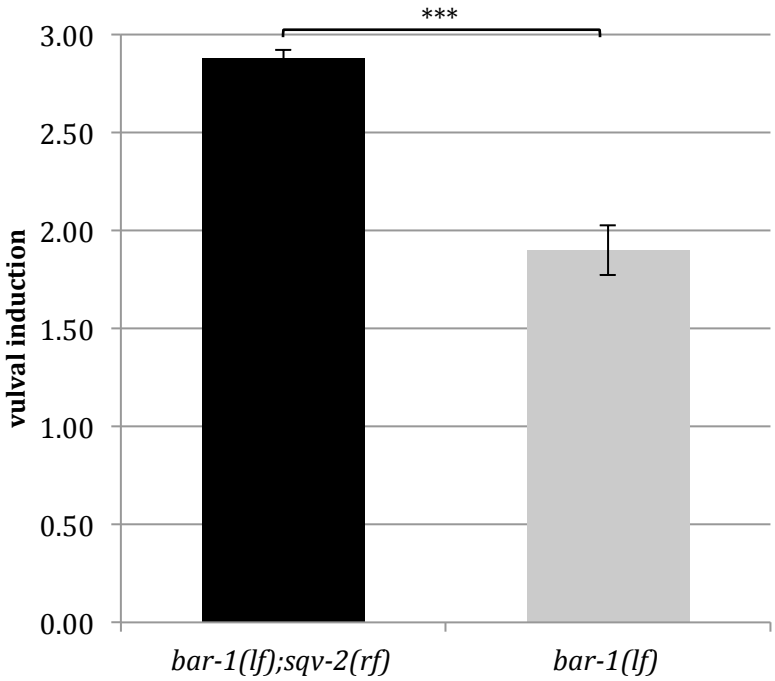

Figure 49: *sqv-2(n2826);bar-1(ga80)* double mutant analysis. The *sqv-2(n2826)* allele increases vulval induction in the double mutant vs. *bar-1(ga80)* single mutant. Error bars =SE, Mann-Whitney-U test, *** p<0.001

Further investigation regarding the insertion of single copies of *sqv-2* of either the N2 or the CB4856 allele into the *sqv-2(n2826)* mutant will clarify the gene as being a natural polymorphic modifier of WNT signalling or not.

Side projects

1.10 Screen to Identify Novel Negative Regulators of the MAPK *mpk-1* During *C. elegans* Oocyte Development

1.10.1 Background:

To date, there is only one direct negative regulator of *mpk-1* known, which is *lip-1* ((Berset, 2001)). To find further candidates, several Mos1 transposon and conventional EMS screens were carried out in the sensitized *mpk-1(ga111)* background (Lackner & Kim, 1998).

1.10.2 Experimental procedure and screen rationale:

We used the *mpk-1(ga111)* temperature sensitive allele that is completely sterile at 25°C. After Mos1 mobilisation (for materials and methods see (Boulin & Bessereau, 2007)) or EMS treatment, worms were shifted from permissive 20°C to restrictive 25°C and screened for rescue of sterility or progeny after several days, indicating the mutation in a gene negatively regulating *mpk-1* (Lackner & Kim, 1998).

1.10.3 Results:

In total, approximately 130'000 F1 animals were screened and no mutation rescuing the *mpk-1(ga111)* sterility at 25°C could be isolated. In addition, *lip-1* as positive candidate was not identified in any of the carried out screens. We therefore decided to stop this project.

1.10.4 Discussion:

mpk-1(ga111) is a highly temperature-dependent allele, and small differences in the incubator caused rescue of sterility and let to the identification of many false positives. Therefore, it would be absolutely necessary to control temperature on the worm's plate more accurately. In addition, since *lip-1* mutational alleles were not identified, I could have crossed the *lip-1(zh15)* allele into the *mpk-1(ga111)* background to test for fertility by myself. At last, *mpk-1* is the terminal member of MAPK signalling, therefore most regulation happens on more upstream components of EGFR/RAS/MAPK signalling, it is unlikely to reveal novel negative regulators downstream or at the level of *mpk-1*. In addition, a proof of concept, namely to identify *lip-1* mutational alleles was not successful, this highly questions the screen to produce valid results.

1.11 Background Modifier of *let-60(n1046)*

1.11.1 Background:

The crossings of the *let-60(n1046)* mutant with different introgression lines revealed two lines of ewIR2;*let-60(n1046)* that display a vulval induction index of almost six combined with a strong unviable phenotype. This effect seems to be independent of the introgression, since one of the lines harbours the ewIR2 introgression the other not, but both with the same vulval induction index.

1.11.2 Explanation:

This observation is possibly due to a background modifier in the *let-60(n1046)* or the ewIR2 strain that was removed during crossing. Since the lines show high unviability, those strains can never be isolated via conventional methods.

1.11.3 Further investigations:

To identify background modifiers, we analysed the data of the whole genome sequence of *let-60(n1046)* and aligned them to the reference N2 genome WS220. In a next step, we checked for non synonymous SNPs in the *let-60(n1046)* which are not found in the N2 reference and obtained the following candidate list (Table 11):

Gene	non synonymous SNP	Counts	Coverage
R119.1	Lys329Asn	15	19
Y71G12B.23	Gln100Leu	5	7
sydn-1	Met301Ile	15	19
ttx-7	Gly206Ala	21	21
T22C1.6	Lys188Gln	5	9
C45G3.5	Glu160Gln	23	24
F36H2.2	Arg366Ala	4	5
ZC247.1	Ala631Val	8	10
lam-3	Lys1589Gln	5	9
Y53H1B.6	Phe79Cys Leu81Val	8 9	8 9
nhr-245	Lys259Thr	5	6
T26E3.6	Glu53Asp	20	21
Y71A12B.17	Lys176Glu	17	17
Y105E8A.24	Gly905Arg	8	8
C50D2.1	Lys327Thr	5	7
R07C3.13	Arg184Lys	20	23
W10G11.19	Glu73Lys	13	14
sea-2	Asn1003Ser	7	9
lact-5	Thr2Ile	20	21

Gene	non synonymous SNP	Counts	Coverage
ins-20	Met15Ile	23	23
C56E6.4	Ile185Asn	16	17
T14B4.2	Ser54Cys Phe55Leu	15 20	16 21
F41G3.2	Gln190Glu	7	9
unc-104	Val495Glu	14	14
col-76	Phe422Tyr	13	16
let-23	Ser1001Phe	11	13
zfp-2	Gly90Arg	16	16
C08H9.3	Val706Ile	20	20
F33H1.3	His249Tyr	20	21
F33H1.4	Ser872Phe	5	5
pro-2	His619Pro	24	24
age-1	Pro332Ser	15	18
ZK930.1	Pro479Leu	20	21
Y38E10A.23	Asn83Thr	12	13
Y46G5A.29	Asp41Asn	9	10
gcn-2	Asp1534Glu	9	9
F15D4.4	Asp514Glu	7	8
Y48C3A.20	Asp125Gly	5	9
tbc-15	Thr88Lys	19	22
eif-3.B	Gly170Val	15	16
trp-2	Pro288Arg	19	20
smi-1	Phe160Cys	20	22
Y54F10AM.7	Thr49Ser	8	10
him-18	Met215Val	18	18
R151.2	Ser323Arg	14	16
ZK507.1	START Gln2Lys	8 8	11 9
K04H4.2	Glu849Lys Gly857Glu	14 17	14 20
mut-7	Glu829STP	5	5
vps-53	Glu634Asp	22	22
Y66D12A.21	Lys209Arg Lys259Arg	5 4	7 5
Y66D12A.14	Gly2186Glu	14	15
Y66D12A.8	Ala144Gly	17	17
srw-9	Met134Leu	17	18
ttm-1	Asn370Thr	17	17
cutl-24	Arg262Lys	12	13
dcap-1	Lys186Glu	19	22
bus-2	Pro8Leu	17	18

Gene	non synonymous SNP	Counts	Coverage
xpc-1	Gly1048Glu	10	12
clec-76	Asp67Asn	18	18
T12E12.3	Pro678Ser	14	14
tag-80	Gln3127His	17	17
acc-2	Leu294His	24	25
srb-17	Val224Ile	21	21
F56C4.4	Tyr61Phe	16	20
pept-2	Glu483Lys	22	22
sdz-13	Arg172Cys	13	13
pfd-1	Asp50Val	13	13
F54E12.2	Met840Ile	22	22
cyp-31A2	Ile312Val	11	11
prx-2	Pro250Ala	5	8
let-60	Gly13Glu	17	18
Y51H4A.6	Phe6Leu	9	11
Y116A8C.1	Gly173Arg	12	13
Y116A8C.26	His156Arg	15	15
Y58G8A.4	Gly72Arg	16	18
F31F4.17	Val382Glu	18	20
Y50D4B.3	His68Pro	19	19
srw-141	Gln352His	5	7
str-83	Thr49Ala	22	23
Y45G5AM.3	Ile14Leu	23	24
srr-4	Thr324Pro	4	5
pqn-13	Ser28Phe	21	21
pst-1	Leu4Ser	5	8
ttn-1	Gln6679Pro	7	8
mec-1	Val32Leu Arg42Ala	5 10	8 13
ftn-1	His147Tyr	23	23
B0507.7	Asn150Lys	25	25
srx-86	Trp186Leu	5	6
unc-61	Leu142Val	22	24
F57A10.2	Ser77STP	17	17
fbxa-69	Lys308Thr	5	9
clec-38	Phe370Val	23	23
C14B4.2	Gln1696STP	20	20
Y43F8C.4	Gln349Pro	5	7
F55A4.2	Asn51Ile	16	17
gap-1	Cys10Arg	22	22
C14A11.5	Tyr418Phe	21	24
C12D12.1	Thr207Ile	17	18

Gene	non synonymous SNP	Counts	Coverage
C15H9.5	Asn194Lys	21	25
hen-1	Cys83STP	15	15
atg-11	His460Asn	4	5
vps-52	Val342Ala	14	17
adt-2	Ser75Pro	25	25
C18A11.6	Ala52Gly	20	21
alh-13	Trp578Cys	17	17
srd-50	Asn117Ile	13	17
sto-5	Lys290Glu	20	21
gcy-11	Glu922Lys	23	23

Table 11: Putative background modifiers in the *let-60(n1046)* genome, dramatically enhancing the muv phenotype and leading to unviability. Data was obtained after aligning *let-60(n1046)* raw sequences to N2 reference genome WS220. Coverage of the variant and total coverage is indicated as counts and coverage respectively. Cases were the alignment found two mutational alleles were ignored and removed from the list.

1.11.4 RNAi of putative modifier genes reveals slight suppression

In a next step, we applied RNAi to knockdown putative modifier genes. We screened for suppression of lethality in three independent rounds. The results are summarised in Table 12.

Gene	1. Screen	2. Screen	3. Screen	significance
ttx-7		*		*
T22C1.6		*	*	**
T26E3.6	*			*
R07C3.13	*	*	*	***
C56E6.4		*		*
let-23	*			*
age-1	*		*	**
ZK930.1		*		*
gcn-2	*			*
F15D4.4	*			*
him-18	*			*
bus-2	*	*		**
clec-76	*	*		**
pfd-1	*			*
F54E12.2			*	*
cyp-31A2	*			*
let-60		*	*	**
Y116A8C.26	*	*		**
srw-141	*	*	*	***
pqn-13		*		*
mec-1		*		*
srx-86		*	*	**

fbxa-69	*			*
C14B4.2	*	*		**
F55A4.2	*			*
C14A11.5		*		*
C12D12.1			*	*
hen-1		*		*
alh-13		*		*

Table 12: RNAi positive candidate genes in the outcrossed *let-60(n1046)* unviable, high muv strain. Indicated are the rounds of screening and if there was any sign of viability restoration visible. Significance sums up the results from all the screening rounds.

1.11.5 Conclusion and Outlook

The *let-60(n1046)* strain possibly harbours a background suppressor mutation, masking its real vulval and lethal phenotype. The nature of the suppressor mutation can either lead to a gain-of-function situation in a negative or to a loss- or reduction-of-function situation in a positive regulator of RAS. Using RNAi, we can only test for the first possibility. It is impossible to detect further enhancement due to the strength of the phenotype. Nevertheless, RNAi knockdown could identify possible modifiers. Next, it would be of interest to test the candidates through mutant and rescue experiments that would restore the function of the suppressor in the *let-60(n1046)* background.

A very different approach would be to start with the outcrossed *let-60(n1046)* mutant and to do further conventional fine mapping of the mutation either using CB4856 or different introgression lines, helping to reduce the number of candidate genes. A more detailed analysis on the residual genes could be carried out including RNAi, mutant and rescue analysis.

It has to be considered that background mutations do not only affect the *let-60(n1046)* mutant strain, but all other strains that were generated via forward genetic screen have do deal with the same problem. Subsequent backcrossing might help to reduce the mutational load coming from random mutagenesis of the genome. But, recent investigation in the *C. elegans* field showed that backcrossing introduced more background mutation than what was removed (Worm breeder gazette, personal communication). No matter what strain is used to backcross, it will always introduce new mutations. Therefore, analysis of a given mutation should always be in the same genomic context. E.g. differences between single and double mutants should always rely on the corresponding cross progeny. Researchers should not compare the double mutant vs. the parental lines, unless someone is interested in finding background modifier mutations. At last, for transgenic animals harbouring extrachromosomal arrays it is conventionally done to analyse at least 3 independent lines, this should be done for any cross comparison, we should not rely on one double mutant line comparing it to the parental.

1.12 WormQTL--public archive and analysis web portal for natural variation data in Caenorhabditis spp. (PMID: 23180786)

My contribution to this work: eQTL and QTL data from the MIRIL sets *let-60(n1046)* and *bar-1(80)* are stored in the online database.

D738–D743 *Nucleic Acids Research, 2013, Vol. 41, Database issue* *Published online 24 November 2012*
doi:10.1093/nar/gks1124

WormQTL—public archive and analysis web portal for natural variation data in *Caenorhabditis* spp

L. Basten Snoek[1], K. Joeri Van der Velde[2], Danny Arends[2], Yang Li[2], Antje Beyer[3], Mark Elvin[4], Jasmin Fisher[3], Alex Hajnal[5], Michael O. Hengartner[5], Gino B. Poulin[4], Miriam Rodriguez[1], Tobias Schmid[5], Sabine Schrimpf[5], Feng Xue[4], Ritsert C. Jansen[2], Jan E. Kammenga[1,*] and Morris A. Swertz[2,6,*]

[1]Laboratory of Nematology, Wageningen University, Wageningen 6708 PB, [2]Groningen Bioinformatics Centre, University of Groningen, Groningen, P.O. Box 11103, 9700 CC, The Netherlands, [3]Microsoft Research Cambridge, Cambridge CB3 0FB, [4]Faculty of Life Sciences, University of Manchester, Manchester M13 9PT, UK, [5]Institute of Molecular Life Sciences, University of Zurich, Zurich CH-8057, Switzerland and [6]Genomics Coordination Center, University of Groningen, University Medical Center Groningen, Groningen, P.O. Box 30001, 9700 RB, The Netherlands

Received August 15, 2012; Revised October 10, 2012; Accepted October 22, 2012

ABSTRACT

Here, we present WormQTL (http://www.wormqtl.org), an easily accessible database enabling search, comparative analysis and meta-analysis of all data on variation in *Caenorhabditis* spp. Over the past decade, *Caenorhabditis elegans* has become instrumental for molecular quantitative genetics and the systems biology of natural variation. These efforts have resulted in a valuable amount of phenotypic, high-throughput molecular and genotypic data across different developmental worm stages and environments in hundreds of *C. elegans* strains. WormQTL provides a workbench of analysis tools for genotype–phenotype linkage and association mapping based on but not limited to R/qtl (http://www.rqtl.org). All data can be uploaded and downloaded using simple delimited text or Excel formats and are accessible via a public web user interface for biologists and R statistic and web service interfaces for bioinformaticians, based on open source MOLGENIS and xQTL workbench software. WormQTL welcomes data submissions from other worm researchers.

INTRODUCTION

Over the past 30 years, the metazoan *Caenorhabditis elegans* has become a premier animal model for determining the genetic basis of quantitative traits (1,2). The extensive knowledge of molecular, cellular and neural bases of complex phenotypes makes *C. elegans* an ideal system for the next endeavour: determining the role of natural genetic variation on system variation. These efforts have resulted in an accumulation of a valuable amount of phenotypic, high-throughput molecular and genotypic data across different developmental worm stages and environments in hundreds of strains (3–19). In addition, a similar wealth has been produced on hundreds of different *C. elegans* wild isolates and other species (20). For example, *C. briggsae* is an emerging model organism that allows evolutionary comparisons with *C. elegans* and quantitative genetic exploration of its own unique biological attributes (21).

This rapid increase in valuable data calls for an easily accessible database allowing for comparative analysis and meta-analysis within and across *Caenorhabditis* species (22). To facilitate this, we designed a public database repository for the worm community, WormQTL (http://www.wormqtl.org). Driven by the PANACEA project of the systems biology program of the EU, its design was tuned to the needs of *C. elegans* researchers via an intensive series of interactive design and user evaluation sessions on a mission to integrate all available data within the project.

As a result, data that were scattered across different platforms and databases can now be stored, downloaded, analysed and visualized in an easily and comprehensive way in WormQTL. On top, the database provides a set of user interfaced analysis tools to search the database and

*To whom correspondence should be addressed. Tel: +31 317 482998; Fax: +31 317 484254; Email: jan.kammenga@wur.nl
Correspondence may also be addressed to Morris A. Swertz. Tel: +31 50 361 7100; Fax: +31 50 361 7230; Email: m.a.swertz@rug.nl

The authors wish it to be known that, in their opinion, the first four authors should be regarded as joint First Authors.

explore genotype–phenotype mapping based on R/qtl (23,24). New data can be uploaded and downloaded using the extensible plain text format for genotype and phenotypes, XGAP (25). There is no limit to the type of data (from gene expression to protein, metabolite or cellular data) that can be accommodated because of its extensible design. All data and tools can be accessed via a public web user interface and programming interfaces to R and REST web services, which were built using the MOLGENIS biosoftware toolkit (26). Moreover, users can upload and share more R scripts as 'plugin' for the colleagues in the community to use directly and run those on a computer cluster using software modules from xQTL workbench (27); this requires login to prevent abuse. All software can be downloaded for free to be used, for example as local mirror of the database, and/or to host new studies.

All the software was built as open source, reusing and building on existing open source components as much as possible. WormQTL is freely accessible without registration and is hosted on a large computational cluster enabling high-throughput analyses at http://www.wormqtl.org. Below we detail the results, methods used to implement the system and future plans.

RESULTS

WormQTL is an online database platform for expression quantitative trait loci (eQTL) exploration to service the worm community and already provides many publicly available data sets (5,9–15,19). New data sets can be uploaded using the XGAP plain file data format. Suitable help pages are provided. Currently, 38 public data sets have been loaded, of which the bulk is xQTL data on 500 strains (introgression lines, recombinant inbred lines (RILs), recombinant inbred advanced intercross lines and natural isolates), 55,000 transcripts, 1594 samples and 1579 markers (Table 1). With this combination of classical phenotypes, molecular profiles and genetics data sets, WormQTL contains all the 'genetical genomics' experiments published to our current knowledge (except for some tiling data). Using WormQTL, researchers can explore many xQTLs across the various studies in different conditions and ages and compare classical QTLs with xQTLs. The main interfaces are 'Find QTLs', 'Genome browser' and'Browse data'.

Find QTLs

QTL is genomic regions associated with phenotypic variation and can be used to study the genetic architecture of traits and to detect potential phenotypic regulators. Recently, the number of QTLs and especially eQTL studies in *C. elegans* has increased greatly. These eQTL studies consist of large data sets that, before WormQTL, were very difficult to access and perform a combined meta-analysis. Therefore, we provide easy access to most of the eQTL studies published, by search, browse and plot functions (Figure 1).

We support relatively simple questions like 'does my gene have an xQTL?' to more advanced ones like 'how do these genes fit into an xQTL network?'. All the matching genes, markers and traits found in the data sets are returned including links to WormBase and literature. Furthermore, WormQTL is the first portal for any species that allows comparison of eQTLs over multiple experiments and environments, giving insight in the plastic nature of genetic regulation.

Genome browser

To find the genes that have a QTL on your favourite position, click 'Genome browser'. Here, you can select from all the different releases of the University of California, Santa Cruz genome releases. You can add tracks from the designated experiments of interest. Then navigate to your favourite location (tip: use open in new window) and collect significant probe identifiers from that region.

Browse data

Complete data sets and accompanying gene, sample and trait identifier lists can be browsed via the 'browse data' user interface. External identifiers anywhere in the data are automatically recognized and enhanced as linkouts to background information, such as links to Wormbase, NCBI, KEGG or Ensembl. All the annotation lists and data matrices can be browsed and searched in a tabular form and can be downloaded as plain text or Excel files. Readers can also download data sets or submit new data sets using the XGAP data format following examples described in the WormQTL help section. Also all data can be accessed programmatically from with R (as whole matrix or per row) or using REST web services, including filtering of the annotations (genes, probes, markers and phenotypes) and services to 'slice' individual lines out of the complete data sets to speed up download and (parallel) analyses. Alternatively, readers can request a login to upload data and new analysis scripts directly.

DISCUSSION

Implementation

All the software was implemented using the open source 'Molecular Genetics Information Systems' MOLGENIS toolkit (26), and in particular one previously existing MOLGENIS application, the extensible xQTL workbench (27) and the R/qtl QTL mapping and visualization package for the R language (23,24). The MOLGENIS toolkit is a Java-based software to generate tailored research infrastructure on demand (22). From a single 'blueprint' describing all biological data structures and user interfaces of the whole system, MOLGENIS autogenerates a full application including user interface, database infrastructure and application programming interfaces (APIs) in R, REST and SOAP.

At the push of a button, MOLGENIS 'generators' automatically translates these models into a database, standard user interfaces for data queries and updates, upload/download tools for tab-delimited data and

Table 1. Overview of data sets currently loaded

Phenotypes	Sample size	Parental strains	Reference	Pubmed link	Growing temperature	Stage
Gene expression	2 × 40 RILs	CB4856; N2	Li *et al.* (10)	17196041	16 and 24°C	(72 h at 16 and 40 h at 24) L4
Gene expression	60 RILs	CB4856; N2	Li *et al.* (11)	20610403	24°C	(40 h) L4
Gene expression	36 × 3 RILs	CB4856; N2	Viñuela *et al.* (14)	20488933	24°C	(40, 96 and 214 h) L4, adult, old
Gene expression	208 RIAILs	CB4856; N2	Rockman *et al.* (5)	20947766	20°C	YA
Feeding curves RNAi exposure	56 RILs × 12 RNAi	CB4856; N2	Elvin *et al.* (15)	22004469	20°C	Multi-generational
Life-history traits	80 RILs	CB4856; N2	Gutteling *et al.* (13)	16955112	12 and 24°C	Egg, L4, YA
Lifespan and pharyngeal-pumping	90 NILs	CB4856; N2	Doroszuk *et al.* (9)	19542186	20°C	All; synchronized
Lifespan, Recovery and reproduction after heat-shock	58 RILs	CB4856; N2	Rodriguez *et al.* (19)	22613270	20 and 35°C heat shock	L4 and adult
Gene expression	6 × 2 parental strains	CB4856 and N2	Viñuela *et al.* (18)	22670229	24°C	(40, 96 and 214 h) L4, adult, old

RILs, recombinant inbred lines; NILs, near isogenic lines; RIAILs, recombinant inbred advanced intercross lines.

scriptable interfaces for programmers to users from within R and via web services. This greatly speeded up the initial software development and also enables rapid extension when, for example, new data types arrive. On top of this foundation, we build the WormQTL specific user interactions such as the 'Find QTLs' and the 'Genome browser' using MOLGENIS 'plug-in' mechanism and the visualizations and plots using the R interface. xQTL workbench is a scalable web platform for the mapping of QTLs at multiple levels: for example, gene expression (xQTL), protein abundance (pQTL), metabolite abundance (mQTL) and phenotype (phQTL) data. The xQTL workbench provided a set of previously developed user interfaces to run R/qtl mapping methods directly from within the WormQTL user interface, the ability to add new analysis procedures in R, data management and data format conversions, all greatly speeding up the generation of new xQTL profiles.

All the data sets were downloaded from their original sources and then formatted using the XGAP data format. XGAP is a simple text file format that uses a directory of tab-delimited files or one Excel file with multiple sheets to load lists of annotations and data matrices. The annotations list all the background information needed to run and interpret the analysis including, for example, genome position information, such as markers, genes, probes and strains. The data matrices describe all the raw, intermediate and result data, such as gene expression, genotypes and QTL *P*-values, with the row names and column names cross linking to the annotations. For example, gene expression is a matrix of 'gene' X 'sample'. Subsequently these data sets were loaded using the MOLGENIS/xQTL data import wizards, which check the files for correctness and give informative feedback if the data are not yet in a format that WormQTL can understand (25). All the annotations are stored in tables in the database; the large data matrices are stored in a optimized binary format to speed up analyses and queries. This format is documented in the WormQTL manual to ease the submission of new data sets from the community. Finally, all the QTL profiles were recalculated according to the specification of the original, or slightly modified when needed, such as to include a previously missing wrongly labelled sample correction. In this process, we greatly benefitted from the integration with xQTL workbench, which enabled us to re-run all these analyses on the computer cluster and add new R analysis procedures when needed, simply from the user interface.

All software is available as open source on http://github.com/molgenis for others to reuse locally, and related technical documentation is available at http://www.xqtl.org and http://www.rqtl.org and http://www.molgenis.org.

Future plans

The current version of WormQTL (June 2012) is a comprehensive, versatile and flexible package. Follow-up plans of more extended versions with new tools and data depend on the demand by the users of WormQTL.

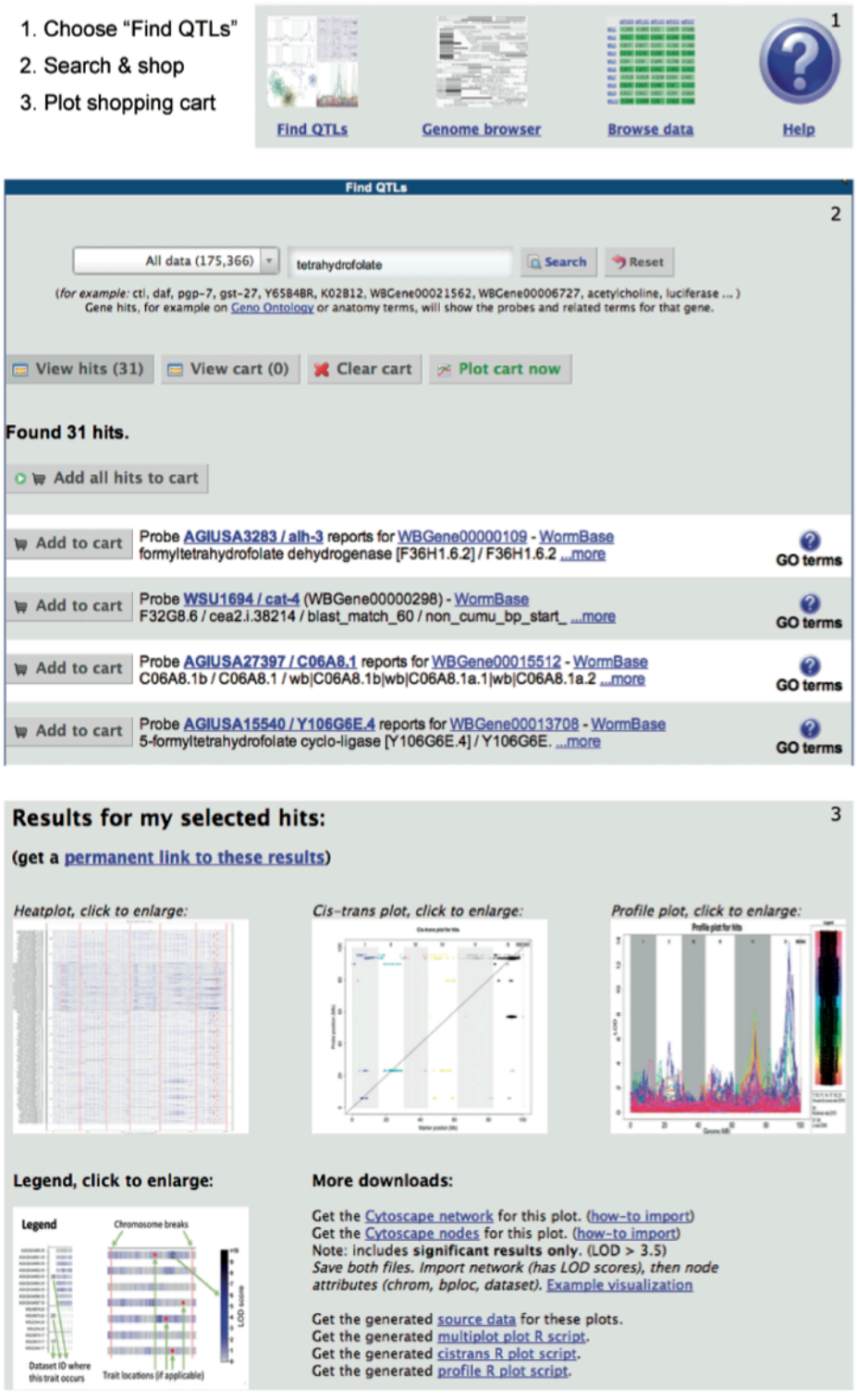

Figure 1. Cross experiment search. (1) Users can search for genes, markers or traits of interest using a google-like search box, optionally filtering for particular types of information. The results include links to WormBase and PubMed where possible. (2) From the resulting list, users can select items in a shopping cart, optionally repeating the search to add more items. (3) Finally, users can plot the contents of the shopping cart on top of all collected QTL data sets showing interesting areas in a heat plot, significant traits in a cis/trans plot and the individual signals in a profile plot. Alternatively, users can browse the QTL profiles using a genome browser, view/download the data set by simply browsing trough all available information or use the scriptable interface to program against. A complete tutorial is available in the help page.

We envisage that in the future, three types of new tools will be developed: (i) visualization tools, (ii) QTL mapping tools and (iii) candidate gene selection tools. Improved visualization tools might include plotting a phenotype against the marker at a certain position; so the two groups become visible at a QTL position. Also plots can be made showing transgression and heritability per microarray probe or gene or histograms of the phenotypic values (and include the parental values if available). Advanced QTL mapping tools might include multi-environment/age mapping or genotype-by-environment analyses, developed in collaboration with the R/qtl team to enable automatic links to this software. The candidate gene selection tools would benefit from the most recent stable release of Wormbase (28), the most widely used platform for worm biology. But also other sources of information like MODENCODE (29) or Wormnet (30) are likely to be connected with WormQTL. A candidate gene selection tool might be implemented in a next version of WormQTL as it is less easy to implement and often needs information beyond WormQTL. One can think of (i) which SNPs/genes/polymorphic genes/transcription factor binding sites and so forth are underlying a eQTL; (ii) which gene, underlying my xQTL, is linked to most of the genes having an xQTL; (iii) which genes are polymorphic and (iv) which other genotypes show a difference in expression and do they share polymorphisms with the parental strains of the RIL population that the xQTL was mapped in. Moreover, WormQTL can be easily expanded to other *Caenorhabditis* species (21).

We believe that WormQTL, which will be continuously curated by the members of this international consortium, is a very attractive database for the growing community of quantitative genetics in worms researchers. We are committed to maintain data and software for the years to come and invite the community to add and share new data and ideas.

ACKNOWLEDGEMENTS

We thank Wormbase for being an easy accessible and versatile data source. We also thank Mark Sterken and Rita Volkers for helpful suggestions, Konrad Zych for graphics design and testing and many members of the *C. elegans* community for their comments and ideas.

FUNDING

The Centre for BioSystems Genomics (CBSG) and the Netherlands Consortium of Systems Biology (NCSB), both of which are part of the Netherlands Genomics Initiative of the Netherlands Organisation for Scientific Research (NWO) (to D.A.); European Community's Health Seventh Framework Programme (FP7/2007-2013) under grant agreement PANACEA [222936 to L.B.S., M.E., T.S., J.E.K., R.C.J.]; ERASysbio-plus ZonMW project GRAPPLE - Iterative modelling of gene regulatory interactions underlying stress, disease and ageing in *C. elegans* [90201066 to L.B.S.]. Funding for open access charge: EU 7th Framework Programme under the Research Project PANACEA (no: 222936).

Conflict of interest statement. None declared.

REFERENCES

1. Gaertner,B. and Phillips,P.C. (2010) *Caenorhabditis elegans* as a platform for molecular quantitative genetics and the systems biology of natural variation. *Genet. Res.*, **92**, 331–348.
2. Kammenga,J.E., Phillips,P.C., de Bono,M. and Doroszuk,A. (2008) Beyond induced mutants: using worms to study natural variation in genetic pathways. *Trends Genet.*, **24**, 178–185.
3. Palopoli,M.F., Rockman,M.V., TinMaung,A., Ramsay,C., Curwen,S., Aduna,A., Laurita,J. and And Kruglyak,L. (2008) Molecular basis of the copulatory plug polymorphism in *Caenorhabditis elegans*. *Nature*, **454**, 1019–1022.
4. Kammenga,J.E., Doroszuk,A., Riksen,J.A.G., Hazendonk,E., Spiridon,L., Petrescu,A.-J., Tijsterman,M., Plasterk,R.H.A. and Bakker,J. (2007) A *Caenorhabditis elegans* wild type defies the temperature-size rule owing to a single nucleotide polymorphism in tra-3. *PLoS Genet.*, **3**, 0358–0366.
5. Rockman,M.V., Skrovanek,S.S. and Kruglyak,L. (2010) Selection at linked sites shapes heritable phenotypic variation in *C. elegans*. *Science*, **330**, 372–376.
6. McGrath,P.T., Rockman,M.V., Zimmer,M., Jang,H., Macosko,E.Z., Kruglyak,L. and Bargmann,C.I. (2009) Quantitative mapping of a digenic behavioral trait implicates globin variation in *C. elegans* sensory behaviors. *Neuron*, **61**, 692–699.
7. Reddy,K.C., Andersen,E.C., Kruglyak,L. and Kim,D.H. (2009) A polymorphism in npr-1 is a behavioral determinant of pathogen susceptibility in *C. elegans*. *Science*, **323**, 382–384.
8. Palopoli,M.F., Rockman,M.V., TinMaung,A., Ramsay,C., Curwen,S., Aduna,A., Laurita,J. and Kruglyak,L. (2008) Molecular basis of the copulatory plug polymorphism in *Caenorhabditis elegans*. *Nature*, **454**, 1019–1022.
9. Doroszuk,A., Snoek,L.B., Fradin,E., Riksen,J.A.G. and Kammenga,J.E. (2009) A genome-wide library of CB4856/N2 introgression lines of *Caenorhabditis elegans*. *Nucleic Acids Res.*, **37**, e110.
10. Li,Y., Alvarez,O.A., Gutteling,E.W., Tijsterman,M., Fu,J., Riksen,J.A.G., Hazendonk,E., Prins,P., Plasterk,R.H., Jansen,R.C. *et al.* (2006) Mapping determinant of gene expression plasticity by genetical genomics in *C. elegans*. *PLoS Genet.*, **2**, 2155–2161.
11. Li,Y., Breitling,R., Snoek,L.B., van der Velde,K.J., Swertz,M.A., Riksen,J., Jansen,R.C. and Kammenga,J.E. (2010) Global genetic robustness of the alternative splicing machinery in *Caenorhabditis elegans*. *Genetics*, **186**, 405–410.
12. Gutteling,E.W., Doroszuk,A., Riksen,J.A.G., Prokop,Z., Reszka,J. and Kammenga,J.E. (2007) Environmental influence on the genetic correlations between life-history traits in *Caenorhabditis elegans*. *Heredity*, **98**, 206–213.
13. Gutteling,E.W., Riksen,J.A.G., Bakker,J. and Kammenga,J.E. (2007) Mapping phenotypic plasticity and genotype-environment interactions affecting life-history traits in *Caenorhabditis elegans*. *Heredity*, **98**, 28–37.
14. Viñuela,A., Snoek,L.B., Riksen,J.A.G. and Kammenga,J.E. (2010) Genome-wide gene expression regulation as a function of genotype and age in *C. elegans*. *Genome Res.*, **20**, 929–937.
15. Elvin,M., Snoek,L.B., Frenjo,M., Klemstein,U., Kammenga,J.E. and Poulin,G.B. (2011) A fitness assay for comparing RNAi effects across multiple *C. elegans* genotypes. *BMC Genomics*, **12**, 510.
16. Chandler,C.H. (2010) Cryptic intraspecific variation in sex determination in *Caenorhabditis elegans* revealed by mutations. *Heredity*, **105**, 473–482.
17. Harvey,S.C., Shorto,A. and Viney,M.E. (2008) Quantitative genetic analysis of life-history traits of *Caenorhabditis elegans* in stressful environments. *BMC Evol. Biol.*, **8**, 15.

18. Viñuela,A., Snoek,L.B., Riksen,J.A.G. and Kammenga,J.E. (2012) Aging uncouples heritability and expression-QTL in *Caenorhabditis elegans*. *G3*, **2**, 597–605.
19. Rodriguez,M., Snoek,L.B., Riksen,J.A.G., Bevers,R.P. and Kammenga,J.E. (2012) Genetic variation for stress-response hormesis in *C. elegans* lifespan. *Exp. Geront.*, **47**, 581–587.
20. Andersen,E.C., Gerke,J.P., Shapiro,J.A., Crissman,J.R., Ghosh,R., Bloom,J.S., Felix,M.A. and Kruglyak,L. (2012) Recent chromosome-scale selective sweeps reshaped genomic diversity in *C. elegans*. *Nat. Genet.*, **29**, 285–290.
21. Ross,J.A., Koboldt,D.C., Staisch,J.E., Chamberlin,H.M., Gupta,B.P., Miller,R.D., Baird,S.E. and Haag,E.S. (2011) *Caenorhabditis briggsae* recombinant inbred line genotypes reveal inter-strain incompatibility and the evolution of recombination. *PLoS Genet.*, **7**, e1002174.
22. Swertz,M.A. and Jansen,R.C. (2007) Beyond standardization: dynamic software infrastructures for systems biology. *Nat. Rev. Genet.*, **8**, 235–243.
23. Broman,K.W., Wu,H., Sen,S. and Churchill,G.A. (2003) R/qtl: QTL mapping in experimental crosses. *Bioinformatics*, **19**, 889–890.
24. Arends,D., Prins,P., Jansen,R.C. and Broman,K.W. (2010) R/qtl: high throughput multiple QTL Mapping. *Bioinformatics*, **26**, 2990–2992.
25. Swertz,M.A., van der Velde,K.J., Tesson,B.M., Scheltema,R.A., Arends,D., Vera,G., Dijkstra,M., Schofield,P., Schughart,K., Hancock,J.M. *et al.* (2010) XGAP: a uniform and extensible data model and software platform for genotype and phenotype experiments. *Genome Biol.*, **11**, R27.
26. Swertz,M.A., Dijkstra,M., Adamusiak,T., van der Velde,K.J., Kanterakis,A., Roos,E.T., Lops,J., Thorisson,G.A., Byelas,G., Muilu,J. *et al.* (2010) The MOLGENIS toolkit: rapid prototyping of biosoftware at the push of a button. *BMC Bioinformatics*, **11(Suppl. 12)**, S12.
27. Arends,D. and van der Velde,K.J. (2012) xQTL workbench: a scalable web environment for multilevel QTL analysis. *Bioinformatics*, **28**, 1042–1044.
28. Yook,K., Harris,T.W., Bieri,T., Cabunoc,A., Chan,J., Chen,W.J., Davis,P., de la Cruz,N., Duong,A., Fang,R. *et al.* (2012) WormBase 2012: more genomes, more data, new website. *Nucleic Acids Res.*, **40**, D735–D741.
29. Gerstein,M.B., Lu,Z.J., Van Nostrand,E.L., Cheng,C., Arshinoff,B.I., Liu,T., Yip,K.Y., Robilotto,R., Rechtsteiner,A., Ikegami,K. *et al.* (2010) Integrative analysis of the *Caenorhabditis elegans* genome by the modENCODE project. *Science*, **330**, 1775–1787.
30. Lee,I., Lehner,B., Crombie,C., Wong,W., Fraser,A.G. and Marcotte,E.M. (2008) A single gene network accurately predicts phenotypic effects of gene perturbation in *Caenorhabditis elegans*. *Nat. Genet.*, **40**, 181–188.

1.13 Hawaii genome assembly (Paper in preparation)

My contribution to this work: Preparation of CB4856 genomic DNA and providing the raw sequencing read data.

1.13.1 Background

The complete genomic sequence of CB4856 is not available. Part of the data is accessible through Wormbase.org through the entry Polymorphisms and natural variants. This lack of reliable information let many laboratories to sequence their own CB4856 strain, without depositing the information on Wormbase.org. In order to provide the community with the complete CB4856 genome, the group of Jan Kammenga took the initiative to collect CB4856 raw sequencing reads from different sequencing platforms and from different labs to newly assemble the CB4856 genome with high coverage. This will further improve the reliability of natural polymorphisms and sequence alterations between Bristol N2 and Hawaii CB4856.

1.14 Combined PANACEA project

1.14.1 Background:

The PANACEA consortium is interested in the investigation of natural variation in complex disease signalling in *C. elegans*. Vulval development as the terminal layer of phenotypic readout is only one aspect of it. To add two more layers of complexity, the transcriptome and the proteome should also be investigated to have a more precise analysis. The combination of all three layers will shed light on the entire mechanism of gene regulation that will eventually lead to a very specific and robust phenotypic outcome.

1.14.2 Experimental approach

Due to different throughput, only a subset of 36 RILs between N2 and CB4856 could be used. Those RILs were chosen to maximize recombination frequency and therefore informational content. RNAi of *let-60*, *lin-12* and *mom-2* was chosen to knockdown the core pathways EGFR/RAS/MAPK, Notch and Wnt respectively. The group of Jan Kammenga took Transcriptome readouts; the group of Michael Hengartner obtained proteomic abundance data and myself collected the phenotypic data by counting vulval induction. The data for vulval induction in the 36 core RILs is summarised below in Table 13.

RILs	EGFR/RAS/MAPK				Notch				Wnt			
	#	VI	STDEV	s.e.m.	#	VI	STDEV	s.e.m.	#	VI	STDEV	s.e.m.
WN13	30	2.98	0.09	0.02	30	2.97	0.13	0.02				
WN14	30	2.70	0.66	0.12	27	2.69	0.46	0.09				
WN31	30	2.93	0.37	0.07	27	2.72	0.45	0.09				

WN41	30	2.83	0.51	0.09	20	2.80	0.30	0.07	30	3.00	0.00	0.00
WN48	30	2.97	0.18	0.03	26	2.58	0.56	0.11	30	3.00	0.00	0.00
WN49	30	2.75	0.77	0.14	30	2.93	0.25	0.05				
WN51	30	3.00	0.00	0.00	30	2.93	0.17	0.03	30	2.97	0.18	0.03
WN52	30	3.00	0.00	0.00	23	2.26	0.56	0.12				
WN54	30	3.00	0.00	0.00	30	2.87	0.29	0.05				
WN58	30	3.00	0.00	0.00	30	2.33	0.53	0.10				
WN60	30	2.83	0.58	0.11	30	2.70	0.50	0.09				
WN61	30	2.90	0.55	0.10	30	2.97	0.18	0.03	30	3.00	0.00	0.00
WN67	30	2.97	0.18	0.03	30	2.88	0.31	0.06	30	3.00	0.00	0.00
WN72	30	3.00	0.00	0.00	30	2.37	0.57	0.10				
WN73	30	2.67	0.80	0.15	30	2.97	0.13	0.02				
WN76	30	2.47	0.96	0.18	30	2.85	0.33	0.06				
WN98	30	2.80	0.70	0.13	30	2.98	0.09	0.02				
WN112												
WN116	30	2.73	0.67	0.12	30	2.58	0.53	0.10	30	3.00	0.00	0.00
WN125	30	2.85	0.60	0.11	28	2.89	0.28	0.05	30	3.00	0.00	0.00
WN129	30	2.77	0.73	0.13	30	2.88	0.28	0.05	30	3.00	0.00	0.00
WN143	30	2.85	0.37	0.07	28	2.66	0.39	0.07				
WN146	30	2.80	0.76	0.14	30	2.70	0.50	0.09				
WN148	30	3.00	0.00	0.00	27	2.57	0.45	0.09				
WN149	30	2.90	0.55	0.10	30	2.77	0.34	0.06				
WN158	30	3.00	0.00	0.00	30	2.77	0.34	0.06				
WN162	30	2.77	0.63	0.11	30	2.57	0.45	0.08				
WN171	30	3.00	0.00	0.00	30	2.73	0.39	0.07				
WN177	30	2.72	0.87	0.16	30	3.00	0.00	0.00				
WN181	30	3.00	0.00	0.00	30	2.27	0.43	0.08				
WN182	30	3.00	0.00	0.00	25	2.36	0.60	0.12				
WN185	30	3.00	0.00	0.00	26	2.75	0.45	0.09	30	3.00	0.00	0.00
WN187	30	3.00	0.00	0.00	24	1.85	0.73	0.15				
WN190	30	2.97	0.18	0.03	30	2.63	0.41	0.08				
WN191	30	3.00	0.00	0.00	30	2.93	0.17	0.03				
WN195	30	2.83	0.55	0.10	30	2.63	0.37	0.07				

Table 13: Combined Panacea experiment. Phenotypic data (vulval induction) is shown after knockdown of *let-60* (EGFR/RAS/MAPK), *lin-12* (Notch) and *mom-2* (Wnt). Due to robustness and/or redundancy in Wnt signalling, mom-2 did not affect vulval induction in the few RILs analysed and was therefore not pursued further.

Overall, there is high variation observed in the Notch, less variation in the EGFR/RAS/MAPK and no variation in the Wnt pathway. This can either be due to the differential effects of the RNAi on vulval induction for the different target genes, or it really reflect natural variation in robustness of different signalling pathways, the latter of course far more interesting for further investigation.

1.14.3 Outlook

Data acquisition is complete for all the partners and has to be evaluated by the groups of Jan Kammenga and Ritsert Jansen.

1.15 Loss-of-function of the Wnt associated β-catenin bar-1 affects transcription and developmental timing in Caenorhabditis elegans (Paper accepted in Sci. Rep.)

My contribution to this work: Analysis of results, reading and revising the manuscript before submission.

SCIENTIFIC REPORTS

OPEN

SUBJECT AREAS:
TRANSCRIPTOMICS
GENE EXPRESSION

Received
27 February 2014

Accepted
23 April 2014

Published
13 May 2014

Correspondence and requests for materials should be addressed to J.E.K. (Jan.Kammenga@wur.nl) or L.B.S. (Basten.Snoek@wur.nl)

* These authors contributed equally to this paper.

Loss-of-function of β-catenin *bar-1* slows development and activates the Wnt pathway in *Caenorhabditis elegans*

M. Leontien van der Bent[1]*, Mark G. Sterken[1]*, Rita J. M. Volkers[1]*, Joost A. G. Riksen[1], Tobias Schmid[2], Alex Hajnal[2], Jan E. Kammenga[1] & L. Basten Snoek[1]

[1]Laboratory of Nematology, Wageningen University, Droevendaalsesteeg 1, 6708 PB Wageningen, The Netherlands, [2]Institute of Molecular Life Sciences, University of Zurich, Winterthurerstrasse 190, CH-8057 Zurich, Switzerland.

C. elegans **is extensively used to study the Wnt-pathway and most of the core-signalling components are known. Four β-catenins are important gene expression regulators in Wnt-signalling. One of these, *bar-1*, is part of the canonical Wnt-pathway. Together with Wnt effector pop-1, bar-1 forms a transcription activation complex which regulates the transcription of downstream genes. The effects of *bar-1* loss-of-function mutations on many phenotypes have been studied well. However, the effects on global gene expression are unknown. Here we report the effects of a loss-of-function mutation *bar-1(ga80)*. By analysing the transcriptome and developmental phenotyping we show that *bar-1(ga80)* impairs developmental timing. This developmental difference confounds the comparison of the gene expression profile between the mutant and the reference strain. When corrected for this difference it was possible to identify genes that were directly affected by the *bar-1* mutation. We show that the Wnt-pathway itself is activated, as well as transcription factors *elt-3, pqm-1, mdl-1* and *pha-4* and their associated genes. The outcomes imply that this response compensates for the loss of functional *bar-1*. Altogether we show that *bar-1* loss-of function leads to delayed development possibly caused by an induction of a stress response, reflected by daf-16 activated genes.**

The Wnt/β-catenin pathway is highly conserved across metazoans and is essential for many cellular functions like cell specialization, cellular migration, adhesion and development. Although a key pathway in invertebrates and vertebrates, the Wnt-signalling pathway yet remains to be fully elucidated[1–3]. A better understanding is required not only from a fundamental biological point of view, but also because it can be important for developing drugs and medical treatments of Wnt associated diseases such as bone diseases and colorectal cancer (reviewed by[4,5]).

The model worm *Caenorhabditis elegans*, a widely studied human model species, has the canonical Wnt-signalling pathway and a variation on this pathway, the asymmetrical cell division pathway. The Wnt pathway has five known Wnt genes: *mom-2, cwn-1, cwn-2, lin-44* and *egl-20*[6]. In the canonical Wnt pathway, the cellular abundance of free β-catenin is controlled by a protein destruction complex which targets free β-catenin for proteasomal degradation. Activation of canonical Wnt-signalling, whereby Wnt binds to a Frizzled/LRP co-receptor, inactivates the destruction complex leading to accumulation of free β-catenin which then functions as a nuclear transcriptional activator. In *C. elegans* four distinct β-catenins have been identified. *Bar-1* is part of the evolutionarily most conserved pathway[7–9], whereas *wrm-1*[10], *hmp-2*[11], and *sys-1*[12] function in a variant of the Wnt pathway regulating asymmetrical cell divisions[6,7]. These β-catenins all seem to play distinct roles in the worm[13].

BAR-1 functions in the post-embryonic stage[8,14,15] where it forms a transcription activation complex with the Wnt effector POP-1[13], similar to the TCF/β-catenin complex in flies and vertebrates[16]. BAR-1 is regulated by the axin-like protein PRY-1, the GSK3β homolog SGG-1 and the APC-like protein APR-1[17,18]. Among the processes influenced by BAR-1 are P12 cell fate specification[14,19] and *mab-5* expression in the neuroblast QL[15,20]. Moreover, BAR-1 is involved in vulval precursor cell specification in the early L1 stage of *C. elegans* through transcriptional activation of the Hox gene *lin-39*. In addition, BAR-1 plays a role in cell fate specification of the vulva during the early L3 stage[8]. The mutation used in this study, *bar-1(ga80)*, affects vulval precursor cell induction which results in an incomplete vulva, a protruding vulva (pvl) and egg-laying defects (egl)[8].

Even though many developmental processes in which *bar-1* is involved are known, the effect of *bar-1* on gene expression is poorly understood. We studied gene expression patterns during the fourth larval stage (L4) of the

worm strain EW15 carrying the β-catenin-loss-of-function point mutation *bar-1(ga80)*. This mutation causes a Glu to Stop codon change at amino acid 97 of the predicted BAR-1 protein. By analysing the transcriptome and developmental phenotyping we show that *bar-1(ga80)* impairs developmental timing. Moreover we found that without a functioning *bar-1* ~ 7,500 genes were affected. Our results further suggest that the loss of *bar-1* is partially compensated by redundancy in the Wnt-signalling pathway, pointing towards a feed-back mechanism between β-catenin activation and the expression levels of Wnt-signalling pathway encoding genes.

Methods

Strains. The following strains were used: EW15 (Bristol N2 strain, carrying the mutation *bar-1(ga80)*) and wild type Bristol N2. Upon arrival in the lab EW15 was outcrossed at least 4 times. Worms were kept in maintenance at 12°C and before experiments started, populations were cleared of males and grown at 20°C until all worms were gravid. All experiments were conducted at 20°C.

Microarray experiment. Strains were stage synchronized by bleaching[21], then grown on 9 cm NGM Petri dishes seeded with *E. coli* OP50. Worms were rinsed of the plates with M9 buffer 48 hours after synchronization, snap-frozen in liquid nitrogen and stored at −80°C before performing gene expression profiling using microarray analysis. The experiment was performed in three independent duplicates.

Egg laying experiment. Strains were synchronised by bleaching, after which approximately 200 eggs from N2 or 300 eggs from EW15 were transferred to a fresh 9 cm NGM dish containing *E. coli* OP50. Starting at 58 hours after bleaching, the production of eggs by the adult worms was observed. Eggs on the plate were scored as: 0 (no eggs), 1 (first 1–100 eggs, first worms have started laying), 2 (100–200 eggs, multiple worms are laying eggs), 3 (>200, most worms are laying eggs, first egg clusters appear) or 4 (many eggs and the first eggs are hatching). The scoring was done every hour. The experiment was performed in three independent duplicates.

Egg hatching experiment. Strains were synchronised by bleaching, after which as many eggs as possible (up to 700 eggs) were placed on a fresh 9 cm NGM dish containing *E. coli* OP50. Observations started immediately after bleaching, for every 30 minutes. Once an egg hatched, the L1 larvae was picked and counted. This was continued until all eggs hatched. The experiment was performed three times.

Microarray sample preparation, scanning and normalization. mRNA isolation was performed using the RNeasy Micro Kit from Qiagen (Hilden, Germany), following the 'Purification of Total RNA from Animal and Human Tissues' -protocol provided with the kit. After this, the 'Two-Color Microarray-Based Gene Expression Analysis; Low Input Quick Amp Labeling' -protocol, version 6.0 from Agilent (Agilent Technologies, Santa Clara, CA, USA) was followed, starting from step 5. The microarrays used were *C. elegans* (V2) Gene Expression Microarray 4 × 44K slides, manufactured by Agilent. Input of total RNA was approximately 200 ng for each replicate. Three independent duplicates per strain were measured. The microarrays were scanned using an Agilent High Resolution C Scanner, using the settings as recommended in the above mentioned manual. Data was extracted with the Agilent Feature Extraction Software version 10.5, following manufacturers' guidelines. For normalization the Limma package for the "R" environment (version 2.13.1 x 64) was used. No background correction of the RNA-array data was performed as recommended by[22]. For within-array normalization of the RNA-array data the Loess method was used and for between-array normalization the Quantile method was used. The obtained log2 normalized intensities (single channel data) were used for further analysis.

Statistical analyses. All statistical analyses were performed using the statistical programming language "R" (version 2.13.1 x 64). A linear model was used to determine the effect and significance of the genotype on the expression levels (probe intensity ~ genotype + error). Using permutations of the original data in the same linear model, we determined thresholds adjusted for multiple testing (FDR 0.05: $-\log10(p) > 2$; FDR 0.01: $-\log10(p) > 3$). To correct for the developmental difference between *bar-1(ga80)* and N2 we used the developmental gene expression data from Snoek *et al.* (2014)[23] together with the gene expression data generated for this study (*bar-1(ga80)* vs. N2) in one linear model (probe intensity ~ sample age + genotype + error). The intensities were corrected for batch effect and for sample age we used an age of 44 hours for the *bar-1(ga80)* samples (as estimated), and 48 hours for the N2 samples. For the samples from Snoek *et al.* (2014) their original ages were used (44 to 58 hours after synchronisation). Genes with $p > 0.05$ for the "sample age" were selected as genes without a developmental effect. Genes with for which the "sample age" effect was opposite to the *bar-1* effect were selected as genes with "effect which was opposite of what one would expect in a relatively slower developed *bar-1(ga80)* mutant".

Enrichment tests were done using a hyper geometric test on the genes with a significant *bar-1(ga80)* effect ($-\log10(p) > 2$), excluding those with a developmental effect (unless stated otherwise). eQTL enrichments were done by selecting the genes with a significant ($-\log10(p) > 3$) linkage to each locus and comparing those against the genes affected by the mutant[24].

Datasets used. The GO-annotation, anatomy terms, protein domains and gene classes were obtained via Wormmart (www.caprica.caltech.edu:9002/biomart/martview/) of the WS220 wormbase release. Genes from Wormbook chapters were obtained from the 2012 version of Wormbook (www.wormbook.org). Expression QTLs (eQTLs) were obtained from WormQTL (www.wormqtl.org;[25,26,49] using the data from[27–29]. Transcription factor binding sites were obtained from[30] Binding sites from DAF-16 were obtained from modENCODE release #32 (www.modencode.org;[31]), and mapped to transcription start sites according to Tepper *et al.* (2013)[32]. KEGG pathways were obtained from Release 65.0 of the Kyoto Encyclopedia of Genes and Genomes (www.genome.jp/kegg/).

Network visualization. The network of the transcription factors and their targets was visualized using Cytoscape (version 2.8.2)[33].

Data storage. All data was stored in WormQTL (www.wormqtl.org)[25,26,49].

Results and discussion

bar-1(ga80) affects gene expression and slows development. We compared the transcriptomes of worms (age of 48 h) of N2 to the *bar-1(ga80)* mutant strain of the same age by microarray analysis. Of the 20,887 genes that were tested on the microarray, 5,772 genes were differentially expressed ($-\log10(p) > 2.0$ at FDR = 0.05). In *bar-1(ga80)*, 51% was down-regulated (2,927 genes), and 49% was up-regulated (2,855 genes) compared to N2. During the initial analyses, we noticed that many of the differentially expressed genes were related to development, for example genes encoding for collagens and vitellogenins. Recently we reported that genome wide gene expression can rapidly and massively change during the L4 stage[23]. To test for the developmental difference within the L4 stage, we compared the differentially expressed genes between N2 and *bar-1(ga80)* with the set of genes reported by Snoek *et al.* (2014)[23] (Figure 1). The differentially expressed genes between *bar-1(ga80)* and N2 were enriched for genes changing during L4 development (hypergeometric test, $p < 1*10^{-200}$). To exactly pinpoint the developmental delay, we used the expression levels which have a linear correlation with L4 developmental timing to estimate the developmental age of the *bar-1(ga80)* and N2 samples. Even though all RNA samples from both genotypes were taken at 48 hours after synchronisation we found that the *bar-1(ga80)* worms developed more slowly (44.4 h ± 0.9) than the N2 samples (47.7 h ± 0.8) (two-sided t-test, $p = 6*10^{-5}$) (Supplementary figure

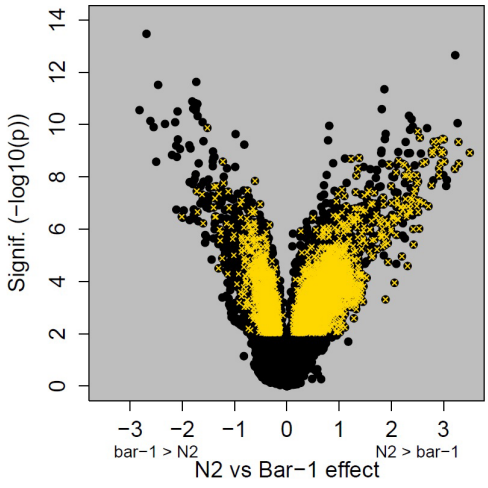

Figure 1 | Genes affected by *bar-1* and development. Volcano plot showing the effects and significance of the transcriptome comparison between *bar-1(ga80)* and N2. The black dots represent the spots on the array, the log2 effect between N2 and *bar-1(ga80)* is shown versus the LOD score. The yellow x indicate spots of genes affected by developmental effects during L4 development[23].

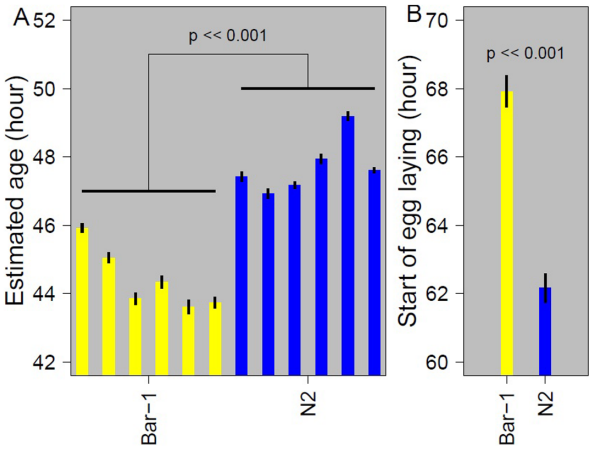

Figure 2 | Age-estimation and start of egg-laying in N2 and *bar-1(ga80)*. A) Age estimates for N2 (blue) and *bar-1(ga80)* (yellow), based on linearly differentially expressed genes during L4 development[23]. The *bar-1(ga80)* mutant is estimated significantly younger than N2 ($p < 1*10^{-4}$). B) Start of egg-laying in hours after synchronization for N2 (blue) and *bar-1(ga80)*. Again, the difference between the two strains is significant ($p < 1*10^{-5}$).

A and Figure 2A) indicating a developmental delay of 3.3 hours after 48 hours.

To confirm this discrepancy we recorded the time until the first eggs were laid in N2 and *bar-1(ga80)*. N2 started laying eggs at ~62 hours and *bar-1(ga80)* started laying eggs at ~68 hours (two-sided t-test, $p = 4*10^{-6}$) (Figure 2B). To investigate whether the delay was caused in part by delayed hatching or slow embryonic development, the time until hatching after synchronization was determined. No difference was found between N2 and *bar-1(ga80)* in time from synchronising the eggs and hatching of those eggs (Supplementary figure B).

The developmental delay of *bar-1(ga80)* increased over time (0 h at 0 h, −3.3 h at 48 h and 6 h at 62 hour). This implies that the mutation affected the entire developmental period from egg to adult. Our results show that *bar-1(ga80)* does not affect a single developmental stage, because than the developmental difference between *bar-1(ga80)* and N2 would remain constant during the subsequent stages.

Analysis incorporating developmental effects. To exclude the effects of the developmental delay of *bar-1(ga80)* from other effects of *bar-1(ga80)* on gene expression, we included the transcriptional effects during L4 development in the analysis (Figure 3). Here we found 7,557 (FDR = 0.05) genes to be affected by the *bar-1(ga80)* mutation either with or without a development effect. Of these genes, 3,920 were up-regulated and 3,637 were down-regulated in the *bar-1(ga80)* mutant (Supplementary figure C).

As developmental effects were very strong and affected many genes[23,34], we selected those genes that did not have a developmental effect ($P < 0.05$) or an effect which was opposite of what one would expect in a relatively slower developed *bar-1(ga80)* mutant (Supplemental figure C). We also selected on effect size (>0.5 or <−0.5) which resulted in 710 down- and 425 up-regulated genes compared to N2 (FDR = 0.05; Supplement Table 1).

BAR-1 strongly affects collagens and hedge-hog signalling. The set of genes down-regulated in *bar-1(ga80)* compared to N2 (Supplement Table 1) contains many non-annotated genes. These genes could complement the genes with known functions, but could also constitute new functions. Furthermore genes like *mai-1*, *dao-4*, *pho-11*, *sta-2*, *plc-2*, *pes-8*, *cnp-2*, *hmit-1.1*, *hmit-1.2*, *gcy-32*, *nlp-23* and *fkb-5* have a strongly reduced expression in *bar-1(ga80)*. These genes

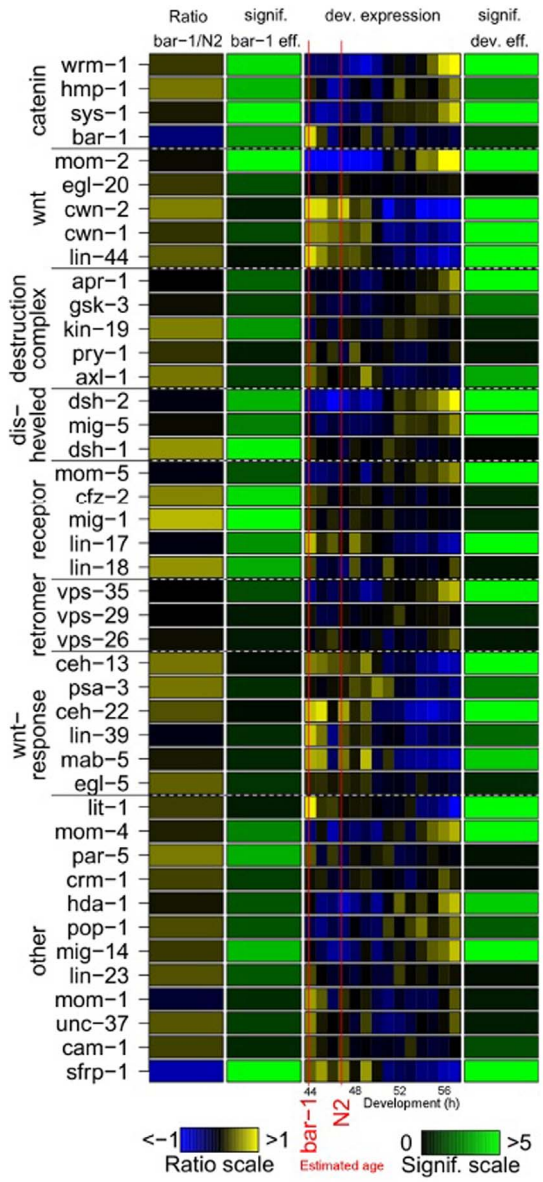

Figure 3 | Effects on Wnt pathway genes. Members of the Wnt pathway are shown by their function. The first column shows the log2-ratio between the *bar-1* mutant and N2, blue indicates lower in *bar-1*, yellow higher in *bar-1*. The second column shows the significance (-log10(p)) of the *bar-1* effect. The third column shows the log2-ratio during L4 stage (44 to 58 hours at 20°C)[23]. Two red lines indicate the relative development of the *bar-1* and N2 samples taken at 48 hours post hatching. Last column shows the significance (-log10(p)) of the developmental effect.

might function together with the strongly down-regulated groups of genes, like collagens (*rol-1*, *bli-2*, *bli-1*, *dpy-3*, *lon-3*), *col*-type genes (*col-175*, *-38*, *-71*, *-120*, *-40*, *-49*, *-138*, *-110*, *-97*, *-79*, *-70*) or other cuticle related components (*cutl-18*, *cutl-28*, *mlt-18*, *mltn-12*, *nas-27* and *gly-1*). Components of hedge-hog (hh) signalling were also much lower expressed in *bar-1(ga80)* such as: the warthog genes *wrt-6* and *wrt-4*; groundhog-like genes *grl-15*, *grl-5* and *grl-14*; hedgehog-like genes, *hog-1*, *grd-2*, *grd-1* and *grd-12*. This shows that hh-signalling is affected by *bar-1(ga80)* mutation. Taken together, BAR-1 activity is most likely required for activation of collagens and other cuticle genes as well as genes involved in hedge-hog signalling.

Expression of Wnt-signalling components. The expression of most Wnt-signalling components changed during development and were

affected by *bar-1(ga80)* mutation (Figure 3) (core-Wnt pathway genes selected by[6]). All four β-catenins were differentially expressed in *bar-1(ga80)*. Expression of *bar-1* was lower whereas *wrm-1, hmp-1* and *sys-1* all showed a slight increase in expression (see 4 upper blocks in the first column of Figure 3). In N2, these three β-catenins showed increased expression levels during L4 development whereas expression of *bar-1* hardly changed throughout the L4 stage in N2 ($p = 0.042$; see 4 upper blocks in the third column of Figure 3).

Of the five Wnt genes in *C. elegans*, only *mom-2* was higher expressed in *bar-1(ga80)*. For the other Wnt genes no significant effect was found. Of the Wnt genes, only *mom-2* expression increased during L4 development, whereas expression of *cwn-1, cwn-2* and *lin-44* decreased ($p < 0.001$ in all cases). *Egl-20* was not differentially expressed throughout L4 and was also not affected by the *bar-1* mutation.

The members of the destruction complex showed no or only minor expression differences between *bar-1(ga80)* and N2 during development. One of the dishevelled genes, *dsh-1*, was affected by the *bar-1* mutation. This gene was higher expressed in *bar-1(ga80)*. It was also the only gene of the three dishevelled genes that did not show a change in expression.

The Wnt receptors *cfz-2, mig-1* and *lin-18* (*ryk/derailed*) were higher expressed in *bar-1(ga80)*, and their expression did not change during development. The two other Wnt-receptors were slightly affected by development. Expression of *mom-5* increased during L4 development whereas *lin-17* expression decreased. Of the other genes, *sfrp-1*, an extracellular active Wnt-inhibitor[35], had a lower expression in the *bar-1* mutant compared to N2. The expression of *sfrp-1* decreased during L4 development in N2. Even though *bar-1(ga80)* showed a developmental delay, the expression of *sfrp-1* decreased compared to N2. Some of the transcription factors known to be involved in the Wnt-pathway, like EOR-1[36] and EGL-27[37] (or associated with the Wnt pathway, like SKN-1[38]), were up regulated, but their targets were not enriched for in the differentially expressed genes set (hypergeometric test, $p > 0.1$).

To summarize, the up-regulation of the other three β-catenins in *bar-1(ga80)* probably compensates for the loss of a functional BAR-1 (Supplement figure C). Intriguingly, not only the β-catenins were higher expressed, but also the Wnt-receptors. Furthermore, the *sfrp-1* gene was down-regulated. Thus, a lack of *bar-1* also affects the Wnt-signalling pathway upstream, which could point to a feed-back-mechanism. As the Wnt encoding gene *mom-2*, the Wnt-receptors *cfz-2*, *mig-1* and *lin-18* and the dishevelled gene *dsh-1* were also up-regulated, our results imply that the Wnt- signalling pathway itself was activated following the knock-down of *bar-1*.

Natural genetic variation in Wnt-pathway genes. All genes part of, or associated with, the Wnt-pathway (Figure 3) are polymorphic across many other *C. elegans* wild type strains[39–41]. Between the two most frequently studied wild types N2 and CB4856 these polymorphisms lead to an amino acid change in almost 50% of the proteins (Supplement text 1). Furthermore enrichments of expression Quantitative Trait Loci (eQTL) of genes with affected transcript levels by *bar-1(ga80)* suggest that polymorphic loci between CB4856 and N2 downstream of or modulated by *bar-1* and Wnt-signalling might be present (Supplement text 1). This indicates that the Wnt-signalling pathway is genetically buffered[42] and the associated genes are possibly co-evolving.

Biological processes affected by bar-1(ga80). To investigate which processes were affected by the *bar-1(ga80)* mutation, we tested enrichment of mutation-affected genes in GO-, KEGG-, Anatomy-, Wormbook-, Gene class- and Protein domain annotations. To distinguish between *bar-1* and developmental effects we excluded all the *bar-1(ga80)* affected genes with a developmental effect from the set of genes used for enrichment analysis (Supplementary Table 2). The results of the complete set of *bar-1(ga80)* affected genes including those with a developmental effect can also be found in Supplementary Table 2.

Genes lower expressed in *bar-1(ga80)* are enriched with genes involved in cuticle constituents ($p < 1*10^{-4}$), proteolysis ($p < 1*10^{-10}$) and the proteasome core complex ($p < 1*10^{-10}$). Whereas the proteolysis and proteasome core complex genes overlapped, they did not overlap with the cuticle constituent genes. Furthermore protein degradation related enrichments were reflected in the multiple categories tested, implying that protein degradation/turn-over might be reduced. Thus, *bar-1(ga80)* affects protein degradation, possibly reflecting the transition of the cell from one state into another.

The group of genes expressed higher in *bar-1(ga80)* consisted of a more diverse set of genes. These genes were especially related to transcriptional regulation, as shown by an enrichment of the GO-terms regulation of transcription ($p < 1*10^{-8}$), sequence specific DNA binding ($p < 1*10^{-8}$), transcription factor activity ($p < 1*10^{-8}$) and nucleus ($p < 1*10^{-7}$). Some indications were found that the Ras-pathway was affected because transcription factors known to be linked to the Ras-pathway were up-regulated, like the RAS inhibitors MDL-1[43] and LIN-15B[44]. The activation of the Ras pathway is further shown by the strong up regulation of *cav-1* in the *bar-1(ga80)* mutant.

Furthermore, also neuron-related terms were represented, as shown by enrichments of the GO-term axon ($p < 1*10^{-6}$), synapse ($p < 1*10^{-4}$) and in the anatomy terms where the three most significantly enriched groups were neuronal ($p < 1*10^{-10}$). The enrichment of these neuronal genes can point in the direction of the aberrant neuron migration that is observed in *bar-1(ga80)*[15], the mutation might affect neuropeptide signalling.

bar-1(ga80) transcription patterns suggest DAF-16 activation. Since enrichment in transcriptional regulation was detected, we used the modENCODE[30,31] set of ChIP-seq determined binding sites to search for enrichment of binding sites for transcription factors. We found that the genes higher expressed in *bar-1(ga80)* were enriched for binding-sites of transcription factors PHA-4, MDL-1, ELT-3 and PQM-1 (hypergeometric test, $P < 1*10^{-2}$). These transcription factors were up-regulated in the *bar-1(ga80)* mutant, except for *elt-3* (Figure 4A). Together with the enrichment found for the binding sites, this indicates that the absence of the β-catenin BAR-1 results in an activation of transcription factors, possibly as a compensatory response. The four transcription factors for which enrichments have been found share binding sites for many of the genes. Over 50% of the up-regulated genes in the transcriptional network were associated with more than one of these four transcription factors (Figure 4B). Furthermore, PQM-1 and MDL-1 also bind near the transcription starting site of PHA-4 and ELT-3 (Supplementary figure D)[30]. This indicates that it is likely that PQM-1 or MDL-1 is involved in the transcriptional activation observed in *bar-1(ga80)*.

Three of these transcription factors: PQM-1[32], MDL-1[45], and ELT-3[46], have been associated with the insulin/IGF-1 signalling pathway and longevity. However, for ELT-3 this relation is debated in more recent literature[47]. Furthermore, PQM-1 is also identified as a promoter of growth, development and reproduction[32]. PQM-1 has an antagonistic interaction with DAF-16, where nuclear translocation of PQM-1 (promoted by DAF-2) results in depletion of DAF-16 from the nucleus (and vice-versa). Tepper *et al.* identified genes regulated by PQM-1 (referred to as class II genes), and genes regulated by DAF-16 (referred to as class I genes). It is also shown that some of the class I genes are also regulated by PQM-1[32]. We tested expression of these genes in the *bar-1(ga80)* versus N2 and found that the class I genes were enriched for in the up-regulated genes (hypergeometric test, $p < 1*10^{-22}$) and slightly but significantly

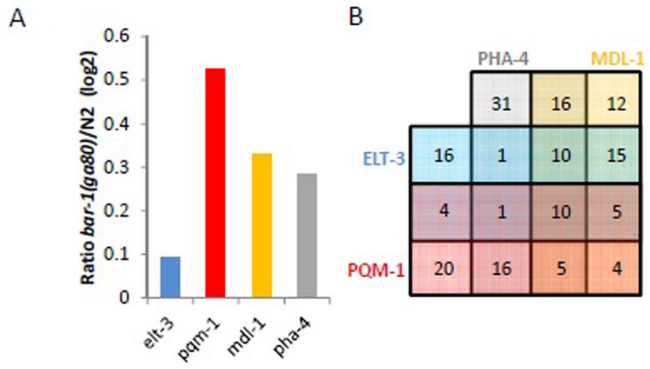

Figure 4 | Transcription factor activity and targets in up-regulated genes. (A) shows the transcript abundance of the four transcription factors enriched for targets among the up-regulated genes in *bar-1(ga80)*. The fold-change in bar-1/N2 is shown. The levels of *pqm-1*, *pha-4*, and *mdl-1* are significantly higher in *bar-1(ga80)* (linear model, $p < 0.01$), whereas this is not the case for *elt-3* (linear model, $p = 0.158$). (B) A Venn-diagram of the up-regulated genes associated with the four enriched transcription factors. There is a high level of overlap between the associations as >50% of the targets are associated with multiple transcription factors.

up-regulated in *bar-1(ga80)* (two-sided t-test, $p < 1*10^{-8}$). Moreover, the specific PQM-1 targets were enriched for in the down-regulated genes (hypergeometric test, $p < 1*10^{-2}$) and were slightly down-regulated (two-sided t-test, $p < 1*10^{-5}$), see also Supplementary figure E and Supplementary Table 3. We also analysed DAF-16 ChIP-seq data[31], and found that the genes up-regulated in *bar-1(ga80)* were enriched for DAF-16 targeted genes (124 out of 425 up-regulated genes, hypergeometric test, $p < 1*10^{-3}$). Based on these results we hypothesize that loss of function of *bar-1(ga80)* leads to induction of a stress response reflecting DAF-16 activation, causing delayed development of the worms.

Conclusion

We studied gene expression patterns during the fourth larval stage (L4) of the strain EW15 carrying the β-catenin-loss-of-function point mutation *bar-1(ga80)* causing a Glu to Stop codon change at amino acid 97 of the predicted BAR-1 protein. To untangle the developmental effects from the effects of the *bar-1* mutation, we used a time-series dataset[23]. We showed that *bar-1(ga80)* results in a slower development, as these worms take on average ~10% more time to develop than Bristol N2. Using the transcriptome to estimate the age of the worms, we found that 48 hours after synchronization, *bar-1(ga80)* worms are transcriptionally most similar to N2 worms at 44–45 hours after synchronization[23]. By measuring the time that egg-deposit starts in *bar-1(ga80)* and Bristol N2, we confirmed this developmental delay. To our knowledge, this has not yet been reported for *bar-1*.

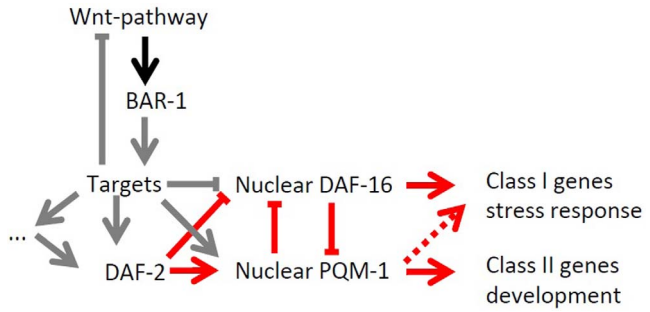

Figure 5 | A model for the *bar-1lof* effects. This model incorporates the findings in this paper (grey) with what is known about the Wnt-pathway regarding to BAR-1 (black)[6] and findings reported about DAF-16 and PQM-1 (red)[32]. It is proposed that (transcriptional) activity of the β-catenin *bar-1* results in a feedback loop, de-activating the Wnt-pathway. Furthermore BAR-1 activity is needed for a correct developmental program, where *bar-1lof* shows indications of a DAF-16-mediated stress response. The exact level of interaction between BAR-1 and the insulin pathway remains to be elucidated.

Analysis of the Wnt-pathway showed that a non-functional *bar-1* causes up-regulation of Wnt-signalling components, *mom-2, cfz-2, mig-1, lin-18, dsh-1, mom-5* and *lin-17*. Together with the down-regulation of Wnt-inhibitor *sfrp-1* this indicates hyper-activation of the Wnt-signalling pathway, suggesting a compensatory mechanism (Figure 5). This is further shown by the modest up-regulation of the other β-catenins, *wrm-1*, *hmp-2* and *sys-1* which all have the potential to substitute for *bar-1* in transcriptional activation[12,48].

Analysis of the genes affected by *bar-1(ga80)* showed that genes up-regulated in *bar-1(ga80)* are enriched for transcription factor- as well as histone- binding sites and for processes like chromosome rearrangement, chromatin factors and neurogenesis. The down-regulated genes were enriched for cuticle components and hh-signalling pathway genes, suggesting *bar-1* directly affects these processes. We found that the transcriptional response induced in *bar-1(ga80)* reflects DAF-16 activation (Figure 5). This also corresponds with the developmental delay we measured. We propose that loss of *bar-1* results in a compensatory/feedback response on the transcriptional level, leading to Wnt-pathway and DAF-16 activation.

1. Buechling, T. & Boutros, M. Wnt signaling signaling at and above the receptor level. *Curr. Top. Dev. Biol.* **97**, 21–53, doi:10.1016/B978-0-12-385975-4.00008-5 (2011).
2. Moon, R. T., Bowerman, B., Boutros, M. & Perrimon, N. The promise and perils of Wnt signaling through beta-catenin. *Science* **296**, 1644–1646, doi:10.1126/science.1071549 (2002).
3. Niehrs, C. The complex world of WNT receptor signalling. *Nat. Rev. Molec. Cell Biol.* **13**, 767–779, doi:10.1038/nrm3470 (2012).
4. Clevers, H. & Nusse, R. Wnt/beta-catenin signaling and disease. *Cell* **149**, 1192–1205, doi:10.1016/j.cell.2012.05.012 (2012).
5. MacDonald, B. T., Tamai, K. & He, X. Wnt/beta-catenin signaling: components, mechanisms, and diseases. *Dev. Cell* **17**, 9–26, doi:10.1016/j.devcel.2009.06.016 (2009).
6. Jackson, B. M. & Eisenmann, D. M. Beta-catenin-dependent Wnt signaling in C. elegans: teaching an old dog a new trick. *Cold Spring Harbor Perspect. Biol.* **4**, a007948, doi:10.1101/cshperspect.a007948 (2012).
7. Eisenmann, D. M. Wnt signaling. *WormBook: the online review of C. elegans biology*, 1–17, doi:10.1895/wormbook.1.7.1 (2005).
8. Eisenmann, D. M., Maloof, J. N., Simske, J. S., Kenyon, C. & Kim, S. K. The beta-catenin homolog BAR-1 and LET-60 Ras coordinately regulate the Hox gene lin-39 during Caenorhabditis elegans vulval development. *Dev.* **125**, 3667–3680 (1998).
9. Gleason, J. E., Szyleyko, E. A. & Eisenmann, D. M. Multiple redundant Wnt signaling components function in two processes during C. elegans vulval development. *Dev. Biol.* **298**, 442–457, doi:10.1016/j.ydbio.2006.06.050 (2006).
10. Rocheleau, C. E. *et al.* Wnt signaling and an APC-related gene specify endoderm in early C. elegans embryos. *Cell* **90**, 707–716 (1997).
11. Costa, M. *et al.* A putative catenin-cadherin system mediates morphogenesis of the Caenorhabditis elegans embryo. *J. Cell. Biol.* **141**, 297–308 (1998).
12. Kidd, A. R., 3rd, Miskowski, J. A., Siegfried, K. R., Sawa, H. & Kimble, J. A beta-catenin identified by functional rather than sequence criteria and its role in Wnt/MAPK signaling. *Cell* **121**, 761–772, doi:10.1016/j.cell.2005.03.029 (2005).
13. Korswagen, H. C., Herman, M. A. & Clevers, H. C. Distinct beta-catenins mediate adhesion and signalling functions in C. elegans. *Nature* **406**, 527–532, doi:10.1038/35020099 (2000).
14. Eisenmann, D. M. & Kim, S. K. Protruding vulva mutants identify novel loci and Wnt signaling factors that function during Caenorhabditis elegans vulva development. *Genet.* **156**, 1097–1116 (2000).
15. Maloof, J. N., Whangbo, J., Harris, J. M., Jongeward, G. D. & Kenyon, C. A Wnt signaling pathway controls hox gene expression and neuroblast migration in C. elegans. *Dev.* **126**, 37–49 (1999).
16. van de Wetering, M. *et al.* Armadillo coactivates transcription driven by the product of the Drosophila segment polarity gene dTCF. *Cell* **88**, 789–799 (1997).
17. Gleason, J. E., Korswagen, H. C. & Eisenmann, D. M. Activation of Wnt signaling bypasses the requirement for RTK/Ras signaling during C. elegans vulval induction. *Gen. Dev.* **16**, 1281–1290, doi:10.1101/gad.981602 (2002).

18. Korswagen, H. C. *et al.* The Axin-like protein PRY-1 is a negative regulator of a canonical Wnt pathway in C. elegans. *Gen. Dev.* **16**, 1291–1302, doi:10.1101/gad.981802 (2002).
19. Jiang, L. I. & Sternberg, P. W. Interactions of EGF, Wnt and HOM-C genes specify the P12 neuroectoblast fate in C. elegans. *Dev.* **125**, 2337–2347 (1998).
20. Whangbo, J. & Kenyon, C. A Wnt signaling system that specifies two patterns of cell migration in C. elegans. *Mol. Cell.* **4**, 851–858 (1999).
21. Sulston, J. E. & Hodgkin, J. in *The nematode Caenorhabditis elegans* (ed Wood, W. B.) 587–606 (Cold Spring Harbor Laboratory 1988).
22. Zahurak, M. *et al.* Pre-processing Agilent microarray data. *BMC Bioinf.* **8**, 142, doi:10.1186/1471-2105-8-142 (2007).
23. Snoek, L. B. *et al.* A rapid and massive gene expression shift marking adolescent transition in C. elegans. *Sci. Rep.* **4**, 3912, doi:10.1038/srep03912 (2014).
24. Terpstra, I. R., Snoek, L. B., Keurentjes, J. J. B., Peeters, A. J. M. & Van den Ackerveken, G. Regulatory Network Identification by Genetical Genomics: Signaling Downstream of the Arabidopsis Receptor-Like Kinase ERECTA. *Plant. Physiol.* **154**, 1067–1078, doi:DOI 10.1104/pp.110.159996 (2010).
25. Snoek, L. B. *et al.* WormQTL--public archive and analysis web portal for natural variation data in Caenorhabditis spp. *Nucl. Ac. Res.* **41**, D738–743, doi:10.1093/nar/gks1124 (2013).
26. van der Velde, K. J. *et al.* WormQTLHD--a web database for linking human disease to natural variation data in C. elegans. *Nucl. Ac. Res.* **42**, D794–801, doi:10.1093/nar/gkt1044 (2014).
27. Vinuela, A., Snoek, L. B., Riksen, J. A. G. & Kammenga, J. E. Genome-wide gene expression regulation as a function of genotype and age in C-elegans. *Genome Res.* **20**, 929–937, doi:DOI 10.1101/gr.102160.109 (2010).
28. Vinuela, A., Snoek, L. B., Riksen, J. A. G. & Kammenga, J. E. Aging Uncouples Heritability and Expression-QTL in Caenorhabditis elegans. *G3-Genes Genom. Genet.* **2**, 597–605, doi:DOI 10.1534/g3.112.002212 (2012).
29. Rockman, M. V., Skrovanek, S. S. & Kruglyak, L. Selection at linked sites shapes heritable phenotypic variation in C. elegans. *Science* **330**, 372–376, doi:10.1126/science.1194208 (2010).
30. Niu, W. *et al.* Diverse transcription factor binding features revealed by genome-wide ChIP-seq in C. elegans. *Genome Res.* **21**, 245–254, doi:DOI 10.1101/gr.114587.110 (2011).
31. Gerstein, M. B. *et al.* Integrative analysis of the Caenorhabditis elegans genome by the modENCODE project. *Science* **330**, 1775–1787, doi:10.1126/science.1196914 (2010).
32. Tepper, R. G. *et al.* PQM-1 Complements DAF-16 as a Key Transcriptional Regulator of DAF-2-Mediated Development and Longevity. *Cell* **154**, 676–690, doi:DOI 10.1016/j.cell.2013.07.006 (2013).
33. Shannon, P. *et al.* Cytoscape: a software environment for integrated models of biomolecular interaction networks. *Genome Res.* **13**, 2498–2504, doi:10.1101/gr.1239303 (2003).
34. Kim, D. H., Grun, D. & van Oudenaarden, A. Dampening of expression oscillations by synchronous regulation of a microRNA and its target. *Nat. Genet.* **45**, 1337–+, doi:Doi 10.1038/Ng.2763 (2013).
35. Harterink, M. *et al.* Neuroblast migration along the anteroposterior axis of C. elegans is controlled by opposing gradients of Wnts and a secreted Frizzled-related protein. *Dev.* **138**, 2915–2924, doi:Doi 10.1242/Dev.064733 (2011).
36. Howard, R. M. & Sundaram, M. V. C. elegans EOR-1/PLZF and EOR-2 positively regulate Ras and Wnt signaling and function redundantly with LIN-25 and the SUR-2 Mediator component. *Gen. Dev.* **16**, 1815–1827, doi:10.1101/gad.998402 (2002).
37. Herman, M. A. *et al.* EGL-27 is similar to a metastasis-associated factor and controls cell polarity and cell migration in C. elegans. *Dev.* **126**, 1055–1064 (1999).
38. Maduro, M. F., Kasmir, J. J., Zhu, J. W. & Rothman, J. H. The Wnt effector POP-1 and the PAL-1/Caudal homeoprotein collaborate with SKN-1 to activate C-elegans endoderm development. *Dev. Biol.* **285**, 510–523, doi:DOI 10.1016/j.ydbio.2005.06.022 (2005).
39. Andersen, E. C. *et al.* Chromosome-scale selective sweeps shape Caenorhabditis elegans genomic diversity. *Nat. Genet.* **44**, 285–290, doi:10.1038/ng.1050 (2012).
40. Thompson, O. *et al.* The million mutation project: a new approach to genetics in Caenorhabditis elegans. *Genome Res.* **23**, 1749–1762, doi:10.1101/gr.157651.113 (2013).
41. Volkers, R. J. *et al.* Gene-environment and protein-degradation signatures characterize genomic and phenotypic diversity in wild Caenorhabditis elegans populations. *BMC Biol.* **11**, 93, doi:10.1186/1741-7007-11-93 (2013).
42. Felix, M. A. & Barkoulas, M. Robustness and flexibility in nematode vulva development. *Trends Genet.* **28**, 185–195, doi:10.1016/j.tig.2012.01.002 (2012).
43. Yuan, J., Tirabassi, R. S., Bush, A. B. & Cole, M. D. The C-elegans MDL-1 and MXL-1 proteins can functionally substitute for vertebrate MAD and MAX. *Oncog.* **17**, 1109–1118, doi:DOI 10.1038/sj.onc.1202036 (1998).
44. Clark, S. G., Lu, X. W. & Horvitz, H. R. The Caenorhabditis-Elegans Locus Lin-15, a Negative Regulator of a Tyrosine Kinase Signaling Pathway, Encodes 2 Different Proteins. *Genet.* **137**, 987–997 (1994).
45. Ackerman, D. & Gems, D. Insulin/IGF-1 and Hypoxia Signaling Act in Concert to Regulate Iron Homeostasis in Caenorhabditis elegans. *PLoS Genet.* **8**, doi:ARTN e1002498 DOI 10.1371/journal.pgen.1002498 (2012).
46. Budovskaya, Y. V. *et al.* An elt-3/elt-5/elt-6 GATA transcription circuit guides aging in C-elegans. *Cell* **134**, 291–303, doi:DOI 10.1016/j.cell.2008.05.044 (2008).
47. Tonsaker, T., Pratt, R. M. & McGhee, J. D. Re-evaluating the role of ELT-3 in a GATA transcription factor circuit proposed to guide aging in C. elegans. *Mech. Ageing. Dev.* **133**, 50–53, doi:DOI 10.1016/j.mad.2011.09.006 (2012).
48. Natarajan, L., Witwer, N. E. & Eisenmann, D. M. The divergent Caenorhabditis elegans beta-catenin proteins BAR-1, WRM-1 and HMP-2 make distinct protein interactions but retain functional redundancy in vivo. *Genet.* **159**, 159–172 (2001).
49. Snoek, L. B. *et al.* Worm variation made accessible: Take your shopping cart to store, link, and investigate! *Worm* **3**, e28357 (2014) http://dx.doi.org/10.4161/worm.28357.

Acknowledgments

LBS was funded by the ERASysbio-plus ZonMW project GRAPPLE (project nr. 90201066). MGS was supported by Graduate School Production Ecology & Resource Conservation. RJMV was funded by the NWO-ALW (project 855.01.151), TS, AH, JAGR and JEK were funded by PANACEA EU FP project contractnr. 222936. We thank Wormbase (www.wormbase.org) for being a rich and versatile source of information. We thank Morris Swertz and Joeri van der Velde for their help with making the data accessible through WormQTL. *Bar-1(ga80)* strain was kindly provided by S. Kim.

Author contributions

M.L.V.D.B., J.A.G.R., M.G.S., R.J.M.V. conducted the experiments. M.G.S., T.S., L.B.S. analysed the results, A.H., J.E.K., R.J.M.V., M.G.S. and L.B.S. wrote the manuscript.

Additional information

Supplementary information accompanies this paper at http://www.nature.com/scientificreports

Competing financial interests: The authors declare no competing financial interests.

How to cite this article: van der Bent, M.L. *et al.* Loss-of-function of β-catenin *bar-1* slows development and activates the Wnt pathway in *Caenorhabditis elegans*. *Sci. Rep.* **4**, 4926; DOI:10.1038/srep04926 (2014).

Discussion and Outlook

1.16 General Considerations

It is a big challenge to uncover the entire mechanism how complex diseases manifest, due to genes with only little effects on the phenotype. The use of recombinant inbred lines to answer biological questions in the field of quantitative genetics is powerful, but alone not useful to investigate complex disease signalling. Vulval development in *C. elegans* and many other biological processes are robust enough to tolerate small fluctuations in gene regulation and produce an unchanged phenotypic outcome (Milloz, Duveau, Nuez, & Félix, 2008). For example, it is not possible to detect any changes in vulval development between N2 Bristol and CB4856 Hawaii, possibly due to buffering mechanisms driven by positive selection for fitness. We therefore decided to use a novel approach by including a sensitised background in the RIL population to circumvent the robustness of the vulva system. We performed an initial pilot screen including the most prominent genes necessary during vulval development in order to find promising candidates to sensitise the RILs with (Table 1). In addition we screened in 3 different backgrounds to exclude background specific effect that limit the potential of further investigation. Most of the N2 gene mutations screened behaved different in the other three genetic backgrounds, but all with similar effects within the wild isolates. Therefore, N2 seems to be the special case, in which continuous lab adaptation and artificial selection may have changed biological processes. The weakening of the strength of mutants for vulval development is a well-known example of and how a system is able to accumulate background suppressor mutations over time. The study of natural isolates is valid, since those genomes are less compromised by artificial lab selection and thus better reflect wild-type situation.

1.17 Technical aspects

1.17.1 *let-60(n1046)* and *bar-1(ga80)* as Promising Sensitised Backgrounds for Further Investigation, but with Limited Genetic Manipulation

From the pilot screen, we found the miIRLs of *let-60(n1046)* and *bar-1(ga80)* to be the most promising candidates for further investigation, due to the high range of phenotypic changes. miRILs of *pry-1(mu38)* were not pursued further due to time constraints, but still reflect a promising sensitized background to pursue further. Unfortunately, *let-60(n1046)* and *bar-1(ga80)* mutants are not best for genetic studies due to their difficult handling. Both, *let-60(n1046)* and *bar-1(ga80)* males are not able to mate and both mutant hermaphrodites display severe vulval phenotypes (muv and pvl, respectively), making crossings more difficult. In

addition *let-60(n1046)* mutants display a large intra-strain variability and might be easily influenced by environmental factors such as temperature and the availability of food (Battu, Froehli Hoier, & Hajnal, 2003). *bar-1(ga80)* mutants seem to have a more robust phenotype, but are still variable as well. But, eventually this is the variability needed to observe natural variation during vulval development. Still surprising is the fact that strong mutants of the two key players in the pathway of EGFR/RAS/MAPK and Wnt signalling (*let-60* and *bar-1* respectively) exhibit so much variability in the phenotype. It is therefore more conceivable that their regulation is far more complex than previously thought. Our approach to find novel natural variations in modifiers of *let-60(n1046)* and *bar-1(ga80)* is very compelling and might lead to the identification of novel drug targets and to further medication for cancer patients.

1.17.2 *let-60(n1046)* and *bar-1(ga80)* Mutants are Full of Background Mutations with Known or Unknown Functions

The concept to regard a mutant strain as harbouring only a single mutation is a wrong assumption. With the rise of next generation sequencing and its drop in cost, researchers were confronted with what everyone already assumed. Mutant strains, despite back- and outcrossing, still contain lots of background mutations with known or unknown functions, generating biological noise and obscuring phenotypes. Since all mutants have benn back- and/or outcrossed multiple times, those mutations have to be linked to the phenotype. After sequencing the *let-60(n1046)* and *bar-1(ga80)* strains (see electronic supplementary information), I was confronted with the same situation. Eventually we could identify 3843 SNPs for *let-60(n1046)* and 14738 SNPs for *bar-1(ga80)*. The main problem is to find casual background mutations and to avoid those in further studies. Due to the high amount of background mutations, it is not possible to test them all. Therefore, this led to the strategy of comparing siblings from the same cross but with different genotypes to filter out biological noise. Background mutations should randomly segregate and therefore using at least three independent sibling lines from the same genotype comparing it to at least three independent siblings from a different genotype should filter out most of the biological noise.

1.17.2.1 *let-60(n1046)* Harbours SNPs in Prominent Genes of the EGFR/RAS/MAPK Pathway.

The *let-60(n1046)* strains MT2124 contains non synonymous SNPs in prominent genes of the EGFR/RAS/MAPK pathway (Table 11), such as *let-23*, *gap-1* and *age-1*, all not physically linked to *let-60(n1046)*. It is not known if these mutations were carried over from the initial chemical mutagenesis, despite back-/outcrossing to generate the *n1046* allele or if these are over time

acquired suppressor mutations. The mutations in *let-23(Ser1001Phe),* and *age-1(Pro332Ser, Asp747Glu)* generate novel alleles with unknown function. According to protein structural domains, the Ser1001Phe allele of *let-23* might interfere with the active site of the kinase, which is at position 1010. In addition, the Pro332Ser allele of *age-1* could impair the PI3K ras-binding domain and the Asp747Glu might affect the PIK domain. The mutation found for *gap-1(Cys10Arg)* is also described as otn18459 by (Sarin et al., n.d.). In summary, the mutations found in the *let-60(n1046)* strain might potentially suppress the *n1046* allele.

1.17.2.2 *bar-1(ga80)* Might have CB4856 Contamination on Chromosome V

After looking more deeply into the *bar-1(ga80)* genomic sequence, I could detect a massive amount of SNPs mapping to certain regions on chromosome V. Wormbase.org identified those SNP as CB4856 specific, indicating that the *bar-1(ga80)* strain contains stretches of CB4856 on chromosome V. Either the original strain from the *Caenorhabditis Elegans* Center (CGC) already contained those stretches or they were introduced in our lab. This fact might explain, why there is a region completely CB4856 for the *bar-1(ga80)* miRILs (Figure 43, chromosome V). Contraindicative is the fact that we always included the parental strains *bar-1(ga80)* and CB4856 in the SNP mapping and they were all the time completely N2 or CB4856 respectively for the markers tested. Nevertheless, and for further studies, the *bar-1(ga80)* mutant has to be outcrossed several times with N2 to remove all those foreign regions.

1.17.3 The Use of Introgression Lines to Verify the *let-60(n1046)* QTLs for Vulval Induction

By using the introgression lines from (Doroszuk et al., 2009) crossed with the *let-60(n1046)* mutant, I made the observation of strong variability within the lines from the same genotype. First, with introgression lines we could separate QTL regions for analysis, neglecting that different QTLs might interact with each other therefore leading to different effects (Figure 17). This was the case for the *let-60(n1046)* miRIL QTL 4 on chromosome 5, which only affected RAS signalling when QTL 1b was present as CB4856 region (compare Figure 18 and Figure 19). Additional introduction of CB4856 at QTL1b position using ewIR17 was able to circumvent this problem. Second, background mutations (Table 11) that segregate randomly can act as modifiers of RAS signalling. Since we do not genotype for background modifiers, every cross progeny line might contain different modifiers altering RAS signalling, introducing genetic variability. Using multiple independent cross progeny lines, all with a different combination of background, modifiers will average out any effect coming from the *let-60(n1046)* specific genetic

background. At last, introgression line crosses of *let-60(n1046)* with ewIR2 produced two lines massively deviating from the parental *let-60(n1046)*, regardless of the presence or absence of the ewIR2 introgression (see 1.11. for more information). In summary, to get a valid estimate for vulval induction, I had to analyse many different independent lines; relying on only one line per genotype would have falsified my data tremendously.

1.17.4 Non-synonymous SNPs as the First Source of Natural Variation

After the verification of the QTL regions using introgression lines, we aligned the parental lines *let-60(n1046)* and CB4856 and analysed SNPs. In order to deal with the immense amount of polymorphisms between the parental strains and to identify natural polymorphic genes affecting RAS signalling, we had to filter our dataset in order to reduce the candidates to a manageable amount for further investigation. Depending on the perspective, non-synonymous SNPs and missing genes in the CB4856 strain seemed to be the most promising sources of natural variation due to their direct influence on the amino acid sequence. We were clear that this is an oversimplification of the biological processes, but choices were limited. We therefore focused on changes on the protein level, excluded synonymous SNPs and sources on the transcript level such as regulatory sequences, miRNAs and pseudogenes as being important for our study. One can argue that it is very likely that a non-synonymous SNP containing genes in addition contains synonymous SNPs and SNPs in regulatory sequences. This is probably true for most of the cases, but the converse is not. Surprisingly, we identified F44F1.1 as a missing gene in CB4856 affecting vulval development, which in fact is annotated as a pseudogene, demonstrating that posttranscriptional regulation are important as well. Further, non-synonymous SNPs in *amx-2* are only one source of variability between N2 and CB4856, another is its highly variable 3' genomic region. Next, we identified *glct-2* to alter Wnt signalling in *bar-1(ga80)* and *sqv-2* identified by the group of Jan Kammenga as being a putative natural modifier of *bar-1(ga80)*. In addition to their non-synonymous SNPs, both the genes contain deletions in the CB4856 genome. *glct-2* is partly deleted and *sqv-2* harbours a deletion in the 3'UTR. It is surprising that many of those genes were initially tested since they harbour non-synonymous SNP but a closer look revealed that they are strongly divergent in the two backgrounds. This indicates that the most promising candidate genes for natural variation, at least in this study, comprise genes with large numbers of sequence alterations between N2 and CB4856.

1.17.5 Extrachromosomal Array Lines are not Suitable for the Identification of Modifier Genes

The use of extrachromosomal arrays to study gene function is well established in the field (Evans, 2006) but certain limitations have to be taken into account. Extrachromosomal arrays are built up through random assembly of the injected DNA. They are comples mixes of multiple functional or non-functional copies of transgenes and co-injection markers. Therefore, more than one extrachromosomal line has to be analysed to exclude for such effects. In addition, the overexpression of transgenes might induce an RNAi related mechanism called co-suppression ((Plasterk & Ketting, 2000)) in which the transgene is rapidly silenced.

The generation of transgenic animals in the *let-60(n1046)* background using *sur-5::gfp* as co-injection marker (Trent Gu, 1998) is problematic and not suitable for further investigation on the functionality of the N2 or CB4856 alleles. Regardless of what was injected, animals containing the gfp-positive array never displayed a vulval induction higher than the gfp negative no array containing siblings, indicating that the effect may arise from the use of *sur-5::gfp* as co-injection marker. *sur-5* was previously identified as negative regulator of *let-60(n1046)* and the overexpression of *sur-5* as extrachromosomal array in a *let-60(n1046)* background strongly suppressed the multivulva phenotype (Trent Gu, 1998). To our surprise, the co-injection marker *sur-5::gfp* is a translational fusion protein, unlike other co-injection marker that only express gfp under a tissue specific promoter. On the one side, it seems plausible that the use of *sur-5::gfp* falsified our transgenesis data. But on the other side, *sur-5::gfp* tested alone in the *let-60(n1046)* background caused no obvious effect, and many lines containing *sur-5::gfp* did not alter vulval induction. One last explanation remains. Comparing animals with to animals without an extrachromosomal array relies on the detectability of the fluorescent protein (here gfp) and hence in the sensitivity of the camera of the microscope. Not being able to detect the gfp, does not indicate the absence of the extrachromosomal array. The signal might be just below detection limit.

A much more elegant way of analysing the function of different alleles is accomplished by using the recently developed MosSCI system ((Robert, Katic, & Bessereau, 2009)) where only one copy per chromosome is integrated, thereby minimising the effects of artificial overexpression and reflecting a more wild-type situations. The drawback of this technique is the use of specific landing sites for integration, thereby excluding the endogenous genomic environment of the transgene.

1.17.6 Results from Western Blot Analysis to Measure Phosphorylated/ Total ERK Ratio have a High Variability in Worms and Human Cell Lines

The use of phosphorylated/total ERK ratio to assess signalling strength is well known (Friedman & Perrimon, 2005), but results are highly variable. Since we used crude whole-worm protein extracts, the variability is not expected to be lower due to sample complexity. Western blots in addition only provide a snapshot of an otherwise changing environment. Phosphorylation and dephosphorylation events are highly dynamic processes and can change within minutes from highest phosphorylation peaks towards dephosphorylation events leading to lower levels ((Olsen et al., 2006), (Fritz et al., 2013)), thereby limiting their potential significance in western blots due to the narrow time window tested. In addition, cell stress such as stretching can induce ERK signalling as well via upregulation of phoshpoERK ((Yamazaki et al., 1995)). In summary, phosphorylation of ERK relies on processes that are highly sensitive and any manipulation of living sample material such as grinding worms or scraping cells from a culture plate to harvest might induce artefacts and therefore have to be as mild and short as possible. Fixation prior to manipulation might as well help to reduce the variability in biological replicates. For further studies in human cells we will use the recently developed toolkit to visualise phosphorylation of ERK on a FRET basis enabling us to produce a continuous time window for analysis, which might help to investigate the activity and dynamics of ERK ((Fritz et al., 2013)).

1.17.7 Measuring Enzymatic Activity of *amx-2* in Crude Worm Protein Extracts is Unsuccessful

We tried to measure enzymatic activity of the N2 and CB4856 alleles of *amx-2* to investigate natural variation in more detail. *amx-2* is homologous to MAOA, which is supposedly able to metabolise biogenic amines into metabolites, thereby producing H_2O_2 as by-product. Therefore, the use of the Amplex Red Monoamine Oxidase kit (lifetechnologies, cat# A12214) should be able to measure *amx-2* activity in total worm protein extracts. Unfortunately, biological replicates differed highly from each other, and results where not reproducible at all. In addition, none of the different protein extracts from different worm strains reacted to the administration of the substrates (tyramine and benzylamine), nor to the addition of MAO inhibitors (Clorgyline and Pargyline). We further purified the mitochondrial fraction using an additional low centrifugation step followed by high centrifugation, (Graham, 2001). This additional purification, intended to exclude other organelles and to further reduce sample complexity, led to no improvement. We also preincubated our protein samples with katalase, which should remove preexisting H_20_2 from the sample prior to experimentation without any success. Since protein extracts did not react to the substrates we believe that we did not measure *amx-2* activity, but

instead and despite the use of katalase, another source of H_20_2 that might be still present in the samples. Also, MAO inhibitors were not able to inhibit *amx-2* in the assays, indicating that those molecules might not be able to inhibit the worm homologue, due to weak conservation. In summary, H_20_2 present in the sample is probably produced through other enzymes. In crude worm extracts we cannot exclude all those parameters and therefore the signal to noise ratio remains high and possibly masks the activity of *amx-2* in the sample. A more precise way to analyse the function of the N2 and CB4856 allele is to purify AMX-2 protein from N2 and CB4856 worm protein extracts and by adding the putative substrates. Since translational gfp reporter constructs were built and transgenic worms were established previously, the purification of the N2 and CB4856 *amx-2* protein should be possible in order to test the enzymatic activity *in vitro*.

1.18 Biological aspects

1.18.1 Known Functions of Monoamine Oxidase A (MAOA)

There exist two humna monoamine oxidase in head-to-tail configuration on the X chromosome (termed MAOA and MAOAB) (Tipton, Boyce, O'Sullivan, Davey, & Healy, 2004). Monoamine oxidase A (MAOA) is located in the outer mitochondrial to regulate general mood, feeling and other social behaviours. Overactivation of MAOA was one of the first shown to cause depressive disorders. Therefore, inhibitors of MAOA were among the first to treat patients suffering from depression (Tipton et al., 2004). Naturally occurring polymorphisms raising or lowering MAOA activity were identified soon thereafter ((McDermott, Tingley, Cowden, Frazzetto, & Johnson, 2009), (Zalsman et al., 2004), (H G Brunner, 1993)). MAOA is responsible for the breakdown of biogenic amines, such as Serotonin, but how this biochemical mechanism might affect the general behaviour of an individual is still unknown. Most of the previous studies focused on MAOA as part of a regulatory network in the nervous system, only limited information is available concerning its role in other tissues, such as the liver and intestine, where it was first discovered (Tipton et al., 2004).

1.18.2 How AMX-2/MAOA Might Interact with LET-60/KRAS

To date, there are only a handful of studies implicating MAOA in cancer signalling ((Rybaczyk et al., 2008), (Yang et al., 2009), (Mikula et al., 2010), (J. Li et al., 2014)) but none could demonstrate the underlying molecular mechanism. In all above mentioned cases, downregulation of MAOA expression or protein abundance seems to correlated with poorer

cancer prognosis. Therefore, determination of MAOA expression levels as well as protein abundance can serve as a novel biomarker for cancer prognosis.

It is difficult to imagine how the mitochondrial enzyme MAOA would be able to affect RAS/MAPK signalling thought to primarily happen in the cytoplasm or the nucleus. However, newer studies found that translocation of oncogenic KRAS to the mitochondrial membrane is often observed and essential for cancer cells to grow anchorage independent ((Hu et al., 2011), (Weinberg et al., n.d.)). It might be possible that AMX-2 interacts with LET-60 at the mitochondrial membrane, but further molecular changes leading to the suppressive action of AMX-2 remain to be elucidated. One possibility might be that AMX-2 is part of a system that regulates the redox steady-state of a cell. The additional loss-of-function of *amx-2* could change the redox equilibrium of cells and lead to an imbalance, which is often observed in cancer cells. It is not known if this process involves direct interaction of AMX-2 and LET-60.

Surprisingly, identification of interacting proteins using the intracellular domain of the let-23/EGF receptor identified mostly mitochondrial proteins involved in the respiratory chain system (see Masterthesis Fabienne Largey). This might be another hint that EGFR/RAS/MAPK signalling could be coupled to components of mitochondriae.

1.18.3 Differences Between the Bristol and the Hawaii Allele of *amx-2*

In this study, we could demonstrate that the activities of the N2 and CB4856 alleles are different. So far we were not able to show which molecular differences account for the different activities. We tried –without success- to assess enzymatic activity using the AmpleRed reagent and Q-PCR to detect changes in expression levels. Q-PCR on one hand worked and indicated that expression levels are not significantly different. Hence, we still need to test enzymatic *amx-2* activity in a reliable way in order to find the reason responsible for the different activities.

1.18.4 How 5-HIAA Suppresses RAS/MAPK Signalling

5-HIAA is the main metabolite of Serotonin (5-HT) (Lesniak et al., 2013) and therefore believed to be an inactive compound. Here, we discovered a novel role of 5-HIAA to negatively regulate MAPK signalling. Hence, the current view of metabolites as being biologically inactive might be wrong. However, we cannot distinguish if the function of 5-HIAA is direct or if it rather serves as a sensor, in which the concentration of 5-HIAA indirectly reflects the enzymatic activity of MAOA or the presence of its substrate 5-HT. We believe that the action of MAOA to suppress

RAS/MAPK signalling relies on the amount of 5-HIAA produced. Under high doses of 5-HT, more 5-HIAA is produced and therefore suppresses signalling more strongly. A loss of function in *amx-2* will result in lower 5-HIAA production, hence the suppression is weakened. We know that in humans 5-HIAA is rapidly excreted through urine, but we cannot exclude that some of it is further metabolised by other enzymes. We can imagine the production of Melatonin (MT) as a second suppressive route, independent of *amx-2* function, but still relying on the presence of 5-HT. To completely abolish Serotonin signalling and its effect on RAS/MAPK signalling we will analyse a mutation in *tph-1* that prevents any endogenous 5-HT production and thereby eliminates both suppressive branches (Sze, Victor, Loer, Shi, & Ruvkun, 2000). We would expect a further increase in RAS/MAPK signalling in the *tph-1(lf);let-60(gf)* as compared to the *amx-2(lf);let-60(gf)* mutant.

1.18.5 Putative Additional Role of AMX-2/MAOA on the Redox State

Mammalian cells possess two types of mechanisms to produce ATP; oxidative phosphorylation happening in mitochondria and glycolysis in the cytosol (Hu et al., 2011). Under normal conditions, cells preferentially produce ATP through the more efficient process of oxidative phosphorylation. In contrast, cancer cells rely on glycolysis, which is the less efficient, but faster way to produce ATP (Hu et al., 2011). In addition, glycolysis delivers anabolic intermediates to build proteins, lipids and nucleic acids, providing cancer cells a fast source of energy and a metabolic advantage over normal cells. This phenomenon was first identified by (O, K, & E, 1924) and is therefore referred to be the Warburg effect. More recent studies implicate KRAS oncogenic transformation to lead to suppression of mitochondrial respiration and to an increase in ROS production, but it is not known how those changes affect cancer signalling and progression. ((Chiaradonna, Gaglio, Vanoni, & Alberghina, 2006a), (Chiaradonna et al., 2006b)). It seems possible that expression of the oncogenic KRAS(G12V) leads to mitochondrial dysfunction via a dramatic change in the mitochondrial membrane potential and to the suppression of respiratory chain complex I, where most of electron leakage occurs to form superoxide ((Jastroch, Divakaruni, Mookerjee, Treberg, & Brand, 2010)). Contraindicating this hypothesis, it was also shown that changes of the respiratory chain further lead to the increase of ROS production and to higher glycolysis (Hu et al., 2011). It might well be that the increase in glycolysis is rather a cellular response than a cause due to the loss of energy production via the respiratory chain. In addition (Weinberg et al., n.d.) could demonstrate that mitochondrial metabolism is necessary for in vivo tumourigenesis and identified complex III of the respiratory chain to produce ROS independent of oxidative phosphorylation, which in turn enables the cells to grow anchorage independently. Furthermore, active translocation of KRAS to the

mitochondria inner membrane is essential, since blockage of KRAS transport prevented mitochondria from becoming dysfunctional ((Hu et al., 2011)).

AMX-2 could be another component influencing the level of ROS via the oxidation of its substrates and at high activity levels might lead to toxicity, eventually suppressing cellular growth and survival. Furthermore, the enzymatic oxidation reaction requires O_2, which might be another limiting factor in cancer cells. This could be one of the reasons why cancer cells shut down expression of pro-apoptotic MAOA in order to prevent loss of O_2 and the production of toxic ROS.

In summary, changes to the redox state of a cell are a general strategy of cancer cells to survive and to become more tumourigenic.

Materials and Methods

1.19 Molecular Biology

1.19.1 Primers:

All primers in Table 14 were diluted in TE buffer to a stock concentration for 100 nM and kept at -20°C in the personal freezer. Primers used for PCR assays were diluted in TE from the stock to a final concentration of 2 nM and kept at 4°C. In addition, sequencing primers were diluted in TE to a concentration of 10 nM.

Genotyping primers

lin-2(n105)	
OTS16	CCTACGCTCGAGAACAAATA
OTS17	GTGGAAAAACCCCAGGTTTT
let-23(sy1)	
OTS18	GGCGATTACTACAACCAACC
OTS19	GCATGATGGCAAATTGTATGAG
let-23(sa62)	
OTS175	AGTTACTGTACGACCCAGATG
OTS176	TGCCAATGAGGGTTTGTTATCT
OTS222	CAGAATCCACAACTCACGAAA
mpk-1(ga111)	
OTS20	GTTCAATGCCTGATGGAGAC
OTS21	CCACATACTCGGTCAAGAACC
OTS24	TCAGGGGTGAGGATTTTT
OTS25	TTCAAATCACGATGGAGCA
OTS26	TACATTCACTCTGCAAATGG
OTS27	GCTGCTTGTTTAGATTTACG
OTS28	CGTAGTTCAATTCAGGGGTG
let-60(n1046)	
OTS22	CCATATTCAACTATGCGTC
OTS23	CTATGGTCGGGTCGTATTC
OTS38	TCATTCTCCGTCGTCTTC
OTS39	CATTTTTTTCAGTTCCAGCC
OTS49	CCAAACTTCTGACTCATC
toe-2(ok2807)	
OTS29	CAGGCTTGGAGGAGATTCTG

OTS30	GCCAAATCTCTGTTTTTCAGG

lin-2(n397)

OTS31	CAGAGAAAAATGCAAACACG

pry-1(mu38)

OTS32	TCTAATTTCCAGACTCCGCC
OTS35	TGTACGCTTAAACCAGGAAT

bar-1(ga80)

OTS33	
	AGATAGACACACACACACAA
OTS36	GAGCATTGTTGCATGTTGGA

lin-39(n1490)

OTS34	AGGATGATGACAAGAAAGGC
OTS37	TGGATATTCAGTGGGTTTTG

lin-12(n302)

OTS40	GATGTGGTTTTGATGGTGA
OTS41	CGTTTCATTATCACAATCAC
OTS42	AAGCCTTGCAGATATTGAGT

CE1-123

OTS68	CTGTTGAGGCTAATGTTTGG
OTS69	ACTTCTCTCGGATCTCATCA

haw5576

OTS70	CAAAAAAGTGGGTGAGCTAT
OTS71	CGCCCAAAGATATTACACCT

haw5575

OTS72	GATAACCGGGACTTTACCAT
OTS73	AAAATCTTACCAGACGGACC

amx-2(ok1235)

OTS149	AGGCTCAGGGTACATTTTAG
OTS150	GTCGTTTCGGTTAATGATGG
OTS174	GGAGCTCGTTGCTGATGTTA
OTS218	CCACGCCTACTACTTCACAAT

tfg-1(ok2290)

OTS153	AGCTCCGGATAAACTTGGGT

OTS154	TATTCCCTTCCCACCAATCA

tfg-1(gk128455)

OTS164	TCCCTTTAAAAAACCCCCGT
OTS165	GGCTCACACTACAAACTACAC

Y10D10A.9(gk125840)

OTS158	CTTTCGTGTCCTTCTAGCTTG
OTS159	CAAGGCGAGAAAGATGACAC

Y10D10A.9(gk125834)

OTS160	ATTTTGCAATCTCCACCACC
OTS161	GAAAACACGGGAAAAATCGG

eif-3.j(gk127104)

OTS162	GGCTGAAAAAGAAGCGATACA
OTS163	GTTTTTCGTGGTTTTCAGGTG

pfd-3(gk125596)

OTS166	CCGGAATTTCTACGCTCAAT
OTS167	TGGGAACTTGATTTTAGGCG

toe-4(tm1580)

OTS187	ACTCATGTGAAATTTTGGGCG
OTS188	TGACGTTGAAGGTAGAGATGAAG

Y18D10A.2(tm3588)

OTS189	CCTTTTCCTATTTTCTGAGCCA

gale-1

OTS183	GGTACTGGTTTTTGGATCGTT
OTS184	TGGGGGTCAATTTCTCTGTTTC

Genomic template

srxa-13

OTS50	ACGCGTTAATTTTTTTCGGGTTGC
OTS51	GAATTCTCTTCATTTTTTTTAGAT
OTS52	TTCGGGTTGCCAATAAACG
OTS53	TCTCGGGTACGTCATCTTTC
OTS54	AACAAGGAAGAACTGGGC
OTS55	AATACCAACCAGCAAGTG

F08A8.1

OTS56	CTATCTATGACACTCCTCCG
OTS57	GTTCGCCATGTTACTGATAT

clec-110

OTS58	CTTGGACAAAACTGCGGAT
OTS59	ACATACGATTCATGCACAAC

W02A11.1

OTS60	CGAAGTCAACATGTCCCATA
OTS61	TCGGTGGAGATAATGAAGGC

F17B5.1

OTS62	GCCCAAACATTTTCCAACTT
OTS63	ATGCATGTGGAAAAGTTGGA

T06G6.6

OTS64	ATGGCTGGCTTCTCGTATAA
OTS65	CCTCTCTGTTTCATCATTCT

bath-34

OTS66	GTGGAGGAAAAGGACGATAA
OTS67	CCCGTTATACATTTTCGCAA

tfg-1

OTS74	TCAGAAAACGCGAAAAATCCAC
OTS75	CTCCAACAATTGCTCTCCAAAT
OTS82	CGTTTAGCCTCAATTTCCTG
OTS83	CGTGGATGAGGACGATGAAG
OTS168	AAAACCTAGGGCAATCCTGGCACGCGTGTTGC
OTS169	AAAACCTAGGCGTGGATGAGGACGATGAAG

toe-4

OTS76	TGCCGTTTTAGCAGCTATTCT
OTS77	AATAGAGTAAAAAGGGGACCAC
OTS84	CTTTAGCAGGTTTTCGGGTC
OTS85	CGGTTGAGGTTGGAAATGTC
OTS147	AAAAGAATTCCGGTTGAGGTTGGAAATGTC
OTS148	AAAAGAATTCCTTTAGCAGGTTTTCGGGTC
OTS151	AAAAGCTAGCCGGTTGAGGTTGGAAATGTC
OTS152	AAAAGCTAGCCTTTAGCAGGTTTTCGGGTC

Y10D10A.2

OTS78	GAAAAAAGAGGTTTGTGGCCG
OTS79	GGTAGGTTTTACGGGACATTTT
OTS86	TAAAACTCACCTCGGCAATG
OTS87	CGAGTGGCAATGATGATGAC
OTS179	AAAACCTAGGCGGGGTGTGTGTGATAACTATT
OTS180	AAAACCTAGGAAGAGGGGTACATGAAGGTTTA

F08A8.5

OTS80	AACGCCTCATAATTTTGTGTGT
OTS81	AGAGCGAGTGAAAATTGAGAAG
OTS88	GCTTCCCGTCCTTTTATCAG
OTS89	CTGAAGAGCGAGTGAAAATTG
OTS90	GCAATCCTGGCACGCGTGTTGC

F44F1.3

OTS91	GCTGACTGTTTTCTGGATCT
OTS92	TAGAATATTGGCAGCATAACCG
OTS170	AAAAGCTAGCGCTGACTGTTTTCTGGATCT
OTS171	AAAAGCTAGCTAGAATATTGGCAGCATAACCG

amx-2

OTS93	CCGCTCAATCATCTCACTTC
OTS94	TGGCCAAAACCACTCAAATT
OTS123	GATTTTGGAGAAGAAACGAGGG
OTS124	ACTTCACTATGTTCCTCTACCG
OTS131	AAAAACTCGAGGATTTTGGAGAAGAAACGAGGG
OTS132	AAAACTCGAGACTTCACTATGTTCCTCTACCG
OTS185	AAAACTCGAGCCGCTCAATCATCTCACTTC
OTS186	AAAACTCGAGTGGCCAAAACCACTCAAATT
OTS196	AAAACCTAGGCCGCTCAATCATCTCACTTC
OTS197	AAAACCTAGGTGGCCAAAACCACTCAAATT
OTS200	AAAAGCTAGCGATTTTGGAGAAGAAACGAGGG
OTS201	AAAAGCTAGCACTTCACTATGTTCCTCTACCG
OTS202	AAAACGTACGCCGCTCAATCATCTCACTTC
OTS203	AAAACGTACGTGGCCAAAACCACTCAAATT
OTS204	AAAAGGATCCCCGCTCAATCATCTCACTTC
OTS205	AAAAGGATCCTGGCCAAAACCACTCAAATT

F44F1.4

OTS95	AGAGACAGACATGGTGGAAG
OTS96	GCGATTGAGTTGTGAGAGAG
OTS99	TCTTCGATTTCTTCAGCCCAC
OTS100	GAGTTGTATCGTTGAGTTGGG
OTS109	ACAATTGTCTCGTTTTCGCC

OTS110	ATGAAGTCTTTTCGAGCGTT
OTS157	GGAGAGTTGTGAAAATCGAGAA

F17B5.4

OTS97	AGTAAAAGTGTTAGACGTCGC
OTS98	AATTGTTCCACCATCCTATCAC

C54C8.2

OTS101	ATATTTGCACATGGGACTTCC
OTS102	AATCCAGGAGACGTAATAGC

W02D9.4

OTS103	CCGCACATTTCGATTATCA
OTS104	GCGCATTTTTGTTGGAGAT

sra-17

OTS105	ATGTATGGAGATGTCGGAGA
OTS106	CTTCAGCGGTTTTGTTCATT

F44F1.1

OTS107	AGAAGAAGAAGAACAAGCGTC
OTS108	GCTCCAAAAGCTCCTCTTC
OTS129	AAAACTCGAGAGAAGAAGAAGAACAAGCGTC
OTS130	AAAACTCGAGGCTCCAAAAGCTCCTCTTC

T26E3.6

OTS111	GGTTTGAAGCGAAAGGAATG
OTS112	CACAAACCAAAGCATATCGG
OTS119	CTCAACCCACACAATATAAGCAAC
OTS120	GGATAAGCGTCAACAACTGGAA

srw-88

OTS113	ACGTCAGGAACCGAAAAAAC
OTS114	CAAACGAAAATACACGGCG
OTS198	AAAAGCTAGCACGTCAGGAACCGAAAAAAC
OTS199	AAAAGCTAGCCAAACGAAAATACACGGCG

pfd-3

OTS115	ATCTTCCAACCAAGCCTTCA
OTS116	TTCTCAGCCAACACACACTG
OTS121	AGTTGGGATTTTTTTGTGCTCC
OTS122	TGGCTGCTGAGATGTTGATTTTC
OTS177	AAAACCTAGGAGTTGGGATTTTTTTGTGCTCC
OTS178	AAAACCTAGGTGGCTGCTGAGATGTTGATTTTC

W04A4.5

OTS117	CTCTTGAAAATATCCGCCCC
OTS118	CAATGAGAGTTTGTGAGCGT

F44F1.6

OTS125	AGAGGCAGTGGAAAAGATAGAC
OTS126	TTTCTCCGTGTCCCTATGTTTC

sepa-1

OTS127	GTCTTCACCAAAACTCACCG
OTS128	AAAGCCTGACAACTCTCTACG

sra-20

OTS133	GGCTCAAGAAAAGCTGGGAATA
OTS134	CCCGTTTTTGGGCATTTTCAC

uba-2

OTS135	GAAAAACTCACCGGAATTGAAG
OTS136	TCAGAATTTACAGCGCTCATC

Y10D10A.8

OTS137	GGTCTTCCTTCCACTTCTTCT
OTS138	GTTTGCCGAGTTTCCGATTTG

Y10D10A.9

OTS139	CGGGGTGTGTGTGATAACTATT
OTS140	AAGAGGGGTACATGAAGGTTTA

gale-1

OTS141	CCTCGTTTTCATTGTTGGCTTC
OTS142	GATGATGACGTAGATGGTGGTG
OTS155	AAAAGCTAGCTTTTATGGGCTGGAAAGTTGTC
OTS156	AAAAGCTAGCGATGATGACGTAGATGGTGGT
OTS181	AAAACCTAGGGATGATGACGTAGATGGTGGTG
OTS182	AAAACCTAGGCCTCGTTTTCATTGTTGGCTTC

ZK12251.1

OTS143	TTGTGGAAAAGTCGGGGTCA
OTS144	CTTTCAGTCGATAATGTGGTGT

eif-3.j

OTS145	ATTTCTGTGTGTTTATGCCGC

OTS146	TCTACCACCGCCATTTTTATCC

glct-2

OTS206	AAAACCTAGGGGCACAACGACCAAAAAGAC
OTS207	AAAACCTAGGATCACCATGCAAATCACGAC
OTS212	AAAACCTAGGGATATCAAAACGAGAAGGCAGGAA
OTS213	AAAACCTAGGCCGTCTGTTCTTTTTTGTGCTAAG
OTS223	AAAACCTAGGAACACTTGGATTGACTCTGC
OTS247	AAAACCTAGGTTCAGGTGTGTGAAGGGTTGA

hsr-9

OTS208	AAAACCTAGGACCTTTCCACTCTTCTTCAAG
OTS209	AAAACCTAGGCATTTCCACCACCTCGTCTTC
OTS214	AAAACCTAGGTTAGAAGACGGAAAGAAAACCCAC
OTS215	AAAACCTAGGGATTATGATTGGATGGACTTGGAG

C15C6.3

OTS210	AAAACCTAGGAATGCCAGAGAGAGGAGAGA
OTS211	AAAACCTAGGCGTACGTCTTTGCTCATTTT
OTS216	AAAACCTAGGTCGTTTTCTTTTCCACCTCCTACA
OTS217	AAAACCTAGGTTGAAAATTACCTCCTCCCCGAGA

elt-2

OTS232	TCTGAGCCCGCTTTCCTTATA
OTS233	CATTCCAGGGTACTTCACGTT

Other

pCFJ151

pCFJ151_1	ATTTAGGTGACACTATAG
pCFJ151_2	CTGTCACACTCGCTAAAAAC
pCFJ151_3	CGCCCAGGAGAACACGTTA

pPD95.67/ pPD95.75

GFPfusionREV_prim	CAACAAGAATTGGGACAACT
M13_reverse_prime	GCTCGTATGTTGTGTGGAA

ttTi5605

OTS172	CGGAAACCAAAGGACGAGAG
OTS173	TGTTTTTGATTGCGTGCGTT
OTS190	GAATGACGAGAGAGTATGCAAAGG
OTS191	CTCACTATAAAAACCCGCTAACTC
OTS192	TGACGTCTTCTTCTGCTTCTTTTC
OTS193	GGAAACGTATGAGAGAGCAGTAAG

OTS194	ATCTTTTCTGGCTCTGCTTCTTC
OTS195	CCTCTTAATGCGTTGTTTCTCTC
NM3880	AGGCAGAATGTGAACAAGACTCG
NM3887	ACCGGAAACCAAAGGACGAGAG
NM3888	ACGCCCAGGAGAACACGTTAG
NM3884	ATCGGGAGGCGAACCTAACTG

amx-2 gene expression

transcriptional

OTS219	AAAAGGATCCTTAGGTTTATTGCTGGAAAAAT
OTS220	AAAAGGATCCCCTTAACCAAATTTCATACCC

translational

OTS221	AAAAGGATCCTGTAGACGCAAAGTCTGTAA

Q-PCR

amx-2

OTS234	TCGTAGATACAGGATCTCAGT
OTS235	AGGGATAGTTGTCTCTTCTTC
OTS236	TTGGATGTTAGTGACGTCAAC
OTS237	TTCATGGTACCCAAATTGTGC
OTS238	TGGAAATTTGGACAACTCCAC
OTS239	CGTTGAATAGTTCAATGTTGGT

amx-1

OTS240	TTGAAATAGACGATAGAAAAGAAG
OTS241	CGCGATTCATTTTTACAGGT
OTS242	GATGAGAAATTTGCATTCCC
OTS243	GCATGACCTCTGACAATAATC
OTS244	TTCTGGAAAGGACCCCAATG
OTS245	GAAGGGTTGCACAGAATTTGTC

sqv-2 operon fusion

OTS224	GTCTTCTACATCCACCACCACCA
OTS225	GCAAATATGTTCGGTAGAATCTCATTAATTTTTGGAGAAAAATTGGTAAA
OTS226	ATGAGATTCTACCGAACATATTTGC
OTS227	CTGTGAGAATGTATGGGTTT
OTS228	CAGAAAAACCCATACATTCTCACAGAATTTCTGAAATTTTAGAGAATTTT
OTS229	GAGACAGTGAAAGATTTGGTGG
OTS230	GGAAAATTTGAGCCAAAAACTAAG
OTS231	AGGAAATGGGGAAAACTAGG
OTS248	CTGTGAGAATGTATGGGTTTTTCTGG
OTS249	TTTGGGGGGAAATAAAGAAAGGG
OTS250	ATTAAATTTGCGACGAGACCC
OTS251	GAAGGCATTGGACGGATTTTAG

OTS252	CCCCGACTCTCTTCATTTTTATC

***let-23* GST fusion**

OTS43	CCCGGGAAGATGTCAACGTATTGG
OTS44	CCCGGGTTAAAGACAAGTTTCCTT
OTS45	CCCGGGAACCAAACTAGACAAAAA
OTS46	TTTAGATCTAGATGTCAACGTATTGG
OTS47	TTTAGATCTTTAAAGACAAGTTTCC
OTS48	TTTAGATCTACCAAACTAGACAAAAA

Table 14: Primer stocks diluted to 100 nM in TE buffer

1.19.2 PCR Reaction and Setup

Phusion High-Fidelity DNA Polymerase, New England Biolabs (NEB)

Reaction

Components	Volume (20 µl)
5x HF or GC buffer	4 µl
2 mM dNTPs	2 µl
2 mM Primer fwd	2 µl
2 mM Primer rev	2 µl
Phusion Polymerase	0.2 µl
template DNA	variable
ddH_2O	to 20 µl

Cycling

Temperature	Time	Cycle
98°C	30 sec	1x
98°C	15-30 sec	30-35x
variable	30 sec	
72°C	15-30 sec/ kb	
72°C	5 min	1x
12°C	∞	

Taq Polymerase, Invitrogen

Reaction

Components	Volume (20 µl)
10x reaction buffer	2 µl
2 mM dNTPs	2 µl
50 mM $MgCl_2$	1 µl
2 mM Primer fwd	2 µl
2 mM Primer rev	2 µl
Taq Polymerase	0.2 µl
template DNA	variable
ddH_2O	to 20 µl

Cycling

Temperature	Time	Cycle
94°C	2 min	1x
94°C	30 sec	30-35x
variable	30 sec	
72°C	1 min/ kb	
72°C	10 min	1x
12°C	∞	

GoTaq Polymerase, Promega

Reaction

Components	Volume (20 µl)
10x reaction buffer	2 µl

Cycling

Temperature	Time	Cycle
94°C	2 min	1x

2 mM dNTPs	2 µl
50 mM $MgCl_2$	1 µl
2 mM Primer fwd	2 µl
2 mM Primer rev	2 µl
GoTaq Polymerase	0.2 µl
template DNA	variable
ddH_2O	to 20 µl

94°C	30 sec	30-35x
variable	30 sec	
72°C	1 min/ kb	
72°C	10 min	1x
12°C	∞	

LongAmp Taq Polymerase, New England Biolabs (NEB)

Reaction

Components	Volume (20 µl)
5x LongAmp reaction buffer	4 µl
2 mM DNTPs	2 µl
2 mM Primer fwd	2 µl
2 mM Primer rev	2 µl
Taq Polymerase	1 µl
template DNA	variable
ddH_2O	to 20 µl

Cycling

Temperature	Time	Cycle
94°C	2 min	1x
94°C	30 sec	30-35x
variable	30-1 min	
65°C	1 min/ kb	
65°C	10 min	1x
12°C	∞	

1.19.3 PCR Loading and Detection

Variable amounts of PCR product were mixed in a 5:1 ratio with loading dye, loaded together with 3 µl of 1 Kb Plus DNA ladder (Invitrogen) and run on 0.5-1 % agarose gel (depending on PCR size) containing a 1:1000 dilution of EtBr stock solution (2 mg/ml). UV transillumination was used to detect DNA fragments.

1.19.4 Restriction Digest

Restriction digests for cloning were carried out in total volume of 20 µl for PCR fragments and vector DNA overnight at 37°C. In addition, digested vectors were routinely dephosphorylated using the Antarctic phosphatase (NEB). Subsequent heat inactivation, if possible, or PCR purification using the GenElute PCR Clean-Up Kit (Sigma-Aldrich) was used to clean PCR fragments and vectors from buffer and residual enzymes. Digested and cleaned DNA was loaded on an agarose gel to estimate concentration

10x digestion buffer	2 µl
template DNA	Variable
restriction enzyme	0.2 µl

ddH_2O	to 20 µl

To consider: If there were undesired fragments after digestion with size > 50 bp, the desired band was cut out in gel and gel purified using the GenElute Gel Extraction Kit (Sigma-Aldrich). The presence of the desired fragment after cutting was checked again on an agarose gel and to estimate concentration.

Restriction digests to screen for alleles (genotyping) was carried out in 10 µl for 3-4 h at 37°C and without further purification analysed on an agarose gel.

1.19.5 DNA Ligation

Purified DNA from section 1.19.4 was ligated using T4 DNA ligase (Fermentas) in a total volume of 20 µl. Fragment and vector DNA were mixed in a ratio anywhere between 1:1 and 1:10 and left for 30 min to 2 h at room temperature.

10x ligation buffer	2 µl
Fragment DNA	Variable
Vector DNA	variable
T4 DNA ligase	1 µl
ddH_2O	to 20 µl

Additional step: Subcloning into the pGEM-T easy system (Promega)

For better handling and manipulation, PCR fragments can be TA cloned into the pGEM-T easy system that made use of the additional A overhang PCR polymerases normaly add to every fragment (see manufacturers protocol). If PCR fragments were obtained form a proofreading polymerase such as Phusion, the addition of A's is necessary, since proofreading eliminates those during PCR amplification. The incubation mixture was incubated in a PCR thermocycler at 70°C for 30 minutes.

purified PCR	5 µl
5x GoTaq PCR Buffer	2 µl
10 µM dATPs	0.2 µl
GoTaq Polymerase	0.2 µl
ddH_2O	2.6 µl

1.19.6 Transformation of Competent *E. coli* Cells

Ligation products form section 1.19.5 were completely transformed using DH10b chemically competent cells. Competent cells were taken from the -80°C freezer an carefully thawed on ice. 100 µl cell suspension was added to 20 µl ligation product, while tubes were kept on ice for another 20-30 minutes. In the meantime, a temperature of 42°C is set on the heating block. Ligation and cell mixture is incubated for 90 sec at 42°C and put back on ice immediately afterwards. 800 µl of cold 2xTY media is added and the tubes are shifted for 30 min to 1 h to 37°C. Cells were then spun at 3500 rpm in a table top centrifuge and supernatant was removed, leaving roughly 50 µl. Cells were dissolved and plated in most of the cases on amp containing plates (other antibiotic or IPTG/x-Gal, if plasmid contains different selection marker).

To consider: For simple retransformation of plasmids, the centrifugation step was omitted, instead 50 µl of uncentrifuged cell suspension was plated.

1.19.7 Minipreparation of Plasmid DNA

Routinely, the rapid boil miniprep protocol was used (Harwood, 1996). Tubes of 2 ml 2xTY containing desired antibiotic resistance (usually amp in 1:1000 dilution) were inoculated with single colonies from plates of section 1.19.6 and left overnight at 37°C. The next day, tubes were centrifuged at 4000 rpm to pellet bacteria. Supernatant was discared and 350 µl STET solution was added. Tubes were vortexted until bacteria pellet completely dissolved. 25 µl of lysozyme was added to each tube and tubes were inverted 2-3 times and incubated for 1 minute at 95°C. Next samples were taken out and centrifuged full speed at 4°C for 8 minutes. The viscous pellet was removed using forceps and 30 µl 3M NaAc (pH 5.2) and 300 µl Isopropanol was added. Tubes were inverted 2-3 times and centrifuged again for 8 minutes at full speed. Supernatant was discarded and pellet was dissolved in 30-50 µl of TE. DNA concentration was measured on the NanoDrop instrument.

1.19.8 Midipreparation of Plasmid DNA

If more and cleaner plasmid DNA was required, the QIAfilter Plasmid Midi Kit (Qiagen) was used according to the manufacturers protocol.

Exception: Optimisations were made to the protocol starting after step 13. Unlike in the protocol, the pellet was dissolved in 400 µl of TE and transferred to a 1.5 ml tube. 40 µl of 3M NaAc (pH 5.2) and 800 µl of ice cold EtOH were added to precipitate the DNA at -80°C for 10-15 minutes. Next, the sample was centrifuged full speed for 15 minutes, the supernatant was discarded and the pellet dissolved in 100 µl TE buffer.

1.19.9 Sequencing of DNA Fragments (Plasmid or PCR)

PCR fragments were purified either by conventional EtOH precipitation (described elsewere) or using the GenElute PCR Clean-Up Kit (Sigma-Aldrich). Plasmids obtained from the miniprep protocol were prepared the same way. Plasmids from Midipreparation needn't any further purification step.

Components	Volume
10 mM primer	1 µl
template DNA	PCR: 15 ng/500 bp Plasmid 200-300 ng
ddH_2O	To 10 µl

1.19.10 Plasmids Obtained

pTS3	Hawaii F44F1.1 region amplified with OTS129 and OTS130 cloned into XhoI site of pCFJ151
pTS4	Bristol F44F1.1 region amplified with OTS129 and OTS130 cloned into XhoI site of pCFJ151
pTS5	Hawaii amx-2 amplified with OTS185 and OTS132 cloned into XhoI site of pCFJ151
pTS6	Bristol amx-2 amplified with OTS131 and OTS132 cloned into XhoI site of pCFJ151
pTS7	Hawaii toe-4 amplified with OTS151and OTS152 cloned into AvrII site of pCFJ151
pTS8	Bristol toe-4 amplified with OTS151 and OTS152 cloned into AvrII site of pCFJ151
pTS9	Hawaii tfg-1 amplified with OTS168 and OTS169 cloned into AvrII site of pCFJ151
pTS10	Bristol tfg-1 amplified with OTS168 and OTS169 cloned into AvrII site of pCFJ151
pTS11	Hawaii F44F1.3 amplified with OTS170 and OTS171 into AvrII site of pCFJ151
pTS12	Bristol F44F1.3 amplified with OTS170 and OTS171 into AvrII site of pCFJ151
pTS13	Hawaii pfd-3 amplified with OTS177 and OTS178 into AvrII site of pCFJ151
pTS14	Bristol pfd-3 amplified with OTS177 and OTS178 into AvrII site of pCFJ151
pTS15	transcriptional reporter construct for CB-amx-2, promoter of CB-amx-2 amplified with OTS219 and OTS220 cloned into BamHI site of pPD95.67

pTS16	transcriptional reporter construct for N2-amx-2, promoter of N2-amx-2 amplified with OTS219 and OTS220 cloned into BamHI site of pPD95.67
pTS17	translational reporter construct for CB-amx-2, genomic region amplified with OTS186 and OTS221 cloned into BamHI, XhoI sites of pPD95.75
pTS18	translational reporter construct for N2-amx-2, genomic region amplified with OTS186 and OTS221 cloned into BamHI, XhoI sites of pPD95.75

1.20 Biochemistry

1.20.1 SDS PAGE

The MiniProtean Electrophoresis System (BioRad) and the following buffers were used:

2x SDS sample buffer DTT or β-mercaptoethanol:	100 mM Tris-Cl pH=6.8, 4% SDS, 0.2% bromophenol blue, 20% glyerols, 200 mM DTT or 200 mM β-mercaptoethanol
1x SDS running buffer:	30.2 g Tris, 188 g Glycine, 50 ml 20% SDS fill to 8 l with dH_2O
Stacking gel 5%:	13.6 ml H2O, 3.4 ml 30% acrylamide mix, 2.5 ml 1.5M Tris pH=8.8, 0.1 ml 20% SDS, 0.2 ml 10% APS, add 20 µl TEMED prior to use and pour immediatly
Separation gel 8%:	2.3 ml H2O, 1.3 ml 30% acrylamide mix, 1.5 ml Tris pH=8.8, 25 µl 20% SDS, add 50 µl 10% APS, 5 µl TEMED prior to use and pour immediatly
Separation gel 12%:	50 ml 1 M Tris, 150 ml 5 M NaCl, 2.5 ml Tween 20, 5l H2O, 25 µl 20% SDS, add 50 µl 10% APS, 5 µl TEMED prior to use and pour immediatly

Depending on the calculated protein size, either 8% or 12% SDS gels were poured. For whole worm protein extract, sample buffer was diluted to 1x and *C. elegans* worms were simply boiled in SDS sample buffer in a ratio of 1 worm/µl for 5-10 min at 95°C, centrifuged afterwards. Proteins in the supernatant were subsequently loaded on the SDS gel and run at 150-180 V for approximately 2 h or until the bromophenol blue running band reached the end of the gel. Gels were further processed for western blots.

1.20.2 Western Blot

The following buffers were used:

Western blot transfer buffer	2.42 g Tris, 11.528 g Glycine, 160 ml Methanol, 640 ml H2O
Washing buffer	50 mM Tris, 150 mM NaCl, 0.05% Tween 20
Blocking buffer	5 g fat free milkpowder, 100 ml TBS-T

Runs as described in section 1.20.1 were taken out from the glass assembly and transferred to a previously Methanol activated PVDF nylon membrane (Milipore) and assembled in the MiniProtean Electrophoresis System according to the manufacturers protocol for blotting 1.5 h at 150 mAh in the cold room. Next, the PVDF membrane was taken out from the stack and transferred to 5% fat-free milk in TBS-T for blocking at RT for 2-3 h or longer. The blocked PVDF membrane was then probed with the desired 1° antibody (diluted to desired concentration in 5% fat free milk/PBS-T) for overnight incubation. The next day, the membrane was washed 3-4 times 10-15 minutes in PBS-T buffer and then probed with the corresponding host 2° antibody conjugated with horseradish peroxidase (HRP) for 2 h at room temperature. The ECL Western blot detection system (GE Healthcare) was used to detect secondary antibodies and therefore the protein of interest.

1.20.3 Antibodies Used

Name	Host	Type	Company	Number
MEK1/2 (D1A5)	Rabbit	Monoclonal	Cell Signaling	#8727
Phospho-MEK1/2 (Ser217/221)	Rabbit	Polyclonal	Cell Signaling	#9121
Anti-MAP Kinase (ERK-1, ERK-2)	Rabbit	Polyclonal	Sigma-Aldrich	M5670
Anti-MAP Kinase, Activated (Diphosphorylated ERK-1&2)	Mouse	Monoclonal	Sigma-Aldrich	M8159
Anti-α–Tubulin	Mouse	Monoclonal	Sigma-Aldrich	T6074

1.21 Worm Handling

1.21.1 *C. elegans* Strains:

Strains were maintained on NGM agar and on OP50 bacteria at 20°C, otherwise stated ((Brenner, 1974)).

The following strains were used in this study:

1.21.1.1 *let-60(n1046)* MIRILs

RIL Number	Strain	Genotype
RIL1	AH1844	*CB4856/N2;let-60(n1046)*
RIL2	AH1845	*CB4856/N2;let-60(n1046)*
RIL3	AH1846	*CB4856/N2;let-60(n1046)*
RIL4	AH1847	*CB4856/N2;let-60(n1046)*
RIL5	AH1848	*CB4856/N2;let-60(n1046)*
RIL6	AH1849	*CB4856/N2;let-60(n1046)*
RIL7	AH1850	*CB4856/N2;let-60(n1046)*
RIL8	AH1851	*CB4856/N2;let-60(n1046)*
RIL9	AH1852	*CB4856/N2;let-60(n1046)*
RIL10	AH1853	*CB4856/N2;let-60(n1046)*
RIL11	AH1854	*CB4856/N2;let-60(n1046)*
RIL12	AH1855	*CB4856/N2;let-60(n1046)*
RIL13	AH1856	*CB4856/N2;let-60(n1046)*
RIL14	AH1857	*CB4856/N2;let-60(n1046)*
RIL15	AH1858	*CB4856/N2;let-60(n1046)*
RIL16	AH1859	*CB4856/N2;let-60(n1046)*
RIL17	AH1860	*CB4856/N2;let-60(n1046)*
RIL18	AH1861	*CB4856/N2;let-60(n1046)*
RL19	AH1862	*CB4856/N2;let-60(n1046)*
RIL20	AH1863	*CB4856/N2;let-60(n1046)*
RIL21	AH1864	*CB4856/N2;let-60(n1046)*
RIL22	AH1865	*CB4856/N2;let-60(n1046)*
RIL23	AH1866	*CB4856/N2;let-60(n1046)*
RIL24	AH1867	*CB4856/N2;let-60(n1046)*
RIL25	AH1868	*CB4856/N2;let-60(n1046)*
RIL26	AH1869	*CB4856/N2;let-60(n1046)*
RIL27	AH1870	*CB4856/N2;let-60(n1046)*
RIL28	AH1871	*CB4856/N2;let-60(n1046)*
RIL29	AH1872	*CB4856/N2;let-60(n1046)*
RIL30	AH1873	*CB4856/N2;let-60(n1046)*
RIL31	AH1874	*CB4856/N2;let-60(n1046)*
RIL32	AH1875	*CB4856/N2;let-60(n1046)*
RIL33	AH1876	*CB4856/N2;let-60(n1046)*

RIL Number	Strain	Genotype
RIL34	AH1877	*CB4856/N2;let-60(n1046)*
RIL35	AH1878	*CB4856/N2;let-60(n1046)*
RIL36	AH1879	*CB4856/N2;let-60(n1046)*
RIL37	AH1880	*CB4856/N2;let-60(n1046)*
RIL38	AH1881	*CB4856/N2;let-60(n1046)*
RIL39	AH1882	*CB4856/N2;let-60(n1046)*
RIL40	AH1883	*CB4856/N2;let-60(n1046)*
RIL41	AH1884	*CB4856/N2;let-60(n1046)*
RIL42	AH1885	*CB4856/N2;let-60(n1046)*
RIL43	AH2119	*CB4856/N2;let-60(n1046)*
RIL44	AH2120	*CB4856/N2;let-60(n1046)*
RIL45	AH2121	*CB4856/N2;let-60(n1046)*
RIL46	AH2122	*CB4856/N2;let-60(n1046)*
RIL47	AH2123	*CB4856/N2;let-60(n1046)*
RIL48	AH2124	*CB4856/N2;let-60(n1046)*
RIL49	AH2125	*CB4856/N2;let-60(n1046)*
RIL50	AH2126	*CB4856/N2;let-60(n1046)*
RIL51	AH2127	*CB4856/N2;let-60(n1046)*
RIL52	AH2128	*CB4856/N2;let-60(n1046)*
RIL53	AH2129	*CB4856/N2;let-60(n1046)*
RIL54	AH2130	*CB4856/N2;let-60(n1046)*
RIL55	AH2131	*CB4856/N2;let-60(n1046)*
RIL56	AH2132	*CB4856/N2;let-60(n1046)*
RIL57	AH2133	*CB4856/N2;let-60(n1046)*
RIL58	AH2134	*CB4856/N2;let-60(n1046)*
RIL59	AH2135	*CB4856/N2;let-60(n1046)*
RIL60	AH2136	*CB4856/N2;let-60(n1046)*
RIL61	AH2137	*CB4856/N2;let-60(n1046)*
RIL62	AH2138	*CB4856/N2;let-60(n1046)*
RIL63	AH2139	*CB4856/N2;let-60(n1046)*
RIL64	AH2140	*CB4856/N2;let-60(n1046)*
RIL65	AH2141	*CB4856/N2;let-60(n1046)*
RIL66	AH2142	*CB4856/N2;let-60(n1046)*
RIL67	AH2143	*CB4856/N2;let-60(n1046)*
RIL68	AH2144	*CB4856/N2;let-60(n1046)*

RIL Number	Strain	Genotype
RIL69	AH2145	*CB4856/N2;let-60(n1046)*
RIL70	AH2146	*CB4856/N2;let-60(n1046)*
RIL71	AH2147	*CB4856/N2;let-60(n1046)*
RIL72	AH2148	*CB4856/N2;let-60(n1046)*
RIL73	AH2149	*CB4856/N2;let-60(n1046)*
RIL74	AH2150	*CB4856/N2;let-60(n1046)*
RIL75	AH2151	*CB4856/N2;let-60(n1046)*
RIL76	AH2152	*CB4856/N2;let-60(n1046)*
RIL77	AH2153	*CB4856/N2;let-60(n1046)*
RIL78	AH2154	*CB4856/N2;let-60(n1046)*
RIL79	AH2155	*CB4856/N2;let-60(n1046)*
RIL80	AH2156	*CB4856/N2;let-60(n1046)*
RIL81	AH2157	*CB4856/N2;let-60(n1046)*
RIL82	AH2158	*CB4856/N2;let-60(n1046)*
RIL83	AH2159	*CB4856/N2;let-60(n1046)*
RIL84	AH2160	*CB4856/N2;let-60(n1046)*
RIL85	AH2161	*CB4856/N2;let-60(n1046)*
RIL86	AH2162	*CB4856/N2;let-60(n1046)*
RIL87	AH2163	*CB4856/N2;let-60(n1046)*
RIL88	AH2164	*CB4856/N2;let-60(n1046)*
RIL89	AH2165	*CB4856/N2;let-60(n1046)*
RIL90	AH2166	*CB4856/N2;let-60(n1046)*
RIL91	AH2167	*CB4856/N2;let-60(n1046)*
RIL92	AH2168	*CB4856/N2;let-60(n1046)*
RIL93	AH2169	*CB4856/N2;let-60(n1046)*
RIL94	AH2170	*CB4856/N2;let-60(n1046)*
RIL95	AH2171	*CB4856/N2;let-60(n1046)*
RIL96	AH2172	*CB4856/N2;let-60(n1046)*
RIL97	AH2173	*CB4856/N2;let-60(n1046)*
RIL98	AH2174	*CB4856/N2;let-60(n1046)*
RIL99	AH2175	*CB4856/N2;let-60(n1046)*
RIL100	AH2176	*CB4856/N2;let-60(n1046)*
RIL101	AH2177	*CB4856/N2;let-60(n1046)*
RIL102	AH2178	*CB4856/N2;let-60(n1046)*
RIL103	AH2179	*CB4856/N2;let-60(n1046)*

RIL Number	Strain	Genotype
RIL104	AH2180	*CB4856/N2;let-60(n1046)*
RIL105	AH2181	*CB4856/N2;let-60(n1046)*
RIL106	AH2182	*CB4856/N2;let-60(n1046)*
RIL107	AH2183	*CB4856/N2;let-60(n1046)*
RIL108	AH2184	*CB4856/N2;let-60(n1046)*
RIL109	AH2185	*CB4856/N2;let-60(n1046)*
RIL110	AH2186	*CB4856/N2;let-60(n1046)*
RIL111	AH2187	*CB4856/N2;let-60(n1046)*
RIL112	AH2188	*CB4856/N2;let-60(n1046)*
RIL113	AH2189	*CB4856/N2;let-60(n1046)*
RIL114	AH2190	*CB4856/N2;let-60(n1046)*
RIL115	AH2191	*CB4856/N2;let-60(n1046)*
RIL116	AH2192	*CB4856/N2;let-60(n1046)*
RIL117	AH2193	*CB4856/N2;let-60(n1046)*
RIL118	AH2194	*CB4856/N2;let-60(n1046)*
RIL119	AH2195	*CB4856/N2;let-60(n1046)*
RIL120	AH2318	*CB4856/N2;let-60(n1046)*
RIL121	AH2196	*CB4856/N2;let-60(n1046)*
RIL122	AH2197	*CB4856/N2;let-60(n1046)*
RIL123	AH2198	*CB4856/N2;let-60(n1046)*
RIL124	AH2199	*CB4856/N2;let-60(n1046)*
RIL125	AH2200	*CB4856/N2;let-60(n1046)*
RIL126	AH2201	*CB4856/N2;let-60(n1046)*
RIL127	AH2202	*CB4856/N2;let-60(n1046)*
RIL128	AH2203	*CB4856/N2;let-60(n1046)*
RIL129	AH2204	*CB4856/N2;let-60(n1046)*
RIL130	AH2205	*CB4856/N2;let-60(n1046)*
RIL131	AH2206	*CB4856/N2;let-60(n1046)*
RIL132	AH2207	*CB4856/N2;let-60(n1046)*
RIL133	AH2208	*CB4856/N2;let-60(n1046)*
RIL134	AH2209	*CB4856/N2;let-60(n1046)*
RIL135	AH2210	*CB4856/N2;let-60(n1046)*
RIL136	AH2211	*CB4856/N2;let-60(n1046)*
RIL137	AH2212	*CB4856/N2;let-60(n1046)*
RIL138	AH2213	*CB4856/N2;let-60(n1046)*

RIL Number	Strain	Genotype
RIL139	AH2214	*CB4856/N2;let-60(n1046)*
RIL140	AH2215	*CB4856/N2;let-60(n1046)*
RIL141	AH2216	*CB4856/N2;let-60(n1046)*
RIL142	AH2217	*CB4856/N2;let-60(n1046)*
RIL143	AH2218	*CB4856/N2;let-60(n1046)*
RIL144	AH2219	*CB4856/N2;let-60(n1046)*
RIL145	AH2220	*CB4856/N2;let-60(n1046)*
RIL146	AH2221	*CB4856/N2;let-60(n1046)*
RIL147	AH2222	*CB4856/N2;let-60(n1046)*
RIL148	AH2223	*CB4856/N2;let-60(n1046)*
RIL149	AH2224	*CB4856/N2;let-60(n1046)*
RIL150	AH2225	*CB4856/N2;let-60(n1046)*
RIL151	AH2226	*CB4856/N2;let-60(n1046)*
RIL152	AH2227	*CB4856/N2;let-60(n1046)*
RIL153	AH2228	*CB4856/N2;let-60(n1046)*
RIL154	AH2229	*CB4856/N2;let-60(n1046)*
RIL155	AH2230	*CB4856/N2;let-60(n1046)*
RIL156	AH2231	*CB4856/N2;let-60(n1046)*
RIL157	AH2232	*CB4856/N2;let-60(n1046)*
RIL158	AH2233	*CB4856/N2;let-60(n1046)*
RIL159	AH2234	*CB4856/N2;let-60(n1046)*
RIL160	AH2235	*CB4856/N2;let-60(n1046)*
RIL161	AH2236	*CB4856/N2;let-60(n1046)*
RIL162	AH2237	*CB4856/N2;let-60(n1046)*
RIL163	AH2238	*CB4856/N2;let-60(n1046)*
RIL164	AH2239	*CB4856/N2;let-60(n1046)*
RIL165	AH2240	*CB4856/N2;let-60(n1046)*
RIL166	AH2241	*CB4856/N2;let-60(n1046)*
RIL167	AH2242	*CB4856/N2;let-60(n1046)*
RIL168	AH2243	*CB4856/N2;let-60(n1046)*
RIL169	AH2244	*CB4856/N2;let-60(n1046)*
RIL170	AH2245	*CB4856/N2;let-60(n1046)*
RIL171	AH2246	*CB4856/N2;let-60(n1046)*
RIL172	AH2247	*CB4856/N2;let-60(n1046)*
RIL173	AH2248	*CB4856/N2;let-60(n1046)*

RIL Number	Strain	Genotype
RIL174	AH2249	*CB4856/N2;let-60(n1046)*
RIL175	AH2250	*CB4856/N2;let-60(n1046)*
RIL176	AH2251	*CB4856/N2;let-60(n1046)*
RIL177	AH2252	*CB4856/N2;let-60(n1046)*
RIL178	AH2253	*CB4856/N2;let-60(n1046)*
RIL179	AH2254	*CB4856/N2;let-60(n1046)*
RIL180	AH2255	*CB4856/N2;let-60(n1046)*
RIL181	AH2256	*CB4856/N2;let-60(n1046)*
RIL182	AH2257	*CB4856/N2;let-60(n1046)*
RIL183	AH2258	*CB4856/N2;let-60(n1046)*
RIL184	AH2259	*CB4856/N2;let-60(n1046)*
RIL185	AH2260	*CB4856/N2;let-60(n1046)*
RIL186	AH2261	*CB4856/N2;let-60(n1046)*
RIL187	AH2262	*CB4856/N2;let-60(n1046)*
RIL188	AH2263	*CB4856/N2;let-60(n1046)*
RIL189	AH2264	*CB4856/N2;let-60(n1046)*
RIL190	AH2265	*CB4856/N2;let-60(n1046)*
RIL191	AH2266	*CB4856/N2;let-60(n1046)*
RIL192	AH2267	*CB4856/N2;let-60(n1046)*
RIL193	AH2268	*CB4856/N2;let-60(n1046)*
RIL194	AH2269	*CB4856/N2;let-60(n1046)*
RIL195	AH2270	*CB4856/N2;let-60(n1046)*
RIL196	AH2271	*CB4856/N2;let-60(n1046)*
RIL197	AH2272	*CB4856/N2;let-60(n1046)*
RIL198	AH2273	*CB4856/N2;let-60(n1046)*
RIL199	AH2274	*CB4856/N2;let-60(n1046)*
RIL200	AH2275	*CB4856/N2;let-60(n1046)*
RIL201	AH2276	*CB4856/N2;let-60(n1046)*
RIL202	AH2277	*CB4856/N2;let-60(n1046)*
RIL203	AH2278	*CB4856/N2;let-60(n1046)*
RIL204	AH2279	*CB4856/N2;let-60(n1046)*
RIL205	AH2280	*CB4856/N2;let-60(n1046)*
RIL206	AH2281	*CB4856/N2;let-60(n1046)*
RIL207	AH2282	*CB4856/N2;let-60(n1046)*
RIL208	AH2283	*CB4856/N2;let-60(n1046)*

RIL Number	Strain	Genotype
RIL209	AH2284	*CB4856/N2;let-60(n1046)*
RIL210	AH2285	*CB4856/N2;let-60(n1046)*
RIL211	AH2286	*CB4856/N2;let-60(n1046)*
RIL212	AH2287	*CB4856/N2;let-60(n1046)*
RIL213	AH2288	*CB4856/N2;let-60(n1046)*
RIL214	AH2289	*CB4856/N2;let-60(n1046)*
RIL215	AH2290	*CB4856/N2;let-60(n1046)*
RIL216	AH2291	*CB4856/N2;let-60(n1046)*
RIL217	AH2292	*CB4856/N2;let-60(n1046)*
RIL218	AH2293	*CB4856/N2;let-60(n1046)*
RIL219	AH2294	*CB4856/N2;let-60(n1046)*
RIL220	AH2295	*CB4856/N2;let-60(n1046)*
RIL221	AH2296	*CB4856/N2;let-60(n1046)*
RIL222	AH2297	*CB4856/N2;let-60(n1046)*
RIL223	AH2298	*CB4856/N2;let-60(n1046)*
RIL224	AH2299	*CB4856/N2;let-60(n1046)*
RIL225	AH2300	*CB4856/N2;let-60(n1046)*
RIL226	AH2301	*CB4856/N2;let-60(n1046)*
RIL227	AH2302	*CB4856/N2;let-60(n1046)*
RIL228	AH2303	*CB4856/N2;let-60(n1046)*

1.21.1.2 *bar-1(ga80)* MIRILs

RIL Number	Strain	Genotype
RIL1	AH2014	*CB4856/N2;bar-1(ga80)*
RIL2	AH2021	*CB4856/N2;bar-1(ga80)*
RIL3	AH2012	*CB4856/N2;bar-1(ga80)*
RIL4	AH1982	*CB4856/N2;bar-1(ga80)*
RIL4	AH2013	*CB4856/N2;bar-1(ga80)*
RIL5	AH2049	*CB4856/N2;bar-1(ga80)*
RIL6	AH2011	*CB4856/N2;bar-1(ga80)*
RIL7	AH2002	*CB4856/N2;bar-1(ga80)*
RIL8	AH2003	*CB4856/N2;bar-1(ga80)*
RIL9	AH2001	*CB4856/N2;bar-1(ga80)*
RIL10	AH2022	*CB4856/N2;bar-1(ga80)*

RIL Number	Strain	Genotype
RIL11	AH2000	*CB4856/N2;bar-1(ga80)*
RIL12	AH2023	*CB4856/N2;bar-1(ga80)*
RIL13	AH2040	*CB4856/N2;bar-1(ga80)*
RIL14	AH2005	*CB4856/N2;bar-1(ga80)*
RIL16	AH2018	*CB4856/N2;bar-1(ga80)*
RIL17	AH2006	*CB4856/N2;bar-1(ga80)*
RIL18	AH2041	*CB4856/N2;bar-1(ga80)*
RIL19	AH2004	*CB4856/N2;bar-1(ga80)*
RIL20	AH2007	*CB4856/N2;bar-1(ga80)*
RIL21	AH2039	*CB4856/N2;bar-1(ga80)*
RIL22	AH2042	*CB4856/N2;bar-1(ga80)*
RIL23	AH2034	*CB4856/N2;bar-1(ga80)*
RIL24	AH2036	*CB4856/N2;bar-1(ga80)*
RIL25	AH2035	*CB4856/N2;bar-1(ga80)*
RIL26	AH2037	*CB4856/N2;bar-1(ga80)*
RIL28	AH2038	*CB4856/N2;bar-1(ga80)*
RIL29	AH2316	*CB4856/N2;bar-1(ga80)*
RIL30	AH2317	*CB4856/N2;bar-1(ga80)*
RIL31	AH2058	*CB4856/N2;bar-1(ga80)*
RIL32	AH2048	*CB4856/N2;bar-1(ga80)*
RIL33	AH2329	*CB4856/N2;bar-1(ga80)*
RIL34	AH2017	*CB4856/N2;bar-1(ga80)*
RIL35	AH2064	*CB4856/N2;bar-1(ga80)*
RIL36	AH2309	*CB4856/N2;bar-1(ga80)*
RIL37	AH2031	*CB4856/N2;bar-1(ga80)*
RIL38	AH2313	*CB4856/N2;bar-1(ga80)*
RIL39	AH2066	*CB4856/N2;bar-1(ga80)*
RIL40	AH1983	*CB4856/N2;bar-1(ga80)*
RIL41	AH2033	*CB4856/N2;bar-1(ga80)*
RIL42	AH1979	*CB4856/N2;bar-1(ga80)*
RIL43	AH2308	*CB4856/N2;bar-1(ga80)*
RIL44	AH1970	*CB4856/N2;bar-1(ga80)*
RIL45	AH2032	*CB4856/N2;bar-1(ga80)*
RIL46	AH1995	*CB4856/N2;bar-1(ga80)*
RIL47	AH2314	*CB4856/N2;bar-1(ga80)*

RIL Number	Strain	Genotype
RIL48	AH2315	*CB4856/N2;bar-1(ga80)*
RIL49	AH2067	*CB4856/N2;bar-1(ga80)*
RIL50	AH1999	*CB4856/N2;bar-1(ga80)*
RIL51	AH1971	*CB4856/N2;bar-1(ga80)*
RIL52	AH2015	*CB4856/N2;bar-1(ga80)*
RIL53	AH2330	*CB4856/N2;bar-1(ga80)*
RIL54	AH1969	*CB4856/N2;bar-1(ga80)*
RIL55	AH 1996	*CB4856/N2;bar-1(ga80)*
RIL56	AH2044	*CB4856/N2;bar-1(ga80)*
RIL57	AH2068	*CB4856/N2;bar-1(ga80)*
RIL58	AH2047	*CB4856/N2;bar-1(ga80)*
RIL59	AH1994	*CB4856/N2;bar-1(ga80)*
RIL60	AH2056	*CB4856/N2;bar-1(ga80)*
RIL61	AH2053	*CB4856/N2;bar-1(ga80)*
RIL62	AH2306	*CB4856/N2;bar-1(ga80)*
RIL63	AH2043	*CB4856/N2;bar-1(ga80)*
RIL64	AH2020	*CB4856/N2;bar-1(ga80)*
RIL65	AH2307	*CB4856/N2;bar-1(ga80)*
RIL66	AH2019	*CB4856/N2;bar-1(ga80)*
RIL67	AH1968	*CB4856/N2;bar-1(ga80)*
RIL68	AH1978	*CB4856/N2;bar-1(ga80)*
RIL69	AH1997	*CB4856/N2;bar-1(ga80)*
RIL70	AH2045	*CB4856/N2;bar-1(ga80)*
RIL71	AH1976	*CB4856/N2;bar-1(ga80)*
RIL72	AH2016	*CB4856/N2;bar-1(ga80)*
RIL73	AH1998	*CB4856/N2;bar-1(ga80)*
RIL74	AH2323	*CB4856/N2;bar-1(ga80)*
RIL75	AH1993	*CB4856/N2;bar-1(ga80)*
RIL75	AH2310	*CB4856/N2;bar-1(ga80)*
RIL77	AH2057	*CB4856/N2;bar-1(ga80)*
RIL78	AH1977	*CB4856/N2;bar-1(ga80)*
RIL79	AH2311	*CB4856/N2;bar-1(ga80)*

1.21.1.3 Introgression Lines (Doroszuk et al., 2009)

LG I: ewIR2

ewIR5

ewIR7

ewIR9

ewIR10

ewIR11

ewIR13

ewIR14

ewIR17

LG II: ewIR21

ewIR23

ewIR26

LG V: ewIR66

ewIR67

ewIR68

1.21.1.4 Genetic Mutant Strains:

LG I: RB1190: *amx-2(ok1235)*

AH893: *pry-1(mu38)*

AH2444: *ewIR2;let-60(n1046)*

LG II: PS1839: *let-23(sa62)*

AH13: *let-23(sy1)*

LG III: MT302: *lin-12(n302)*

AH1115: *lin-12(n379)*

MT1514: *lin-39(n709)*

MT4306: *lin-39(n1490); unc-36(e251)*

SD939: *mpk-1(ga111);unc-79(e1068)*

LG IV: SD551: *let-60(ga89)*

MT2124: *let-60(n1046)*

MT4866: *let-60(n2021)*

MT822: *lin-1(n304)*

AH102: *lip-1(zh15)*

LG X: AH12: *gap-1(ga133)*

SD294: *lin-2(n397)*

EW15: *bar-1(ga80)*

1.21.1.5 Strains With Extrachromosomal Arrays:

AH2468	*let-60(n1046)II;zhEx502[toe-4;sur-5:gfp]*
AH2469	
AH2470	
AH2471	*let-60(n1046)II;zhEx502[amx-2;sur-5:gfp]*
AH2472	
AH2473	
AH2474	
AH2475	
AH2479	*let-60(n1046)II;zhEx507[Y18D10A.2;sur-5::gfp]*
AH2780	
AH2781	*let-60(n1046)II;zhEx511[F44F1.1;sur-5::gfp]*
AH2782	
AH2783	
AH2793	
AH2794	
AH2784	*let-60(n1046)II;zhEx514[tfg-1;sur-5::gfp]*
AH2785	
AH2786	
AH2787	*let-60(n1046)II;zhEx507[Y18D10A.2;sur-5::gfp]*
AH2788	
AH2789	*let-60(n1046)II;zhEx507[F44F1.3;sur-5::gfp]*
AH2790	
AH2791	
AH2792	
AH2799	*let-60(n1046)II;zhEx515[tfg-1;sur-5::gfp]*

AH2800	*let-60(n1046)II;zhEx516[C54C8.2;sur-5::gfp]*
AH2801	
AH2802	

OLB11: *rde-1(ne219);Ex?[elt-2p::rde1(+);pRF4]*

AH2927: *let-60(n1046);rde-1(ne219);zhEx418?[lin-31::rde-1;myo-2::mCherry]*

1.21.1.6 Integrated Strains:

SD806: *him-5(e1490); gaIs36?[HS-mpk-1(+), HS-dmek]*

SD1059: *gaIs37?[HS-mpk-1(+), HS-dmek]*

AH552: *let-60(n1046); saIs14?[lin-48::gfp]*

1.21.1.6.1 MosSCI Strains and Siblings:

AH3002	*let-60(n1046)* sibling lines from crosses
AH3003	
AH3004	
AH3005	
AH3009	
AH3016	
AH3017	
AH3019	
AH3020	
AH3026	
AH3027	
AH2999	*amx-2(ok1235);let-60(n1046)* sibling lines from crosses
AH3000	
AH3001	
AH3010	
AH3021	
AH3022	
AH3025	
AH2926	
AH3035	

AH3011	*amx-2(ok1235);zhIs74;let-60(n1046)*
AH3012	
AH3036	
AH3040	
AH3046	
AH3047	
AH3048	
AH3049	
AH3007	*amx-2(ok1235);zhIs73;let-60(n1046)*
AH3008	
AH3013	
AH3014	
AH3024	
AH3041	
AH3042	
AH3043	
AH3015	*zhIs73;let-60(n1046)*
AH3018	
AH3023	*zhIs74;let-60(n1046)*
AH3029	*zhEx532*
AH3030	*zhEx533*
AH3031	

1.21.2 Crossings

Males were either picked from spontaneous occurence, generated via heat-shock or N2 males were crossed with the desired strain to obtain heterozygous male progeny used for further crossing. For heatshock treatment 20 L4 hermaphrodites were picked per plate and incubated 5 h at 33°c in a waterbath. the F1 generation was checked for males and used directly or for self-crosses to obtain more male progeny.

4-5 hermaphrodites were crossed with 12-15 males on NGM plates containing a small spot of OP50 (“mating plate”) at 20°C. Animals were left for mating for 2 days. Hermaphrodites were singled out on NGM plates containing OP50 and left for another 2-3 days. Plates were checked for male cross progeny, indicating successful crossing. Plates not containing males were discarded. Next, 5-10 F1 hermaphrodites were singled out on new NGM plates containing OP50. After 3 days F2 progeny was screened for desired phenotype or randomly picked and lysed for further genotyping.

1.21.3 Worm Lysis and Genotyping

10-12 adult hermaphrodites were lysed per 10 µl lysis mix.

Worm lysis mix	For 10 µl
10x lysis buffer	1 µl
Proteinase K	0.6 µl
ddH_2O	8.4 µl

Cycling	
65°C	60 min
95°C	15 min
12°C	∞

Genotyping was done using the Taq (Invitrogen), GoTaq (Promega) or LongAmp (NEB) polymerases and their respective setup (see 1.19.2). 2 µl wormlysate per 20 µl PCR mix was used.

1.21.4 Worm Liquid Culture (as Described in Wormbook Methods)

1.21.4.1 Na22 Worm Food

To feed *C. elegans* in liquid media (see 1.21.4.2), Na22 bacteria were prepared in high quantity in superbroth media. The superbroth media was inoculated with Na22 bacteria the evening before and let shake at 37°C overnight. The next day, the media was centrifuged for 15 min at 4000 rpm and supernatant was discarded. The pelleted bacteria were then dissolved in a little as possible 2xTY media, aliquoted into 15 ml falcon tubes and stored at -20°C.

1.21.4.2 Worm Liquid Setup

To obtain the necessary quantity of *C. elegans* for applications such as extraction of total genomic DNA or RNA, worms were grown in liquid media consisting of s-basal supplemented with the following per 100 ml:

100 ml	s-basal
300 µl	1M $MgSO_4$
300 µl	1M $CaCl_2$
1 ml	K-Citrate pH=6
1 ml	100x trace metals
1 ml	100x Pen/Strep
100 µl	1000x Nystatin
100 µl	Cholesterol (5 mg/ml)
4 ml	Na22 worm food (see 1.21.4)

Worms from two to three confluent small NGM plates were used to inoculate 100 ml worm liquid media. Worm liquid cultures were shaken on a platform rocker at 150 rpm for up to one

week or until desired worm quantity was obtained. Na22 bacteria were thereby added as needed.

1.21.4.3 Harvesting Worm Liquid Cultures

To recover and harvest grown animals in liquid cultures, sucrose floating was used. 100 ml cultures were split into two 50 ml falcon tubes. Worms were washed two to three times with ice cold 0.1 M NaCl and centrifugation at 2000 rpm. Per 50 ml falcon tube, 20 ml of 60% sucrose was added to 20 ml of worm suspension, quickly mixed by inversion and subsequently centrifuged at 5000 rpm for 5 minutes without the decelerating centrifuge brake. Due to the density difference of healthy worms vs. worm debris and bacterial contamination, worm will flow on top and are removed with a widened Pasteur pipette to a fresh 50 ml falcon tube. Worms are washed again two to three times as described before and eventually combined in smaller tubes. Cleaned animals are aliquoted in 1.5 ml tubes, flash frozen in liquid N_2 and stored at -80°C.

1.21.5 Cleaning of Contaminated *C. elegans* Stocks

Two methods were routinely used to clean contaminated stocks.

1.21.5.1 Drop Bleach Method

C. elegans gravid hermaphrodites are transferred from the contaminated plate and deposed in a droplet of 1:1 dilution of 10-15% sodium hypochloride and 2 M NaOH on a clean NGM plate to dissolve.

1.21.5.2 Tube Bleach Method

Worms from one to two contaminated plates are rinsed into a 15 ml falcon tube and centrifuged at 1000 rpm for 1 minute. Supernatant was aspired until a residual volume of 1 ml. 70 µl 10-15% sodium hypochloride and 200 µl 2 M NaOH were added. Worms were dissolved for 5-10 minutes with occasional inversion of the tube. Next, the 15 ml falcon tube was completely filled with ddH_2O to neutralise. Eggs were subsequently spun at 2000 rpm, supernatant was removed till 0.5 ml and residual liquid was plated on several fresh NGM plates.

1.21.6 RNAi Gene Knockdown

Gene knockdown in *C. elegans* was carried out using RNAi feeding according to (Kamath, Martinez-Campos, Zipperlen, Fraser, & Ahringer, 2000).

1.21.6.1 Preparation of Ampicillin and Tetracycline Containing Agar Plates

3-4 g of bacterial agar was added to 200 ml 2xTY media and and heated in the microwave until agar completely dissolved. The media was cooled down to 50°C and 200 µl of ampicillin and 200 µl of tetracycline were added. Plates were poured and let to dry for two to three days at room temperature. RNAi bacterial clones were streaked out on plates (4-8 clones per plate) and let grow overnight at 37°C.

1.21.6.2 NGM RNAi Test Plates

The following media were used and prepared prior to the test plates:

KPO_4 buffer pH6

1 M $MgSO_4$

1 M $CaCl_2$

1 M IPTG

0.5 liter media was prepared to obtain 40-45 RNAi test plates:

1.5g NaCl

1.25g Peptone

9.5g Bacto Agar)

0.5ml Cholesterol (5mg/ml)

up to 0.5 liter with ddH_2O

The RNAi media was autoclaved together with KPO_4 buffer, 1 M $MgSO_4$ and 1 M $CaCl_2$. Next the media was cooled down to 55°C and the following were added:

12.5ml KPO_4 Buffer pH6

0.5ml 1 M $MgSO_4$

0.5ml 1 M $CaCl_2$

1.5ml 1 M IPTG

0.5 ml Ampicillin

RNAi media was subsequently poured into small petri dishes and let to cool down and dry at room temperature for 3 days. In the meantime, an appropriate volume of 2xTY media was inoculated with previously streaked out RNAi bacterial clones and let to grow either 8 hours or overnight at 37°C. Next, 200-300 µl liquid bacteria culture was plates on RNAi test plates and let to dry for another one to two days at room temperature. Worms were added via conventional bleach methods (1.21.5.1 or 1.21.5.2).

1.21.7 NGM Plates Containing 5-HT, 5-HIAA, DOPA or MT

Standard NGM plates were supplemented with different concentrations of Serotonin (5-HT), 5-Hydroxyindoleacetic acid (5-HIAA), Dopamine (DOPA) or Melatonin (MT) and kept in dark at 4°C until use.

1.22 Mammalian Cells

All manipulations described here were carried out in a sterile fume hood, solely used for cell culture work.

1.22.1 Cell Lines Used:

M010817: human melanoma

HCT116: colon carcinoma

MB-MDA223: breast adenocarcinoma

HEK: human embryonic kidney

1.22.2 Cell Culturing

Human cancer cell lines were kept in culture flasks or on coated plates in an incubator at 37°C with 5% CO_2.

1.22.2.1 M010817

Cells were kept in RPMI medium (Dulbecco) supplemented with 10% FCS.

1.22.2.2 HCT116, MB-MDA223, HEK

Cells were kept in DMEM medium (Dulbecco) supplemented with 10% FCS.

1.22.3 Passaging and Trypsination

Cells were conventionally passaged/ harvested using trypsination. Cells were washed once with PBS and 1-2 ml (depending on the size of the culture flask) of trypsin solution was added to the cells. Cells were rocked to remove surface adherence. The cell suspension was pippeted up and down until only a homogenous single cell suspension with no clumps was visible under the microscope. Depending on further applications, cells were diluted to the appropriate density and seeded in new culture flask or on plates. The appropriate amount of growth medium was added and cells were placed back in 37°C inbuator.

1.22.4 MTT Assay

This is an assay to measure cell viability (Mosmann, 1983). The yellow 3-(4,5-dimethythiazol-2-yl)-2,5-diphenyl tetrazolium bromide (MTT) diffuses into the cells and is thereby converted through the action of the mitochondrial succinate dehydrogenase into the insoluble purple formazan. The cells are lysed using an organic solvent such as ispropanol and the formazan is solubilised and can me measured on a photospectrometer. Since only metabolically active cells can convert MTT into formazan, the readout indirectly reflects the amount of viable cells in solution.

Reagents:

PBS

MTT solution: 5mg/ml in PBS, freshly prepared and kept in dark at 4°C

Lysis solution: 0.1 N HCl in isopropanol

Procedure:

Cells were collected from a culture bottle and counted using a haemocytometer. Next, 4000 cells per well were seeded into 96 well culture plates and kept in 200 µl of either RPMI supplemented with 10% FCS (M010817) or in 200 µl of DMEM supplemented with 10% FCS (HCT116, MB-MDA231) for 24 h at 37°C 5% CO_2. The next day, almost all growth medium was aspired and 200 µl of fresh medium supplemented with different concentrations of 5-HIAA was added. Cells were incubated at 37°C 5% CO_2 for 48 h. Next, 40 µl of MTT solution was added per well and cells were left for 3-4 hours at 37°C 5% CO_2. Medium was aspired completely and 200 µl of Lysis solution was added. Pipetting up and down thereby helped to dissolve any formazan clumps. 94 well plates were covered with aluminium foil and absorption at 600 nm was read on a plate reader.

Appendix

1.23 *let-60(n1046)* miRILs

1.23.1 Raw Data Genotypes


lysate
46
47
48
49
50
51
52
53
54
55
56
57
58
59
60
61
62
63
64
65
66
67
68
69
70
71
72
73
74
75
76
77
78
79
80
81
82
83
84
85
86
87
88
89
90
91
92
93
94
95
96
97
98
99
100
2H1-17
2H1-10a
2H1-07
2H1-18a
2H1-03
2H1-27
2H1-14
2H1-01
2H1-23
2H1-15
2H1-08
2H1-06
2H2-04a
2H2-16
2H2-07
2H2-13
2H2-19
2H2-02
2H2-20
2H2-25
2H2-27
2H2-09
2H2-10
2H2-12
2H3-17a
2H3-07
2H3-06
2H3-08
2H3-28
2H3-15
2H3-04
2H3-02
2H3-05a
2H3-35
2H3-10a
2H3-11
2H3-13
2H4-04a
2H4-5
2H4-06
2H4-16
2H4-08
2H4-17
2H4-18
2H4-19
2H4-20
2H4-21
2H4-12
2H5-13
2H5-03a
2H5-14
2H5-05
2H5-16
2H5-17
2H5-18
2H5-11
2H5-12
2H5-08
2H5-21a2
2H5-09
2HX-17
2HX-08
2HX-13
2HX-15
2HX-10
2HX-24
2HX-07
2HX-12
2HX-11
2HX-21a
2HX-06
2HX-22a3


lysate
101
102
103
104
105
106
107
108
109
110
111
112
113
114
115
116
117
118
119
120
121
122
123
124
125
126
127
128
129
130
131
132
133
134
135
136
137
138
139
140
141
142
143
144
145
146
147
148
149
150
151
152
153
154
155


lysate
156
157
158
159
160
161
162
163
164
165
166
167
168
169
170
171
172
173
174
175
176
177
178
179
180
181
182
183
184
185
186
187
188
189
190
191
192
193
194
195
196
197
198
199
200
201
202
203
204
205
206
207
208
209
210
ZH1-17
ZH1-10a
ZH1-07
ZH1-18a
ZH1-03
ZH1-27
ZH1-14
ZH1-01
ZH1-23
ZH1-15
ZH1-08
ZH1-06
ZH2-04a
ZH2-16
ZH2-07
ZH2-13
ZH2-19
ZH2-02
ZH2-20
ZH2-25
ZH2-27
ZH2-09
ZH2-10
ZH2-12
ZH3-17a
ZH3-07
ZH3-06
ZH3-08
ZH3-28
ZH3-15
ZH3-04
ZH3-02
ZH3-05a
ZH3-35
ZH3-10a
ZH3-11
ZH3-13
ZH4-04a
ZH4-5
ZH4-06
ZH4-16
ZH4-08
ZH4-17
ZH4-18
ZH4-19
ZH4-20
ZH4-21
ZH4-12
ZH5-13
ZH5-03a
ZH5-14
ZH5-05
ZH5-16
ZH5-17
ZH5-18
ZH5-11
ZH5-12
ZH5-08
ZH5-21a2
ZH5-09
ZHX-17
ZHX-08
ZHX-13
ZHX-15
ZHX-10
ZHX-24
ZHX-07
ZHX-12
ZHX-11
ZHX-21a
ZHX-06
ZHX-22a3

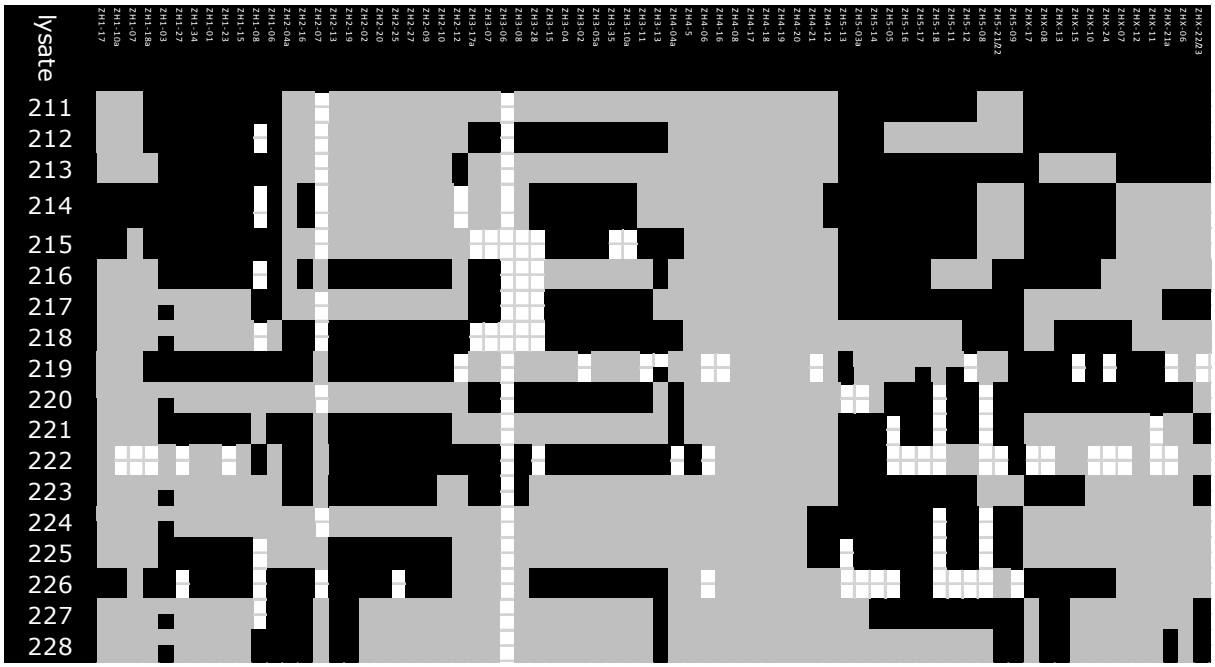

Figure 50: Raw genotype data of *let-60(n1046)* miRILs. Lines are sorted by increasing number. Chromosomes I-V from left to right, grey indicates Bristol and black indicates Hawaii genomic regions.

1.24 *bar-1(ga80)* miRILs

1.24.1 Raw Data Genotypes

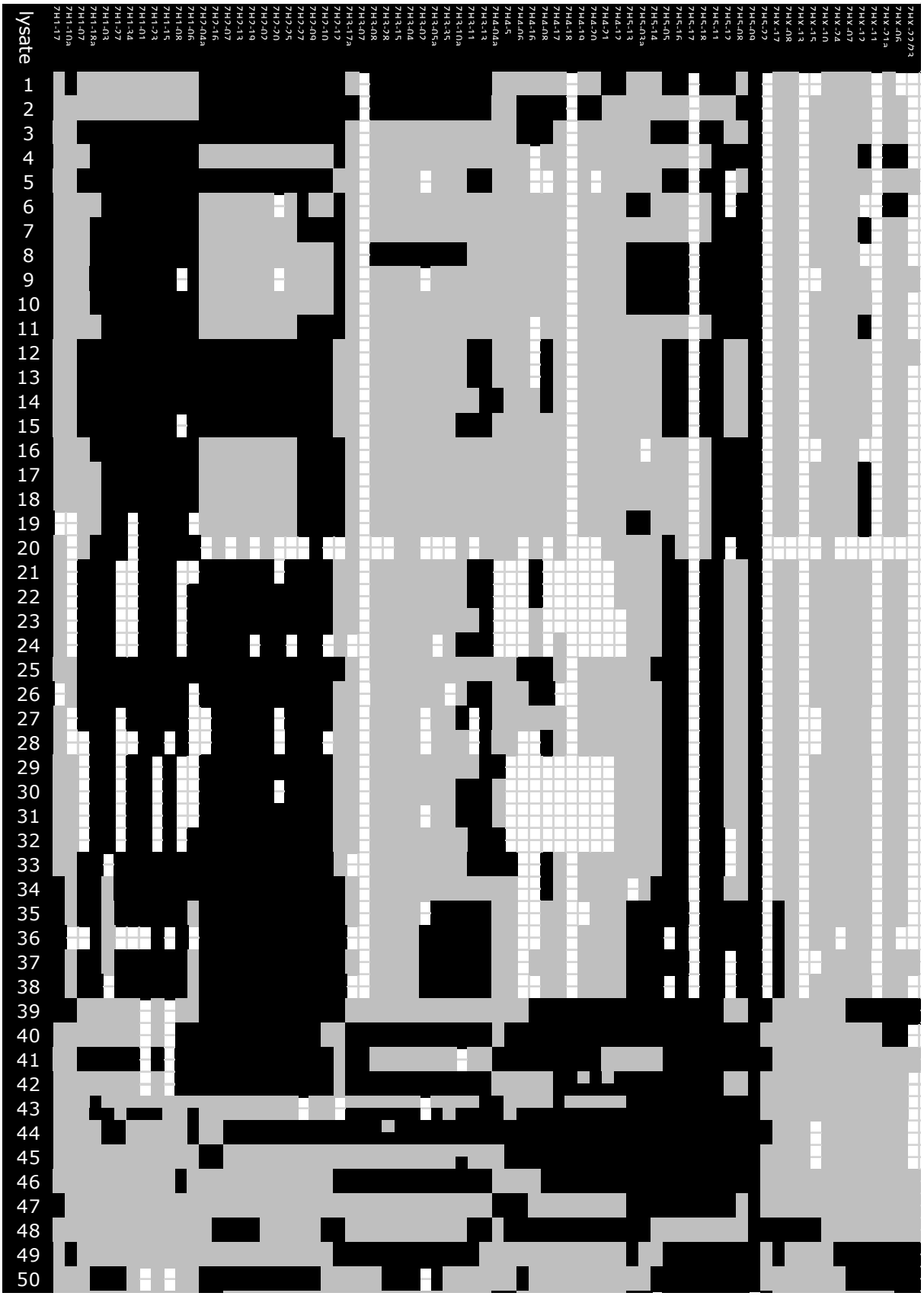

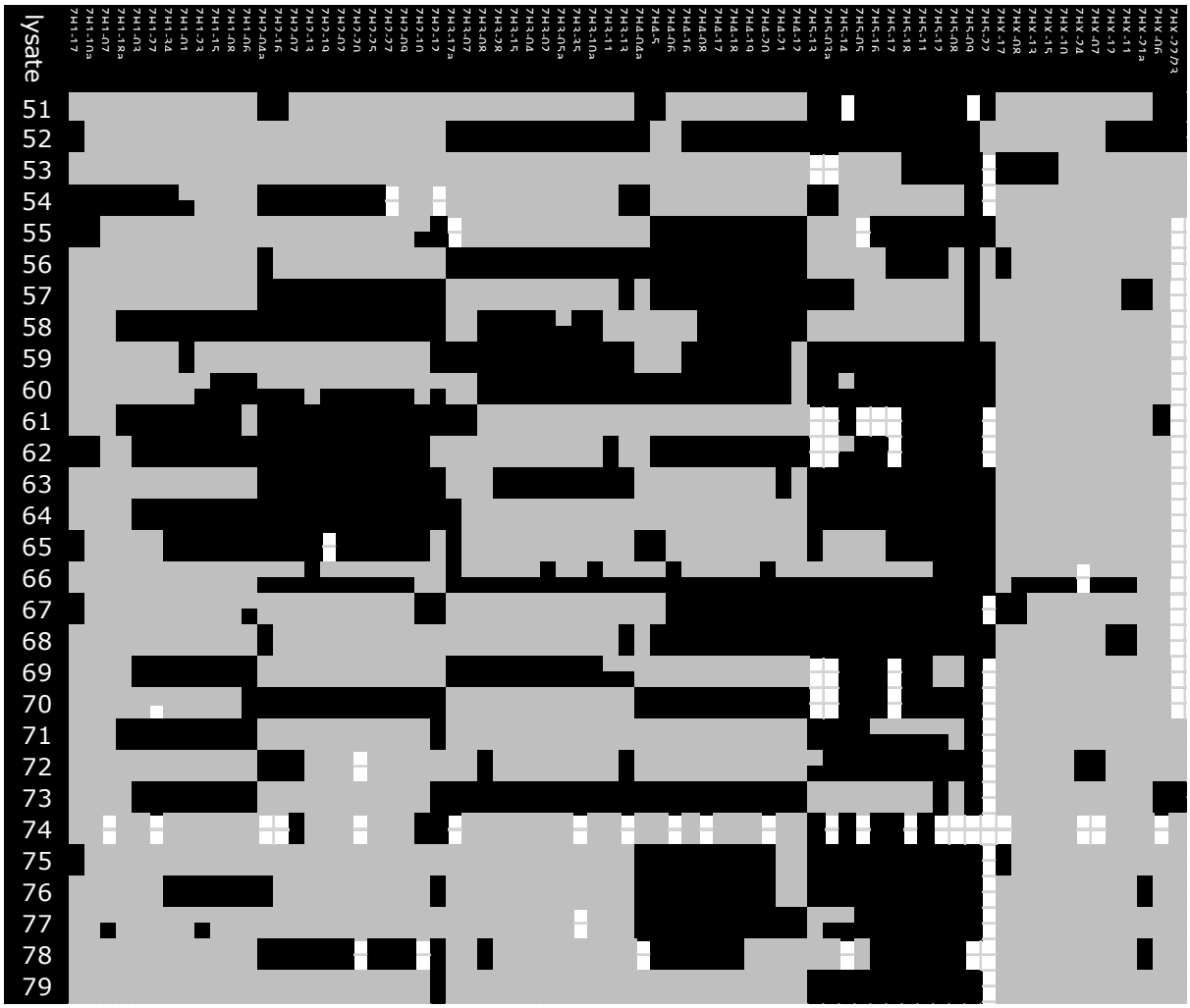

Figure 51: Raw genotype data of *bar-1(ga80)* miRILs. Lines are sorted by increasing number. Chromosomes I-V from left to right, grey indicates Bristol and black indicates Hawaii genomic regions.

Alex Hajnal, C. W. W. S. K. K. (1997). Inhibition of Caenorhabditis elegans vulval induction by gap-1 and by let-23 receptor tyrosine kinase. *Genes & Development*, *11*(20), 2715–2728. doi:10.1101/gad.11.20.2715

Antoshechkin, I., & Han, M. (2002). The C. elegans evl-20 Gene Is a Homolog of the Small GTPase ARL2 and Regulates Cytoskeleton Dynamics during Cytokinesis and Morphogenesis. *Developmental Cell*, *2*(5), 579–591. doi:10.1016/S1534-5807(02)00146-6

Aroian, R. V., Koga, M., Mendel, J. E., Ohshima, Y., & Sternberg, P. W. (1990). The let-23 gene necessary for Caenorhabditis elegans vulval induction encodes a tyrosine kinase of the EGF receptor subfamily. *Nature*, *348*(6303), 693–699. doi:10.1038/348693a0

Barstead, R. (2001). Genome-wide RNAi. *Current Opinion in Chemical Biology*, *5*(1), 63–66. doi:10.1016/S1367-5931(00)00173-3

Battu, G., Froehli Hoier, E., & Hajnal, A. (2003). The C. elegans G-protein-coupled receptor SRA-13 inhibits RAS/MAPK signalling during olfaction and vulval development. *Development*, *130*(12), 2567–2577. doi:10.1242/dev.00497

Beitel, G. J., Tuck, S., Greenwald, I., & Horvitz, H. R. (1995). The Caenorhabditis elegans gene lin-1 encodes an ETS-domain protein and defines a branch of the vulval induction pathway. *Genes & Development*, *9*(24), 3149–3162.

Berset, T. (2001). Notch Inhibition of RAS Signaling Through MAP Kinase Phosphatase LIP-1 During C. elegans Vulval Development. *Science*, *291*(5506), 1055–1058. doi:10.1126/science.1055642

Berset, T. A. (2005). The C. elegans homolog of the mammalian tumor suppressor Dep-1/Scc1 inhibits EGFR signaling to regulate binary cell fate decisions. *Genes & Development*, *19*(11), 1328–1340. doi:10.1101/gad.333505

Bivona, T. G., Quatela, S. E., Bodemann, B. O., Ahearn, I. M., Soskis, M. J., Mor, A., et al. (2006). PKC Regulates a Farnesyl-Electrostatic Switch on K-Ras that Promotes its Association with Bcl-Xl on Mitochondria and Induces Apoptosis. *Molecular Cell*, *21*(4), 481–493. doi:10.1016/j.molcel.2006.01.012

Boguski, M. S., & McCormick, F. (1993). Proteins regulating Ras and its relatives. *Nature*, *366*(6456), 643–654. doi:10.1038/366643a0

Boulin, T., & Bessereau, J.-L. (2007). Mos1-mediated insertional mutagenesis in Caenorhabditis elegans. *Nature Protocols*, *2*(5), 1276–1287. doi:10.1038/nprot.2007.192

Brenner, S. (1974). The genetics of Caenorhabditis elegans. *Genetics*, *77*(1), 71–94.

Capon, D. J., Chen, E. Y., Levinson, A. D., Seeburg, P. H., & Goeddel, D. V. (1983). Complete nucleotide sequences of the T24 human bladder carcinoma oncogene and its normal homologue. *Nature*, *302*(5903), 33–37. doi:10.1038/302033a0

Casey, P. J., Solski, P. A., Der, C. J., & Buss, J. E. (1989). p21ras is modified by a farnesyl isoprenoid. *Proceedings of the National Academy of Sciences of the United States of America*, *86*(21), 8323–8327.

Chang, C. (2000). Caenorhabditis elegans SOS-1 is necessary for multiple RAS-mediated developmental signals. *The EMBO Journal*, *19*(13), 3283–3294. doi:10.1093/emboj/19.13.3283

Chang, E. H., Gonda, M. A., Ellis, R. W., Scolnick, E. M., & Lowy, D. R. (1982). Human genome contains four genes homologous to transforming genes of Harvey and Kirsten murine sarcoma viruses. *Proceedings of the National Academy of Sciences of the United States of America*, *79*(16), 4848–4852.

Charles W Whitfield, C. B. T. B. S. H. S. K. K. (1999). Basolateral Localization of the Caenorhabditis elegans Epidermal Growth Factor Receptor in Epithelial Cells by the PDZ Protein LIN-10. *Molecular Biology of the Cell*, *10*(6), 2087.

Chesire, D. R., Ewing, C. M., Sauvageot, J., Bova, G. S., & Isaacs, W. B. (2000). Detection and analysis of ?-catenin mutations in prostate cancer. *The Prostate*, *45*(4), 323–334. doi:10.1002/1097-0045(20001201)45:4<323::AID-PROS7>3.0.CO;2-W

Chiaradonna, F., Gaglio, D., Vanoni, M., & Alberghina, L. (2006a). Expression of transforming K-Ras oncogene affects mitochondrial function and morphology in mouse fibroblasts. *Biochimica et Biophysica Acta (BBA) - Bioenergetics*, *1757*(9-10), 1338–1356.

doi:10.1016/j.bbabio.2006.08.001
Chiaradonna, F., Sacco, E., Manzoni, R., Giorgio, M., Vanoni, M., & Alberghina, L. (2006b). Ras-dependent carbon metabolism and transformation in mouse fibroblasts. *Oncogene*, *25*(39), 5391–5404. doi:10.1038/sj.onc.1209528
Clandinin, T. R., Katz, W. S., & Sternberg, P. W. (1997). Caenorhabditis elegansHOM-C Genes Regulate the Response of Vulval Precursor Cells to Inductive Signal. *Developmental Biology*, *182*(1), 150–161. doi:10.1006/dbio.1996.8471
Clark, S. G., Chisholm, A. D., & Horvitz, H. R. (1993). Control of cell fates in the central body region of C. elegans by the homeobox gene lin-39. *Cell*, *74*(1), 43–55.
Costa, M. (1998). A Putative Catenin-Cadherin System Mediates Morphogenesis of the Caenorhabditis elegans Embryo. *The Journal of Cell Biology*, *141*(1), 297–308. doi:10.1083/jcb.141.1.297
Dalpé, G., Brown, L., & Culotti, J. G. (2005). Vulva morphogenesis involves attraction of plexin 1-expressing primordial vulva cells to semaphorin 1a sequentially expressed at the vulva midline. *Development*, *132*(6), 1387–1400. doi:10.1242/dev.01694
DeFeo, D., Gonda, M. A., Young, H. A., Chang, E. H., Lowy, D. R., Scolnick, E. M., & Ellis, R. W. (1981). Analysis of two divergent rat genomic clones homologous to the transforming gene of Harvey murine sarcoma virus. *Proceedings of the National Academy of Sciences of the United States of America*, *78*(6), 3328–3332.
Doroszuk, A., Snoek, L. B., Fradin, E., Riksen, J., & Kammenga, J. (2009). A genome-wide library of CB4856/N2 introgression lines of Caenorhabditis elegans. *Nucleic Acids Research*, *37*(16), e110–e110. doi:10.1093/nar/gkp528
Eastman, Q., & Grosschedl, R. (1999). Regulation of LEF-1/TCF transcription factors by Wnt and other signals. *Current Opinion in Cell Biology*, *11*(2), 233–240. doi:10.1016/S0955-0674(99)80031-3
Eisenmann, D. M., & Kim, S. K. (2000). Protruding vulva mutants identify novel loci and Wnt signaling factors that function during Caenorhabditis elegans vulva development. *Genetics*, *156*(3), 1097–1116.
Eisenmann, D. M., Maloof, J. N., Simske, J. S., Kenyon, C., & Kim, S. K. (1998). The beta-catenin homolog BAR-1 and LET-60 Ras coordinately regulate the Hox gene lin-39 during Caenorhabditis elegans vulval development. *Development*, *125*(18), 3667–3680.
Evans, T. C. (2006). Transformation and microinjection. *WormBook*.
Friedman, A., & Perrimon, N. (2005). High-throughput approaches to dissecting MAPK signaling pathways. *Error*, *40*(3), 262–271. doi:10.1016/j.ymeth.2006.05.002
Fritz, R. D., Letzelter, M., Reimann, A., Martin, K., Fusco, L., Ritsma, L., et al. (2013). A Versatile Toolkit to Produce Sensitive FRET Biosensors to Visualize Signaling in Time and Space. *Science Signaling*, *6*(285), rs12. doi:10.1126/scisignal.2004135
Frøkjær-Jensen, C., Wayne Davis, M., Hopkins, C. E., Newman, B. J., Thummel, J. M., Olesen, S.-P., et al. (2008). Single-copy insertion of transgenes in Caenorhabditis elegans. *Nature Genetics*, *40*(11), 1375–1383. doi:10.1038/ng.248
Gaertner, B. E., & Phillips, P. C. (2010). Caenorhabditis elegans as a platform for molecular quantitative genetics and the systems biology of natural variation. *Genetics research*, *92*(5-6), 331–348. doi:10.1017/S0016672310000601
Ghai, R., Mobli, M., Norwood, S. J., Bugarcic, A., Teasdale, R. D., King, G. F., & Collins, B. M. (2011). Phox homology band 4.1/ezrin/radixin/moesin-like proteins function as molecular scaffolds that interact with cargo receptors and Ras GTPases. *Proceedings of the National Academy of Sciences*, *108*(19), 7763–7768. doi:10.1073/pnas.1017110108
Gilman, A. G. (1987). G proteins: transducers of receptor-generated signals. *Annual review of biochemistry*, *56*, 615–649. doi:10.1146/annurev.bi.56.070187.003151
Gleason, J. E. (2002). Activation of Wnt signaling bypasses the requirement for RTK/Ras signaling during C. elegans vulval induction. *Genes & Development*, *16*(10), 1281–1290. doi:10.1101/gad.981602
Graham, J. M. (2001). *Isolation of Mitochondria from Tissues and Cells by Differential Centrifugation*. *onlinelibrary.wiley.com*. Hoboken, NJ, USA: John Wiley & Sons, Inc.

doi:10.1002/0471143030.cb0303s04
H G Brunner, M. R. N. P. V. Z. N. G. A. A. H. V. G. E. C. W. M. A. K. H. H. R. B. A. V. O. (1993). X-linked borderline mental retardation with prominent behavioral disturbance: phenotype, genetic localization, and evidence for disturbed monoamine metabolism. *American Journal of Human Genetics*, *52*(6), 1032.
Hall, A., Marshall, C. J., Spurr, N. K., & Weiss, R. A. (1983). Identification of transforming gene in two human sarcoma cell lines as a new member of the ras gene family located on chromosome 1. *Nature*, *303*(5916), 396–400. doi:10.1038/303396a0
Hancock, J. F., Paterson, H., & Marshall, C. J. (1990). A polybasic domain or palmitoylation is required in addition to the CAAX motif to localize p21ras to the plasma membrane. *Cell*, *63*(1), 133–139. doi:10.1016/0092-8674(90)90294-O
Hand, P. H., Thor, A., Wunderlich, D., Muraro, R., Caruso, A., & Schlom, J. (1984). Monoclonal antibodies of predefined specificity detect activated ras gene expression in human mammary and colon carcinomas. *Proceedings of the National Academy of Sciences of the United States of America*, *81*(16), 5227–5231.
Hannah S Seidel, M. V. R. L. K. (2008). Widespread genetic incompatibility in C. elegans maintained by balancing selection. *Science (New York, N.Y.)*, *319*(5863), 589. doi:10.1126/science.1151107
Hardin, J., & King, R. S. (2008). The long and the short of Wnt signaling in C. elegans. *Current Opinion in Genetics & Development*, *18*(4), 362–367. doi:10.1016/j.gde.2008.06.006
Harwood, A. J. (1996). The Rapid Boiling Method for Small-Scale Preparation of Plasmid DNA. In *link.springer.com* (Vol. 58, pp. 265–268). New Jersey: Humana Press. doi:10.1385/0-89603-402-X:265
Herman, R. K., & Hedgecock, E. M. (1990). Limitation of the size of the vulval primordium of Caenorhabditis elegans by lin-15 expression in surrounding hypodermis. *Nature*, *348*(6297), 169–171. doi:10.1038/348169a0
Hill, R. J., & Sternberg, P. W. (1992). The gene lin-3 encodes an inductive signal for vulval development in C. elegans. *Nature*, *358*(6386), 470–476. doi:10.1038/358470a0
Hu, Y., Lu, W., Chen, G., Wang, P., Chen, Z., Zhou, Y., et al. (2011). K-rasG12V transformation leads to mitochondrial dysfunction and a metabolic switch from oxidative phosphorylation to glycolysis. *Cell Research*, *22*(2), 399–412. doi:10.1038/cr.2011.145
Hwang, H.-Y., Olson, S. K., Brown, J. R., Esko, J. D., & Horvitz, H. R. (2003). The Caenorhabditis elegans Genes sqv-2 and sqv-6, Which Are Required for Vulval Morphogenesis, Encode Glycosaminoglycan Galactosyltransferase II and Xylosyltransferase. *jbc.org*, *278*(14), 11735–11738. doi:10.1074/jbc.C200518200
Jastroch, M., Divakaruni, A. S., Mookerjee, S., Treberg, J. R., & Brand, M. D. (2010). Mitochondrial proton and electron leaks. *Essays in biochemistry*, *47*, 53–67. doi:10.1042/bse0470053
Kalgutkar, A. S., Dalvie, D. K., & Castagnoli, N. (2001). Interactions of nitrogen-containing xenobiotics with monoamine oxidase (MAO) isozymes A and B: SAR studies on MAO substrates and inhibitors. *Chemical research in …*.
Kamath, R. S., Martinez-Campos, M., Zipperlen, P., Fraser, A. G., & Ahringer, J. (2000). Effectiveness of specific RNA-mediated interference through ingested double-stranded RNA in Caenorhabditis elegans. *Genome Biology*, *2*(1), research0002.1. doi:10.1186/gb-2000-2-1-research0002
Kishore, R. S., & Sundaram, M. V. (2002). ced-10 Rac and mig-2 function redundantly and act with unc-73 trio to control the orientation of vulval cell divisions and migrations in Caenorhabditis elegans. *Developmental Biology*, *241*(2), 339–348. doi:10.1006/dbio.2001.0513
Korinek, V. (1997). Constitutive Transcriptional Activation by a beta -Catenin-Tcf Complex in APC-/- Colon Carcinoma. *Science*, *275*(5307), 1784–1787. doi:10.1126/science.275.5307.1752
Korswagen, H. C., Herman, M. A., & Clevers, H. C. (2000). Distinct [beta]-catenins mediate adhesion and signalling functions in C. elegans : Article : Nature. *Nature*, *406*(6795), 527–532. doi:10.1038/35020099

Kyriakis, J. M., App, H., Zhang, X.-F., Banerjee, P., Brautigan, D. L., Rapp, U. R., & Avruch, J. (1992). Raf-1 activates MAP kinase-kinase. *Nature*, *358*(6385), 417–421. doi:10.1038/358417a0

Lackner, M. R., & Kim, S. K. (1998). Genetic analysis of the Caenorhabditis elegans MAP kinase gene mpk-1. *Genetics*, *150*(1), 103–117.

Lesniak, W. G., Jyoti, A., Mishra, M. K., Louissaint, N., Romero, R., Chugani, D. C., et al. (2013). Concurrent quantification of tryptophan and its major metabolites. *Analytical Biochemistry*, *443*(2), 222–231. doi:10.1016/j.ab.2013.09.001

Li, J., Yang, X.-M., Wang, Y.-H., Feng, M.-X., Liu, X.-J., Zhang, Y.-L., et al. (2014). Monoamine oxidase A suppresses hepatocellular carcinoma metastasis by inhibiting the adrenergic system and its transactivation of EGFR signaling. *Journal of Hepatology*. doi:10.1016/j.jhep.2014.02.025

Li, P., Wood, K., Mamon, H., Haser, W., & Roberts, T. (1991). Raf-1: A kinase currently without a cause but not lacking in effects. *Cell*, *64*(3), 479–482. doi:10.1016/0092-8674(91)90228-Q

Liu, J., Phillips, B. T., Amaya, M. F., Kimble, J., & Xu, W. (2008). The C. elegans SYS-1 Protein Is a Bona Fide β-Catenin. *Developmental Cell*, *14*(5), 751–761. doi:10.1016/j.devcel.2008.02.015

Maloof, J. N., & Kenyon, C. (1998). The Hox gene lin-39 is required during C. elegans vulval induction to select the outcome of Ras signaling. *Development*, *125*(2), 181–190.

Maniatis, T. (1999). A ubiquitin ligase complex essential for the NF-kappaB, Wnt/Wingless, and Hedgehog signaling pathways. *Genes & Development*, *13*(5), 505–510.

Masckauchán, T. N. H., Shawber, C. J., Funahashi, Y., Li, C.-M., & Kitajewski, J. (2005). Wnt/β-Catenin Signaling Induces Proliferation, Survival and Interleukin-8 in Human Endothelial Cells. *Angiogenesis*, *8*(1), 43–51. doi:10.1007/s10456-005-5612-9

Maydan, J. S., Lorch, A., Edgley, M. L., Flibotte, S., & Moerman, D. G. (2010). Copy number variation in the genomes of twelve natural isolates of Caenorhabditis elegans. *BMC Genomics*, *11*(1), 62. doi:10.1186/1471-2164-11-62

McDermott, R., Tingley, D., Cowden, J., Frazzetto, G., & Johnson, D. D. P. (2009). Monoamine oxidase A gene (MAOA) predicts behavioral aggression following provocation. *Proceedings of the National Academy of Sciences*, *106*(7), 2118–2123. doi:10.1073/pnas.0808376106

Mikula, M., Rubel, T., Karczmarski, J., Goryca, K., Dadlez, M., & Ostrowski, J. (2010). Integrating proteomic and transcriptomic high-throughput surveys for search of new biomarkers of colon tumors. *Functional & Integrative Genomics*, *11*(2), 215–224. doi:10.1007/s10142-010-0200-5

Miller, J. R., & Moon, R. T. (1996). Signal transduction through beta-catenin and specification of cell fate during embryogenesis. *Genes & Development*, *10*(20), 2527–2539.

Miller, L. M., Gallegos, M. E., Morisseau, B. A., & Kim, S. K. (1993). lin-31, a Caenorhabditis elegans HNF-3/fork head transcription factor homolog, specifies three alternative cell fates in vulval development. *Genes & Development*, *7*(6), 933–947.

Milloz, J., Duveau, F., Nuez, I., & Félix, M.-A. (2008). Intraspecific evolution of the intercellular signaling network underlying a robust developmental system. *Genes & Development*, *22*(21), 3064–3075. doi:10.1101/gad.495308

Miskowski, J., Li, Y., & Kimble, J. (2001). The sys-1 Gene and Sexual Dimorphism during Gonadogenesis in Caenorhabditis elegans. *Developmental Biology*, *230*(1), 61–73. doi:10.1006/dbio.2000.9998

Mor, A., Campi, G., Du, G., Zheng, Y., Foster, D. A., Dustin, M. L., & Philips, M. R. (2007). The lymphocyte function-associated antigen-1 receptor costimulates plasma membrane Ras via phospholipase D2. *Nature Cell Biology*, *9*(6), 713–719. doi:doi:10.1038/ncb1592

Morin, P. J. (1997). Activation of beta -Catenin-Tcf Signaling in Colon Cancer by Mutations in beta -Catenin or APC. *Science*, *275*(5307), 1787–1790. doi:10.1126/science.275.5307.1787

Mosmann, T. (1983). Rapid colorimetric assay for cellular growth and survival: Application to proliferation and cytotoxicity assays. *Journal of Immunological Methods*, *65*(1-2), 55–63. doi:10.1016/0022-1759(83)90303-4

Myers, T. R., & Greenwald, I. (2007). Wnt signal from multiple tissues and lin-3/EGF signal from the gonad maintain vulval precursor cell competence in Caenorhabditis elegans. *Proceedings of the National Academy of Sciences*, *104*(51), 20368–20373. doi:10.1073/pnas.0709989104

Nakano, H., Yamamoto, F., Neville, C., Evans, D., Mizuno, T., & Perucho, M. (1984). Isolation of

transforming sequences of two human lung carcinomas: structural and functional analysis of the activated c-K-ras oncogenes. *Proceedings of the National Academy of Sciences of the United States of America*, *81*(1), 71–75.

Natarajan, L., Witwer, N. E., & Eisenmann, D. M. (2001). The divergent Caenorhabditis elegans beta-catenin proteins BAR-1, WRM-1 and HMP-2 make distinct protein interactions but retain functional redundancy in vivo. *Genetics*, *159*(1), 159–172.

Niv, H. (2002). Activated K-Ras and H-Ras display different interactions with saturable nonraft sites at the surface of live cells. *The Journal of Cell Biology*, *157*(5), 865–872. doi:10.1083/jcb.200202009

O, W., K, P., & E, N. (1924). Über den Stoffwechsel der Carcinomzelle. *Biochem Z*, (152), 309–344.

Olsen, J. V., Blagoev, B., Gnad, F., Macek, B., Kumar, C., Mortensen, P., & Mann, M. (2006). Global, In Vivo, and Site-Specific Phosphorylation Dynamics in Signaling Networks. *Cell*, *127*(3), 635–648. doi:10.1016/j.cell.2006.09.026

Omerovic, J., Laude, A. J., & Prior, I. A. (2007). Ras proteins: paradigms for compartmentalised and isoform-specific signalling. *Cellular and Molecular Life Sciences*, *64*(19-20), 2575–2589. doi:10.1007/s00018-007-7133-8

Plasterk, R. H. A., & Ketting, R. F. (2000). A genetic link between co-suppression and RNA interference in : C. elegans : Abstract : Nature. *Nature*, *404*(6775), 296–298. doi:10.1038/35005113

Plowman, S. J., Muncke, C., Parton, R. G., & Hancock, J. F. (2005). H-ras, K-ras, and inner plasma membrane raft proteins operate in nanoclusters with differential dependence on the actin cytoskeleton. *Proceedings of the National Academy of Sciences*, *102*(43), 15500–15505. doi:10.1073/pnas.0504114102

Prior, I. A., & Hancock, J. F. (2012). Ras trafficking, localization and compartmentalized signalling. *Seminars in Cell & Developmental Biology*, *23*(2), 145–153. doi:10.1016/j.semcdb.2011.09.002

Pylayeva-Gupta, Y., Grabocka, E., & Bar-Sagi, D. (2011). RAS oncogenes: weaving a tumorigenic web. *Nature reviews. Cancer*, *11*(11), 761–774. doi:10.1038/nrc3106

R H Hruban, A. D. V. M. G. J. O. D. H. V. W. D. C. A. S. N. G. T. W. K. K. K. B. J. L. C. J. L. B. (1993). K-ras oncogene activation in adenocarcinoma of the human pancreas. A study of 82 carcinomas using a combination of mutant-enriched polymerase chain reaction analysis and allele-specific oligonucleotide hybridization. *The American Journal of Pathology*, *143*(2), 545.

Rao, T. P., & Kühl, M. (2010). An updated overview on Wnt signaling pathways: a prelude for more. *Circulation research*, *106*(12), 1798–1806. doi:10.1161/CIRCRESAHA.110.219840

Rasola, A., Sciacovelli, M., Chiara, F., Pantic, B., Brusilow, W. S., & Bernardi, P. (2010). Activation of mitochondrial ERK protects cancer cells from death through inhibition of the permeability transition. *Proceedings of the National Academy of Sciences*, *107*(2), 726–731. doi:10.1073/pnas.0912742107

Reddy, E. P., Reynolds, R. K., Santos, E., & Barbacid, M. (1982). A point mutation is responsible for the acquisition of transforming properties by the T24 human bladder carcinoma oncogene. *Nature*, *300*(5888), 149–152. doi:10.1038/300149a0

Riddle, D. L. (1982). Developmental Biology of Caenorhabditis elegans: Symposium Introduction. *Journal of nematology*, *14*(2), 238–240.

Robert, V. J. P., Katic, I., & Bessereau, J.-L. (2009). Mos1 transposition as a tool to engineer the Caenorhabditis elegans genome by homologous recombination. *Error*, 1–7. doi:10.1016/j.ymeth.2009.02.013

Roy, S., Plowman, S., Rotblat, B., Prior, I. A., Muncke, C., Grainger, S., et al. (2005). Individual Palmitoyl Residues Serve Distinct Roles in H-Ras Trafficking, Microlocalization, and Signaling. *Molecular and Cellular Biology*, *25*(15), 6722–6733. doi:10.1128/MCB.25.15.6722-6733.2005

Rubinfeld, B., Robbins, P., El-Gamil, M., Albert, I., Porfiri, E., & Polakis, P. (1997). Stabilization of beta-catenin by genetic defects in melanoma cell lines. *Science*, *275*(5307), 1790–1792.

Rybaczyk, L. A., Bashaw, M. J., Pathak, D. R., & Huang, K. (2008). An indicator of cancer: downregulation of Monoamine Oxidase-A in multiple organs and species. *BMC Genomics*,

9(1), 134. doi:10.1186/1471-2164-9-134
Salser, S. J., Loer, C. M., & Kenyon, C. (1993). Multiple HOM-C gene interactions specify cell fates in the nematode central nervous system. *Genes & Development*, *7*(9), 1714–1724.
Santos, E., Martin-Zanca, D., Reddy, E. P., Pierotti, M. A., Porta, Della, G., & Barbacid, M. (1984). Malignant activation of a K-ras oncogene in lung carcinoma but not in normal tissue of the same patient. *Science*, *223*(4637), 661–664.
Sarin, S., Bertrand, V., Bigelow, H., Boyanov, A., Doitsidou, M., Poole, R. J., et al. (n.d.). Analysis of Multiple Ethyl Methanesulfonate-Mutagenized Caenorhabditis elegans Strains by Whole-Genome Sequencing.
Sato, J. D., & Kan, M. (2001). Media for culture of mammalian cells. *Current protocols in cell biology / editorial board, Juan S. Bonifacino ... [et al.]*, *Chapter 1*, Unit–Uni2. doi:10.1002/0471143030.cb0102s00
Sefton, B. M., Trowbridge, I. S., Cooper, J. A., & Scolnick, E. M. (1982). The transforming proteins of Rous sarcoma virus, Harvey sarcoma virus and Abelson virus contain tightly bound lipid. *Cell*, *31*(2 Pt 1), 465–474.
Sharma-Kishore, R., White, J. G., Southgate, E., & Podbilewicz, B. (1999). Formation of the vulva in Caenorhabditis elegans: a paradigm for organogenesis. *Development*, *126*(4), 691–699.
Shemer, G., & Podbilewicz, B. (2002). LIN-39/Hox triggers cell division and represses EFF-1/fusogen-dependent vulval cell fusion. *Genes & Development*, *16*(24), 3136–3141.
Shimizu, K., Goldfarb, M., Suard, Y., Perucho, M., Li, Y., Kamata, T., et al. (1983). Three human transforming genes are related to the viral ras oncogenes. *Proceedings of the National Academy of Sciences of the United States of America*, *80*(8), 2112–2116.
Sternberg, P. W., & Horvitz, H. R. (1986). Pattern formation during vulval development in C. elegans. *Cell*, *44*(5), 761–772. doi:10.1016/0092-8674(86)90842-1
Stetak, A., Gutierrez, P., & Hajnal, A. (2008). Tissue-specific functions of the Caenorhabditis elegans p120 Ras GTPase activating protein GAP-3. *Developmental Biology*, *323*(2), 166–176. doi:10.1016/j.ydbio.2008.08.026
Sze, J. Y., Victor, M., Loer, C., Shi, Y., & Ruvkun, G. (2000). Food and metabolic signalling defects in a Caenorhabditis elegans serotonin-synthesis mutant. *Nature*, *403*(6769), 560–564. doi:10.1038/35000609
Tabin, C. J., Bradley, S. M., Bargmann, C. I., Weinberg, R. A., Papageorge, A. G., Scolnick, E. M., et al. (1982). Mechanism of activation of a human oncogene. *Nature*, *300*(5888), 143–149. doi:10.1038/300143a0
Taparowsky, E., Shimizu, K., Goldfarb, M., & Wigler, M. (1983). Structure and activation of the human N-ras gene. *Cell*, *34*(2), 581–586. doi:10.1016/0092-8674(83)90390-2
Taparowsky, E., Suard, Y., Fasano, O., Shimizu, K., Goldfarb, M., & Wigler, M. (1982). Activation of the T24 bladder carcinoma transforming gene is linked to a single amino acid change. *Nature*, *300*(5894), 762–765. doi:10.1038/300762a0
Tipton, K. F., Boyce, S., O'Sullivan, J., Davey, G. P., & Healy, J. (2004). Monoamine oxidases: certainties and uncertainties. *Current medicinal chemistry*, *11*(15), 1965–1982.
Trent Gu, S. O. M. H. (1998). Caenorhabditis elegans SUR-5, a Novel but Conserved Protein, Negatively Regulates LET-60 Ras Activity during Vulval Induction. *Molecular and Cellular Biology*, *18*(8), 4556. Retrieved from http://www.ncbi.nlm.nih.gov/pmc/articles/PMC109041/pdf/mb004556.pdf
Vergara, I. A., Tarailo-Graovac, M., Frech, C., Wang, J., Qin, Z., Zhang, T., et al. (2014). Genome-wide variations in a natural isolate of the nematode Caenorhabditis elegans - 1471-2164-15-255.pdf. *BMC Genomics*, *15*(1), 255. doi:10.1093/bioinformatics/btp352
Weinberg, F., Hamanaka, R., Wheaton, W. W., Weinberg, S., Joseph, J., Lopez, M., et al. (n.d.). Mitochondrial metabolism and ROS generation are essential for Kras-mediated tumorigenicity. *pnas.org*.
Willert, K., & Nusse, R. (1998). β-catenin: a key mediator of Wnt signaling. *Current Opinion in Genetics & Development*, *8*(1), 95–102. doi:10.1016/S0959-437X(98)80068-3
Yamazaki, T., Komuro, I., Kudoh, S., Zou, Y., Shiojima, I., Mizuno, T., et al. (1995). Mechanical stress activates protein kinase cascade of phosphorylation in neonatal rat cardiac myocytes.

Journal of Clinical Investigation, *96*(1), 438–446. doi:10.1172/JCI118054

Yang, B., Jiang, J., Du, H., Geng, G., Jiang, Z., Yao, C., et al. (2009). Decreased monoamine oxidase (MAO) activity and MAO-A expression as diagnostic indicators of human esophageal cancers. *Biomarkers*, *14*(8), 624–629. doi:10.3109/13547500903207688

Yoo, A. S., Bais, C., & Greenwald, I. (2004). Crosstalk between the EGFR and LIN-12/Notch pathways in C. elegans vulval development. *Science*, *303*(5658), 663–666. doi:10.1126/science.1091639

Zalsman, G., Huang, Y.-Y., Harkavy-Friedman, J. M., Oquendo, M. A., Ellis, S. P., & Mann, J. J. (2004). Relationship of MAO-A promoter (u-VNTR) and COMT (V158M) gene polymorphisms to CSF monoamine metabolites levels in a psychiatric sample of caucasians: A preliminary report. *American Journal of Medical Genetics Part B: Neuropsychiatric Genetics*, *132B*(1), 100–103. doi:10.1002/ajmg.b.30094

Zipperlen, P., Nairz, K., Rimann, I., Basler, K., Hafen, E., Hengartner, M., & Hajnal, A. (2005). A universal method for automated gene mapping. *Genome Biology*, *6*(2), R19. doi:10.1186/gb-2005-6-2-r19

Acknowledgements:

I would like to thank Alex for the opportunity to work on this encouraging, interdisciplinary project and more importantly, to take and supervise me as a Ph.D. student. Further I thank all the members of the PANACEA project. I would not be here now, without your great support and inspiration, it was a pleasure to have met you and discussed with you all on our half-yearly meetings. In particular, I thank Basten for his big support on the analysis of quantitative genetics data and all things related. I enjoyed working with you a lot. I am further grateful for the help of Miriam, who did the experiments for the eQTL studies and part of the *bar-1(ga80)* miRIL project. In addition I would like to thank Jan as being an amazing PANACEA project manager.

Next I would like to thank all previous and current members of the Hajnal lab. I enjoyed the nice atmosphere in the lab and on lab excursions. I will miss you people. In particular, I would like to thank Fabienne as being a wonderful and highly motivated master student, carrying out most of the *bar-1(ga80)* miRIL project. I am also thankful for the entire lab scientific input, especially Michi, with whom I spent many hours discussing. In addition, Erika's technical expertise supported me to perform many of my molecular biology experiments. She further advanced my project by helping and carrying out many western blots and soft agar cell growth experiments. I am very thankful for this. Another thank goes to Martin, that mapped all the miRILS and ILs and the Functional Genomics Center Zürich for their help with whole genome sequencing and data analysis. At last I thank the two Biology Undergraduate Summer School students Leontien and Evelin, for their big help to advance and to support the project.

Further thanks go to the members of my thesis committee, Ueli Grossniklaus, Homayoun Bagheri and Ralf Sommer for all their scientific input, advice and support during my entire Ph.D. studies.

Another thanks goes to Irene for her support on organisational issues, Fedex mail handling and for her reminders to add oligos to the database, which otherwise would not be there.

I am also grateful to have the opportunity to work as a teacher for the life science learning center, giving courses about *C. elegans* biology.

Furthermore, and most importantly, I thank my parents that made it possible for me to study biology at the University of Zürich and eventually to become a Ph.D. I further thank Ari for her tremendous support and for being always a great motivator during my studies and as a dear friend. At last I would like to thank Sabrina who supports me and keeps my life happy; with her I can share all my ups and downs. Thank you all.

Lebenslauf

Persönliche Angaben:

Name:	Tobias Schmid
Geburtstag:	5. April 1983
Heimatort:	Schübelbach, SZ
Zivilstand:	ledig
Nationalität:	Schweizer

Ausbildung:

seit 09/2014:	**Research Associate** bei Prof. Dr. A. Hajnal am Institut für Molekulare Biologie der Universität Zürich
12/2014:	**Promotion zum Dr. sc. nat.** verliehen von der Mathematisch-naturwissenschaftlichen Fakultät der Universität Zürich Titel der Doktorarbeit: “Quantitative genetic analysis of *C. elegans* vulval development.”
03/2009 – 09/2014:	**Doktoratsstudium in Biologie** Mathematisch-naturwissenschaftliche Fakultät der Universität Zürich
01/2009:	**Master of Science in Genetik** (Note: 5.4) Titel der Masterarbeit: “Identification of interaction proteins of the *C. elegans* calsyntenin-2 homologue *casy-1*, an episodic memory related gene.”
10/2007 – 01/2009:	**Masterstudium** Mathematisch-naturwissenschaftliche Fakultät der Universität Zürich
06/2007:	**Bachelor of Science in Biologie** (Note: 5.3)
10/2003 – 06/2007:	**Bachelorstudium** Mathematisch-naturwissenschaftliche Fakultät der Universität Zürich
1999 – 2003:	**Matura Typus MAR** Kantonsschule Wettingen, AG Akzentfach: Mathematik Schwerpunktsfach: Biologie und Chemie Ergänzungsfach: Geographie

Sprachen:

Deutsch:	Muttersprache
English:	fliessend in Wort und Schrift

Französisch:	Grundkenntnisse

EDV Kentnisse:

Microsoft Word:	sehr gut
Microsoft Excel:	sehr gut
Microsoft Powerpoint:	sehr gut
Adobe Illustrator:	gut
Adobe Photoshop:	gut
Endnote:	Grundkenntnisse
Openlab:	Grundkenntnisse
Sequencher:	gut
CLC Bio:	gut

Technisches Wissen/ praktische Erfahrung:

DNA/RNA:	Extraktion, Purifikation, diverse PCRs
Protein:	Expression, Extraktion, Purifikation, SDS-PAGE, Western-blot, IP, Co-IP
Klonieren:	bakterielle Transformation, Restriktionsverdau, Ligation, etc.
Genetik:	CRISPR/Cas9 Transgenese, Ballistische und injektionelle Transgenese in C. elegans
Mikroskopie:	Licht- sowie Fluoreszentmikroskopische Analysen

Lehrtätigkeit/ Supervision:

2008 – 2014:	diverse Assistenzen in Entwicklungsbiologie-, Genetik- und Medizinkursen
01/2011 – 01/2012:	Betreuung von Fabienne Largey als Masterstudentin
07/2011 – 09/2011:	Betreuung von Leontien van der Bent als BUSS Studentin
07/2012 – 09/2012:	Betreuung von Evelin Despot Slade als BUSS Studentin
08/2014 – 12/2014:	Betreuung von Katharina Jovic als Austauschstudentin

Nebenuniversitäre Tätigkeiten:

seit 2010:	Kursleiter für das Life Science Learning Center Zürich
03/2003 – 02/2009:	20% Anstellung als Mitarbeiter im Vertrieb/ Verkauf der Lebensmittelabteilung der Manor AG.

Freizeitaktivitäten:

Aquaristik, züchten exotischer Pflanzen, Lesen von Romane im Sci-Fi und Fantasy Genre, Wintersport.

Referenzen:

Masterarbeit und Doktorat: Prof. Dr. A. Hajnal, +41 44 635 48 54, alex.hajnal@imls.uzh.ch
Life Science Learning Center: Dr. L. Leumann, +41 44 635 31 46, lorenz.leumann@access.uzh.ch